INTEGRATED NON-INVASIVE CARDIOVASCULAR IMAGING

A Guide for the Practitioner

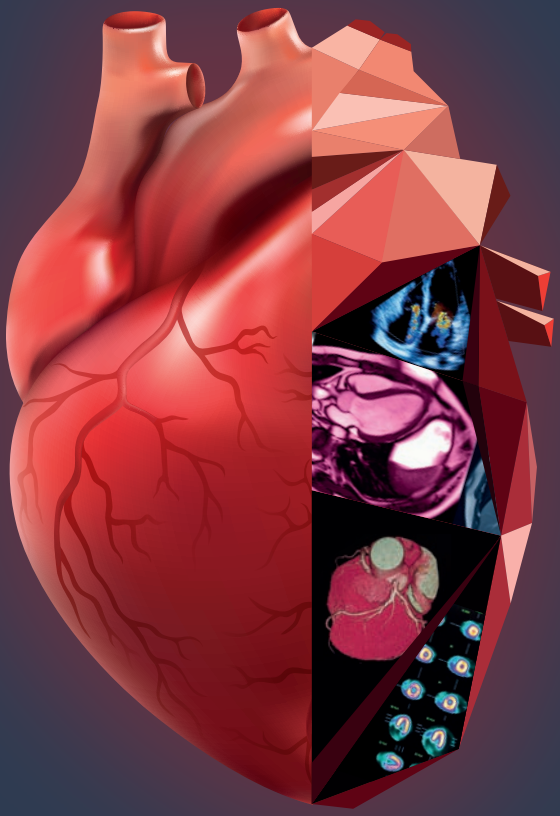

Maurizio Dondi, Diana Paez, Paolo Raggi, Leslee J. Shaw, Mani Vannan

IAEA
International Atomic Energy Agency

INTEGRATED NON-INVASIVE CARDIOVASCULAR IMAGING: A GUIDE FOR THE PRACTITIONER

The following States are Members of the International Atomic Energy Agency:

AFGHANISTAN
ALBANIA
ALGERIA
ANGOLA
ANTIGUA AND BARBUDA
ARGENTINA
ARMENIA
AUSTRALIA
AUSTRIA
AZERBAIJAN
BAHAMAS
BAHRAIN
BANGLADESH
BARBADOS
BELARUS
BELGIUM
BELIZE
BENIN
BOLIVIA, PLURINATIONAL STATE OF
BOSNIA AND HERZEGOVINA
BOTSWANA
BRAZIL
BRUNEI DARUSSALAM
BULGARIA
BURKINA FASO
BURUNDI
CAMBODIA
CAMEROON
CANADA
CENTRAL AFRICAN REPUBLIC
CHAD
CHILE
CHINA
COLOMBIA
COMOROS
CONGO
COSTA RICA
CÔTE D'IVOIRE
CROATIA
CUBA
CYPRUS
CZECH REPUBLIC
DEMOCRATIC REPUBLIC OF THE CONGO
DENMARK
DJIBOUTI
DOMINICA
DOMINICAN REPUBLIC
ECUADOR
EGYPT
EL SALVADOR
ERITREA
ESTONIA
ESWATINI
ETHIOPIA
FIJI
FINLAND
FRANCE
GABON
GEORGIA
GERMANY
GHANA
GREECE
GRENADA
GUATEMALA
GUYANA
HAITI
HOLY SEE
HONDURAS
HUNGARY
ICELAND
INDIA
INDONESIA
IRAN, ISLAMIC REPUBLIC OF
IRAQ
IRELAND
ISRAEL
ITALY
JAMAICA
JAPAN
JORDAN
KAZAKHSTAN
KENYA
KOREA, REPUBLIC OF
KUWAIT
KYRGYZSTAN
LAO PEOPLE'S DEMOCRATIC REPUBLIC
LATVIA
LEBANON
LESOTHO
LIBERIA
LIBYA
LIECHTENSTEIN
LITHUANIA
LUXEMBOURG
MADAGASCAR
MALAWI
MALAYSIA
MALI
MALTA
MARSHALL ISLANDS
MAURITANIA
MAURITIUS
MEXICO
MONACO
MONGOLIA
MONTENEGRO
MOROCCO
MOZAMBIQUE
MYANMAR
NAMIBIA
NEPAL
NETHERLANDS
NEW ZEALAND
NICARAGUA
NIGER
NIGERIA
NORTH MACEDONIA
NORWAY
OMAN
PAKISTAN
PALAU
PANAMA
PAPUA NEW GUINEA
PARAGUAY
PERU
PHILIPPINES
POLAND
PORTUGAL
QATAR
REPUBLIC OF MOLDOVA
ROMANIA
RUSSIAN FEDERATION
RWANDA
SAINT LUCIA
SAINT VINCENT AND THE GRENADINES
SAMOA
SAN MARINO
SAUDI ARABIA
SENEGAL
SERBIA
SEYCHELLES
SIERRA LEONE
SINGAPORE
SLOVAKIA
SLOVENIA
SOUTH AFRICA
SPAIN
SRI LANKA
SUDAN
SWEDEN
SWITZERLAND
SYRIAN ARAB REPUBLIC
TAJIKISTAN
THAILAND
TOGO
TRINIDAD AND TOBAGO
TUNISIA
TURKEY
TURKMENISTAN
UGANDA
UKRAINE
UNITED ARAB EMIRATES
UNITED KINGDOM OF GREAT BRITAIN AND NORTHERN IRELAND
UNITED REPUBLIC OF TANZANIA
UNITED STATES OF AMERICA
URUGUAY
UZBEKISTAN
VANUATU
VENEZUELA, BOLIVARIAN REPUBLIC OF
VIET NAM
YEMEN
ZAMBIA
ZIMBABWE

The Agency's Statute was approved on 23 October 1956 by the Conference on the Statute of the IAEA held at United Nations Headquarters, New York; it entered into force on 29 July 1957. The Headquarters of the Agency are situated in Vienna. Its principal objective is "to accelerate and enlarge the contribution of atomic energy to peace, health and prosperity throughout the world".

INTEGRATED NON-INVASIVE CARDIOVASCULAR IMAGING: A GUIDE FOR THE PRACTITIONER

M. DONDI, D. PAEZ, P. RAGGI, L.J. SHAW, M. VANNAN

INTERNATIONAL ATOMIC ENERGY AGENCY
VIENNA, 2021

COPYRIGHT NOTICE

Marketing and Sales Unit, Publishing Section
International Atomic Energy Agency
Vienna International Centre
PO Box 100
1400 Vienna, Austria
fax: +43 1 26007 22529
tel.: +43 1 2600 22417
email: sales.publications@iaea.org
www.iaea.org/publications

Printed by the IAEA in Austria
June 2021
STI/PUB/1931

IAEA Library Cataloguing in Publication Data

Names: International Atomic Energy Agency.
Title: Integrated non-invasive cardiovascular imaging : a guide for the practitioner / International Atomic Energy Agency.
Description: Vienna : International Atomic Energy Agency, 2021. | Series: -, ISSN ; no. | Includes bibliographical references.
Identifiers: IAEAL 21-01421 | ISBN 978–92–0–133021–5 (paperback : alk. paper) | ISBN 978–92–0–133121–2 (pdf) | ISBN 978–92–0–101621–8 (epub) | ISBN 978–92–0–101721–5 (mobipocket)
Subjects: LCSH: Heart — Imaging. | Nuclear medicine. | Radioisotopes in cardiology. | Single-photon emission computed tomography. | Tomography, Emission.
Classification: UDC 616.12:616-073 | STI/PUB/1931

FOREWORD

Cardiovascular disease is a major contributor to premature morbidity and mortality worldwide, and improving human health through early and effective diagnostic imaging is an effective means to positively influence the health of a population. Through efforts within the IAEA, numerous initiatives have been developed, or are underway, to promote quality medical imaging practices for the detection and guided treatment of cardiovascular disease. These regional and global training and educational programmes emphasize the importance of worldwide standards for instrumentation, protocols, appropriate use, and high quality image interpretation and reporting practices.

The importance of addressing cardiovascular diseases and other non-communicable diseases is recognized by United Nations organizations. Under United Nations Sustainable Development Goal 3, to ensure healthy lives and to promote well being for everyone at all ages, the target is to reduce premature non-communicable disease mortality by one third by 2030. The Global Action Plan, designed by the World Health Organization, aims at preventing and controlling non-communicable diseases and offers a roadmap and policy options. The aim is to prevent heart attacks and strokes and to achieve a 25% relative reduction in premature mortality from non-communicable diseases by 2025.

Integrated cardiovascular imaging is an evolving concept. Recent advances in technology have contributed to the development of new imaging modalities and the refinement of existing ones, leading to major improvements in the accuracy of diagnosing cardiovascular and other diseases. While modality centric knowledge and expertise have been the primary drivers of improvement in each modality, this has also contributed to imagers working in silos, which has resulted in limited intermodality coordination and collation of information relevant for patient care. Non-invasive imaging tools to diagnose and stratify risk in cardiac disease and to guide its management include echocardiography, coronary computed tomography angiography (CCTA), cardiac magnetic resonance (CMR) imaging and nuclear cardiology, using either single photon emission computed tomography (SPECT) or positron emission tomography (PET) coupled with computed tomography (CT). Each of these techniques has distinct characteristics that allow the evaluation of details of the anatomy of the heart, its physiology or both. Depending on a patient's characteristics and the various potential clinical presentations, some of these techniques may be better suited for some patients than other techniques, either for the initial work-up of a certain condition or as a follow-up method to evaluate a condition already identified.

The IAEA plays an integral role in the development of clinical trial evidence and in the development of guidance documents to synthesize available data into

optimal strategies of care. Examples of IAEA sponsored research can be found in recent publications.

The availability of technology is quite heterogeneous worldwide. Some countries have access to only the most basic tools to evaluate the heart, such as electrocardiogram, exercise treadmill/bicycle test and echocardiography. Other countries have various degrees of access to more advanced imaging technologies, such as SPECT, CCTA, CMR imaging and PET–CT. It is advisable that physicians use all the diagnostic potential of any techniques available, applying internationally accepted standard protocols, and that the results be interpreted and acted upon appropriately.

This publication provides comprehensive guidance on the rationale for and implementation of integrated cardiovascular imaging for practitioners. Imaging experts can embrace optimal strategies of cardiovascular imaging to address an array of clinical conditions. By applying high quality evidence published in peer reviewed literature, vast opportunities are available to improve the lives of patients at risk of and diagnosed with cardiovascular disease, many of whom will benefit from the use of cardiovascular imaging to guide optimal therapeutic decision making.

The IAEA is grateful to all who contributed to the drafting and review of this publication, in particular P. Raggi (Canada), L.J. Shaw (United States of America) and M. Vannan (United States of America). The IAEA acknowledges the contributions of the late Ravi Kashyap of the Division of Human Health. The IAEA officers responsible for this publication were M. Dondi and D. Paez of the Division of Human Health.

EDITORIAL NOTE

CONTENTS

Chapter 1

INTRODUCTION

1.1. BACKGROUND

Integrated cardiovascular imaging is an evolving concept. Recent advances in technology have contributed to the development of new imaging modalities and the refinement of existing ones, leading to major improvements in the accuracy of diagnosing cardiovascular and other diseases. While modality centric knowledge and expertise have been the primary drivers of improvement in each modality, this has also contributed to imagers working in silos, resulting in limited intermodality coordination and collation of information relevant for patient care. Non-invasive imaging tools to diagnose and stratify risk in cardiac disease and to guide its management include echocardiography, coronary computed tomography angiography (CCTA), cardiac magnetic resonance (CMR) and nuclear cardiology, using either single photon emission computed tomography (SPECT) or positron emission tomography (PET) coupled with computed tomography (CT). Each of these techniques has distinct characteristics that allow the evaluation of details of the anatomy of the heart, its physiology or both. Depending on a patient's characteristics and the various potential clinical presentations, some of these techniques may be better suited for some patients than other techniques, either for the initial work-up of a certain condition or as a follow-up method to evaluate a condition already identified.

1.2. OBJECTIVE

Availability of technology worldwide is quite heterogeneous. Some countries have access to only the most basic tools to evaluate the heart, such as electrocardiogram (ECG), exercise treadmill/bicycle test (ETT) and echocardiography. Other countries will have various degrees of access to more advanced imaging technologies, such as SPECT, SPECT–CT, CCTA, CMR and PET–CT. The objective of this publication is to provide physicians a comprehensive information on the use of all the diagnostic potential of the technique available, so that internationally accepted standard protocols are applied, and that the results are interpreted and acted upon appropriately. Guidance provided here, describing good practices, represents expert opinion but does not constitute recommendations made on the basis of a consensus of Member States.

1.3. SCOPE

This publication provides comprehensive guidance on the rationale for and implementation of integrated cardiovascular imaging for practitioners. Imaging experts can embrace optimal strategies of cardiovascular imaging to address an array of clinical conditions. By applying high quality evidence published in peer reviewed literature, vast opportunities are available to improve the lives of patients at risk of and diagnosed with cardiovascular disease, many of whom will benefit from the use of cardiovascular imaging to guide optimal therapeutic decision making.

1.4. STRUCTURE

This publication is structured in two parts. Part I provides technical information on the different techniques; Part II addresses their clinical applications.

Part I

FUNDAMENTALS OF NON-INVASIVE CARDIAC IMAGING

Chapter 2

NUCLEAR CARDIOLOGY: SINGLE PHOTON EMISSION COMPUTED TOMOGRAPHY

A. PEIX, J. VITOLA, E. GARCIA, D. SOBIC SARANOVIC, M. DONDI

Single photon emission computed tomography (SPECT) is the most widely applied nuclear medicine technique in cardiology. It is based on the use of single photon emitting radiopharmaceuticals that have the property of entering myocardial cells proportional to regional blood flow. This property allows the imaging of myocardial perfusion using detecting devices for either X rays or gamma rays. Indeed, the extraction of those radiopharmaceuticals increases proportionally in a myocardial territory perfused by a patent coronary artery than in a segment perfused by a stenosed vessel, enabling differentiation between the normal and the hypoperfused myocardium. Computer algorithms have been developed to automatically and objectively process and quantify these images.

Myocardial perfusion imaging (MPI) has a widespread clinical use because of its well documented diagnostic accuracy for assessing coronary artery disease (CAD), as well as its prognostic value [2.1]. Recent advances in SPECT instrumentation have made it possible to improve image quality while reducing study time, radiation dose to the patient and overall cost. In addition, new software solutions have improved image resolution and helped to limit image noise. In this chapter, a general review of recent advances in this field is presented. The IAEA has published detailed guidance on SPECT MPI implementation in Ref. [2.1].

2.1. HARDWARE

In most nuclear cardiology laboratories today, SPECT cameras based on a technology developed in 1958 by Anger [2.2] are used, together with standard parallel hole collimators, to image the heart. Basic filtered back projection algorithms are then used to reconstruct cardiac images [2.3]. Typically, these studies require 15–20 min to be completed.

Recently, newer ultrafast cameras based on cadmium zinc telluride (CZT) solid state detectors have been introduced, allowing a five to tenfold increase in count sensitivity at no loss or even at a gain in resolution, resulting in the potential for acquiring a stress MPI scan with a standard radiopharmaceutical injected dose within 2 min or less. Several clinical trials have been published using CZT cameras, showing that a stress/rest MPI protocol with 4 and 2 min

CZT acquisitions has an equivalent diagnostic performance compared with stress/rest conventional SPECT [2.4–2.6]. Another development for conventional SPECT cameras is the modification of the electronics, system geometry and collimation to significantly improve the imaging performance of rotating SPECT cameras [2.7, 2.8].

2.2 SOFTWARE

For gamma cameras, the time of acquisition of an MPI study is dependent on the resolution required to resolve perfusion defects in the myocardium above the noise due to inherent limited count sensitivity. The resolution and sensitivity of parallel hole collimators depend on the shape, length and size of the holes [2.9], and this represents the main drawback of the technology. To account for that limitation, image reconstruction has been improved using software that considers and corrects for the distance between the detector and the source, in this case the myocardium. This is known as resolution recovery and reduces noise and improves spatial resolution compared with the previously utilized filtered back projection [2.9].

Reconstruction using resolution recovery is inherently iterative. Although it takes more calculations and time than filtered back projection, a favourable characteristic of resolution recovery is its ability to account for the factors that degrade SPECT images in the reconstruction process. The most widely used iterative reconstruction method is maximum likelihood expectation maximization (MLEM) [2.10]. A shortcut to the MLEM algorithm is known as ordered subset expectation maximization, which is the approach commonly implemented in most commercial systems [2.9].

Another important improvement has been the introduction of solid state detector cameras, such as the newer CZT cameras, which allow reconstruction of SPECT acquisition together with the quantification of myocardial blood flow, similar to that carried out with ^{13}N ammonia positron emission tomography (PET) [2.11]. From a clinical point of view, these instrumentation and software improvements provide a significant reduction in acquisition time for an MPI study, with the advantages of offering greater patient comfort owing to the studies being shorter and a decreased incidence of artefacts due to patient motion. The radiation dose to the patient and staff is also lower.

2.3. HYBRID SPECT–CT IMAGING SYSTEMS

Hybrid systems, which physically couple a computed tomography (CT) scanner with either a PET or a SPECT scanner, are now used in routine clinical practice. The coupled CT scanner is commonly used for attenuation correction but, if equipped with adequate software and an adequate number of slices, may be used to evaluate the coronary artery calcium score (CACS) or to perform coronary computed tomography angiography (CCTA). An advantage of these systems is that they can provide, in one imaging study, comprehensive cardiac evaluation of anatomical information from the CT scan and physiological information from the PET or SPECT scan [2.12].

2.3.1. Techniques

SPECT MPI is currently performed using the gated technique, where the acquisition is synchronized with the electrocardiogram (ECG) signal, and is usually referred to as GSPECT, where the G stands for gated. Performed after either physical or pharmacological stress, this well validated nuclear cardiology technique has the capability of evaluating the extent and severity of myocardial ischaemia and measuring the size of an infarct, as well as regional wall motion and left ventricular function [2.13].

2.3.2. Types of stress used in GSPECT procedures

Physical exercise is the stress of choice for all patients who do not present baseline ECG abnormalities that might preclude interpretation of the results and impact the ability to exercise adequately. It covers a broad spectrum including the diagnosis of obstructive CAD, risk assessment and prognosis in symptomatic patients or those with previous history of CAD, and evaluation of therapeutic interventions [2.14].

Exercise testing can be done using a treadmill or an ergometric bicycle. Each modality has its own advantages and disadvantages; both modalities are equally useful, and the choice depends on the experience and preferences of the laboratory. Although exercise testing should be the stress modality of choice for MPI, it could be substituted by pharmacological stress in patients with exercise limitations, as well as in those with left bundle branch block or paced rhythms who may show artefactual perfusion defects in the septal territories [2.15]. The indications for the use of pharmacological stress are as follows:

(a) Neurological diseases.
(b) Muscular diseases.

(c) Skeletal diseases.
(d) Peripheral vascular disease.
(e) Reduced exercise capacity or inability to achieve at least submaximal heart rate owing to:
    — Chronic obstructive lung disease;
    — Diabetes mellitus or neuropathy;
    — Poor physical training;
    — Poor motivation;
    — Morbid obesity;
    — Mental conditions.
(f) Left bundle branch block.
(g) Pace rhythms.
(h) Ventricular pre-excitation (Wolff–Parkinson–White syndrome).

The pharmacological stress agents belong to two groups: vasodilators, such as dipyridamole, adenosine and regadenoson; and inotropic drugs such as dobutamine. The contraindications for the use of vasodilators and inotropic drugs, as well as the different protocols that can be used, are clearly presented in the American Society of Nuclear Cardiology imaging guidelines for SPECT nuclear cardiology procedures (stress, protocols, tracers) [2.16]. As a general recommendation, Fig. 2.1 shows an algorithm to help to optimize the stress test used in MPI, considering the interpretability of the ECG and the ability of the patient to exercise.

2.3.3. Acquisition and interpretation of images

Acquisition parameters and reconstruction filters are extensively covered in Ref. [2.1] on the implementation of SPECT for MPI. The assessment of the quality of the study as well as of the perfusion and ventricular contractility is the first step in MPI clinical interpretation. In addition, quantification using several commercially available software packages is a very important tool in MPI because it provides an objective assessment of the different parameters evaluated, including the extent and severity of the ischaemia and the infarct size. Combining perfusion and function information with the exercise information helps the clinician to establish appropriate ischaemia guided management and is the main strength of the technique.

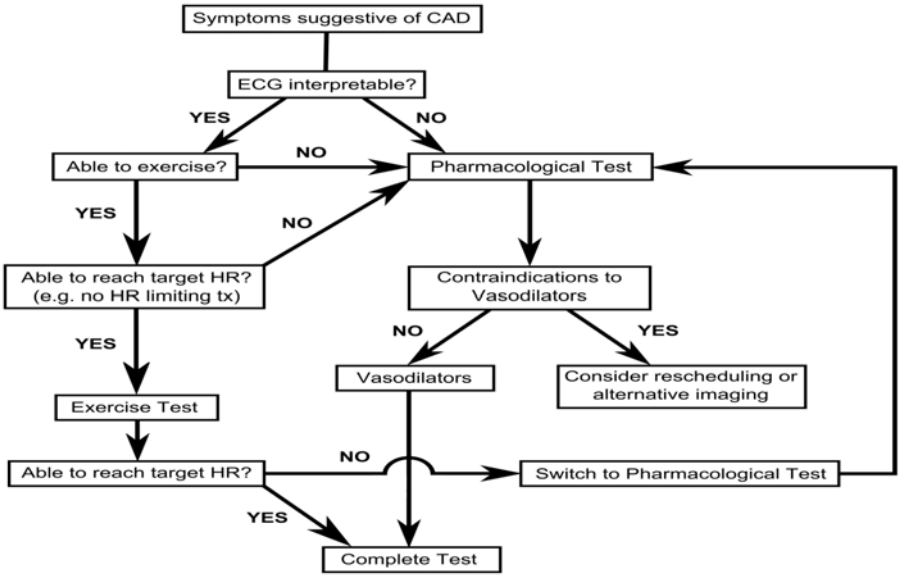

FIG. 2.1. Optimization of stress test in MPI. Source: See fig. 4.1 of Ref. [2.1]. Note: CAD — coronary artery disease; ECG — electrocardiogram; HR — heart rate.

2.3.4. Reporting

The standardized myocardial segmentation and nomenclature for tomographic imaging of the heart should be followed [2.17] and the following information should be provided.

2.3.4.1. Perfusion defect severity and size

The perfusion defect severity correlates with the severity of CAD and can be scored as follows:

— Absent uptake = 4;
— Severely reduced uptake = 3;
— Moderately reduced uptake = 2;
— Mildly reduced uptake = 1;
— Normal uptake = 0.

The perfusion defect size correlates with the extent of CAD and can be calculated using either software or visual scoring.

2.3.4.2. Summed stress, rest and difference scores

The summed scores consider both the extent and severity of myocardial perfusion defects in each of the 17 myocardial segments, as defined by the American Heart Association [2.17]. The sum of the scores on the 17 left ventricular myocardial segments of the stress image is called the summed stress score. The difference between the stress and rest scores is the summed difference score. The scores are interpreted as follows:

— Summed stress score: Includes ischaemia and infarction. A summed stress score ≤3 is consistent with a normal result, while 4–8 is a mild defect, 9–12 is a moderate defect and >12 is a severe defect.
— Stress and rest scores: This is the magnitude of a fixed defect, and generally represents the size and severity of a myocardial infarction.
— Summed difference score: This expresses the magnitude of defect reversibility or ischaemia. A summed difference score of 1–3 represents mild ischaemia, 4–7 moderate ischaemia and >7 severe ischaemia.

2.3.4.3. Left ventricular ejection fraction

Left ventricular ejection fraction (LVEF) can be assessed using GSPECT, which produces a highly reproducible measurement of LVEF and assessment of regional wall motion. This also allows a better assessment of perfusion defects, differentiating scars from attenuation artefacts, to improve the specificity of the test and risk stratification. The normal lower limit of LVEF is typically 50%, although values as low as 45% have been reported in men with a low likelihood of CAD [2.1]. Normal limits of LVEF may be higher in individuals with a low body mass index (e.g. women and people of certain ethnicities) because of the partial volume effect. LVEF may be underestimated in individuals with a large heart and a thinned myocardium owing to the resolution limitations of the imaging system. For values beyond 70%, LVEF should be reported as greater than 70%. Similarly, an indication of less than 10% should be reported for all values below 10%.

Although the GSPECT acquisition is typically performed 45–60 min after injection at peak stress, this time lapse prevents the acquisition of a real post-stress test. However, that value should be reported together with the rest LVEF and the difference between values (delta ejection fraction). A significant post-stress decline in LVEF might be an indicator of prolonged post-ischaemic myocardial ‘stunning’, especially when perfusion defects are reversible [2.18]. A stress LVEF value of 5 absolute points or lower than the rest LVEF value is generally associated with a high risk of cardiac events. It has been shown that

when post-stress image acquisition is performed within 15 min of injection, the test has a higher sensitivity to detect post-ischaemic stunning [2.19].

Left ventricular volumes, both end diastolic and end systolic, should also be routinely reported for both stress and rest images (in mL) because these values also have significant prognostic implications.

2.3.4.4. Regional left ventricular function and wall motion

Regional wall motion is an important parameter that can be visually assessed and scored as the following:

— Normal = 0;
— Mild hypokinesia = 1;
— Moderate hypokinesia = 2;
— Severe hypokinesia = 3;
— Akinesia (infarct) = 4;
— Dyskinesia (infarct, aneurysm) = 5.

Another important piece of information is wall thickening assessed quantitatively (as a percentage of thickening from diastole to systole) and expressed in scores and colour scaled polar plots. Wall thickening can also be evaluated using a semiquantitative scale where:

— Normal = 0;
— Mild reduction in thickening = 1;
— Moderate to severe reduction in thickening = 2;
— No thickening = 3.

Phase analysis of gated MPI studies has been applied to investigate asynchronous myocardial contraction and is now available in certain software packages. The method has been shown to be useful in assessing the need for resynchronization therapy and to evaluate its results [2.20, 2.21]. It may also help to identify the heart failure patients most likely to experience cardiac events [2.22, 2.23]. Figures 2.2–2.4 show examples of how quantification can be performed using MPI SPECT techniques.

2.3.4.5. Transient ischaemic dilation

Transient ischaemic dilation is defined as an apparent enlargement of the left ventricle on images taken after stress as compared with rest conditions. A ratio of 1.2 or above is considered pathological for physical stress MPI; while for

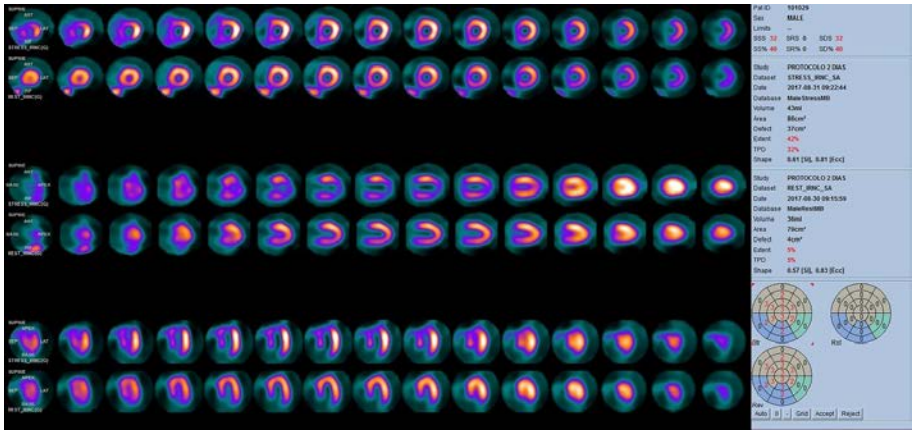

FIG. 2.2. 80 year old male patient referred for investigation of atypical chest pain and fatigue on exertion. He was able to exercise on the treadmill without any chest pain but showed ischaemic changes on the ECG (Duke treadmill score of intermediate risk). SPECT images show a severe defect involving a large area of the left anterior descending branch territory, completely normalized at rest. The summed stress score is 32, the summed rest score is 0 and the summed difference score is 32, consistent with pure ischaemia involving part of the anterior wall, the septum and the whole apex. (Courtesy of J. Vitola, Curitiba, Brazil.)

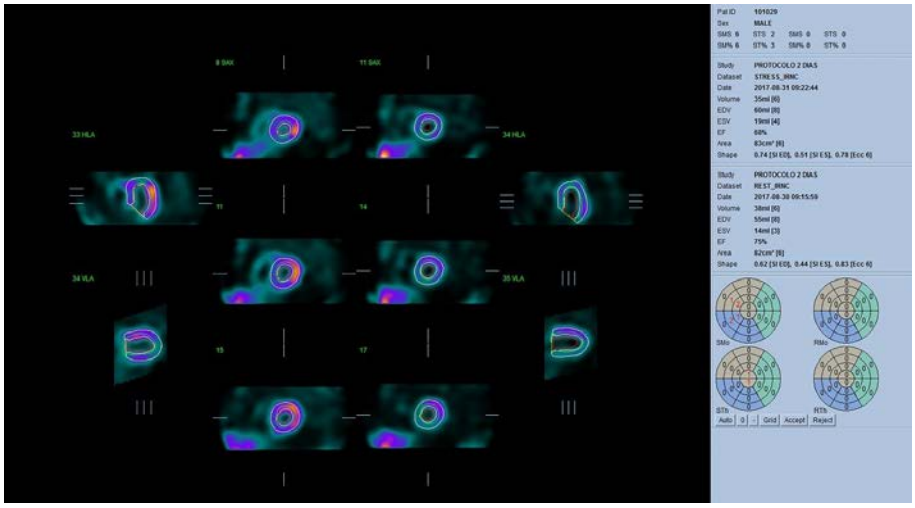

FIG. 2.3. These images are for the same patient as in Fig. 2.2. Quantification of motion shows abnormalities after stress — septal hypokinesia (polar map labelled SMo for stress motion) and mildly decreased apical thickness observed (STh) but normal at rest (RMo, RTh) — all secondary to ischaemia induced myocardial stunning. (Courtesy of J. Vitola, Curitiba, Brazil.)

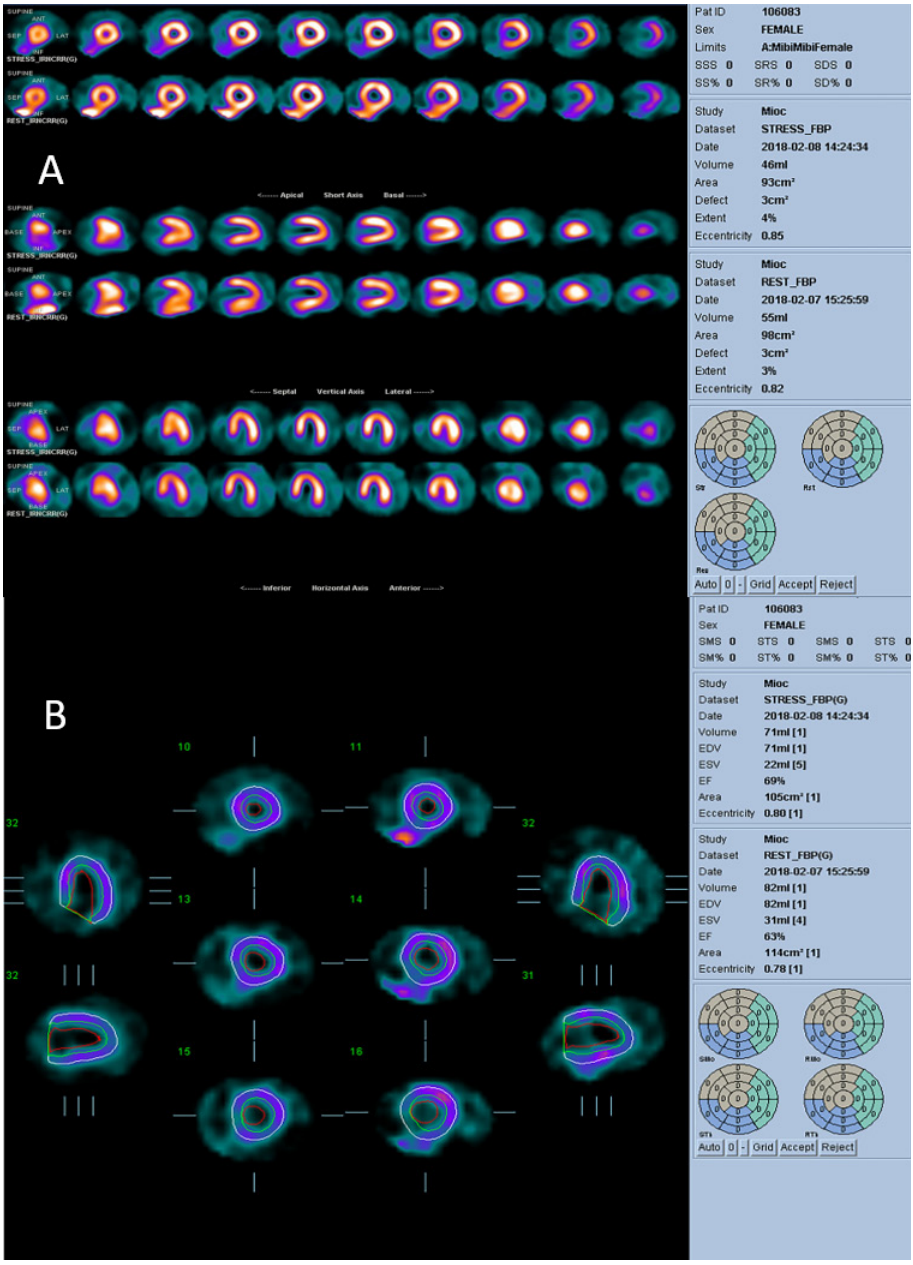

FIG. 2.4. 41 year old female patient referred for atypical chest pain with borderline positive ST segment changes on the stress ECG. (A) SPECT images showing normal perfusion as well as (B) normal quantitative analysis. (Courtesy of J.Vitola, Curitiba, Brazil.)

pharmacological stress MPI, 1.3 is the upper limit. Transient ischaemic dilation can result from severe regional or diffuse ischaemia and may be especially useful when there is suspicion of 'balanced' ischaemia, which is a well known cause of false negative perfusion scans. It could also be due to diffuse subendocardial ischaemia causing an apparent enlargement of the left ventricular cavity during stress [2.24, 2.25].

2.3.4.6. Lung to heart ratio

Increased uptake of perfusion tracers in the lungs results in a high lung to heart ratio and carries a significant adverse prognosis since it reflects poor left ventricular function. When using ^{99m}Tc labelled compounds, a lung to heart ratio is considered abnormal when greater than 0.44; while when using ^{201}Tl, a lung to heart ratio greater than 0.50 is considered significant. Increased lung uptake is due to elevated left ventricular end diastolic pressure as a consequence of poor left ventricular function. Owing to the inherently different characteristics of the two tracers, ^{201}Tl MPI is more sensitive for this parameter, since post-stress images are obtained sooner after stress than with ^{99m}Tc labelled compounds.

2.3.4.7. Right ventricular uptake

Because of its low wall thickness, typically one third thinner than that of the left ventricle, the right ventricle myocardium normally shows very mild uptake of the tracer and is faintly seen. Higher than normal right ventricular uptake may represent severe left ventricular ischaemia and should be considered a specific marker of multivessel CAD or involvement of the left main coronary artery [2.26], causing left ventricular dysfunction and an increase in pulmonary arterial pressure.

2.3.4.8. High risk scan features

The following MPI findings are associated with an elevated risk of cardiac events:

— Multiple, extensive and severe perfusion defects;
— Perfusion defects in the region of the left anterior descending coronary artery;
— Transient dilation of the left ventricle;
— Transient increase in right ventricular tracer uptake;
— Increased pulmonary uptake of radiotracer;
— Transient wall motion abnormalities;

— Post-ischaemic myocardial stunning, when post-stress LVEF is lower than rest LVEF.

2.4. SAFETY

The application of strategies to reduce radiation dose in MPI is of crucial importance. The two fundamental principles of medical radiation protection are justification and optimization. Justification requires that any procedure involving radiation is performed for the appropriate clinical indication [2.27] or, in other words, the right test for the right patient at the right time, taking into account the three As of awareness, appropriateness and audit.

Optimization refers to performing the test appropriately according to the ALARA (as low as reasonably achievable) principle, keeping radiation as low as possible while ensuring diagnostically acceptable image quality. The American Society of Nuclear Cardiology recommends a median dose of ≤9 mSv for an MPI study [2.28]. As part of the IAEA Nuclear Cardiology Protocols Study (INCAPS) [2.29], a committee of international experts identified eight best practices aimed at optimization for nuclear cardiology laboratories:

(1) Avoid thallium stress testing. Thallium-201 has a much longer physical half-life (73 h) than ^{99m}Tc (6 h), and therefore stays in the body longer, exposing a patient to ionizing radiation for a long time after its utility for diagnostic imaging has passed, with a resulting higher radiation dose than ^{99m}Tc labelled compounds.
(2) Avoid dual isotope testing. It is associated with the highest radiation doses of all SPECT MPI studies.
(3) Avoid too much technetium. The effective dose should average less than 15 mSv for all studies in a laboratory using only technetium injections; for most patients, a considerably lower dose should be possible [2.30].
(4) Avoid too much thallium. For average weight patients, 93–110 MBq is considered adequate for diagnostic quality MPI images and a maximum of 130 MBq of ^{201}Tl should be used for stress testing or rest/redistribution imaging.
(5) Perform stress-only imaging. In INCAPS, stress-only imaging was found to reduce radiation dose by 64% [2.30]. Prognostic data from over 20 000 patients suggest that stress-only imaging achieves this radiation reduction without compromising patient outcomes [2.31].
(6) Use camera based dose reduction strategies. Advanced image reconstruction software with iterative reconstruction, resolution recovery and noise reduction algorithms are available and enable the reduction of administered

activity while maintaining image quality [2.32]. The use of advanced SPECT hardware, including cardiac focused collimators or high efficiency CZT cameras, can also help in reducing administered activity. Radiation effective dose could be reduced to as little as 1 mSv [2.33].

(7) Use weight based dosing for technetium. The amount of injected technetium activity should be based on patient weight and habitus. Larger patients generally need higher doses than smaller patients to achieve good image quality (see table 4.4 of Ref. [2.1] for a range of activities for each protocol).

(8) Avoid inappropriate dosing that can lead to shinethrough artefacts. If there is a six hour delay between injections, no more than half the activity from the first injection will remain and shine through into the second set of images, and therefore a 1:2 ratio of injected activity should be adequate [2.1]. In general, using a 1:4 ratio of injected activities in a one-day stress/rest or rest/stress study (e.g. a 300 MBq first injection and a 1200 MBq second injection) will always ensure an adequate count ratio to minimize the risk of significant shinethrough artefacts [2.1]. This does not reduce radiation dose but may in fact increase it. However, it prevents the performance of low quality, inadequate studies that could need to be repeated, therefore submitting the patient to a new administration of a radiopharmaceutical.

2.5. KEY MESSAGES

(1) GSPECT MPI with induced stress (either physical or pharmacological) is a well validated nuclear cardiology technique available in countries with all levels of income, and it enables the evaluation of the extent, severity and localization of myocardial ischaemia, as well as regional wall motion, left ventricular function and measurement of infarct size.

(2) From a clinical point of view, instrumentation and software improvements (mainly new ultrafast cameras and the resolution recovery for iterative reconstruction) allow a significant reduction of acquisition time for an MPI study, with the following advantages:
   (i) Decreased artefacts due to patient motion;
   (ii) Decrease in the radiation dose absorbed by the patient and staff (same or better diagnostic image quality as that obtained with older equipment but with a much lower radiopharmaceutical dose);
   (iii) High count efficiency that allows true stress acquisitions of myocardial function, as well as dynamic acquisition of SPECT tracers, similar to that achievable with PET tracers;
   (iv) Dynamic imaging that potentially opens the door to the quantification of blood flow and coronary flow reserve.

(3) Several MPI findings are associated with a high risk of cardiac events, namely:
   (i) Multiple, extensive and severe perfusion defects;
   (ii) Perfusion defects in the territory of the left anterior descending coronary artery (excluding a mild defect in the apical region);
   (iii) Transient dilation of the left ventricle;
   (iv) Transient increase in right ventricular tracer uptake;
   (v) Increased pulmonary uptake of radiotracer;
   (vi) Transient wall motion abnormalities;
   (vii) Post-ischaemic myocardial stunning (post-stress LVEF lower than rest LVEF).

(4) Optimization of nuclear cardiology practice requires adherence to the following eight best practices:
   (i) Avoid thallium stress testing;
   (ii) Avoid dual isotope testing;
   (iii) Avoid too much technetium;
   (iv) Avoid too much thallium;
   (v) Perform stress-only imaging;
   (vi) Use camera based dose reduction strategies;
   (vii) Use weight based dosing for technetium;
   (viii) Avoid inappropriate dosing that can lead to shinethrough artefacts.

REFERENCES TO CHAPTER 2

[2.1] INTERNATIONAL ATOMIC ENERGY AGENCY, Nuclear Cardiology: Guidance on the Implementation of SPECT Myocardial Perfusion Imaging, IAEA Human Health Series No. 23 (Rev. 1), IAEA, Vienna (2016).

[2.2] ANGER, H.O., Scintillation camera, Rev. Sci. Instrum. **29** (1958) 27–33.

[2.3] GARCIA, E.V., FABER, T.L., Advances in nuclear cardiology instrumentation: Clinical potential of SPECT and PET, Curr. Cardiovasc. Imag. Rep. **2** (2009) 230–237.

[2.4] PATTON, J.A., SLOMKA, P.J., GERMANO, G., BERMAN, D.S., Recent technologic advances in nuclear cardiology, J. Nucl. Cardiol. **14** (2007) 501–513.

[2.5] SHARIR, T., et al., High-speed myocardial perfusion imaging: Initial clinical comparison with conventional dual detector anger camera imaging, J. Am. Coll. Cardiol. Imag. **1** (2008) 156–163.

[2.6] SHARIR, T., et al., 2.09: Validation of quantitative analysis of high-speed myocardial perfusion imaging — Comparison to conventional SPECT imaging, J. Nucl. Cardiol. **15** (2008) 4–5.

[2.7] FUNK, T., KIRCH, D.L., KOSS, J.E., BOTVINICK, E., HASEGAWA, B.H., A novel approach to multipinhole SPECT for myocardial perfusion imaging, J. Nucl. Med. **47** (2006) 595–602.

[2.8] STEELE, P.P., KIRCH, D.L., KOSS, J.E., Comparison of simultaneous dual-isotope multipinhole SPECT with rotational SPECT in a group of patients with coronary artery disease, J. Nucl. Med. **49** (2008) 1080–1089.

[2.9] GARCIA, E.V., FABER, T.L., New trends in camera and software technology in nuclear cardiology, Cardiol. Clin. **27** (2009) 227–236.

[2.10] SHEPP, L.A., VARDI, Y., Maximum likelihood reconstruction for emission tomography, IEEE Trans. Med. Imag. **1** (1982) 113–122.

[2.11] BEN BOUALLÈGUE, F., et al., SPECT myocardial perfusion reserve in patients with multivessel coronary disease: Correlation with angiographic findings and invasive fractional flow reserve measurements, J. Nucl. Med. **56** (2015) 1712–1717.

[2.12] DI CARLI, M.F., HACHAMOVITCH, R., New technology for noninvasive evaluation of coronary artery disease, Circulation **115** (2007) 1464–1480.

[2.13] JAARSMA, C., et al., Diagnostic performance of noninvasive myocardial perfusion imaging using single-photon emission computed tomography, cardiac magnetic resonance, and positron emission tomography imaging for the detection of obstructive coronary artery disease: A meta-analysis, J. Am. Coll. Cardiol. **59** (2012) 1719–1728.

[2.14] GIBBONS, R.J., et al., ACC/AHA 2002 guideline update for exercise testing: Summary article, Circulation **106** (2002) 1883–1892.

[2.15] TRAVAIN, M.I., WEXLER, J.P., Pharmacological stress testing, Semin. Nucl. Med. **29** (1999) 298–318.

[2.16] HENZLOVA, M.J., DUVALL, W.L., EINSTEIN, A.J., TRAVIN, M.I., VERBERNE, H.J., ASNC imaging guidelines for SPECT nuclear cardiology procedures: Stress, protocols, and tracers, J. Nucl. Cardiol. **23** (2016) 606–639.

[2.17] CERQUEIRA, M.D., et al., Standardized myocardial segmentation and nomenclature for tomographic imaging of the heart: A statement for healthcare professionals from the Cardiac Imaging Committee of the Council on Clinical Cardiology of the American Heart Association, Circulation **105** (2002) 539–542.

[2.18] MARCASSA, C., et al., Impact of imaging protocol on left ventricular ejection fraction using gated-SPECT myocardial perfusion imaging, J. Nucl. Cardiol. **24** (2017) 1292–1301.

[2.19] MUT, F., et al., Detection of post-exercise stunning by early gated SPECT myocardial perfusion imaging: Results from the IAEA multi-center study, J. Nucl. Cardiol. **21** (2014) 1168–1176.

[2.20] CHEN, J., et al., SPECT myocardial perfusion imaging for the assessment of left ventricular mechanical dyssynchrony, J. Nucl. Cardiol. **18** (2011) 685–694.

[2.21] ZHOU, W., et al., Development and validation of an automatic method to detect the latest contracting viable left ventricular segments to assist guide CRT therapy from gated SPECT myocardial perfusion imaging, J. Nucl. Cardiol. **25** (2018) 1948–1957.

[2.22] PEIX, A., et al., Gated SPECT myocardial perfusion imaging, intraventricular synchronism, and cardiac events in heart failure, Clin. Nucl. Med. **39** (2014) 498–504.

[2.23] PEIX, A., et al., Stress–rest myocardial perfusion scintigraphy and adverse cardiac events in heart failure patients, MEDICC Rev. **17** (2015) 33–38.

[2.24] WEISS, A.T., et al., Transient ischaemic dilation of the left ventricle on stress thallium-201 scintigraphy: A marker of severe and extensive coronary artery disease, J. Am. Coll. Cardiol. **9** (1987) 752–759.

[2.25] MCLAUGHLIN, M.G., DANIAS, P.G., Transient ischemic dilation: A powerful diagnostic and prognostic finding of stress myocardial perfusion imaging, J. Nucl. Cardiol. **9** (2002) 663–667.

[2.26] WILLIAMS, K.A., SCHNEIDER, C.M., Increased stress right ventricular activity on dual isotope perfusion SPECT: A sign of multivessel and/or left main coronary artery disease, J. Am. Coll. Cardiol. **34** (1999) 420–427.

[2.27] MALONE, J., et al., Justification of diagnostic medical exposures: Some practical issues — Report of an International Atomic Energy Agency consultation, Br. J. Radiol. **85** (2012) 523–538.

[2.28] CERQUEIRA, M.D., et al., Recommendations for reducing radiation exposure in myocardial perfusion imaging, J. Nucl. Cardiol. **17** (2010) 709–718.

[2.29] EINSTEIN, A.J., et al., Current worldwide nuclear cardiology practices and radiation exposure: Results from the 65 country IAEA Nuclear Cardiology Protocols Cross-sectional Study (INCAPS), Eur. Heart J. **36** (2015) 1689–1696.

[2.30] MERCURI, M., et al., Estimating the reduction in the radiation burden from nuclear cardiology through use of stress-only imaging in the United States and worldwide, JAMA Intern. Med. **176** (2016) 269–273.

[2.31] CHANG, S.M., NABI, F., XU, J., RAZA, U., MAHMARIAN, J.J., Normal stress-only versus standard stress/rest myocardial perfusion imaging: Similar patient mortality with reduced radiation exposure, J. Am. Coll. Cardiol. **55** (2010) 221–230.

[2.32] PICCINELLI, M., GARCIA, E.V., Advances in software for faster procedure and lower radiotracer dose myocardial perfusion imaging, Prog. Cardiovasc. Dis. **57** (2015) 579–587.

[2.33] EINSTEIN, A.J., et al., Radiation dose and prognosis of ultra-low-dose stress-first myocardial perfusion SPECT in patients with chest pain using a high-efficiency camera, J. Nucl. Med. **56** (2015) 545–551.

Chapter 3

NUCLEAR CARDIOLOGY: POSITRON EMISSION TOMOGRAPHY

L.J. SHAW, M. DONDI, E. ALEXANDERSON, I. CARVAJAL, V. LARA, J. CARRASCO

3.1. BASIC PRINCIPLES

Positron emission tomography (PET) is a non-invasive technique that employs positron emitting radionuclides labelled to biological molecules, capturing the molecular and cellular events targeted by the metabolic behaviour of the carrier molecule itself. Unlike other imaging techniques, such as computed tomography (CT) or magnetic resonance imaging (MRI), which provide anatomical or structural information, PET captures metabolic and functional information. The radionuclides used in PET decay through the emission of a particle called a positron or beta plus particle (β+). After the positron has been emitted from the parent, it undergoes an annihilation process that begins immediately after the interaction with electrons in the surrounding matter. This reaction results in the production of two annihilation photons, which have 511 keV of energy and are antiparallel and at a 180° angle relative to one another [3.1–3.3].

The interactions of the pair of annihilation photons are detected and provide spatial–temporal information about the biodistribution of the radiopharmaceutical. The acquisition of the image is by coincidence detection, analysing two photons from the same annihilation process with a certain energy (energetic window), both of them arriving within a certain time period (temporal window), but at polar opposites (the photons are antiparallel).

Although PET is widely used in oncology, cardiac PET is emerging as an important modality for the detection of physiologically significant coronary artery disease (CAD) [3.4], for the evaluation of infiltrative diseases (e.g. sarcoidosis), the assessment of myocardial viability and for infective imaging (e.g. endocarditis). PET for the detection of CAD may be combined with CT to collect measures of myocardial perfusion with anatomical findings of obstructive stenosis and atherosclerotic plaque.

Quantification of myocardial blood flow (MBF) is also possible with PET. There is indeed increasing information as to the value of measurement of absolute MBF, at rest and peak hyperaemia, and with the ratio calculation

of coronary flow reserve (CFR). Indeed, PET is considered the gold standard for measuring MBF [3.5]. The ability of PET–CT to non-invasively determine regional MBF at rest and at peak hyperaemia during stress allows the calculation of CFR, which carries important prognostic information independent of rest and stress myocardial perfusion data. CFR is measured in the three main coronary artery territories and as a global measure, and allows for the identification of flow limitations within the epicardial coronary arteries [3.4, 3.5].

PET acquisitions in list mode permit a comprehensive evaluation of several parameters, including perfusion, volumes and left ventricular ejection fraction (LVEF). Quantification software provides analysis of static, gated and dynamic datasets in a single session, facilitating inclusion of all quantitative results for clinical interpretation [3.6]. Finally, dynamic reconstruction of the data allows the computation of absolute regional MBF in $mL \cdot g^{-1} \cdot min^{-1}$ at stress and rest and, consequently, measurement of CFR. CFR is particularly useful in the setting of 'balanced' ischaemia when all the epicardial coronary arteries are involved and static imaging may not identify all the hyperperfused territories [3.6]. CFR is computed as the ratio of MBF at stress divided by rest and can be obtained within seconds with minimal user interaction [3.6].

3.1.1. Hardware

PET equipment uses rings of detectors coupled to photomultiplier tubes. In general, the diameter of the detector rings is 80–90 cm, which is suitable for clinical imaging. The intrinsic spatial resolution of the detectors is about 3 mm, while the spatial resolution of the system is approximately 4.5 mm near the centre of the field of view.

PET has improved in 3-D imaging and the sensitivity of a PET device is at least two to three orders of magnitude greater than that of conventional cardiac single photon emission computed tomography (SPECT). Thus, the advantages of PET include an increase in the resolution and precision of the image, allowing for improved image quantification and better image quality.

3.1.2. Software

A recent advance in reconstruction algorithms is the 3-D modelling of the maps of the punctual dispersion function. In addition, reconstruction algorithms of the time of flight have been implemented, so the information from annihilation photons with a different time of arrival to the detectors can be used to its fullest. This information is used during the image reconstruction process to predict the exit of the signal. With this method, the effective resolution diminishes to 2 mm, which in turn brings better image quality and contrast.

3.2. CARDIAC PET RADIOTRACERS[1]

There are several PET myocardial tracers, including ^{82}Rb–RuCl, ^{13}N ammonia, ^{15}O water and flurpiridaz, which may be used to evaluate myocardial perfusion and assess blood flow quantitation. To assess metabolism and viability, ^{11}C acetate and ^{18}F-fluorodeoxyglucose (^{18}F-FDG) may be used.

3.2.1. ^{82}Ru

Rubidium-82, with a physical half-life of 1.25 min, can be produced by an ^{82}Sr/^{82}Rb generator. It behaves as a potassium analogue through active transport by the Na^+/K^+ adenosine triphosphatase pump. The positron range of ^{82}Rb is 8.1 mm, resulting in low image resolution. The myocardial extraction fraction of ^{82}Rb is about 65%, and its more prominent non-linear myocardial uptake with increasing blood flow compared with ^{13}N ammonia results in a relatively lower myocardial contrast resolution than with ^{13}N ammonia [3.7–3.10]. Nonetheless, owing to its ease of production and relatively lower cost, ^{82}Rb is the most commonly used PET radioisotope for myocardial imaging with the most robust evidence with regard to the detection of obstructive CAD and the prediction of major adverse CAD events.

3.2.2. ^{13}N ammonia

Nitrogen-13 ammonia, with a physical half-life of 9.96 min, requires an on-site cyclotron for its production. It is taken up by the myocardium by passive free diffusion across cell membranes as ammonia (NH_3), where it equilibrates with its charged form, ammonium (NH_4^+), and is trapped inside the cell by conversion through glutamine synthase to ^{13}N glutamine. The positron range of ammonia is 2.53 mm, resulting in an intermediate high image resolution tracer. The myocardial extraction fraction is approximately 80% and is linear with increasing blood flow. The combination of the high first pass myocardial extraction fraction and the relatively long physical half-life may account for the high contrast resolution, which permits visual and semiquantitative evaluation of myocardial perfusion abnormalities on stress and rest images. Nitrogen-13 ammonia has been validated and is used clinically for the measurement of rest and stress myocardial perfusion and calculation of CFR [3.9, 3.10].

[1] Based on Ref. [3.7].

3.2.3. ^{15}O water

Oxygen-15 water, with a physical half-life of 2.09 min, requires an on-site cyclotron for production. Myocardial uptake is through passive diffusion; it has a 4.14 mm positron range resulting in an intermediate image resolution. The myocardial extraction fraction is close to 100%. Nevertheless, myocardial perfusion image quality with ^{15}O water is suboptimal because of low count density, related to the short physical and biological half-life of this tracer. Thus, the measurement of regional or segmental myocardial perfusion abnormalities is not possible owing to issues with image quality. However, the measurement of rest and stress MBF and CFR is possible [3.9, 3.10].

3.2.4. Flurpiridaz

Flurpiridaz (^{18}F fluorobenzyl triphenyl phosphonium) binds with high affinity to the mitochondrial complex I of the electron transport chain. This tracer, currently evaluated in Phase III studies [3.11], shows a 94% flow independent extraction fraction, implying a linear relationship between uptake and MBF, an important attribute for stress MBF measurements with an excellent image quality and high target (i.e. heart) to background ratio [3.11–3.15]. The long physiological half-life of ^{18}F (110 min) permits its distribution as a single unit dose on a daily basis by delivery from a central production site, which ensures reduction of the tracer cost. Moreover, it allows for the application of the perfusion agent during a treadmill exercise test, as well as with vasodilator stress.

3.2.5. ^{18}F-FDG

Currently, the gold standard for assessing myocardial viability is ^{18}F-FDG. As an analogue of glucose, it is taken up by myocytes via facilitated diffusion through a sarcolemma glucose transporter, followed by phosphorylation by a hexokinase to ^{18}FDG-6-phosphate. After phosphorylation, the molecule is trapped intracellularly without undergoing further metabolism. As a result, ^{18}F-FDG is effectively fixed in the myocardium in a manner proportional to the transport rate of the glucose transporter and the activity of hexokinase [3.16, 3.17].

3.3. IMAGING PROTOCOLS

3.3.1. MPI and MBF quantification

Dilsizian et al. [3.18] report that patient preparation is similar to the preparation for stress/rest myocardial SPECT imaging. This includes an overnight fast of 6 h or more, avoidance of caffeinated beverages for at least 12 h and avoidance of theophylline containing medications for 48 h [3.18, 3.19]. For imaging, Dilsizian et al. [3.18] report that the patient should be in a supine position, with the arms out of the camera field of view. This can be tolerated by nearly all patients, provided there is some method to support the patient's arms. Alternatively, an overhead bar has often been used as a handhold for arm support.

Owing to the shortest half-lives of PET tracers, such as and ^{15}O and ^{82}Rb, there is no need to wait for radioactive decay between rest and stress imaging, so the patient generally remains in the scanner throughout the rest–stress imaging protocol [3.7, 3.18]. A standard cardiac PET–CT protocol is shown in Fig. 3.1.

For ^{82}Rb, imaging starts with a CT scout and transmission CT for attenuation correction purposes. A rapid infusion, over about 10–30 s, follows the CT scan, while the patient is at rest. The dose (750–1500 MBq) is calculated based on body weight (e.g. 10–15 MBq/kg). Acquisition in list mode begins immediately and lasts 6–8 min (14 × 5 s, 6 × 10 s, 3 × 20 s, 3 × 30 s, 1 × 90 s) [3.7, 3.20, 3.21]. Pharmacological stress is then administered, without the need for any delay, while the patient remains in the scanner. To this purpose, immediately after completion of the rest study, an intravenous vasodilator infusion is administered. At peak hyperaemia, a second dose of ^{82}Rb (750–1500 MBq) is injected, and images

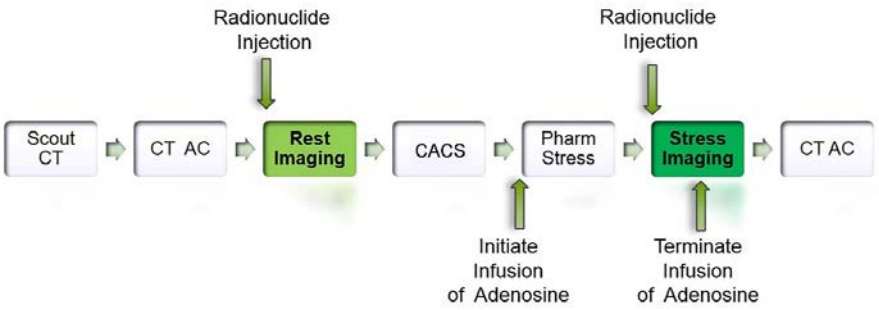

FIG. 3.1. The standard cardiac PET–CT protocol includes the scout of the CT, attenuation correction CT (labelled 'CT AC' in the figure), followed by image acquisition of the rest/stress PET portion. In addition, if clinically indicated, either coronary artery calcium score (CACS) or coronary computed tomography angiography (CCTA) can be acquired.

are recorded in the same manner as during rest imaging. The whole acquisition is generally electrocardiography and respiration gated and can be completed in less than 30 min.

For ^{15}O water, the imaging protocol consists of injection of 350–1100 MBq of the tracer at rest, followed by dynamic imaging for 4–5 min (14 × 5 s, 3 × 10 s, 3 × 20 s, 4 × 30 s). Pharmacological stressor administration may begin shortly after the completion of rest image acquisition. Again, 350–1100 MBq of the tracer is injected, this time at peak hyperaemia, followed by dynamic imaging for 4–5 min [3.7, 3.19, 3.22].

For ^{13}N ammonia, the acquisition time is longer (10–20 min), and a 30–40 min delay between the rest and stress study is typically required to allow for isotope decay. Less activity is injected (350–750 MBq) to minimize radiation dose. A ^{13}N ammonia standard protocol involves an injection of 740 MBq at rest, followed by a 10 min image acquisition protocol. Thirty minutes later, pharmacological stress is administered with a second injection of 740 MBq of ^{13}N ammonia and images are acquired [3.7]. For the measurement of absolute flow, dynamic acquisition from the time of injection is required. Uptake is relatively rapid (often complete within 90 s), and radioactive decay (10 min half-life) is fast [3.7, 3.19, 3.22]. Figure 3.2 shows examples of normal MBF and Fig. 3.3 of abnormal MBF. The ability of MBF quantification to show triple vessel disease revealed by a reduction of CFR in all three epicardial vessel territories is notable. This is a definite improvement in comparison with SPECT myocardial perfusion imaging (MPI).

3.3.2. Myocardial viability and sarcoid imaging

The study of viability with PET is based on perfusion–metabolism mismatch. To differentiate scar tissue from normal myocardium, patients scheduled for a viability study using ^{18}F-FDG PET should also be submitted to MPI and, if PET perfusion agents are not available, the ^{18}F-FDG images can be interpreted in conjunction with SPECT perfusion images. Perfusion images acquired using a suitable PET perfusion agent are acquired with the same PET system and can be displayed with similar parameters as the ^{18}F-FDG images. In cases of cardiac sarcoid imaging, the same concept applies, as it does to studies performed to identify changes of active sarcoid granulomas to normal myocardium, or progression to scar tissue in response to therapy [3.20, 3.21]. Exclusion of CAD is also important, as left ventricular dyssynergia may reflect either a hibernating myocardium or myocardial inflammation [3.23]. Li et al. [3.16] find that to maximize myocardial uptake, ^{18}F-FDG is normally administered after an oral glucose load or insulin clamp. Acipimox, which decreases serum fatty acids by inhibiting lipolysis and indirectly stimulates cardiac ^{18}F-FDG uptake, is an alternative clamp option.

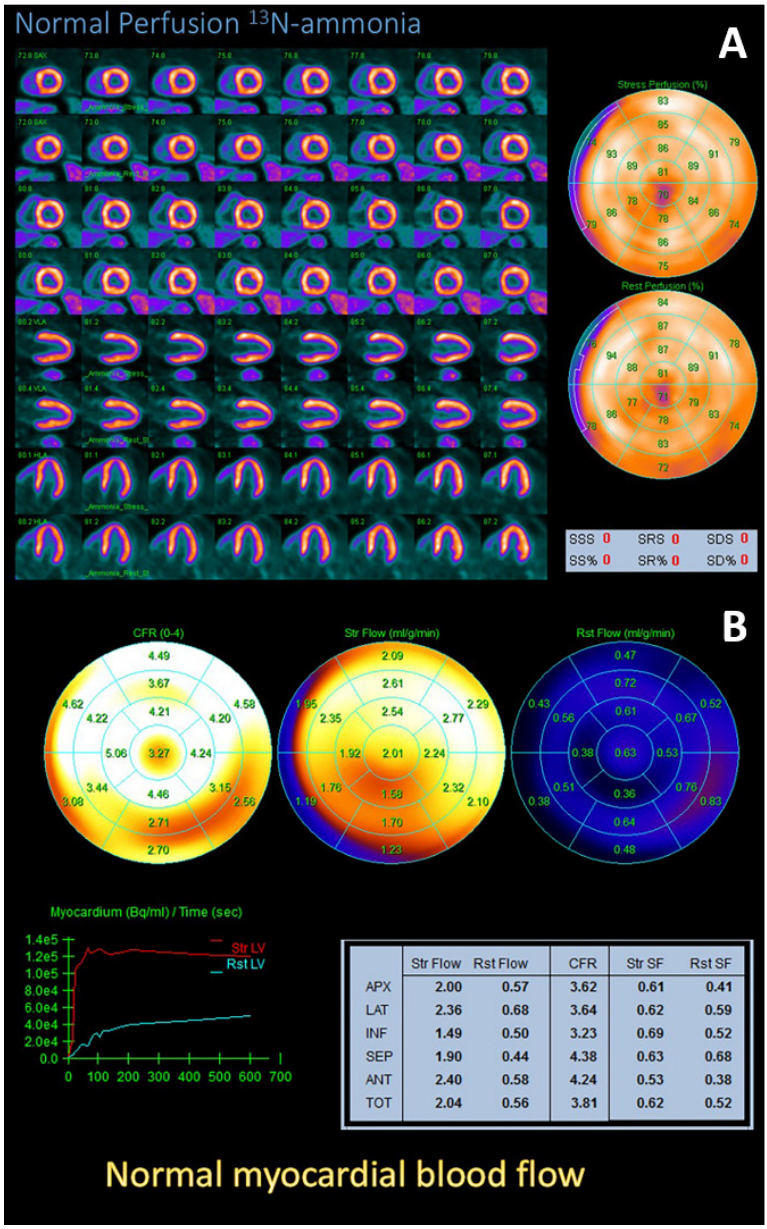

FIG. 3.2. Normal MPI with ^{13}N ammonia PET–CT. (A) The short and long axis of tomographic slides and polar map show no perfusion defect. Semiquantitative scoring system reports score zero for all parameters. (B) Polar maps and time–activity curves of absolute regional MBF in mL·g^{-1}·min^{-1} at stress and rest.

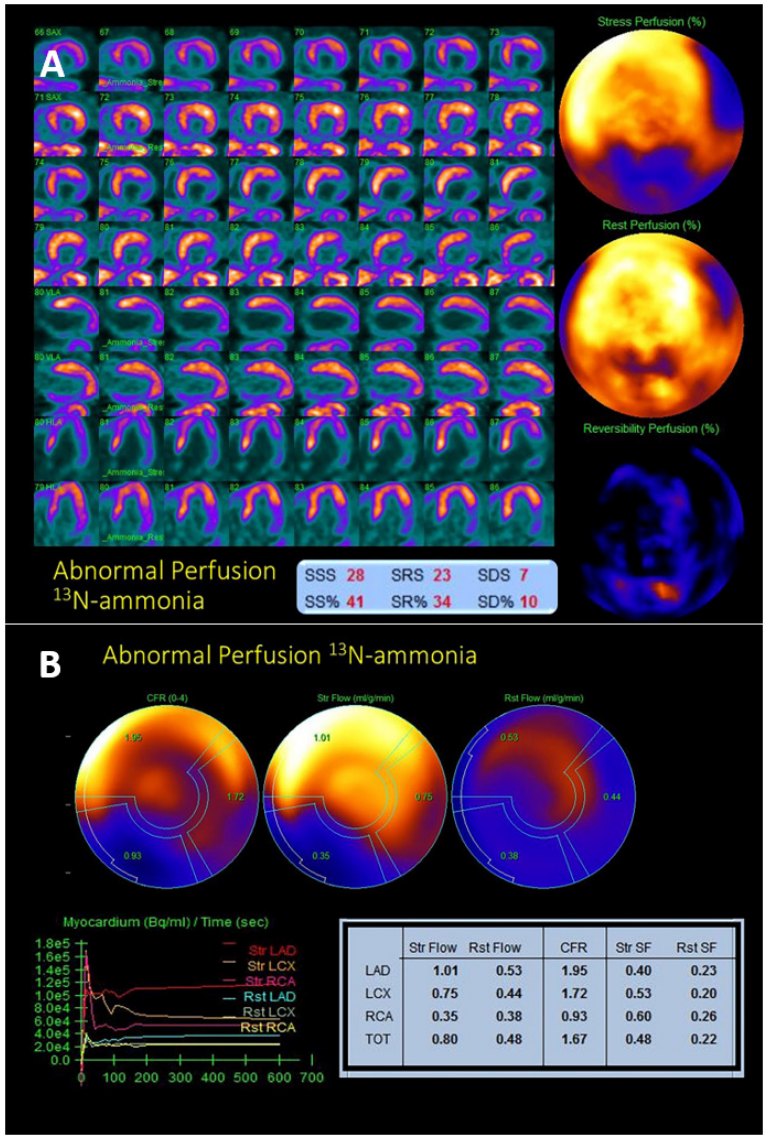

	Str Flow	Rst Flow	CFR	Str SF	Rst SF
LAD	1.01	0.53	1.95	0.40	0.23
LCX	0.75	0.44	1.72	0.53	0.20
RCA	0.35	0.38	0.93	0.60	0.26
TOT	0.80	0.48	1.67	0.48	0.22

FIG. 3.3. Abnormal perfusion detected with ^{13}N ammonia PET–CT. (A) The study shows an abnormal myocardial perfusion with severe inferior wall defect with moderate reversibility. The same pattern is shown for the lateral wall where the defect is only partially reversible, with a posterolateral area of possible limited scar. The summed difference score is 10%. (B) Quantification shows severely diminished MBF in the territory of the right coronary artery with the lower CFR. The left circumflex artery and the left anterior descending artery are also affected. The study is compatible with triple vessel disease.

Viability studies with ^{18}F-FDG are combined with MPI (using ^{13}N ammonia, ^{82}Rb or ^{99m}Tc labelled compounds) to quantify the mismatch between myocardial perfusion and ^{18}F-FDG metabolic activity. In the fasting state, the normal myocardium preferentially utilizes free fatty acids and ^{18}F-FDG myocardial uptake is low and heterogeneous [3.16]. Clinically, this is defined as a myocardial segment with preserved glucose utilization within hypoperfused or dysfunctional myocardium (flow–metabolism mismatch) [3.16]. Whereas uptake of ^{18}F-FDG indicates viability, lack of uptake could either indicate non-viable tissue or viable tissue that was utilizing substrates other than glucose. The aim of ^{18}F-FDG imaging is the identification of viable myocardium. By comparison, a non-viable segment will exhibit a concordant reduction in myocardial perfusion and ^{18}F-FDG uptake (matched defect) [3.16, 3.24].

According to a meta-analysis, the extent of viable myocardium leading to improved survival with revascularization over medical therapy was estimated to be 25.8% (95% CI: 16.6–35.0%) using ^{18}F-FDG-perfusion mismatch overall (22.5% for PET with ^{18}F-FDG/NH_3, 29.2% for PET with ^{18}F-FDG/^{99m}Tc) [3.25]. An example of a viability study using ^{18}F-FDG and ^{99m}Tc tetrofosmin is shown in Fig. 3.4.

3.3.3. Coronary artery calcium scoring with PET–CT

The diffusion of hybrid PET–CT scanners allows for the identification of the presence and the extent of coronary artery calcium within the epicardial coronary arteries [3.26]. The extent of coronary artery calcium reflects the atherosclerotic plaque burden and is an excellent means to risk stratify patients for major adverse CAD events. The coronary artery calcium score (CACS) is calculated as the product of the area of coronary artery calcium plaque and the density of the plaque (measured in Hounsfield Units). Other factors to consider are the number of involved vessels, the location of the plaques (e.g. proximal left anterior descending coronary artery) and the size and number of lesions. All these are also particularly helpful when PET findings are integrated. Table 3.1 reports a summary of CAD event rates based on CACS.

3.3.4. Display of PET perfusion rest–stress and perfusion–metabolism images

Normalization of stress perfusion with resting perfusion images is commonly performed by using the myocardial maximal intensity pixel (MIP) value. Each perfusion study is then normalized to its own maximum. The metabolism images are normalized to the counts in the same myocardial region on the resting perfusion images [3.6, 3.23–3.25].

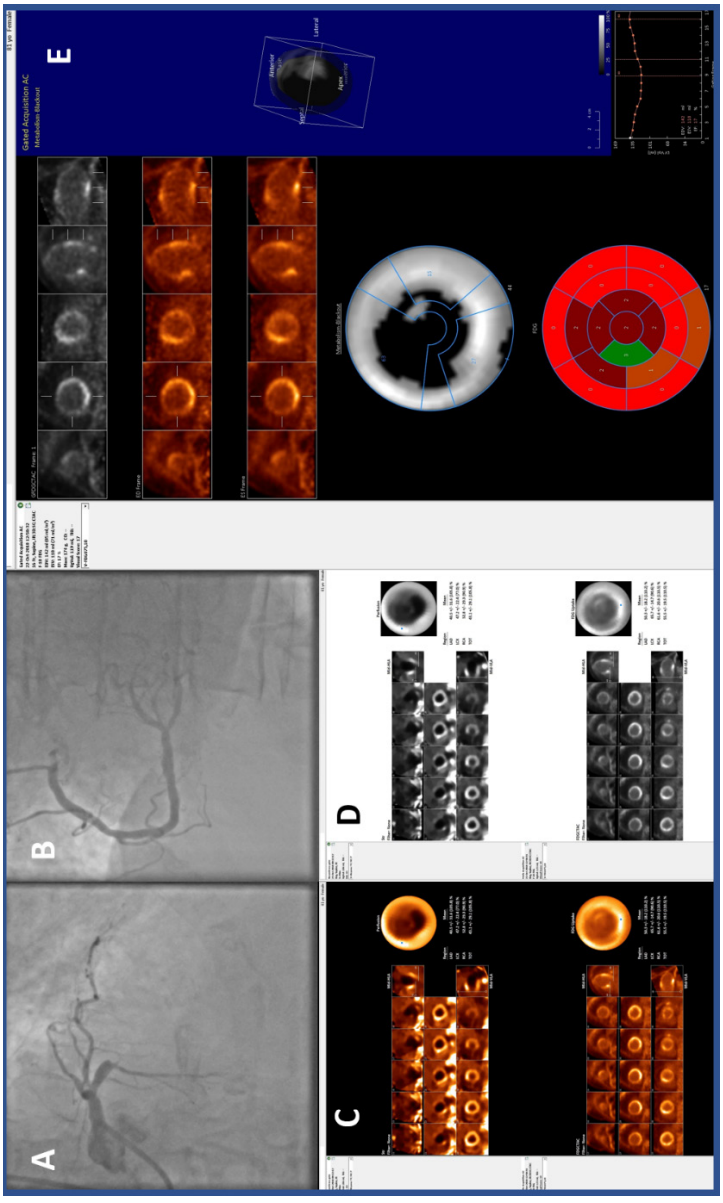

FIG. 3.4. Viability study with SPECT MPI and ^{18}F-FDG PET. Coronary angiography showing (A) a proximal occlusion of the left anterior descending coronary artery and (B) patent right coronary artery. First study rest MPI with ^{99m}Tc tetrofosmin showing absent perfusion in the left anterior descending coronary artery territory ((C) and (D), upper rows). The second study with ^{18}F-FDG PET after glucose load shows some degree of preserved viability in the left anterior descending coronary artery territory second study ((C) and (D), lower rows). Gated PET (E) showing severe left ventricular dysfunction as seen from the time–activity curve ((E), lower right corner).

TABLE 3.1. SUMMARY OF CARDIOVASCULAR RISK BASED ON CORONARY ARTERY CALCIUM SCORE
(see table 2 of Ref. [3.27])

CACS	Framingham Risk Score equivalent	10 year event rate (%)
0	Very low	1.1–1.7
1–100	Low	2.3–5.9
101–400	Intermediate	12.8–16.4
401–999	High	22.5–28.6
≥1000	Very high	>37

Dilsizian et al. [3.18] report that it is necessary to examine the transaxial, coronal and sagittal views (i.e. the not yet reoriented images) to assess the alignment for the attenuation correction images (rest and stress perfusion and metabolism). If the images are not correctly aligned because of patient or cardiac motion, this may cause serious image artefacts, especially when only one set of attenuation correction images has been applied to all emission images for attenuation correction [3.18].

For the interpretation and comparison of perfusion and metabolism images, slices of all datasets should be displayed aligned and adjacent to one another [3.18]. Polar maps of PET rest and stress perfusion images and ^{18}F-FDG metabolic images are commonly used for visual and semiquantitative assessment. These polar maps, while useful, "should not be considered a substitute for the examination of the standard short-axis and long-axis cardiac tomographic slices" [3.18].

3.3.5. Elements of a comprehensive cardiac PET report

Accurate reporting is one of the most critical steps in cardiac imaging. The report is the final product of a complex process, involving substantial human and material resources. Quality reports are typically concise and include all the relevant elements for the referring physician:

(a) Patient demographics and indications for the study.

(b) Methods:
  (i) Technique and radiotracer dose.
  (ii) Stress test information, if applicable.
  (iii) Metabolic preparation (in case of viability studies).
  (iv) Technique for attenuation correction and calcium scoring (when applicable).
(c) MPI findings:
  (i) Qualitative and semiquantitative estimates of rest and stress perfusion, including the presence or absence of reversible, partially reversible or fixed defects and their size, severity and location.
  (ii) For ease of interpretation, the percentage of abnormally perfused myocardium, based on segmental scoring.
(d) MPI and ^{18}F-FDG findings:
  (i) Qualitative and semiquantitative estimates of ^{18}F-FDG uptake in all segments, but particularly those with abnormal rest perfusion and contractile motion.
  (ii) Description of perfusion–metabolism pattern (match, mismatch, non-transmural match).
(e) Quantification of absolute blood flow at rest and stress, reporting CFR by vascular territory (i.e. right coronary artery, left anterior descending and left circumflex territories) and globally.
(f) From the gated study:
  (i) Left ventricular volumes.
  (ii) Regional wall motion.
  (iii) Rest and peak stress (if available) LVEF.
(g) CACS, if applicable:
  (i) CACS.
  (ii) Location, size, and extent of coronary artery calcium within each vascular territory to aid in the interpretation of MPI and CFR findings.
(h) Conclusions should mention a comprehensive interpretation of myocardial perfusion results in conjunction with stress electrocardiogram changes, rest and stress ejection fraction and the presence or absence of transient ischaemic dilation of the left ventricle, as well as CACS:
  (i) For MPI (perfusion):
    — Overall abnormal perfusion findings (ischaemia, scar, or partial viability and peri-infarction ischaemia) for each vascular territory;
    — Territories with reduced CFR should also be identified.
  (ii) For MPI and ^{18}F-FDG (viability):
    — Comprehensive interpretation of ^{18}F-FDG findings in conjunction with perfusion data (scar, ischaemia, hibernation

or combined findings) for each affected vascular territory or myocardial segment;
— A statement about the estimated likelihood of contractile recovery following revascularization, based on PET findings.

3.4. KEY MESSAGES

(1) PET is a non-invasive technique providing information based on the use of positron emitting radionuclides.
(2) All PET scans are acquired with CT as a hybrid technique and may provide both anatomical and functional information with the advantage of image correction from attenuation and dispersion in PET scans using CT images.
(3) Novel high resolution PET has been implemented resulting in improved image resolution with better image quality and contrast.
(4) Improvements in hardware make the sensitivity of PET 2–3 times higher than conventional SPECT, increasing the value of image quantification.
(5) Cardiac PET radiotracers have a short physical half-life and are used to evaluate physiological abnormalities of myocardial perfusion, CFR and viability.
(6) PET is a very well established technique allowing the quantification of absolute blood flow and CFR. Both measurements increase the diagnostic and prognostic power of PET perfusion imaging.

REFERENCES TO CHAPTER 3

[3.1] BAILEY, D.L., TOWNSEND, D.W., VALK, P.E., MAISEZ, M.N. (Eds), Positron Emission Tomography: Basic Sciences, Springer (2005).
[3.2] INTERNATIONAL ATOMIC ENERGY AGENCY, Cyclotron Produced Radionuclides: Principles and Practice, Technical Reports Series No. 465, IAEA, Vienna (2008).
[3.3] INTERNATIONAL ATOMIC ENERGY AGENCY, Cyclotron Produced Radionuclides: Physical Characteristics and Production Methods, Technical Reports Series No. 468, IAEA, Vienna (2009).
[3.4] SCHINDLER, T.H., Cardiac PET/computed tomography applications and cardiovascular outcome, PET Clin. **10** (2015) 441–459.
[3.5] CAMICI, P.G., RIMOLDI, O.E., The clinical value of myocardial blood flow measurement, J. Nucl. Med. **50** (2009) 1076–1087.
[3.6] SLOMKA, P., BERMAN, D.S., ALEXANDERSON, E., GERMANO, G., The role of PET quantification in cardiovascular imaging, Clin. Transl. Imaging **2** (2014) 343–358.

[3.7] MADDAHI, J., PACKARD, R.R.S., Cardiac PET perfusion tracers: Current status and future directions, Semin. Nucl. Med. **44** (2014) 333–343.

[3.8] BERGMANN, S.R., HACK, S., TEWSON, T., WELCH, M.J., SOBEL, B.E., The dependence of accumulation of $^{13}NH_3$ by myocardium on metabolic factors and its implications for quantitative assessment of perfusion, Circulation **61** (1980) 34–43.

[3.9] KRIVOKAPICH, J., HUANG, S.C., PHELPS, M.E., MACDONALD, N.S., SHINE, K.I., Dependence of $^{13}NH_3$ myocardial extraction and clearance on flow and metabolism, Am. J. Physiol. **242** (1982) 536–542.

[3.10] SCHINDLER, T.H., et al., Quantitative assessment of myocardial blood flow: Clinical and research applications, Semin. Nucl. Med. **44** (2014) 274–293.

[3.11] WIYAPORN, K., et al., Optimization of imaging protocols for myocardial blood flow (MBF) quantification with ^{18}F-flurpiridaz PET, Phys. Med. **42** (2017) 127–134.

[3.12] HUISMAN, M.C., et al., Initial characterization of an ^{18}F-labeled myocardial perfusion tracer, J. Nucl. Med. **49** (2008) 630–636.

[3.13] YU, M., et al., Assessment of ^{18}F-labeled mitochondrial complex I inhibitors as PET myocardial perfusion imaging agents in rats, rabbits, and primates, Eur. J. Nucl. Med. Mol. Imaging **36** (2009) 63–72.

[3.14] NEKOLLA, S.G., et al., Evaluation of the novel myocardial perfusion positron-emission tomography tracer ^{18}F-BMS-747158-02: Comparison to ^{13}N-ammonia and validation with microspheres in a pig model, Circulation **119** (2009) 2333–2342.

[3.15] SHERIF, H.M., et al., Simplified quantification of myocardial flow reserve with flurpiridaz F 18: Validation with microspheres in a pig model, J. Nucl. Med. **52** (2011) 617–624.

[3.16] LI, Y., ZHANG, W., WU, H., LIU, G., Advanced tracers in PET imaging of cardiovascular disease, Biomed. Res. Int. (2014) 504532.

[3.17] TAWAKOL, A., et al., In vivo ^{18}F-fluorodeoxyglucose positron emission tomography imaging provides a noninvasive measure of carotid plaque inflammation in patients, J. Am. Coll. Cardiol. **48** (2006) 1818–1824.

[3.18] DILSIZIAN, V., et al., ASNC imaging guidelines/SNMMI procedure standard for positron emission tomography (PET) nuclear cardiology procedures, J. Nucl. Cardiol. **23** (2016) 1187–1226.

[3.19] DEPUEY, E.G., GARCIA, E.V. (Eds), Updated Imaging guidelines for nuclear cardiology procedures: Part 1, J. Nucl. Cardiol. **8** (2001).

[3.20] CHAREONTHAITAWEE, P., et al., Joint SNMMI–ASNC expert consensus document on the role of ^{18}F-FDG PET/CT in cardiac sarcoid detection and therapy monitoring, J. Nucl. Cardiol. **24** (2017) 1341–1353.

[3.21] SKALI, H., SCHULMAN, A.R., DORBALA, S., ^{18}F-FDG PET/CT for the assessment of myocardial sarcoidosis, Curr. Cardiol. Rep. **15** (2013) 352.

[3.22] EL FAKHRI, G., et al., Reproducibility and accuracy of quantitative myocardial blood flow assessment with ^{82}Rb PET: Comparison with ^{13}N-ammonia PET, J. Nucl. Med. **50** (2009) 1062–1071.

[3.23] HULTEN, E., et al., Cardiac sarcoidosis: State of the art review, Cardiovasc. Diag. Ther. **6** (2016) 50–63.

[3.24] SLART, R.H., et al., Imaging techniques in nuclear cardiology for the assessment of myocardial viability, Intern. J. Cardiovasc. Imag. **22** (2006) 63–80.

[3.25] INABA, Y., CHEN, J.A., BERGMANN, S.R., Quantity of viable myocardium required to improve survival with revascularization in patients with ischemic cardiomyopathy: A meta-analysis, J. Nucl. Cardiol. **17** (2010) 646–654.

[3.26] BRODOV, Y., et al., Combined quantitative assessment of myocardial perfusion and coronary artery calcium score by hybrid ^{82}Rb PET/CT improves detection of coronary artery disease, J. Nucl. Med. **56** (2015) 1345–1350.

[3.27] HECHT, H.S., Coronary artery calcium scanning: Past, present, and future, J. Am. Coll. Cardiol. Cardiovasc. Imag. **8** (2015) 579–596.

Chapter 4

ECHOCARDIOGRAPHY

X. ZHOU, G. HONG, M.A. VANNAN

Echocardiography is the most commonly performed test worldwide for the diagnostic and prognostic assessment of a range of cardiac diseases [4.1]. It combines safety and a relatively low cost. Due to its ease of implementation and the structural and haemodynamic information it provides, echocardiography has become an attractive first test for almost any suspected cardiac disease. Doppler echocardiography offers haemodynamic data often comparable to those obtained with invasive approaches. However, the current challenge is to ensure an appropriate use of these easily applied techniques. This chapter provides a brief overview on the fundamental techniques of echocardiography.

4.1. PHYSICS OF ECHOCARDIOGRAPHY

Echocardiography utilizes ultrasound, which has a frequency greater than 20 000 cycles per second (i.e. beyond the hearing spectrum). Several principles of ultrasound physics are involved in the creation of an image that can be used for clinical applications. An ultrasound can be mustered into a beam and directed towards a target of a defined density and stiffness. As ultrasound propagates through tissue, it causes consecutive waves of compression and rarefaction of the particles encountered on its line of propagation. The sum of one compression and rarefaction comprises one cycle. When an ultrasound meets border zones between objects of different composition, it is partly reflected (i.e. returned towards the source), refracted (i.e. directed at a different angle to continue through the target) and attenuated (i.e. continues to travel straight through the medium but part of it is absorbed as it penetrates the object). A sound is characterized by its wavelength (distance between two consecutive waves), frequency (number of wavelengths per unit of time) and amplitude (width between the peak and trough of a single wave). The velocity of propagation of ultrasound is the product of frequency and wavelength ($v = f \lambda$), thus frequency and wavelength are inversely correlated: the higher the frequency the shorter the wavelength (see Fig. 4.1). This is important for image quality and resolution (i.e. clarity of details). A higher frequency sound travels a shorter distance than a lower frequency sound. Hence for near objects for which a high image resolution is desired (e.g. the details of the subendocardial space in intravascular ultrasound imaging), an ultrasound with high frequency and

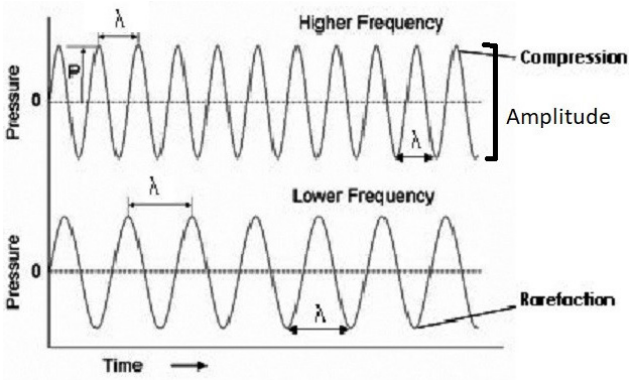

FIG. 4.1. Schematic representation of ultrasound waves and their travel distance, depending on wavelength and frequency. Note: λ — wavelength; P — pressure.

short wavelength is used, while the opposite is true for distant or deeper objects (e.g. imaging the heart in a patient with emphysema).

The velocity of propagation of ultrasound is also directly proportional to the stiffness and indirectly proportional to the density of a medium. The latter is also known as impedance (i.e. resistance) of a medium. As a result, sound travels faster in bone that is stiffer than fat tissue or water. However, bone attenuates (absorbs, scatters, reflects) a sound more than soft tissue does. Consequently, sound travels more quickly in bone but only for a short distance.

The amplitude of ultrasound is a measure of the strength of the signal represented by its ability to compress and rarefy tissue particles and is measured in decibels (dB). Power is a measure of the transfer of energy by the ultrasound to the medium it traverses and is measured in watts (W) over a given area (e.g. W/cm^2). Power is the equivalent of loudness, and as the ultrasound is attenuated while traveling through tissue, it slowly loses its intensity or power.

The transducer is an essential part of the echocardiographic instrumentation. The transducer is made of piezoelectric crystals that vibrate and produce an ultrasound when electricity is applied to them. Similarly, the returning waves are converted to an electrical signal that is sent to the computer to generate an image.

As the ultrasound travels through media of different composition, it is reflected by objects and surfaces larger than its wavelength and produces what are known as specular echoes. A typical example would be the reflection of sound by a valve leaflet. Other reflecting structures, smaller than the ultrasound wavelength, cause the ultrasound to be diffracted and scattered in multiple directions, causing a substantial reduction in the signal returning to the transducer. These are called scattered echo, and a typical example is the echo produced by the myocardial fibres.

As the ultrasound leaves the transducer, it is neatly packed into a tubular beam that represents the near field for imaging. Eventually, the beam diverges into the far field, where the image quality decreases due to the greater scatter and refraction. Since the diameter of the transducer surface is directly proportional to the length of the near field, and the ultrasound frequency indirectly proportional, an ideal transducer could be conceived as one with a large surface capable of emitting a high frequency ultrasound. The trade offs are that the space between ribs may not permit the use of a large surface transducer and — discussed above — the higher the frequency, the lower the penetration of sound into tissue. Manufacturers address these divergent needs by inserting a lens at the tip of the transducer or by building the piezoelectric crystal array in a concave shape. Both of these approaches aim at improving image quality by focusing the ultrasound beam on the near field.

The most frequently used echocardiographic mode is B mode, where B stands for brightness. B mode echocardiography is a 2-D display of echoreflective structures where the intensity of the reflected ultrasound is converted to a certain degree of brightness for video display. B mode is used for both M mode and 2-D imaging. Previously, only the amplitude of the returning ultrasound signals was used to detect cardiac structures. This method was called A mode echocardiography and is a 1-D representation of the structures, with the amplitude of the returning signal being proportional to the intensity of the signal reflected from an interface. A mode is now obsolete. In M mode imaging, the motion of structures towards and away from the ultrasound transducer is shown in one axis. The temporal changes in the structures are displayed along the perpendicular axis. In current clinical practice, a combination of B mode and M mode echocardiography is used.

4.2. 2-D AND 3-D ECHOCARDIOGRAPHY

Routinely performed B mode echocardiography is a 2-D representation of a structure and changes within it over time. The structures displayed are those along the path of the transmitted ultrasound beam. The beam is planar with minimal thickness, so that the image obtained is a representation of the structure in a single plane. Using an ultrasound beam that has a greater thickness to include all the structures in the region yields a volume image. This is called 3-D echocardiography and with it, all structures within the ultrasound beam can be seen (see Fig. 4.2). Currently, 2-D echocardiography is the universal standard. There are distinct advantages of 3-D echocardiography compared with 2-D, and this will likely result in increased usage in the foreseeable future.

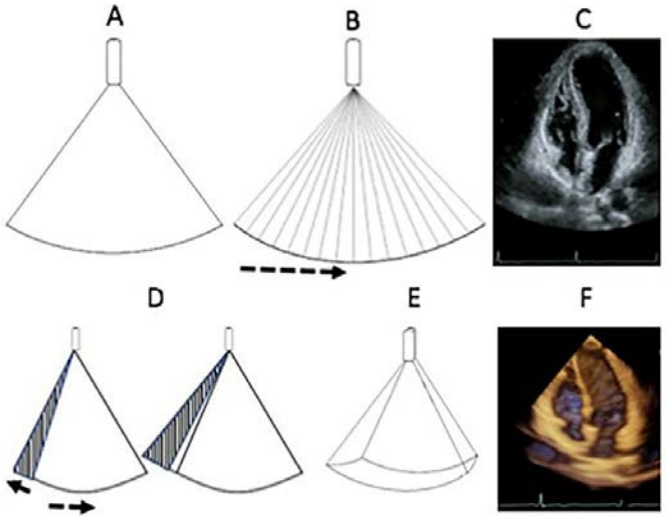

FIG. 4.2. 2-D and 3-D echocardiography. (A, B) A narrow beam of ultrasound is swept across various planes and a 2-D image of the cardiac chambers is rendered in C. (D, E) In 3-D echocardiography, a beam with greater thickness is used to include all the structures within a certain volume, rendering the image in F.

4.3. DOPPLER ECHOCARDIOGRAPHY

In Doppler echocardiography, ultrasound waves are used to measure the speed and direction of blood flow in the heart chambers, across cardiac valves and in blood vessels. The target is the moving red blood cells in all these locations. Sound waves are transmitted from the ultrasound transducer towards the target (red blood cells) at a certain frequency, and these waves impinge on the target and return at a different frequency to the transducer. The movement of the red blood — the flow — may be perfectly parallel to the incident ultrasound waves or the angle may not be perfectly parallel to the transmitted ultrasound waves and there may be an angle of incidence.

4.3.1. Spectral Doppler imaging

The difference in the transmitted and received frequencies (Doppler shift) relates to the velocity of the target and the angle between the ultrasound wave and the moving target. Spectral Doppler imaging depicts the velocity, timing and direction of flow (signals above the baseline represent flow towards the transducer and below). There are three types of Doppler imaging commonly used in clinical practice [4.2].

4.3.1.1. Pulsed wave Doppler imaging

Pulsed wave Doppler imaging is a method in which pulses of ultrasound waves are sent at a certain frequency called pulse repetition frequency. After a single transmission, the reflected sound waves from different targets at different depths arrive back to the transducer at different times. After these are received, another pulse of ultrasound is transmitted and the process is repeated. Since the speed of ultrasound in tissue is known, the location of the reflectors can be determined so that flow velocity at a specific site can be ascertained. The site of interrogation is where the sample volume is placed by the observer. Pulsed wave Doppler imaging can measure velocities only up to a maximum value, which is usually one half of the pulse repetition frequency (Nyquist limit) or typically a maximum of 2 m/s. Velocities beyond this maximum are usually displayed as aliased signals. The pulse repetition frequency varies inversely with the depth of the sample volume, so that the closer the sample volume is to the transducer, the higher the velocity that can be recorded by the pulsed wave. The pulsed wave spectrum shows the dispersion of velocities with a wider dispersion in the centre (darker) and narrower dispersion at the outer edges (brighter), which also represent the most frequent (modal) velocities at the site of interrogation. Pulsed wave Doppler imaging is used to measure low velocity laminar flows at specific sites and is commonly used for the measurement of stroke volume (from which valvular regurgitant volume and orifice area can be computed) and shunt flow volumes. If applied to tissue imaging, it is useful to assess ventricular diastolic function.

4.3.1.2. Continuous wave Doppler imaging

In continuous wave Doppler imaging, the transducer emits and receives ultrasound continuously and not in sequence. Blood flow velocities all along the ultrasound path are depicted and there is no limit to the maximum velocity that can be resolved. There is no Nyquist limit. The continuous wave spectrum shows the full profile of the velocities with the outer borders representing the highest velocities. Continuous wave Doppler imaging is used to measure gradients across valves and shunts and other high velocity flows. Gradients can be used to compute intracardiac pressures.

4.3.1.3. Colour flow Doppler imaging

Colour flow Doppler imaging is a pulsed wave Doppler technique in which multiple gates are used along the multiple ultrasound beam (multigated) to display blood flow using a colour scheme that represents direction, mean velocities and degree of turbulence. At each sampling gate, the frequency shift is converted to a

present colour scheme in which flow towards the transducer (positive frequency shift) is shown in red and away from the transducer (negative frequency shift) is shown in blue. This colour flow map is superimposed on B mode or M mode images. Within each colour, a range of shades is used to show the variation in the velocities within the Nyquist limit, with lighter shades representing higher velocities. When the Nyquist limit is exceeded, there is colour aliasing that is shown as colour reversal. Turbulence is the difference between the mean velocity and the individual velocities (variance) in the region of interest, and the colour green is used to depict variance. Colour flow Doppler imaging is used for the semiquantitative assessment of regurgitant and shunt flows, and in the computation of orifice areas using the proximal isovelocity surface area (PISA) method.

4.3.2. Tissue Doppler imaging

Tissue Doppler imaging is a pulsed wave technique used to record myocardial displacement velocities. When a low pass filter is used (instead of the high pass filter used for flows), low myocardial velocities can be recorded. Mitral annular tissue Doppler imaging is used to assess myocardial function; pulsed wave signals above the baseline depict myocardial shortening velocity and those below the baseline depict lengthening velocity. Pulsed wave tissue Doppler imaging of the mitral annulus is also used to assess left ventricular diastolic function. Colour flow Doppler imaging can also be used to measure tissue displacement velocities, from which myocardial deformation (strain) can be quantified. Figure 4.3 shows the principle of Doppler imaging and Fig. 4.4 shows examples of each of the Doppler imaging methods.

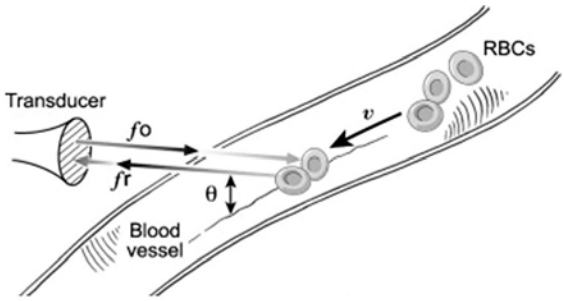

FIG. 4.3. Principles of Doppler echocardiography. (Figure modified and reproduced from Ref. [4.3] with permission). Θ — angle of incidence; fo — transmitted frequency; fr — received frequency; RBCs — red blood cells; v — velocity of red blood cells.

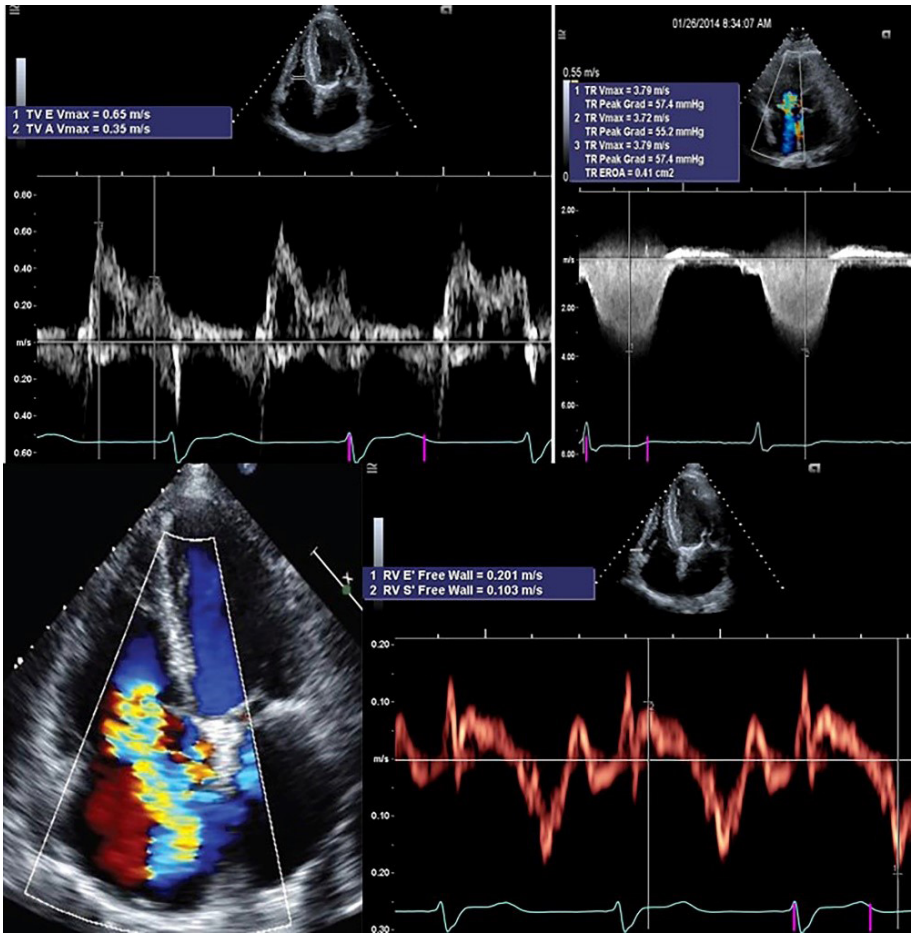

FIG. 4.4. Examples of Doppler imaging in the same patient. (Top left) Spectral pulsed wave Doppler of tricuspid flow velocity. (Top right) Continuous wave Doppler is utilized to measure the velocity of regurgitant blood flow across the tricuspid valve. (Bottom left) Colour flow Doppler showing tricuspid regurgitation. (Bottom right) Example of tissue Doppler imaging used to assess right ventricular function.

4.4. SPECKLE TRACKING ECHOCARDIOGRAPHY

Speckle tracking echocardiography is an echocardiographic imaging technique in which myocardial speckles (the brightness that myocardial pixels emit when hit by ultrasound) are tracked from one frame to the next throughout the cardiac cycle. The tracking of the displacement (motion) of these myocardial pixels can be represented in various ways. One such method is shown in Fig. 4.5,

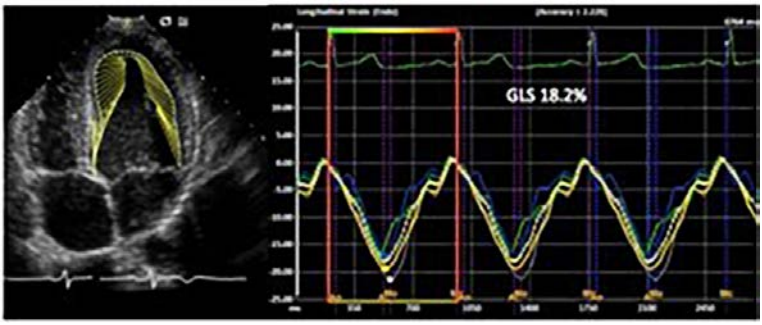

FIG. 4.5. Speckle tracking echocardiography. (Left) Velocity vector imaging, which is a speckle tracking algorithm. The vectors in yellow represent the deformation of the myocardium in systole. The length of the vectors correlates with the magnitude of deformation and the direction of the arrows represents the net direction of myocardial deformation (longitudinal, circumferential, radial). (Right) The curves show data for longitudinal deformation for three cardiac cycles and the average longitudinal deformation. The global longitudinal strain is 18.2%.

in which the length of the arrows is proportional to the magnitude of displacement and the direction in which they are pointing represents the predominant direction of myocardial motion [4.4], hence the term velocity vector imaging.

Motion or displacement is deformation of the muscle and therefore speckle tracking echocardiography essentially quantifies myocardial deformation. The latter is otherwise called strain, and the rate of change of deformation is called the strain rate. Strain can be measured for the entire myocardium (global strain), for a region (regional strain) or for a segment (segmental strain). Myocardial strain measured by speckle tracking echocardiography has been validated against magnetic resonance imaging for normal and diseased myocardium. The most exciting application of speckle tracking echocardiography for strain measurements is its ability to detect subclinical myocardial dysfunction not detectable by current indices of chamber function, specifically for the left ventricle. There is hope that myocardial strain may either replace or refine ejection fraction as an index of left ventricular dysfunction. However, there are technical challenges in speckle tracking echocardiography that will have to be overcome before it can be reliably used. There is a relatively wide variation in repeat measurements in the same patient using the same machine and speckle tracking echocardiography technique. This variation has been reduced in the most recent versions of speckle tracking echocardiography algorithms and will continue to improve. Another challenge is the considerable difference in strain measurements obtained in the same patient with different echocardiographic equipment. This limits the comparability of the results when examining longitudinal changes in myocardial function measured with different machines, and the comparability of results

obtained in different imaging laboratories. These issues have stimulated efforts to standardize measurements across imaging platforms. Global longitudinal strain has emerged as the most reproducible and clinically meaningful index, which is a positive step forward. During the course of this standardization effort, however, it became clear that there are still significant variations in the measurement of global longitudinal strain between machines, hence the current recommendation that the same machine be used in serial measurements of strain in same patient over time.

4.5. TRANSTHORACIC AND TRANSOESOPHAGEAL ECHOCARDIOGRAPHY

Ultrasound imaging of the heart performed by placement of the transducer on the chest wall is called transthoracic echocardiography (TTE). This is the most common form of echocardiography and is entirely non-invasive. It is also the optimal way to assess the size and function of chambers, evaluate flows and valves and use Doppler techniques to assess cardiac haemodynamics. However, the acoustic windows may be limited by narrow rib spaces, lung disease or chest deformities that may prevent adequate visualization of structures by TTE. In these situations, echocardiography may be performed from an oesophageal location; this is called transoesophageal echocardiography (TEE). The transducer is built on the end of an endoscope, which is then placed in the mid-oesophagus for most of the TEE examination. TEE may be also used in addition to TTE for specific indications even when the latter is of adequate quality. Some of the key indications for the use of TEE and TTE include:

— Suboptimal TTE, especially for valve disease, endocarditis, left atrial pathology and aortic diseases;
— Detailed assessment of mitral valve disease;
— Cardiac source of emboli;
— Guidance of structural heart interventions.

4.6. 3-D ECHOCARDIOGRAPHY

Recent developments in transducer technology (evolution from electrocardiographically gated to real time data acquisition), and data processing speed have significantly improved the clinical applicability of 3-D echocardiography in daily practice [4.5]. Furthermore, artificial intelligence and automation in 3-D echocardiography have provided additional impetus to use this technique in routine practice. Both 3-D TTE and TEE (see Fig. 4.6) are now

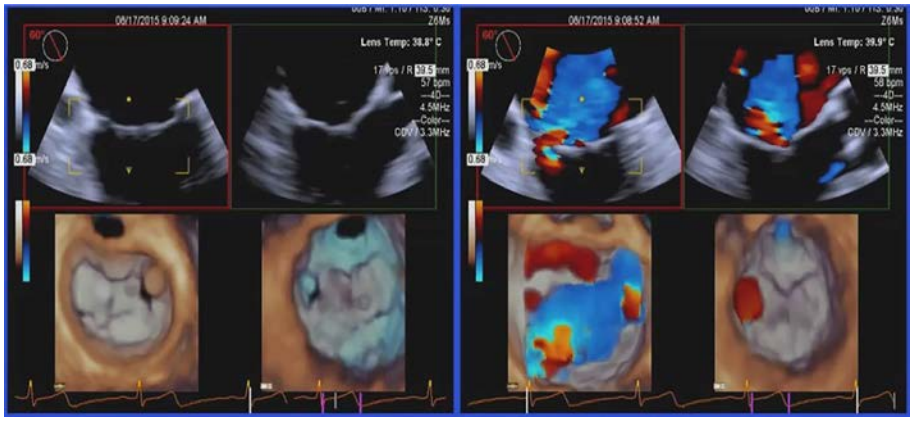

FIG. 4.6. Examples of 2-D TEE (top left) and 3-D TEE (bottom left). (Top right) Colour Doppler superimposed on the 2-D images and demonstrates mitral valve regurgitation. (Bottom right) 3-D representation of the mitral valve and the associated regurgitant jet.

established techniques and have well proven indications, especially in structural heart disease. Some of the key indications for 3-D echocardiography in the current guidelines include:

— Measurement of left ventricular volumes and ejection fraction: 3-D TTE.
— Quantification of mitral valve area in mitral stenosis: 3-D TTE and TEE.
— Quantification of severity of mitral regurgitation: 3-D TTE and TEE.
— Detailed assessment of mitral valve anatomy in degenerative mitral regurgitation: 3-D TEE.
— Tricuspid valve anatomy: 3-D TTE and TEE.
— Planning and guidance of structural heart interventions.

In addition to the above, there are other indications which are rapidly evolving and may become proven applications in the near future: right ventricular ejection fraction and left atrium volume are two such indications.

4.7. CONTRAST ECHOCARDIOGRAPHY

One of the significant advances in echocardiography has been the use of intravenous microbubble contrast to enhance the left heart for better contour definition [4.6]. There are at least three such contrast agents, commercialized under the brand names of Definity (Lantheus, United States of America), Optison (GE Healthcare, United States of America) and SonoVue (Bracco, Italy),

which are approved in various parts of the world for use in echocardiography. The indication is salvage of suboptimal echocardiograms (see Fig. 4.7). The microbubbles usually have a phospholipid shell encasing an inert heavy gas. When exposed to ultrasound, the gas escapes into the blood stream and the signal that emanates during bubble destruction is seen as contrast signal. In addition to left ventricular function application, myocardial perfusion imaging (MPI) has been explored. Although, this application has a sound physiological basis and small studies have shown promise, MPI has not yet been approved as a clinical indication. All contrast agents have an excellent safety profile, and the only absolute contraindication is limited to previously demonstrated allergy to the agent. Most recently, the suspicion and presence of transient right-to-left shunt was removed from the contraindication list. Use in pregnancy is cautioned, and safety in this instance has not been tested or demonstrated.

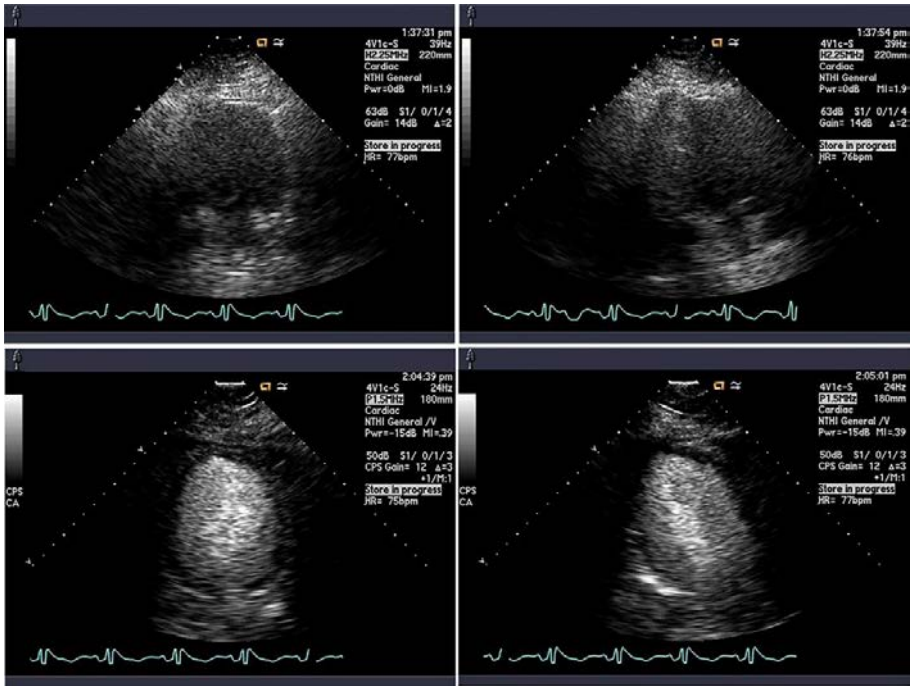

FIG. 4.7. Echocardiographic study using intravenous microbubble contrast.

4.8. KEY MESSAGES

(1) Bidimensional echocardiography is a readily available non-invasive technique widely applied to the study of ventricular and valvular function.
(2) 3-D echocardiography has limited but expanding indications such as accurate assessment of left ventricular volumes and function, and valvular structure and function.
(3) Doppler echocardiography can be used to assess severity of valvular disease, shunt volumes as well as ventricular function.
(4) Speckle tracking is a new technique that allows assessment of pre-clinical left ventricular systolic dysfunction.
(5) Transesophageal echocardiography is an excellent tool to assess valvular structure and function, exclude infective endocarditis, identify the presence of left atrial masses and thrombi, and plan structural heart disease interventions.

REFERENCES TO CHAPTER 4

[4.1] FEIGENBAUM, H., ARMSTRONG, W.F., RYAN, T., Feigenbaum's Echocardiography, 6th edn, Lippincott Williams and Wilkins, Philadelphia, PA (2005).
[4.2] OH, J.K., SEWARD, J.B., TAJIK, A.J., The Echo Manual, 3rd edn, Lippincott Williams and Wilkins, Philadelphia, PA (2006).
[4.3] ANAVEKAR, N.S., OH, J.K., Doppler echocardiography: A contemporary review, J. Cardiol. **54** (2009) 347–358.
[4.4] VOIGT, J.-U., et al., Definitions for a common standard for 2D speckle tracking echocardiography: Consensus document of the EACVI/ASE/Industry Task Force to standardize deformation imaging, Eur. Heart J. Cardiovasc. Imag. **16** (2015) 1–11.
[4.5] LANG, R.M., et al., EAE/ASE recommendations for image acquisition and display using three-dimensional echocardiography, Eur. Heart J. Cardiovasc. Imag. **13** (2012) 1–46.
[4.6] PORTER, T.R., et al., Clinical applications of ultrasonic enhancing agents in echocardiography: 2018 American Society of Echocardiography guidelines update, J. Am. Soc. Echocardiogr. **31** (2018) 241–274.

Chapter 5

CARDIAC MAGNETIC RESONANCE IMAGING

A. MEAVE, D. CUEVAS, B. DOMINGUES, M. PÉREZ, C. BUCCIARELLI-DUCCI

Magnetic resonance imaging (MRI) allows the accurate non-invasive and radiation free evaluation of the heart and vascular structures, with high contrast and large field of view without the restriction of an acoustic window. Cardiac magnetic resonance (CMR) is currently the standard of reference for the measurement of chamber volumes, and its high accuracy in tissue characterization has an excellent correlation with biopsy. It is therefore an imaging technique particularly suitable for serial studies and the close monitoring of changes in chamber dimensions or the severity of valvular abnormalities that can impact clinical management.

5.1. BASICS OF MAGNETIC RESONANCE IMAGING

Magnetic resonance data are acquired from the properties in hydrogen nuclei, which are present in water and fat within tissue. Each proton acts like a tiny magnet because of an intrinsic property known as nuclear spin, which gives rise to a small magnetic field (magnetic moment). The magnetic moments (spins) are naturally randomly oriented so that their magnetic fields do not sum but rather cancel one another out. In the presence of a static magnetic field, they tend to align towards or against this field.

The excess of proton magnetic moments combines to form a net magnetic field or net magnetization along the z axis of the external magnetic field, becoming the source of the magnetic resonance signal, which is ultimately detected and imaged. The greater the applied magnetic field strength, the greater the excess of protons aligned with the magnetic field and the greater the size of the net magnetization. A typical clinical MRI system will have a magnetic strength of 1.5 T, but 3 T systems are also increasingly available.

To be able to generate a signal, the net magnetization vector is tipped into the transverse plane by applying a small magnetic field rapidly changing at radio frequencies for a small period of time (pulse). The field is applied by a transmitter coil at a particular Larmor frequency (defined by the Larmor equation), determined by the strength of the magnetic field. The gyromagnetic ratio has a value of 42.6 MHz/T for the proton, also known as resonant frequency, as protons only absorb energy (resonate) at this frequency. After a 90° radiofrequency

pulse is applied, energy is absorbed, the net magnetization rotates away from the longitudinal direction into the transverse plane (transverse magnetization) and the longitudinal magnetization becomes zero. The magnetization then realigns back with the main magnetization vector), which is called longitudinal (T1) relaxation. The value of T1 is the time it takes for the longitudinal magnetization to reach 63% of its final value and is characteristic of specific tissues; it is the source of contrast in T1 weighted images. After the radiofrequency pulse protons rotate together in a coherent fashion within the *xy* plane, the angle they point to is known as the phase angle. Spins with similar phase angles are considered in phase; when relaxation occurs, there is loss of coherence and they no longer rotate together (and therefore are considered out of phase) and consequently, there is a decay of the transverse magnetization known as T2 relaxation [5.1, 5.2]. All the information acquired during the MRI scan is then transformed into an image using the Fourier transform.

5.2. CARDIAC MAGNETIC RESONANCE

CMR can acquire a specific fraction of the cardiac cycle in a steady state free precession (SSFP) sequence. It relies on a steady state of magnetization in which the longitudinal and transverse magnetizations are at equilibrium with the use of radiofrequency pulses [5.3].

To evaluate cardiac function, the standard CMR protocol (see Fig. 5.1) includes SSFP cine images in a short axis stack from the mitral valve plane through the apex (see Fig. 5.2), vertical long axis, four chamber long axis and left ventricle outflow tract long axis. The inclusion of an optional transaxial stack of cines covering the right ventricle should be considered to evaluate right ventricular volumes [5.4]. The characterization of myocardial oedema is performed in T2 weighted imaging (see Fig. 5.3) in which blood is seen as a dark signal and oedema as a bright signal in the myocardium. These images present some interpretation challenges as they are prone to artefacts caused by slow blood flow. Visual qualitative analysis is usually sufficient in injuries such as acute myocardial infarction and acute myocarditis [5.4, 5.5].

Images acquired to assess cardiac iron deposition in diseases such as thalassaemia major are referred to as T2* (star) images, as these images are strongly influenced by the presence of magnetic susceptibility effects due to iron deposition.

First pass perfusion is a technique that allows the detection of ischaemia; a perfusion defect is seen after the contrast arrival and passage through the left ventricular myocardium. Qualitative analysis is made comparing different

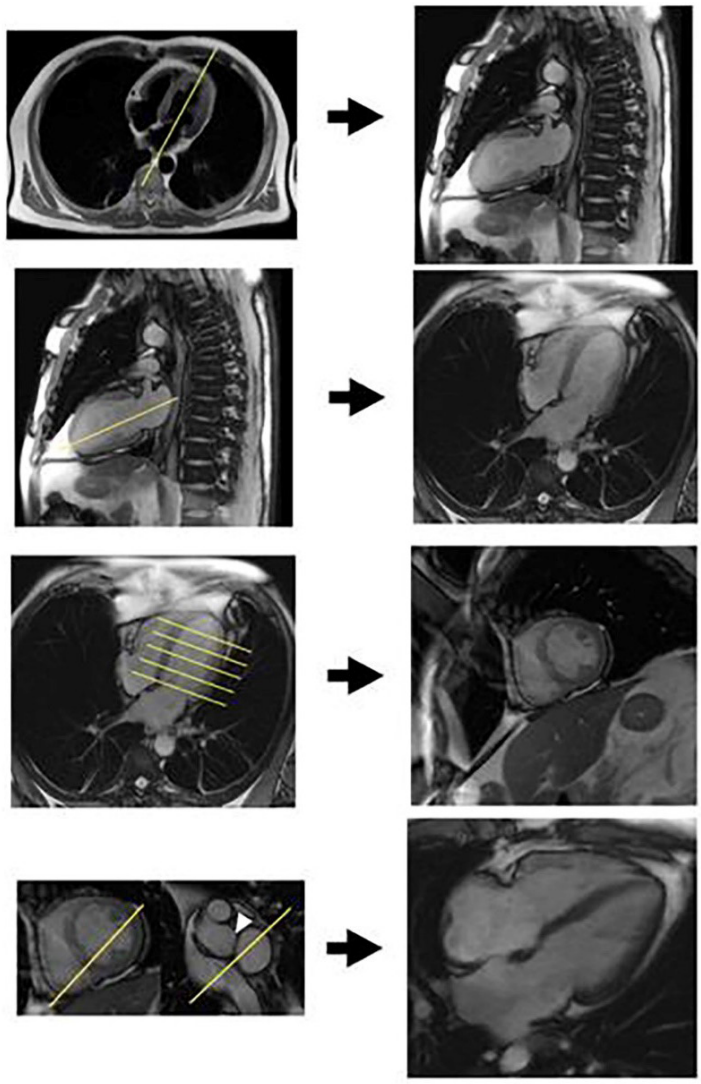

FIG. 5.1. Cardiac view acquisition. Transaxial fast turbo spin echocardiography or half-Fourier single shot images (top left, first row). Single shot SSFP vertical long axis is planned in transaxial images, aligning through the apex and the centre of the mitral valve (second row). Horizontal long axis aligned through the apex and the centre of mitral valve in the previous vertical long axis (third row). Short axis stack is obtained using the horizontal long axis and aligning perpendicularly to the septum. Finally, a more accurate horizontal long axis SSFP cine is obtained aligning through the anterior papillary muscle and the right ventricular apex, avoiding the aortic root (white arrowhead in the left lower bottom panel).

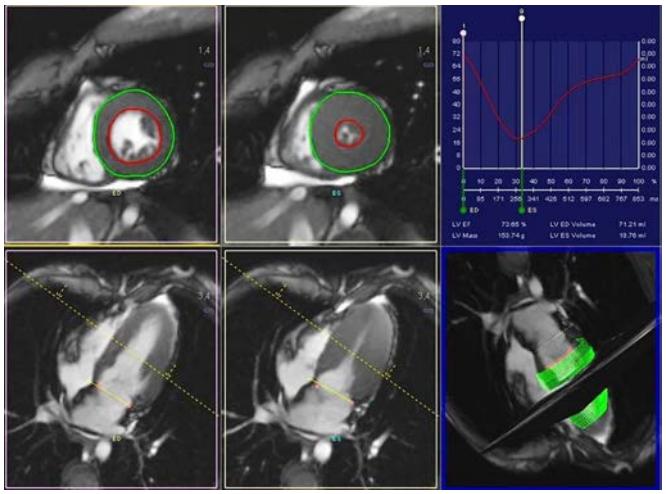

FIG. 5.2. Transaxial fast turbo spin echo or half-Fourier single shot images (upper row, left and middle image). Single shot SSFP vertical long axis is planned in transaxial images, aligning through the apex and the centre of the mitral valve (second row, left and middle image). Short axis stack is obtained using the horizontal long axis and aligning perpendicularly to the septum (lower row, right sided image). The final left ventricular ejection fraction calculation is shown in the right upper insert.

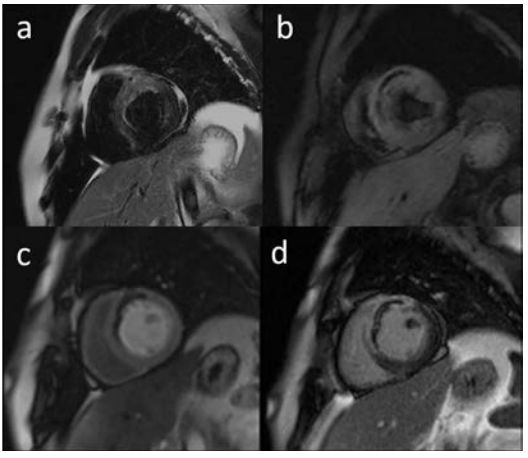

FIG. 5.3. Basic CMR short axis images in a case of acute myocardial infarction. (a) T2 shows increased intensity in the left anterior descending artery territory; (b) T2 depicts a lineal hypointensity in the injured myocardium consistent with haemorrhage. First pass image (c) allows the visualization of a perfusion defect, which persists in late gadolinium enhancement acquisition (d) a feature of no reflow phenomenon. The mural extent is also visualized.*

regions to identify relative hypoperfusion. These defects should persist beyond the peak of myocardial enhancement and for several R–R intervals.

Late gadolinium enhancement (LGE) occurs at least ten minutes after administration and inversion time is set to null the signal of the normal myocardium. LGE occurs in tissue with an increased volume of distribution of gadolinium and slower washout, such as in myocarditis and myocardial infarction. This is a very accurate method to characterize myocardial injury because of its high spatial and contrast resolution.

5.3. BLOOD FLOW EVALUATION USING CMR

CMR can be used to evaluate blood flow using phase contrast or velocity encoded techniques, based on the principle that moving protons change phase in proportion to their velocity [5.6]. Velocity encoded cine MRI imaging provides not only a qualitative assessment of flow but also allows an accurate quantification of key haemodynamic parameters such as flow velocity, flow volume and pressure gradients [5.6]. Hom et al. [5.6] report that the data obtained with velocity encoded MRI are generally reliable and reproducible. However, the "velocity and volume of blood flow may be underestimated if the vessel of interest is not imaged in a plane exactly perpendicular to the direction of flow" [5.6].

Because of the slow acquisition and low spatial resolution compared with computed tomography, the examination of coronary arteries with magnetic resonance angiography is currently not considered appropriate in patients with chest pain symptoms and intermediate pre-test probability of coronary artery disease. The origin and proximal portions of the coronary arteries or dilated vessels can be successfully visualized with CMR, which can subsequently be useful in the diagnosis of anomalous coronary artery origins and in Kawasaki disease [5.7].

5.4. 4-D FLOW CARDIAC MAGNETIC RESONANCE

Dyverfeldt et al. [5.8] report on this is a relatively novel technology that allows a more comprehensive assessment of the pulsatile blood flow through the heart and great vessels (aorta, pulmonary arteries). It has a typical spatial resolution of 1.5 mm × 1.5 mm × 1.5 mm to 3 mm × 3 mm × 3 mm, a typical temporal resolution of 30–40 ms, and an acquisition time of approximately 5–25 min. It refers to phase contrast CMR with flow encoding in all three spatial directions that is resolved relative to all three dimensions of space, and to time

during the cardiac cycle. The main advantage over 2-D flow imaging is the acquisition of images of flow with higher reproducibility in all spatial dimensions.

5.5. SAFETY CONSIDERATIONS

CMR is contraindicated in patients with certain devices. In 2005, ASTM International developed a set of terms to prevent confusion and accidents. 'MR safe' is used to describe an item with no known hazards in any MRI environment. 'MR conditional' is used to describe an item with no known demonstrated hazards in one specific MRI environment once pre-specified conditions have been applied, for example, the field strength (devices tested at 1.5 T may not be safe at 3 T). 'MR unsafe' is used to describe an item known to pose hazards in all MRI environments and exposure is to be avoided [5.9].

In cases of patients with non-MRI-conditional pacemakers or implantable cardioverter defibrillators, recommendations are to have personnel capable of programming the device be present during the examination. If pharmacological stress is administered, a physician trained in advanced cardiac life support should always be present and life support instruments should be available. Heart rhythm and blood pressure needs to be monitored during the stress and recovery phase [5.10].

The use of gadolinium based contrast is contraindicated in patients with stage 4 or 5 chronic kidney disease, as well as in patients with severe acute renal failure, owing to concerns with regard to nephrogenic systemic fibrosis, which might develop in these patients. This risk should be weighed against the clinical benefit of the potential diagnostic information in individual scenarios, as stated by the Radiological Society of North America.[1]

5.6. KEY MESSAGES

(1) CMR has developed into an imaging method with multiple useful cardiovascular applications.
(2) To obtain the best results from CMR, application by a knowledgeable expert is necessary.
(3) Potential hazards must be considered, particularly in patients with implanted devices and MRI conditional devices.

---

[1] See www.rsna.org/uploadedfiles/rsna/content/role_based_pages/media/rsna-gadolinium-position-statement.pdf

(4) Currently, CMR is the method of choice for the study of ventricular volumes, ventricular function and tissue characterization; continuous technology improvements will expand its clinical applications in the near future.

REFERENCES TO CHAPTER 5

[5.1] RIDGWAY, J.P., Cardiovascular magnetic resonance physics for clinicians: Part I, J. Cardiovasc. Magn. Reson. **12** (2010) 71–99.

[5.2] HENDRICK, R.E., The AAPM/RSNA physics tutorial for residents. Basic physics of MR imaging: An introduction, Radiographics **14** (1994) 829–846.

[5.3] RAJIAH, P., BOLEN, M.A., Cardiovascular MR imaging at 3 T: Opportunities, challenges, and solutions, Radiographics **34** (2014) 1612–1635.

[5.4] SCHULZ-MENGER, J., et al., Standardized image interpretation and post processing in cardiovascular magnetic resonance: Society for Cardiovascular Magnetic Resonance (SCMR) Board of Trustees Task Force on Standardized Post Processing, J. Cardiovasc. Magn. Reson. **15** (2013) 35–54.

[5.5] RAJIAH, P., DESAI, M.Y., KWON, D., FLAMM, S.D., MR imaging of myocardial infarction, Radiographics **33** (2013) 1383–1412.

[5.6] HOM, J.J., ORDOVAS, K., REDDY, G.P., Velocity-encoded cine MR imaging in aortic coarctation: Functional assessment of hemodynamic events, Radiographics **28** (2008) 407–416.

[5.7] SAKUMA, H., Coronary CT versus MR angiography: The role of MR angiography, Radiology **258** (2011) 340–349.

[5.8] DYVERFELDT, P., et al., 4D flow cardiovascular magnetic resonance consensus statement, J. Cardiovasc. Magn. Reson. **17** (2015) 17–72.

[5.9] WOODS, T.O., Standards for medical devices in MRI: Present and future, J. Cardiovasc. Magn. Reson. Imag. **26** (2007) 1186–1189.

[5.10] WOODARD, P.K., ACR practice guideline for the performance and interpretation of cardiac magnetic resonance imaging (MRI), J. Am. Coll. Radiol. **3** (2006) 665–676.

Chapter 6

CARDIAC COMPUTED TOMOGRAPHY

Z. QIAN, D. BERMAN, M.C. WILLIAMS

6.1. BASIC PRINCIPLES

Computed tomography (CT) is an X ray based tomographic imaging technique that produces transaxial images of the human body. Since its invention in the 1970, it has rapidly evolved from the earliest generation model, which took 4.5 min to acquire a single image, to the modern multidetector row CT scanners that are able to acquire a 3-D volumetric image in under 200 ms. Cardiac computed tomography (CCT) has gained wide clinical acceptance since the introduction of the 64 detector row CT scanners in the early 2000s.

The three major components of a CT scanner are a rotating gantry, a reconstruction workstation and an image reading workstation. The X ray source, the collimator and the X ray detectors reside in the CT gantry (see Fig. 6.1). X ray beams are emitted by the X ray source, passing through the collimator and the patient, and are collected by the X ray detectors, which are located at the opposite side of the gantry from the X ray source. A collimator is a device that restricts and aligns X ray beams to reduce radiation dose and improve image quality. It can be placed on both the X ray source side and the X ray detector side. The detector width of a multidetector row CT scanner in the *z* axis determines the maximum axial spatial resolution. The in-plane spatial resolution of a CT image is determined by multiple factors, such as the X ray focal spot size (X ray beam width) and the detector spacing in the circumferential direction. In practice, the in-plane spatial resolution can be calculated by dividing the size of the field of view by the image matrix size.

During a CT scan, the gantry rotates quickly around the patient to gather the attenuation information from different angles (see Fig. 6.1). With a conventional single source scanner, the gantry needs to rotate by a little more than 180° to reconstruct a complete cross-sectional CT image. The temporal resolution of the CT scanner, like the shutter time of a camera, is defined as the length of time that it takes to complete this partial gantry rotation time. The higher the gantry rotation speed is, the greater the extent to which the CT scanner can freeze the fast motion of a beating heart.

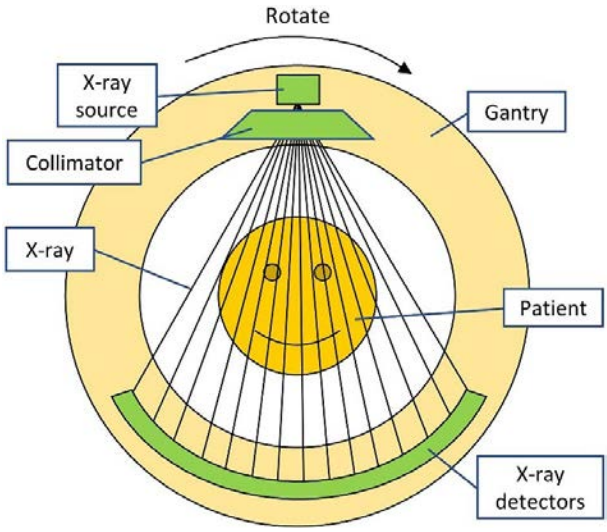

FIG. 6.1. Structure of the computed tomography gantry.

Tube voltage and tube current are two important parameters in CT image acquisition. The tube voltage, measured in kiloelectron volts (keV), determines the energy (i.e. penetration ability) of X ray photons. The tube current, measured in milliamperes (mA), determines the number of the X ray photons leaving the X ray source per unit of time. The settings of the tube voltage and tube current are closely related to image noise, tissue contrast and the associated radiation dose (see Table 6.1).

Tissue characterization in CT is based on the tissue's ability to attenuate X ray photons. The X ray attenuation coefficient, μ, is positively related to the

TABLE 6.1. THE PROS AND CONS OF INCREASING THE TUBE VOLTAGE AND TUBE CURRENT

	Pros	Cons
keV ↑	Image noise ↓	Radiation* ↑ Tissue contrast ↓
mA ↑	Image noise ↓ Tissue contrast ↑	Radiation ↑

* The radiation dose is proportional to the square of the keV.

tissue's radiodensity and inversely proportional to the energy of the X ray photon. The pixel value in a CT image is defined as the CT number and is quantified in Hounsfield Units (HU). It is a relative measurement of the tissue's X ray attenuation coefficient compared with that of water. By definition, the CT number of water is 0, and 1 HU difference in the CT number reflects 0.1% difference in tissue attenuation. The brightness of a CT image seen on a computer screen is determined by both the CT numbers and the window level.

Because μ is inversely proportional to the energy of the X ray photon, the CT number of a tissue other than water varies slightly with different tube voltage. Therefore, tissue cut-offs in HU need to be adjusted when tube voltage changes. For example, the cut-off of coronary artery calcium is 130 HU below the current guideline for performing coronary artery calcium score (CACS), in which the tube voltage is set to 120 keV. Using a lower keV will reduce radiation dose and as a result a higher cut-off to define calcium will be required to avoid underestimation of the CACS [6.1].

CT imaging involves heavy computation during image reconstruction. A typical CCT study contains hundreds or thousands of 2-D images. This raises an infrastructural requirement for the secure and efficient transfer and storage of large datasets. Many picture archiving and communication systems are available to meet this requirement. Most of these also provide image viewing and image analysis functionalities. However, for the reading of CCT studies, dedicated post-processing software is more commonly used in practice, as discussed below.

6.2. COMPUTED TOMOGRAPHY HARDWARE AND SOFTWARE

6.2.1. Minimum standards

Coronary computed tomography angiography (CCTA) and CACS are the two most commonly performed CCT studies in clinical practice. CCTA is a contrast enhanced CT study using an injection of iodine based contrast agent to examine the anatomy of the coronary arteries for stenosis and atherosclerosis. CCTA has been performed on 4, 8, 16, and 40 slice CT scanners. However, because of the small anatomy and the fast motion of the coronary arteries, 64 slice CT is currently the minimum standard for performing CCTA. Other minimum CT hardware requirements for CCTA include the capability to perform electrocardiogram (ECG) gating, fast gantry rotation (gantry rotation time ≤ 350 ms) and a small detector width (≤0.625 mm). For the injection of the contrast agent during the CCTA study, a dual head power injector comes highly recommended.

CACS is a non-contrast-enhanced CT study that aims to detect and quantify calcium deposits in the coronary arteries. It has been established as an effective screening tool for coronary artery disease (CAD) and a strong predictor for future coronary events in asymptomatic patients. CACS was traditionally performed on electron beam CT scanners. Nowadays, CACS is performed on multidetector row CT scanners. CACS can be performed on a lower end non-cardiac scanner for qualitative grading. For instance, visual grading of the CACS in non-ECG-gated low dose CT for lung cancer screening has been reported [6.2, 6.3].

6.2.2. Recent developments

Since 2000, there have been great advances in CT hardware technology. Such technical development has significantly expanded the indications for cardiovascular CT imaging. It has also greatly improved image quality, and substantially reduced imaging associated radiation exposure to patients.

There have been several advancements in CT hardware. Firstly, the X ray detectors have been re-engineered to improve spatial resolution and increase the axial coverage of a single gantry rotation. 256 and 320 row detectors have been implemented, which expands the axial coverage to up to 16 cm. This allows the CT scanner to image the whole heart in a single heartbeat, and therefore avoids the issues of segmental misalignment and contrast inconsistency caused by combining reconstructed image volumes from multiple heartbeats.

Secondly, more powerful X ray sources have been developed to increase the maximum output capacity of the tube current. This allows CT acquisition at a lower tube voltage, which reduces radiation dose. Reducing tube voltage improves image contrast, with the potential benefit of reducing the volume of iodinated contrast required for CT cardiac angiography (particularly advantageous for patients with renal disease).

Thirdly, the temporal resolution of CT scanners has been improved, mainly owing to the increases in the gantry rotation speed. In addition, a dual source CT scanner, whose CT gantry is equipped with two sets of X ray sources and detectors, was introduced. The new generation of dual source CT scanners have temporal resolutions as low as 60 ms.

Fourthly, efforts are being made to improve the ability of CT to differentiate between materials with similar attenuation density. The principle of these techniques is to integrate the attenuation measurements that are derived under multiple X ray energy spectra, so-called spectral CT. A variety of imaging techniques have been utilized to achieve this, including rapidly switching the X ray tube voltage, employing multilayer detectors and implementing dual X ray sources with different tube voltages. However, the improved diagnostic ability

must be balanced against the increased radiation dose. One of the most recent advancements in CT imaging is photon counting CT [6.4, 6.5].

Software improvements in CT include new reconstruction algorithms, including iterative and model based reconstruction algorithms. These can improve the image quality with reduction in tube current or tube voltage, which will reduce radiation dose.

6.2.3. Software for coronary computed tomography angiography

The CCTA analysis software provides a visualization and interpretation platform for the diagnostic evaluation of CCTA scans. The 3-D image volume of the CCTA scan is often displayed in three orthogonal views as shown in Fig. 6.2. Most CCTA software also provides a volumetric rendering function that removes the ribcage and illustrates the heart in 3-D for a more direct visualization of the coronary arteries, as shown in the upper right of Fig. 6.2. Image manipulation tools, such as window levelling, and image translation, rotation and scaling, are provided as part of the basic image viewing functions.

For the interpretation of the CCTA scans (see Fig. 6.3), most CCTA software provides automated or semi-automated functions for coronary artery

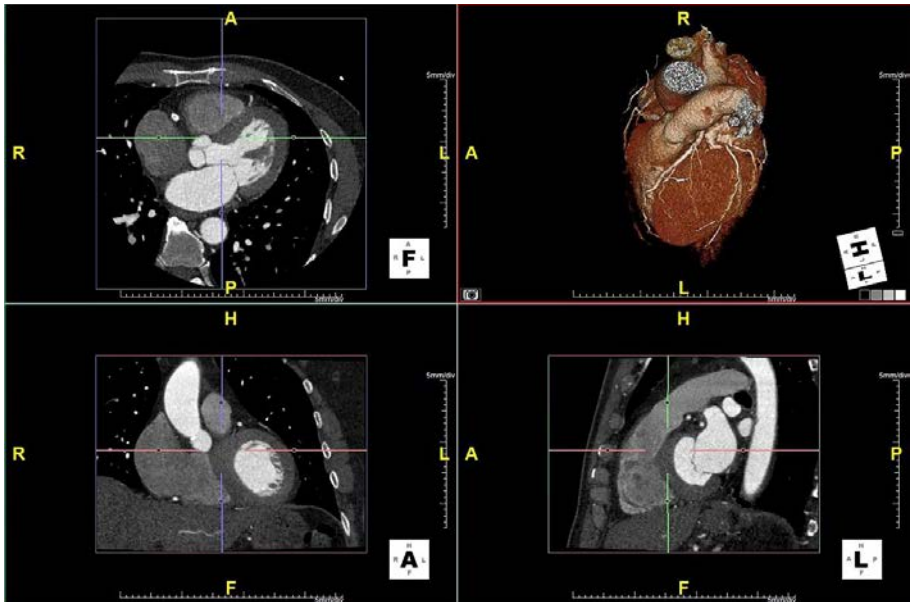

FIG. 6.2. A typical image visualization panel of the CCTA software. The 3-D image is depicted in three orthogonal views (top left and bottom left and right) and a 3-D volumetric rendering view (top right).

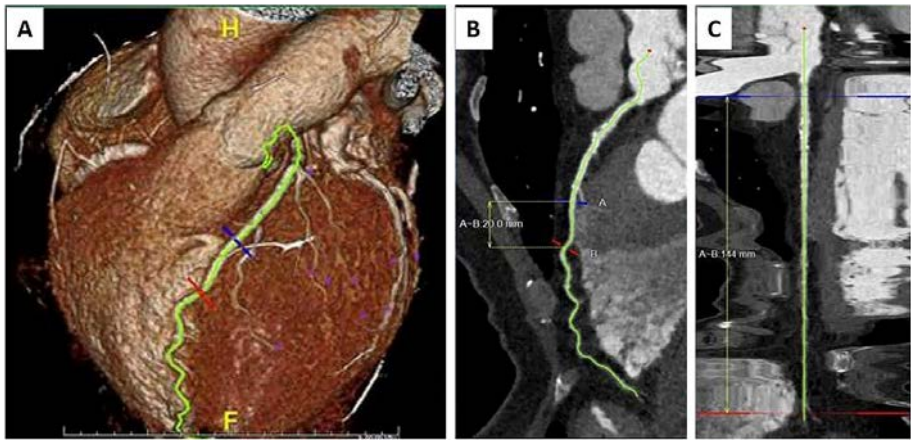

FIG. 6.3. The centreline of the left anterior descending artery is automatically extracted by the CCTA software and displayed in the 3-D volumetric rendering view (A), the curved multiplanar reformatting view (B) and the straightened multiplanar reformatting view (C).

detection and arterial centreline extraction. Some software optionally provides automated segmentation tools for the vessel lumen and vessel wall, based on the detection and grading of identified vessel stenosis and atherosclerosis. However, caution must be exercised when using these automated tools. For example, the automatically derived vessel centreline should be carefully reviewed. If any error is presented, the vessel centreline has to be corrected manually. Most CCTA software also provides a number of reformatting image display options to facilitate the visual inspection of the coronary arteries, such as curved multiplanar reformatting (see Fig. 6.3(B)), straightened multiplanar reformatting (see Fig. 6.3(C)) and maximum intensity projection. The assessment of coronary arteries can also be performed manually using oblique reformats, but this is a more challenging method.

The characterization of an atherosclerotic plaque in CCTA scans is based on the attenuation of the atherosclerotic plaque. Using user defined attenuation thresholds in HU, some CCTA software provide functions to classify the atherosclerotic plaques into different compositional categories, such as the non-calcified plaque, mixed plaque and calcified plaque. A variety of vulnerable plaque criteria have been developed, such as the presence of low attenuation plaques, spotty calcifications, positive remodelling of the vessel and the napkin ring pattern [6.6]. These features can be visually identified using one or more of the reformatting image display methods.

In addition to the coronary findings, CCTA software is potentially capable of providing extra pathophysiological information depending on the specific

CCTA scan protocol. For example, when using full R–R retrospective ECG gating, it is possible to calculate the left ventricular end diastolic volume, the left ventricular end systolic volume, the left ventricular ejection fraction and the left ventricular mass. However, this is at the cost of an increased radiation dose. It is also possible to perform CT myocardial perfusion imaging (MPI) after pharmacological stress and delayed enhancement imaging. Recently, some vendors have developed software to assess the CT based fractional flow reserve from CCTA using computational fluid dynamic techniques [6.7].

6.2.4. Software for determining the coronary artery calcium score

CACS analysis software provides an interface that allows the user to browse through the 3-D CACS data and identify calcified coronary lesions, based on which the software calculates the CACS. Most CACS software programs provide three calcium scoring methods: the Agatston score, the volume score and the mass score [6.8]. The Agatston score has undergone extensive validation over the past two decades and is currently the most widely used scoring method. The volume score and mass score were introduced to address some of the limitations of the Agatston score, most notably its limited reproducibility. However, fewer data exist supporting the clinical validity of these two methods, and therefore they are less used in practice.

6.3. TECHNIQUES

6.3.1. Patient preparation

CCTA and CACS should be performed for appropriate indications [6.9]. The imaging procedure and why it is being performed should be discussed with the patient prior to the procedure. Some potential contraindications or cautions for the use of CCTA or CACS are shown in Table 6.2, but these should be considered on a case by case basis.

Heart rate control is essential for coronary artery imaging in order to optimize image quality and minimize radiation dose. A target heart rate of less than 60 beats per minute is recommended if possible [6.10]. For patients with faster heart rates, imaging may still be possible, but adjustments to the protocol will be required. Oral or intravenous beta blockers (such as metoprolol) are the most commonly used medications to reduce the heart rate, unless there are contraindications. Ivabradine (a direct I(f) current inhibitor) may also be used. For patients undergoing CT for non-coronary imaging, rate limiting medication may not be required depending on the scanner used.

TABLE 6.2. POTENTIAL CAUTIONS OR CONTRAINDICATIONS TO CCTA AND CACS

Both CCTA and CACS	CCTA only
Inability to cooperate with scan (e.g. cannot lie flat or cannot breath hold for the required time) Pregnancy Clinical instability	Anaphylaxis or allergy to contrast Renal impairment

Glyceryl trinitrate administered sublingually causes vasodilation of the coronary arteries and has been shown to improve diagnostic accuracy in CCTA. Administration of glyceryl trinitrate is therefore recommended prior to coronary CT, unless contraindicated (see Ref. [6.11] for more detailed information on patient preparation prior to CCTA or CACS).

6.3.2. CCTA image acquisition

CCTA imaging involves a contrast enhanced ECG gated scan of the heart. The parameters required for the scan will depend on heart rate and patient body habitus. Using scout images, a scan range should be selected to cover the length of the heart. If coronary artery bypass grafts are present, the scan range should commence more cranially, at the level of the clavicles. Tube current and tube voltage can be manually selected based on body habitus or automatically selected based on the scout images. The choice of scan protocol will depend on the rate and regularity of the heartbeat.

For patients with a heart rate of less than 60 beats per minute prospectively ECG triggered axial acquisition can be performed with a narrow acquisition window (typically 70–80% of the resolution recovery interval). For patients with a higher heart rate, a widened acquisition window to include end systolic phases may be required (typically 30–80%). Retrospective ECG triggered helical or spiral acquisitions obtain information throughout the cardiac cycle, with or without tube current modulation. This may be considered for patients with an irregular or rapid heart rate or when additional information on valvular or ventricular function is required. This technique has the highest radiation dose and therefore should only be considered when other options are not possible.

CT scanner technology continues to evolve. Scanners with a wide detector range (up to 160 cm) have been developed and have the capability of imaging the heart in a single rotation. This can aid cardiac imaging by eliminating ‘stair-step’ artefacts. Dual source CT scanners can interleave images from two sets of

detectors and can perform high pitched imaging of the heart at a low radiation dose. Further evolution in hardware and software will continue to improve image quality and reduce radiation dose.

CCTA imaging uses iodinated contrast to opacify the coronary arteries so that the coronary artery lumen can be assessed. A variety of types and concentrations of iodinated contrast are available. The volume and rate of contrast can be tailored to the patient's body habitus, heart rate, cardiac function and scanning indication. After the contrast injection, CCTA imaging is started using a timed bolus or bolus triggering technique, depending on the available technology. Imaging is performed during a breath hold, which should be practised with the patient prior to imaging.

6.3.3. CCTA image analysis

CCTA images are assessed on a dedicated workstation with the ability to view axial images, multiplanar reformations and curved planar reformations. The coronary arteries are evaluated using a 17 segment model, and the presence and type of atherosclerotic plaque is assessed. Coronary artery stenoses are visually assessed and classified based on the presence of luminal stenosis. In addition, recent research suggests that CCTA can be used to identify potentially vulnerable atherosclerotic plaque that may identify patients at increased risk of subsequent coronary events [6.12]. CCTA images also cover non-cardiac structures including the lungs, bones, breast, oesophagus and upper abdomen. These structures should also be interrogated to identify non-cardiac causes of chest pain, such as pulmonary embolism, or other important incidental findings, such as lung cancer.

The CCTA report can be summarized using the Coronary Artery Disease – Reporting and Data System (CAD–RADS), which is applied on a per patient basis for the most clinically relevant stenosis, usually the most severe stenosis. This classifies patients into one of five groups and provides management advice for patients with stable chest pain or acute chest pain [6.13].

6.4. ADVANCED CCT TECHNIQUES

Advanced CCT techniques include CT MPI and computational fluid dynamic techniques to assess fractional flow reserve from resting CCTA images. CT MPI involves the acquisition of additional contrast enhanced ECG gated images during pharmacological stress. Images are acquired either at the peak of contrast enhancement (snapshot imaging) or during the wash-in and washout of contrast (dynamic imaging). Computational fluid dynamic techniques model haemodynamic parameters from anatomical information obtained from resting

CCTA and can estimate fractional flow reserve from these data [6.14]. CT based fractional flow reserve measurement estimates a ratio of pressure before and after a stenosis and can be used for decision making regarding percutaneous coronary intervention. Data currently suggest that CT based fractional flow reserve measurements correlate with invasive fractional flow reserve values and its measurement may be helpful in patients with intermediate to high grade stenosis to define lesion specific ischaemia [6.15].

6.4.1. CACS image acquisition and reconstruction

Imaging for coronary artery calcification involves a non-contrast ECG gated scan. The scan range should be limited to cover just the heart and coronary arteries. The phase of acquisition will depend on the heart rate, and should be as small as necessary to acquire adequate images (between 65% and 80% of the resolution recovery interval or focused on 75% of the R–R interval are typical options). Calcium scoring is performed with a tube voltage of 120 keV, standardized tube current, 3 mm contiguous slices and a filtered back projection reconstruction algorithm. However, imaging can be performed at a lower radiation dose by adjusting these parameters or using new reconstruction algorithms. Care should be taken if this is done, as the resulting calcium score may be over- or underestimated and appropriate caveats should be provided in the report [6.16].

6.4.2. CACS image analysis

Coronary artery calcification can be visually identified on non-contrast CT images as material within the anatomical distribution of the coronary arteries that has a high attenuation, typically above 130 HU. Semiquantitative methods can be used to assess the amount of calcification present. However, the presence or absence of coronary artery stenoses cannot be determined.

The most common method to quantify coronary artery calcification on CT is the Agatston method. To calculate the Agatston score, semi-automated software is used to measure the area of calcification in the location of the coronary arteries, defined as material greater than 1 mm^2 that has an attenuation density of above 130 HU. The area of calcification is then multiplied by a weighting factor dependent on the peak signal intensity within the lesion. These values are summed to give vessel specific and total Agatston scores [6.17]. Percentiles based on age, sex and ethnicity have been developed based on large population studies [6.18]. Other scoring systems include the volume score and the mass score. As mentioned above, the CAC–RADS is a standardized reporting tool developed to improve communication of CACS reports, which divides patients into four groups depending on the amount of calcification [6.19].

6.4.3. Coronary artery calcification on non-dedicated imaging

Coronary artery calcification can be identified on CT imaging performed for non-cardiac indications. This includes CT performed for lung cancer screening, suspected malignancy, trauma or for other reasons. This provides an opportunity to identify potentially asymptomatic patients at increased risk of CAD. These non-contrast, non-gated CT scans use different imaging parameters compared with CACS image acquisition, therefore quantitative scoring methods may under- or overestimate calcium scores. In addition, motion artefacts can affect coronary artery calcium quantification. Ordinal scores and simple visual assessment can identify coronary artery calcification and help to perform basic risk stratification. Using these methods, the amount of calcification can be divided into very low, mildly increased, moderately increased and moderate to severely increased [6.19].

6.4.4. Non-coronary cardiac imaging

CCT can also image a variety of non-coronary pathology, including the cardiac valves and chambers, cardiac tumours and pericardial diseases. To optimize CT images for non-coronary pathology, a variety of adjustments are required compared with CCTA.

To image the cardiac valves and chambers, adjustments may be required to the contrast protocol compared with coronary imaging. More specifically, opacification of the right heart may require a longer duration of injection and a larger contrast volume. Non-contrast images may also be useful to quantify the degree of calcification in the aortic or mitral valve.

As for coronary imaging, motion artefacts can be reduced by using ECG gating. If imaging throughout the cardiac cycle is required, dynamic CT (i.e. continuous acquisition throughout the cardiac cycle) can be performed. However, in view of the potential high radiation dose, alternative imaging modalities such as echocardiography should be considered first. Additional image reconstructions with metal artefact reduction may be beneficial in the presence of metal prosthetic valves.

Imaging prior to transcatheter aortic valve implantation or transcatheter aortic valve replacement involves both cardiac imaging and the assessment of the peripheral arteries [6.20]. Images are obtained from the aortic arch (and in some centres from the circle of Willis) to the level of the femoral heads. Images of the left ventricular outflow tract require ECG gating, but images of the peripheral vessels do not. Depending on the CT scanner used, this can be performed in a single image or two separate images for the chest and abdomen/pelvis.

Cardiac valves, chambers and the pericardium can be assessed by reviewing axial, coronal and sagittal images. In addition, using double oblique tools, the 3-D dataset can be re-oriented to standard cardiac views (e.g. short axis, two chamber, four chamber and three chamber) for the improved assessment of cardiac structures. Images perpendicular to the valve planes can also be created to assess valve structure and function.

Specialized software is available for CT assessments prior to structural interventions such as transcatheter aortic valve implantation, transcatheter aortic valve replacement or transcatheter mitral valve implantation. Measurements prior to transcatheter aortic valve implantation include the dimensions of the aortic annulus, the distance between the annulus and coronary arteries, the angle of the aortic valve and the minimum diameter of the aorta and peripheral arteries.

6.5. SAFETY

6.5.1. Radiation dose parameters

Many radiation dose parameters are provided on a CT scanner console. CT dose index is a measure of the radiation output of the CT scanner and provides an estimate of the average dose per centimetre over the scanned length. Dose–length product is the product of the CT dose index and the scan length. When recording the radiation dose of a CT scan, both CT dose index and dose–length product should be documented.

Effective radiation dose in mSv can be calculated from dose–length product by multiplying by a conversion factor. However, effective dose was devised to assess population radiation exposure and may not be the most appropriate metric for individual assessment. The choice of conversion factor can significantly impact the quoted effective radiation dose and therefore should always be stated. Several thoracic conversion factors have previously been used to calculate the radiation dose for CCT (e.g. 0.014 $mSv \cdot mGy^{-1} \cdot cm^{-1}$ and 0.021 $mSv \cdot mGy^{-1} \cdot cm^{-1}$). However, these underestimate radiation dose owing to the use of out of date weighting factors and the fact that CCT has a smaller scan range compared with thoracic imaging containing an increased proportion of radiosensitive breast tissue. The conversion factor for CCT is actually scanner and protocol dependent and a higher conversion factor of 0.026 $mSv \cdot mGy^{-1} \cdot cm^{-1}$ is more appropriate for the assessment of population radiation dose in CCT [6.21].

6.5.2. Radiation dose of CCTA

The radiation dose of CCTA has significantly decreased with the use of new hardware and software technology. State of the art scanners are capable of routine sub-millisievert CCTA. However, the quest for low radiation dose imaging should not reduce image quality or diagnostic accuracy. The average radiation dose of CCTA in multicentre studies in the range of 4–10 mSv [6.22, 6.23]. Registry studies have identified an average dose–length product of 209 mGy/cm and 259 mGy/cm [6.23, 6.24].

6.5.3. Radiation dose risks

The risks of radiation dose come from both stochastic and deterministic effects. Deterministic effects are tissue reactions that occur with a short latency period when the radiation dose exceeds a tissue specific threshold. These include skin erythema and hair loss. These effects should not occur at the doses used in appropriately performed CCT. Stochastic effects are the long term probabilistic risks of future effects, such as the risk of malignancy. The potential increased risk of subsequent malignancy is particularly important for younger patients and female patients. Therefore, radiation dose for CCT should follow the ALARA (as low as reasonably achievable) principle.

6.5.4. Iodinated contrast

CCTA involves the use of iodinated contrast, which has potential risks including anaphylaxis and contrast induced nephropathy. The volume of contrast required can be tailored to the patient's body mass index, cardiac function and scan indication. Patients at potential risk of contrast induced nephropathy include patients with pre-existent renal impairment, clinical instability and dehydration. Knowledge of the clinical history, recent renal function laboratory tests and current medications is important. Local and national guidelines should be followed to reduce the risk of contrast induced nephropathy (e.g. see Ref. [6.25]).

Supervised prehydration may reduce the risk of contrast nephropathy. Patients taking metformin and who have a glomerular filtration rate of less than 30 $mL \cdot min^{-1} \cdot 1.73\ m^{-2}$ are at risk of lactic acidosis precipitated by iodinated contrast. For such patients, or for those with an unknown glomerular filtration rate, metformin should be withheld for 48 h and estimated glomerular filtration rate assessed prior to re-commencing metformin.

6.5.5. Other medication

Beta blockers and glyceryl trinitrate are generally safe medications that are widely used. The presence of any contraindications or cautions should be assessed prior to the administration of medications. Beta blockers will reduce heart rate and blood pressure and glyceryl trinitrate may cause headache.

6.6. KEY MESSAGES

(1) CT imaging of the heart is a widely used technique to assess the heart and coronary arteries.
(2) Non-contrast imaging can assess coronary artery calcium.
(3) Contrast enhanced images can assess the presence of coronary artery stenoses and atherosclerotic plaque composition.
(4) ECG gating is essential for CCTA.
(5) A variety of hardware and software developments can improve image quality.

REFERENCES TO CHAPTER 6

[6.1] NAKAZATO, R., et al., Coronary artery calcium scoring using a reduced tube voltage and radiation dose protocol with dual-source computed tomography, J. Cardiovasc. Comput. Tomogr. **3** (2009) 394–400.
[6.2] KIRSCH, J., et al., Detection of coronary calcium during standard chest computed tomography correlates with multi-detector computed tomography coronary artery calcium score, Int. J. Cardiovasc. Imag. **28** (2012) 1249–1256.
[6.3] CHANDRA, D., et al., Assessment of coronary artery calcium by chest CT compared with EKG-gated cardiac CT in the multicenter AIDS cohort study, PLoS One **12** (2017).
[6.4] MCCOLLOUGH, C.H., Coronary artery calcium: A multi-institutional, multimanufacturer international standard for quantification at cardiac CT, Radiology **243** (2007) 527–538.
[6.5] CORMODE, D.P., et al., Multicolor spectral photon-counting computed tomography: In vivo dual contrast imaging with a high count rate scanner, Sci. Rep. **7** (2017) 4784–4795.
[6.6] STEFANADIS, C., ANTONIOU, C.K., TSIACHRIS, D., PIETRI, P., Coronary atherosclerotic vulnerable plaque: Current perspectives, J. Am. Heart Assoc. **6** (2017).
[6.7] LU, M.T., et al., Noninvasive FFR derived from coronary CT angiography: Management and outcomes in the PROMISE trial, J. Am. Coll. Cardiol. Cardiovasc. Imag. **10** (2017) 1350–1358.

[6.8] RUMBERGER, J.A., KAUFMAN, L., A Rosetta stone for coronary calcium risk stratification: Agatston, volume, and mass scores in 11,490 individuals, Am. J. Roentgenol. **181** (2003) 743–748.

[6.9] TAYLOR, A.J., et al., ACCF/SCCT/ACR/AHA/ASE/ASNC/NASCI/SCAI/SCMR 2010 Appropriate Use Criteria for Cardiac Computed Tomography, J. Am. Coll. Cardiol. **56** (2010) 1864–1894.

[6.10] SADAMATSU, K., KOIDE, S., NAKANO, K., YOSHIDA, K., Heart rate control with single administration of a long-acting β-blocker at bedtime before coronary computed tomography angiography, J. Cardiol. **65** (2015) 293–297.

[6.11] ABBARA, S., et al., SCCT guidelines for the performance and acquisition of coronary computed tomographic angiography: A report of the Society of Cardiovascular Computed Tomography Guidelines Committee, J. Cardiovasc. Comput. Tomogr. **10** (2016) 435–449.

[6.12] MOTOYAMA, S., et al., Plaque characterization by coronary computed tomography angiography and the likelihood of acute coronary events in mid-term follow-up, J. Am. Coll. Cardiol. **66** (2015) 337–346.

[6.13] CURY, R.C., et al., CAD–RADS^{TM} Coronary Artery Disease – Reporting and Data System: An expert consensus document of the Society of Cardiovascular Computed Tomography (SCCT), the American College of Radiology (ACR) and the North American Society for Cardiovascular Imaging (NASCI), J. Cardiovasc. Comput. Tomogr. **10** (2016) 269–281.

[6.14] MATHEW, R.C., GOTTBRECHT, M., SALERNO, M., CT–FFR to guide coronary angiography and intervention, Interv. Cardiol. Clin. **7** (2018) 345–354.

[6.15] ALFAKIH, K., BYRNE, J., MONAGHAN, M., CT coronary angiography: A paradigm shift for functional imaging tests, Open Heart **5** (2018).

[6.16] GREENLAND, P., BLAHA, M.J., BUDOFF, M.J., ERBEL, R., WATSON, K.E., Coronary calcium score and cardiovascular risk, J. Am. Coll. Cardiol. **72** (2018) 434–447.

[6.17] AGATSTON, A.S., et al., Quantification of coronary artery calcium using ultrafast computed tomography, J. Am. Coll. Cardiol. **15** (1990) 827–832.

[6.18] MCCLELLAND, R.L., CHUNG, H., DETRANO, R., POST, W., KRONMAL, R.A., Distribution of coronary artery calcium by race, gender, and age: Results from the Multi-ethnic Study of Atherosclerosis (MESA), Circulation **113** (2006) 30–37.

[6.19] HECHT, H.S., et al., 2016 SCCT/STR guidelines for coronary artery calcium scoring of noncontrast noncardiac chest CT scans: A report of the Society of Cardiovascular Computed Tomography and Society of Thoracic Radiology, J. Cardiovasc. Comput. Tomogr. **11** (2017) 74–84.

[6.20] CHOURDAKIS, E., et al., The role of echocardiography and CT angiography in transcatheter aortic valve implantation patients, J. Geriatr. Cardiol. **15** (2018) 86–94.

[6.21] TRATTNER, S., et al., Cardiac-specific conversion factors to estimate radiation effective dose from dose–length product in computed tomography, J. Am. Coll. Cardiol. Cardiovasc. Imag. **11** (2018) 64–74.

[6.22] CASTELLANO, I.A., et al., A prospective national survey of coronary CT angiography radiation doses in the United Kingdom, J. Cardiovasc. Comput. Tomogr. **11** (2017) 268–273.

[6.23] HAUSLEITER, J., et al., Image quality and radiation exposure with prospectively ECG-triggered axial scanning for coronary CT angiography: The Multicenter, Multivendor, Randomized PROTECTION-III Study, J. Am. Coll. Cardiol. Cardiovasc. Imag. **5** (2012) 484–493.

[6.24] SCOT-HEART INVESTIGATORS, CT coronary angiography in patients with suspected angina due to coronary heart disease (SCOT-HEART): An open-label, parallel-group, multicentre trial, Lancet **385** (2015) 2383–2391.

[6.25] THE ROYAL AUSTRALIAN AND NEW ZEALAND COLLEGE OF RADIOLOGISTS, Iodinated Contrast Media Guideline, RANZCR, Sydney (2018).

Part II

CLINICAL APPLICATIONS

Chapter 7

INTEGRATED NON-INVASIVE CARDIOVASCULAR IMAGING IN ROUTINE CLINICAL PRACTICE

G. KARTHIKEYAN, J. VITOLA, M. DONDI, D. PAEZ, C. BUCCIARELLI-DUCCI

Since 2000, advances in technology have contributed to the development of new imaging modalities and the refinement of existing ones, leading to major improvements in the accuracy of diagnosing cardiovascular (and other) disease. While modality centric knowledge and expertise has been the primary driver for improvement within each modality, this has also contributed to individual silo working among imagers, resulting in limited intermodality coordination and collation of information relevant for patient care. Several authorities have argued against the modality centric approach and called for greater cooperation between imagers and the integration of information from multiple modalities [7.1, 7.2] to make the best treatment decisions for their patients. This chapter provides comprehensive guidelines on the rationale for and implementation of integrated cardiovascular imaging for practitioners.

7.1. CONCEPT

Integrated cardiovascular imaging is an evolving concept, and there are arguably many ways to describe it. Two essential components for a valid definition of the concept are: (i) the shift away from individual imaging modalities, towards a disease specific approach; and (ii) integration aimed at optimizing clinical decision making. A working definition is as follows: integrated cardiovascular imaging is the optimal use of multiple imaging modalities to obtain complementary information about a disease process, to aid in diagnosis and determine aetiology and prognosis, with the ultimate objective of effectively guiding clinical decision making. Integrated imaging is often confused with multimodality ‘fusion’ imaging. Integration in this chapter refers to the putting together of information obtained from several separate modalities and does not require the integration of software or hardware platforms to fuse images from one modality to another.

Integrated imaging does not imply the indiscriminate use of multiple tests in the same patient. On the other hand, more than one imaging modality can be applied in the context of integrated imaging with the purpose of obtaining complementary information. As an example, in patients with right sided failure

where there is suspicion of constrictive pericarditis, echocardiography and tissue Doppler imaging provide information regarding the presence and absence of diastolic filling patterns. Computed tomography (CT) can complement the assessment by measuring pericardial thickness, and cardiac magnetic resonance (CMR) can provide information about pericardial thickness and inflammation, as well as ruling out inflammatory or restrictive cardiomyopathies that are in the differentials of constrictive pericarditis. Combining the findings from these modalities can lead to a more certain and accurate diagnosis. It may be noted that testing in the context of integrated imaging should be sequential, starting from the first line recommended modality (usually cost efficient and readily available) to the more sophisticated and expensive. Knowledge of the previous test is advisable to maximize the complementarity of the subsequent tests. Individual imaging modalities can often establish the diagnosis, but more complex and intricated cases benefit from integrated imaging information.

Imaging tools to diagnose, stratify risk and guide management in cardiac disease non-invasively include echocardiography, coronary computed tomography angiography (CCTA), magnetic resonance imaging (MRI) and nuclear cardiology using either single photon emission computed tomography (SPECT) or positron emission tomography–computed tomography (PET–CT). Each of these techniques has distinct characteristics that allow the evaluation of details of the anatomy and/or the physiology of the heart. Depending on the patient's characteristics and the various potential clinical presentations, some of these techniques may be better suited for some patients than other techniques, either for the initial work-up of a certain condition or as a follow-up method to evaluate a condition already identified.

The distribution of technology worldwide is heterogeneous, as previously documented by Vitola et al. [7.3]. Some countries have access to only the most basic tools to evaluate the heart, such as electrocardiography, the exercise treadmill/bicycle test (ETT) and echocardiography. Other countries will have various degrees of access to more advanced imaging technology, such as SPECT, SPECT–CT, CCTA, CMR and PET–CT. Therefore, it is advisable that physicians use all the diagnostic techniques available, applying internationally accepted standard protocols, and that the results be interpreted and acted upon appropriately.

7.2. INTEGRATING THE BASICS: ETT AND ECHOCARDIOGRAPHY

Following a medical interview, a complete physical exam and a 12 lead rest electrocardiogram (ECG), the ETT and echocardiography are two of the most basic but extremely important tools to evaluate the heart. They provide

complementary information with regard to the physiology, structure and activity of the heart — information that can certainly be integrated. Despite their limitations, several decades following their initial development they remain extremely useful and widely applied in the routine practice of cardiology worldwide. To be able to offer ETT, a patient needs to be able to exercise and the ECG needs to be suitable for interpreting potential changes during exercise. Therefore, ETT is not advisable in patients with left bundle branch block or a pacemaker.

ETT is widely used for risk stratification, as the variables obtained with this test (i.e. exercise capacity) reflect parameters regarding the physiology of the heart that carry important prognostic value. For example, a patient that can sustain a high workload exercise will most often fare well prognostically (i.e. there are no 'major' dysfunctions). Other variables from ETT that should be considered in risk stratification are [7.4]:

(a) ST segment depression;
(b) Number of abnormal leads (the more, the worse);
(c) Duration of the ST segment depression during the recovery period post-exercise (the longer, the worse);
(d) Magnitude of ST segment depression (the more, the worse);
(e) Pattern of ST segment depression, whether horizontal, down sloping or up sloping (down sloping being the worst);
(f) Its occurrence earlier or later into exercise (the earlier, the worse);
(g) Chronotropic response (a slow increase and a delayed decrease in heart rate);
(h) Blood pressure response (a drop during exercise);
(i) Development of malignant arrhythmias (ventricular tachycardia or ventricular fibrillation, in particular).

ETT is also used for the diagnosis of coronary artery disease (CAD) but has lower sensitivity and specificity compared with other diagnostic tests (higher number of false positives or false negatives). Coupling ETT with an imaging test such as echocardiography can increase the diagnostic accuracy of the test.

Echocardiography is widely available and is an extremely useful modality for the investigation of a large diversity of cardiac conditions. Its main advantages are: no ionizing radiation; its relatively small and portable equipment; and its relatively low cost. Echocardiography can offer a resting anatomical and functional cardiac assessment or, used in combination with either ETT or pharmacological agents such as dobutamine or adenosine/dipyridamole, may evaluate the presence and extent of inducible myocardial ischaemia. Limitations to echocardiography include it being an operator dependent technique, the significant interobserver variability depending on experience and the need for an

adequate acoustic window. Echocardiography is also particularly challenging to perform in patients with chronic obstructive pulmonary disease or obesity.

7.2.1. Integrating with more advanced imaging using nuclear cardiology and computed tomography

Nuclear cardiology has an established role in the diagnosis and prognosis of patients with suspected or known CAD. Importantly, it can be used as a gatekeeper for unnecessary invasive coronary angiography and revascularizations. Known limitations include the use of ionizing radiation, complexities relating to the installation and operation of this technology, and costs. The appropriate use of technology and appropriate use criteria have been published on the use of nuclear cardiology (see Ref. [7.5]), but in general terms the patients that would benefit from it are those found to be at intermediate risk of CAD on ETT. The literature supports the solid role of nuclear cardiology to stratify risk in several groups of patients, including those with suspected or known CAD, following coronary artery bypass graft or percutaneous coronary intervention, left bundle branch block, pacemakers, an inability to exercise, preoperative evaluation, chronic obstructive pulmonary disease, atrial fibrillation, chronic renal failure, patients with diabetes mellitus and the elderly. Importantly, many of these patients can be evaluated under physiological conditions using exercise instead of pharmacological stress agents.

Over time, it has been noted that occasionally a nuclear cardiology test would determine that risk was underestimated in patients who had previously been identified by an ETT as low risk. Similarly, a negative nuclear cardiology study, showing normal perfusion and normal left ventricular function, does not infer the absence of CAD. It implies, instead, the absence of significant CAD, and therefore a lower risk estimate, with a higher accuracy compared with ETT alone. CT can nicely integrate the information obtained with ETT and nuclear cardiology, helping to identify those patients without major ischaemia but who have CAD, as shown either by an elevated CACS [7.6–7.8] or by the diagnosis of non-obstructive CAD on contrast CCTA, triggering more aggressive prevention.

7.2.2. Integrating basic modalities with other modalities

The basic modalities, ETT and echocardiography, can be integrated with other, progressively more available modalities such as PET–CT and CMR, which are both becoming more widely available worldwide for use in the clinical diagnosis of a variety of diseases, including cardiovascular disease. PET–CT plays a major role in oncology, while MRI proves optimal for imaging soft tissue, including nervous tissue and musculoskeletal tissue, as well as prostate

and breast tissue. Both technologies are also increasingly being applied to the cardiovascular system, particularly CMR, as indicated in the current European Society of Cardiology, American College of Cardiology and American Heart Association clinical practice guidelines (see Ref. [7.9]). Education of the imaging community and referring physicians is key in ensuring the appropriate use of the various imaging modalities in different clinical contexts.

7.2.3. Key aspects for successful integration between modalities

The successful integration of imaging modalities can only be achieved by focusing the patient at the centre, rather than focusing on the techniques. Physicians should also make the most of the technology available locally but be informed of the pros and cons of other modalities.

The choice of a given technique should also include considerations of the technique's effectiveness for the suspected diagnosis, patient comfort, availability and cost constraints. Conceptually, all the modalities described in this publication can be placed under the same 'umbrella', within a given institution, or be part of different institutions, in which case integration and willingness for cooperation should start with the leadership of these different institutions. In any case, the most important aspect for cooperation is to develop a culture of teamwork to achieve the best patient management.

Another very important aspect is an awareness of the strengths and limitations of the different techniques to establish the grounds for fertile cooperation. Recently, publications on the appropriate use criteria for distinct modalities have become available (see Ref. [7.9]). These facilitate a better understanding of the best usage in specific clinical scenarios. Key aspects for the leadership team to consider for the successful integration of a multimodality team include:

— Building an environment to promote team work and cooperation;
— Connecting the entire team — those who are working directly with patients and those who are not;
— Promoting integration and cooperation instead of competition;
— Leadership behaving in a fair way with all team members;
— Developing a culture of quality and excellence within all departments;
— Training specialty residents from clinical programmes, especially cardiology fellows, on the basics of all modalities;
— Promoting appropriate use criteria for all imaging modalities.

7.3. FUTURE OF INTEGRATED CARDIOVASCULAR IMAGING

Cardiovascular imaging is at a crossroads. The value of integrated cardiovascular imaging in the current context of care now needs to be measured. Demonstrating the value of integrated cardiovascular imaging in improving clinical outcomes or improving the efficiency of diagnostic and/or management decisions is also warranted [7.10]. The implementation of integrated imaging into routine clinical practice would require multimodality imaging training and the creation of imaging departments or imaging centres [7.11].

Integrated cardiovascular imaging that is patient centred and disease driven will inevitably displace modality centred imaging paradigms in clinical practice. It is for imagers and clinicians to prepare adequately for this transition. The collaboration between cardiology, radiology and nuclear medicine specialists is key to the successful implementation of integrated cardiovascular imaging in clinical practice.

7.4. KEY MESSAGES

(1) Integrated cardiovascular imaging represents a shift away from individual imaging modalities, towards a disease specific approach.
(2) Its aim is to optimize clinical decision making by merging complementary information about a disease process.
(3) It should not be confused with multimodality fusion imaging and it does not require the integration of software or hardware platforms to fuse images from one modality to another.

REFERENCES TO CHAPTER 7

[7.1] DOUGLAS, P.S., et al., The future of cardiac imaging: Report of a think tank convened by the American College of Cardiology, J. Am. Coll. Cardiol. Cardiovasc. Imag. **9** (2016) 1211–1223.

[7.2] CHANDRASHEKHAR, Y., NARULA, J., To be or not to be a multimodality imager! J. Am. Coll. Cardiol. Cardiovasc. Imag. **10** (2017) 715–717.

[7.3] VITOLA, J.V., et al., Assessing the need for nuclear cardiology and other advanced cardiac imaging modalities in the developing world, J. Nucl. Cardiol. **16** (2009) 956–961.

[7.4] VITOLA, J.V., et al., Outcome of patients with high-risk Duke treadmill score and normal myocardial perfusion imaging on SPECT, J. Nucl. Cardiol. **23** (2016) 1291–1300.

[7.5] PATEL, M.R., et al., ACC/AATS/AHA/ASE/ASNC/SCAI/SCCT/STS 2017 appropriate use criteria for coronary revascularization in patients with stable ischaemic heart disease, J. Nucl. Cardiol. **24** (2017) 1759–1792.

[7.6] CHANG, S.M., et al., Value of CACS compared with ETT and myocardial perfusion imaging for predicting long-term cardiac outcome in asymptomatic and symptomatic patients at low risk for coronary disease: Clinical implications in a multimodality imaging world, J. Am. Coll. Cardiol. Cardiovasc. Imag. **8** (2015) 134–144.

[7.7] CHO, I., et al., Incremental prognostic utility of coronary CT angiography for asymptomatic patients based upon extent and severity of coronary artery calcium: Results from the Coronary CT Angiography Evaluation for Clinical Outcomes International Multicenter (CONFIRM) Study, Eur. Heart J. **36** (2015) 501–508.

[7.8] GREEN, R., et al., Negative predictive value of stress myocardial perfusion imaging and coronary computed tomography angiography: A meta-analysis, J. Nucl. Cardiol. **25** (2018) 1588–1597.

[7.9] VON KNOBELSDORFF-BRENKENHOF F., PILZ, G., SCHULZ-MENGER J., Representation of cardiovascular magnetic resonance in the AHA/ACC guidelines, J. Cardiovasc. Magn. Reson. **19** (2017) 70.

[7.10] HENDEL, R.C., et al., Appropriate use of cardiovascular technology: 2013 ACCF appropriate use criteria methodology update, J. Am. Coll. Cardiol. **61** (2013) 1305–1317.

[7.11] CHANDRASHEKHAR, Y., et al., Implementing multimodality imaging in the future, J. Am. Coll. Cardiol. Cardiovasc. Imag. **9** (2016) 91–98.

Chapter 8

APPROPRIATE USE OF NON-INVASIVE CARDIAC IMAGING TECHNIQUES

P. RAGGI, L.J. SHAW

The use of cardiovascular imaging has more than doubled in high income countries since 2010. Despite the frequently adduced reasoning that the population is ageing and the complexity of disease states is increasing, the exponential increase in imaging utilization has been regarded as the result of inappropriate overuse. Over time, this has caused a growing concern among payors and government agencies, as the cost of imaging has soared in the absence of clear indications that outcomes are being substantially affected. In an attempt to slow the growth in utilization, payors in North America began proposing drastic cuts to reimbursement for imaging procedures, and professional organizations responded by developing lists of appropriate indications for imaging. Problematically, various procedures were often deemed appropriate or inappropriate by a team of experts without the support of solid evidence. Guidelines from different organizations at times conflicted with one another, creating confusion among users. In addition, regional variations in technology availability and professional expertise rendered implementation difficult. As a result, the utilization of appropriate imaging has been slow to occur and remains inhomogeneous within some countries and regions. Emerging economies may face similar challenges as imaging technologies become more widely available, and they may benefit from some of the lessons identified in more economically advanced regions of the world.

8.1. FRAMEWORK OF APPROPRIATE IMAGING GUIDELINES

Imaging overutilization seems to be a concern for many countries [8.1]. In the absence of solid evidence that imaging has contributed to improving the outcome of cardiovascular disease, physicians are potentially facing severe restrictions to accessing it. Professional societies in North America have been involved for some time in creating a set of criteria to guide members using imaging modalities and to educate referring physicians as to their best application. The American College of Radiology issued the first set of guidelines in 1994 [8.2]. These were meant as a guide to referring doctors as to which test was best to answer the clinical question but not to which approach was the most appropriate to follow.

The American College of Cardiology and several other professional associations devised numerous structured guidelines concerning the appropriate application of echocardiography [8.3–8.6], nuclear cardiology [8.7], cardiac magnetic resonance imaging [8.8], and cardiac computed tomography (CT) [8.8, 8.9], multimodality imaging [8.10–8.12] and imaging for patients admitted with chest pain to the emergency department [8.13]. The need for constant updating of the guidelines makes them cumbersome and demands considerable effort. Regional differences in technology availability and professional expertise make the export of guidelines between countries and continents very problematic. Nonetheless, many countries have recognized the increasing importance of implementing some guidance for referring physicians to improve patient flow, reduce waste and reduce both direct risk (e.g. radiation exposure) and indirect risk (unnecessary further testing) for the patients. Since appropriate use criteria should be regarded as a living document owing to the need for frequent updates, many countries have adopted North American or European guidelines and adapted them to their realities [8.14–8.17].

There are several potential reasons for the expanding use of non-invasive testing: imaging is easy and perceived to be safe; patients often demand action of their physicians; and imaging is frequently included as part of their demands. Physicians may be ‘playing defensive medicine’ and may feel safer having ordered and obtained a test to exclude a condition even if the pre-test probability of disease is low. Finally, physicians may derive a financial incentive from referring patients to facilities they own or manage.

Several publications have reported a clear increase in image utilization. For example, a 5.5% yearly increase in de novo echocardiographic tests and a 10.6% yearly increase for repeat testing has been reported between 2001 and 2009 [8.18]. At a single North American centre, the prevalence of moderately to severely abnormal myocardial perfusion imaging (MPI) scans declined from 40.9% to 8.9% between 1991 and 2009 [8.19]; while a considerable amount of this reduction may have been due to successful therapies for coronary artery disease, there is a reasonable doubt that some of the decline may have been due to overuse of MPI. Intriguing, however, is the fact that other publications showed a lack of overutilization of imaging techniques even in situations where a more substantial use was required or recommended [8.20, 8.21]. The situation may be quite different in developing economies owing to the difficulty of accessing imaging techniques, or in countries with a growing incidence of atherosclerosis. In both instances, underutilization rather than overutilization of imaging is potentially harmful. In fact, underutilization may hamper the opportunity to make the correct diagnosis and to institute appropriate therapies, ultimately bringing harm to the patient. In this light, the appropriate use criteria proposed by

professional associations are not advocating the rationing of resources, but rather a rational implementation of imaging to achieve the best clinical results.

8.2. DEFINITION OF APPROPRIATENESS AND APPLICATION OF GUIDELINES

The RAND criteria define a procedure as being appropriate if the expected overall health benefits of performing it exceed the potential adverse consequences for the patient [8.22, 8.23]. The American College of Cardiology extended this definition to imaging and suggested that a test may be considered appropriate if the incremental information derived from it exceeds the potential negative consequences of its performance by a reasonably wide margin [8.24].

Appropriateness should be established through a process of consensus between the members of a panel who should consider the best possible evidence to reach an agreement [8.25]. Most guidelines are written in a manner that indicates that they are fairly flexible suggestions and are not meant to be prescriptive. This takes into consideration the fact that while a procedure may be more appropriate in a certain situation, another could or should be considered appropriate depending on technology availability and local expertise, among other factors.

There are several issues with the implementation of appropriate use criteria. The complex nature of the appropriate use criteria statements render them difficult to memorize and to apply for professionals who are not experts in the field. It has been reported that there was poor agreement between cardiologists and several other medical professionals in identifying the appropriateness of stress nuclear tests performed in a single academic medical centre [8.26]. Similarly, disagreement exists between imaging specialists with regard to the classification of appropriateness of echocardiography in as many as 31% of cases in a single academic medical centre with a very high volume of procedures [8.27]. Periodical updating of the appropriate use criteria is required to maintain their applicability to the constantly changing medical environment, and this complicates matters further. It is therefore important to put a significant effort into educating the users with a variety of on-line material, live seminars and other educational opportunities. To assess the adherence to guidelines after the American College of Cardiology had released several iterations of them, the trend in appropriateness between the first and second set of appropriate use criteria for several imaging procedures was compared [8.28]. The authors showed a significant increase in appropriate test ordering for CT angiography as well as for transthoracic echocardiography and transoesophageal echocardiography (although the improvement for the latter two techniques was

small), but no change for stress echocardiography and nuclear stress testing was seen [8.28]. There was no significant decline in the ordering of tests that could have been considered 'rarely appropriate' prior to the test based on the presence of defined indications [8.28]. Therefore, these data showed a modest effect of appropriate use criteria updates on physicians' attitude towards test ordering. The American College of Cardiology attempted to simultaneously educate providers and engage patients in the conversation about the utility of an indication for various procedures (not limited to imaging) by introducing the Choosing Wisely campaign. Four of the top five priorities involved educating users about avoiding unnecessary imaging procedures. A recent publication [8.29] reports the results of an intervention aimed at educating a sample of physicians in Canada and the United States of America on echocardiography appropriate use criteria, with the aim of reducing the ordering of procedures rarely appropriate. They conclude that the proportion of 'rarely appropriate' orders was significantly lower, albeit small in absolute terms, in the intervention group than in the control group (8.8% vs 10.1%, $p = 0.039$) [8.29]. Interestingly, the total volume of tests ordered by the intervention and control group was the same, hence the educational intervention did not reduce overall utilization. Despite the emphasis on improving the appropriateness of test ordering to date, there is very little evidence that adhering to the appropriate use criteria improves outcome. In fact, despite a mostly appropriate utilization of echocardiography at one academic centre, the results inspired a change in management in only one third of the cases [8.30], suggesting that the majority of tests were obtained for confirmatory reasons and could potentially have been avoided.

8.3. FUTURE DIRECTIONS

It has become increasingly clear that the management of imaging needs to change to protect access for physicians and patients to this vital component of medical care [8.31]. In this light, the value of imaging needs to be demonstrated beyond its ability to reach a correct diagnosis. In a value based system, imaging should become efficient and effective [8.32].

An efficient utilization of imaging requires the elimination of superfluous testing, such as testing that leads to more downstream imaging because of inaccurate or inconclusive information provided by the first test. 'Effective utilization' refers to a strategy that improves health outcomes for a given cost.

In most traditional cost effectiveness analyses, the output is measured in quality adjusted life years (QALY) gained, and it refers to the cost of extending a year of good quality life in a patient submitted to an intervention. There are several limitations to the concept of cost effectiveness when applied to imaging.

The most important one is the obvious fact that imaging does not save lives. Rather, it is the responsibility of the physician ordering the test and obtaining the results to act upon the information and to improve a patient's outcome. Of course, the test should have been obtained for the correct indication and should provide actionable information.

Another important limitation inherent in cost effectiveness analyses is the type and number of assumptions upon which the calculations are made. For example, the years of follow-up in studies used for the calculation of QALY may be as short as 2–5 years but the extrapolation is for a lifetime gain. The cost of imaging procedures may be quite different when considering private versus government based insurance plans and differ substantially from region to region. Finally, some analyses take into consideration all direct (i.e. imaging, medications, hospitalizations) and indirect costs (i.e. time for a patient to be off work), while others are less inclusive.

To demonstrate that imaging is of value in the care of a patient and should continue to be implemented, there is a need to conduct comparative effectiveness analyses where cost and outcome are compared. This type of assessment does not imply an automatic limitation of imaging access or the elimination of an imaging procedure because it is more costly upfront. In this methodology, the main strategy is to show that one approach compared with another obtains the same results at a lower cost, or with superior results if it is more expensive. Therefore, comparative analysis could be described as the selection of the best among competing choices [8.32].

Ultimately, to protect imaging from severe curtailing, a coordinated approach by physicians, professional organizations, payors and government agencies will be necessary [8.31]. There is a need to develop new outcome measures to demonstrate the value of imaging, since lifesaving per se is not the best goal, as discussed in this chapter [8.31]. Linking large outcome and imaging databases may help to establish the value of imaging using innovative approaches. The insertion of cascade ordering (i.e. a stepwise question and answer approach to ordering a test) in electronic medical systems should help with better implementation of appropriate use criteria [8.33]. More and better education of primary users and referring physicians as far as appropriate uses of imaging is desirable [8.34–8.36]. Collaboration between industry and government agencies to expand research initiatives and define new goals of research is highly advisable. Ultimately, the future of imaging is largely in the hands of the users, and it is up to them to demonstrate that its use is worth the expense to attain better health outcomes.

8.4. KEY MESSAGES

(1) The utilization of cardiovascular imaging has more than doubled in high income countries since 2010.
(2) The exponential increase in imaging utilization has been interpreted as partially due to inappropriate overuse.
(3) To curb the growth in utilization, payors in the United States of America introduced drastic cuts to reimbursement for imaging procedures and professional organizations developed lists of appropriate indications for imaging. Several more guidelines were also developed in Europe and in other parts of the world, albeit with a less systematic effort.
(4) Imaging recommendations are often based on the opinion of experts in the field rather than on solid data collected via randomized trials and different professional societies have at times issued conflicting recommendations.
(5) Regional variations in technology availability and professional expertise, as well as the difficulty of interpreting the guidelines, have reduced their effective and widespread implementation.
(6) In the current high income economic environment, imaging is expected to be efficient (eliminating superfluous testing) and effective (improving health outcomes for a reasonable cost).
(7) Comparative effectiveness refers to the selection of the best imaging option among competing choices to show that one approach compared with another obtains the same results at a lower cost, or with superior results if more expensive.
(8) Cascade test ordering should be inserted in electronic medical systems for a better implementation of guideline recommendations, and users should receive more in-depth education on appropriate uses of imaging.
(9) New outcome measures should be developed to demonstrate the value of imaging since ‘lifesaving’ is not the goal of imaging, but the result of implementing therapeutic measures in response to imaging information.
(10) The linkage of large clinical databases with imaging databases may help to establish the value of imaging.

REFERENCES TO CHAPTER 8

[8.1] EUROPEAN SOCIETY OF RADIOLOGY, Summary of the proceedings of the international forum 2016: “Imaging referral guidelines and clinical decision support — How can radiologists implement imaging referral guidelines in clinical routine?”, Insights Imag. **8** (2017) 1–9.

[8.2] CASCADE, P.N., Setting appropriateness guidelines for radiology, Radiology **192** (1994) 50A–54A.

[8.3] DOUGLAS, P.S., et al., ACCF/ASE/AHA/ASNC/HFSA/HRS/SCAI/SCCM/SCCT/SCMR 2011 appropriate use criteria for echocardiography, J. Am. Soc. Echocardiogr. **24** (2011) 229–267.

[8.4] DOUGLAS, P.S., et al., ACCF/ASE/ACEP/AHA/ASNC/SCAI/SCCT/SCMR 2008 appropriateness criteria for stress echocardiography, Circulation **117** (2008) 1478–1497.

[8.5] CAMPBELL, R.M., et al., ACC/AAP/AHA/ASE/HRS/SCAI/SCCT/SCMR/SOPE 2014 appropriate use criteria for initial transthoracic echocardiography in outpatient pediatric cardiology, J. Am. Coll. Cardiol. **64** (2014) 2039–2060.

[8.6] FLACHSKAMPF, F.A., et al., Recommendations for transoesophageal echocardiography: EACVI update 2014, Eur. Heart J. Cardiovasc. Imag. **15** (2014) 353–365.

[8.7] HENDEL, R.C., et al., ACCF/ASNC/ACR/AHA/ASE/SCCT/SCMR/SNM 2009 appropriate use criteria for cardiac radionuclide imaging, J. Am. Coll. Cardiol. **53** (2009) 2201–2229.

[8.8] HENDEL, R.C., et al., ACCF/ACR/SCCT/SCMR/ASNC/NASCI/SCAI/SIR 2006 appropriateness criteria for cardiac computed tomography and cardiac magnetic resonance imaging, J. Am. Coll. Cardiol. **48** (2006) 1475–1497.

[8.9] TAYLOR, A.J., et al., ACCF/SCCT/ACRA/AHA/ASE/ASNC/NASCI/SCAI/SCMR 2010 appropriate use criteria for cardiac computed tomography, Circulation **122** (2010) 525–555.

[8.10] DOHERTY, J.U., KORT, S., MEHRAN, R., SCHOENHAGEN, P., SOMAN, P., ACC/AATS/AHA/ASE/ASNC/HRS/SCAI/SCCT/SCMR/STS 2017 appropriate use criteria for multimodality imaging in valvular heart disease, J. Am. Coll. Cardiol. **70** (2017) 1647–1672.

[8.11] AKERS, S.R., et al., ACR Appropriateness Criteria chronic chest pain: High probability of coronary artery disease, J. Am. Coll. Radiol. **14** (2017) 71–80.

[8.12] COSYNS, B., et al., European Association of Cardiovascular Imaging (EACVI) position paper: Multimodality imaging in pericardial disease, Eur. Heart J. Cardiovasc. Imag. **16** (2015) 12–31.

[8.13] RYBICKI, F.J., et al., 2015 ACR/ACC/AHA/AATS/ACEP/ASNC/NASCI/SAEM/SCCT/SCMR/SCPC/SNMMI/STR/STS appropriate utilization of cardiovascular imaging in emergency department patients with chest pain, J. Am. Coll. Cardiol. **67** (2016) 853–879.

[8.14] ANDREINI, D., et al., Clinical recommendations on cardiac–CT in 2015: A position paper of the working group on Cardiac–CT and Nuclear Cardiology of the Italian Society of Cardiology, J. Cardiovasc. Med. **17** (2016) 73–84.

[8.15] YOON, Y.E., et al., 2014 Korean guidelines for appropriate utilization of cardiovascular magnetic resonance imaging: A joint report of the Korean Society of Cardiology and the Korean Society of Radiology, Korean Circ. J. **44** (2014) 359–385.

[8.16] KIM, Y.J., et al., Korean guidelines for the appropriate use of cardiac CT, Korean J. Radiol. **16** (2015) 251–285.

[8.17] BECK, K.S., et al., 2017 Multimodality appropriate use criteria for noninvasive cardiac imaging: Expert consensus of the Asian Society of Cardiovascular Imaging, Cardiovasc. Imag. Asia **1** (2017) 156–165.

[8.18] BLECKER, S., et al., Temporal trends in the utilization of echocardiography in Ontario, 2001 to 2009, J. Am. Coll. Cardiol. Cardiovasc. Imag. **6** (2013) 515–522.

[8.19] ROZANSKI, A., et al., Temporal trends in the frequency of inducible myocardial ischaemia during cardiac stress testing: 1991 to 2009, J. Am. Coll. Cardiol. **61** (2013) 1054–1065.

[8.20] FARMER, S.A., et al., Hospital-level variation in use of cardiovascular testing for adults with incident heart failure: Findings from the Cardiovascular Research Network Heart Failure Study, J. Am. Coll. Cardiol. Cardiovasc. Imag. **7** (2014) 690–700.

[8.21] KERR, E.A., CHEN, J., SUSSMAN, J.B., KLAMERUS, M.L., NALLAMOTHU, B.K., Stress testing before low-risk surgery: So many recommendations, so little overuse, JAMA Intern. Med. **175** (2015) 645–647.

[8.22] BROOK, R.H., et al., A method for the detailed assessment of the appropriateness of medical technologies, Int. J. Technol. Assess. Health Care **2** (1986) 53–63.

[8.23] FITCH, K., et al., The RAND/UCLA Appropriateness Method User's Manual, RAND Corporation, Santa Monica, CA (2001).

[8.24] HENDEL, R.C., et al., Appropriate use of cardiovascular technology: 2013 ACCF appropriate use criteria methodology update, J. Am. Coll. Cardiol. **61** (2013) 1305–1317.

[8.25] MURPHY, M.K., et al., Consensus development methods, and their use in clinical guideline development, Health Technol. Assess. **2** (1998) 1–88.

[8.26] YE, S., et al., Can physicians identify inappropriate nuclear stress tests? An examination of inter-rater reliability for the 2009 appropriate use criteria for radionuclide imaging, Circ. Cardiovasc. Qual. Outcomes **8** (2015) 23–29.

[8.27] AGGARWAL, N.R., WUTHIWAROPAS, P., KARON, B.L., MILLER, F.A., PELLIKKA, P.A., Application of the appropriateness criteria for echocardiography in an academic medical center, J. Am. Soc. Echocardiogr. **23** (2010) 267–274.

[8.28] FONSECA, R., NEGISHI, K., OTAHAL, P., MARWICK, T.H., Temporal changes in appropriateness of cardiac imaging, J. Am. Coll. Cardiol. **65** (2015) 763–773.

[8.29] BHATIA, R.S., et al., Improving the appropriate use of transthoracic echocardiography: The Echo WISELY trial, J. Am. Coll. Cardiol. **70** (2017) 1135–1144.

[8.30] MATULEVICIUS, S.A., et al., Appropriate use and clinical impact of transthoracic echocardiography, JAMA Intern. Med. **173** (2013) 1600–1607.

[8.31] DOUGLAS, P.S., et al., The future of cardiac imaging: Report of a think tank convened by the American College of Cardiology, J. Am. Coll. Cardiol. Cardiovasc. Imag. **9** (2016) 1211–1223.

[8.32] SHAW, L.J., Cost-effectiveness and future implications for cardiovascular imaging, Can. J. Cardiol. **29** (2013) 350–357.

[8.33] LIN, F.Y., et al., Impact of an automated multimodality point-of-order decision support tool on rates of appropriate testing and clinical decision making for individuals with suspected coronary artery disease: A prospective multicenter study, J. Am. Coll. Cardiol. **62** (2013) 308–316.

[8.34] DUDZINSKI, D.M., et al., Effect of educational intervention on the rate of rarely appropriate outpatient echocardiograms ordered by attending academic cardiologists: A randomized clinical trial, JAMA Cardiol. **1** (2016) 805–812.

[8.35] BHATIA, R.S., MILFORD, C.E., PICARD, M.H., WEINER, R.B., An educational intervention reduces the rate of inappropriate echocardiograms on an inpatient medical service, J. Am. Coll. Cardiol. Cardiovasc. Imag. **6** (2013) 545–555.

[8.36] BHATIA, R.S., DUDZINSKI, D.M., MILFORD, C.E., PICARD, M.H., WEINER, R.B., Educational intervention to reduce inappropriate transthoracic echocardiograms: The need for sustained intervention, Echocardiography **31** (2014) 916–923.

Chapter 9

CURRENT EVIDENCE AND LESSONS LEARNED FROM RANDOMIZED TRIALS IN CARDIOVASCULAR IMAGING

L.J. SHAW, M.C. WILLIAMS, C. BUCCIARELLI-DUCCI

Cardiovascular disease imparts a heavy financial burden and impacts the lives of millions of patients around the world, leading to loss of societal productivity coupled with premature morbidity and mortality [9.1, 9.2]. For imaging to contribute to a healthier patient population, new standards require a demonstrable impact on important clinical outcomes. This chapter highlights the rationale for employing clinical trials in cardiovascular imaging and provide recent examples of net health benefit resulting from non-invasive strategies of cardiovascular care in published literature. Although in decades past, the available clinical trial evidence was less developed, currently there is robust evidence that the use of cardiovascular imaging can guide clinical management decisions and, in some cases, improve clinical outcomes [9.3, 9.4]. Preceding a discussion of available clinical trials, some guidelines will be described as to evidentiary standards applied in cardiovascular imaging and the hierarchy of quality for evaluating clinical trials and registries. This will be followed by a description of how evidence standards evolve and makes the transition from observational findings to impacting patient outcome. Finally, an overview of existing clinical trials and how they contribute to devising appropriate indications for cardiovascular imaging and guided therapeutic strategies of care will be presented.

9.1. HIERARCHY OF CLINICAL RESEARCH EVIDENCE IN CARDIOVASCULAR IMAGING

The guidelines in this chapter are to be considered in the context of evidentiary standards and prioritizations in medicine. Figure 9.1 depicts a pyramid of evidence revealing a ranking of lower quality to high quality evidence for cardiovascular imaging. Importantly for this discussion, randomized trials are the highest level of evidence and have the most consequential implications for imaging guided strategies [9.5]. However, readers should note that this pyramid reflects how evidence is developed; that is, the single site series can lead to multicentre registries and then to clinical trials as one piece of evidence contributes to an unfolding of higher and higher quality evidence.

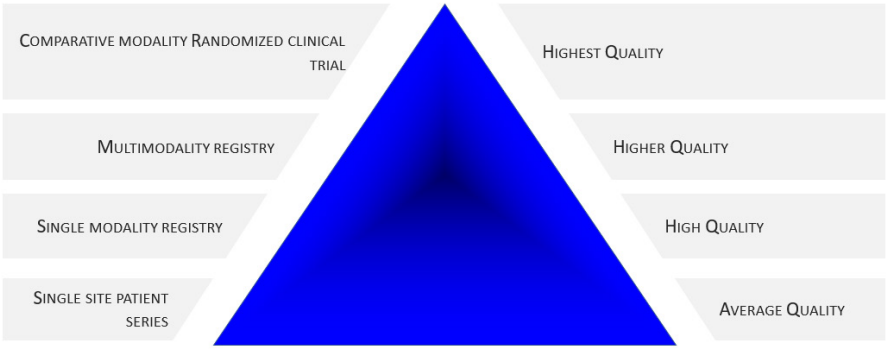

FIG. 9.1. Quality ranking of cardiovascular imaging evidence. Source: see fig. 3 of Ref. [9.5].

An understanding of this hierarchy can allow the reader to appreciate the quality ranking for all evidence.

The primary rationale for supporting randomized trials pertains to the minimal impact of selection and other biases on the final results. For observational series, clinical outcome differences, such as higher or lower mortality, are not only influenced by imaging but also by clinical factors such as age, risk factors and related comorbidities. However, in a randomized trial of an anatomical versus a functional imaging procedure, for example, differences in outcome can be directly compared because clinical factors should be similarly distributed between the two arms of the trial. The result is that the differences in outcome are not mitigated by other clinical factors, but exist owing to differences between the imaging guided strategies. Care should be taken to understand that complicated clinical trials may have issues of generalizability owing to the challenges and selectivity of enrolment.

9.2. EVIDENTIARY STANDARDS FOR QUALITY CARDIOVASCULAR IMAGING

The hierarchy of evidence shown in Fig. 9.1 is important, since it relates to the development of clinical indications for testing (see Chapter 8 for a detailed discussion on the appropriate indications for cardiovascular imaging). Appropriateness criteria rely on high quality evidence to develop ‘appropriate’ indications and, where data are lacking, ‘rarely appropriate’ indications. For example, as high quality evidence is available for stable ischaemic heart disease, many indications are deemed appropriate for the evaluation of symptomatic patients. However, evidence is either lacking or insufficient for the evaluation

of asymptomatic individuals, and for this reason these indications are generally categorized as 'rarely appropriate'. This chapter contributes to discussions on clinical trials as the available evidence forms the basis for assigning an indication as appropriate or not.

Thus, in general, the higher the levels of evidence, the more likely a test indication will be appropriate, and this will also correspond to support within clinical practice guidelines. A more detailed description of developing quality standards has recently been published by the American Heart Association Cardiovascular Imaging and Intervention Subcommittee [9.5].

9.3. LESSONS LEARNED FROM OBSERVATIONAL DATA: EXAMPLES IN NUCLEAR CARDIOLOGY

When a new technology is developed, it is incumbent upon all relevant stakeholders to initiate the process of evidence development. This is important for varying populations around the world. A greater understanding of diagnostic accuracy or risk stratification in diverse populations remains core to developing observational evidence that contributes to the development of clinical trials. This foundation of observational data in guiding clinical trial design is important so that findings can directly impact clinical practice. There are several examples of this in the published literature that can help to guide the reader's understanding of developing evidentiary standards.

One example is the application of stress myocardial perfusion imaging (MPI) for the evaluation of stable ischaemic heart disease [9.6, 9.7]. The development of this evidence has contributed greatly to the development of numerous class I indications and appropriate use criteria for stable ischaemic heart disease. These indications were based on decades of observational findings that began with single centre data on the diagnostic accuracy of stress MPI in smaller patient series and were followed by larger, prognostic series including multicentre and multinational registries, and later by controlled and randomized clinical trial evidence. Over this period of time, the observational registries increased in size and number as participating centres allowed for greater representation of diverse patient cohorts. Moreover, the larger sample sizes also allowed for comparison of differences in cardiovascular mortality, which is often not possible in smaller patient cohorts. In these larger cohorts, exploratory analysis evaluated therapeutic risk reduction with coronary revascularization versus medical therapy [9.8–9.10]. This observational evidence was instrumental in providing supportive evidence that was later used in the design of several therapeutic randomized trials for stable ischaemic heart disease [9.11, 9.12].

9.4. DEFINING COMPARATIVE EFFECTIVENESS

There is an important difference and consideration between a controlled clinical trial and a randomized clinical trial. A controlled clinical trial includes rigorous data collection where patients may undergo one or more cardiovascular imaging procedures. An example of a controlled clinical trial is the Evaluation of Integrated Cardiac Imaging for the Detection and Characterization of Ischemic Heart Disease (EVINCI) trial [9.13], which compared the diagnostic accuracy achieved in 475 patients undergoing coronary computed tomography angiography (CCTA) plus one or more stress imaging procedures (stress MPI, echocardiography or cardiac magnetic resonance, CMR) and invasive coronary angiography. The rigour of this design with its mandatory testing places it in the controlled clinical trial category; however, there was no randomization in this trial.

By comparison, several recent examples of randomized clinical trials have been published, such as the Scottish Computed Tomography of the Heart (SCOT-HEART) trial [9.14] and the Prospective Multicenter Imaging Study for Evaluation of Chest Pain (PROMISE) [9.15]. In the PROMISE trial, there was a randomization of more than 10 000 patients to an anatomical (non-invasive CCTA) compared with a functional testing (stress electrocardiography, echocardiography or stress myocardial perfusion single photon emission computed tomography, SPECT) strategy [9.16]. In the PROMISE trial, the primary comparison was the effectiveness of the anatomical versus functional testing strategy at 2–3 years of follow-up; the primary endpoint was death, myocardial infarction or procedural complications. Both trials are discussed in more detail later in this chapter. These two types of trial are examples of the highest quality cardiovascular imaging evidence. Randomized trials that compare one imaging test or strategy with another, such as the example of the PROMISE trial, are also considered comparative effectiveness trials. For imaging, a comparative effectiveness trial includes randomization to one test versus another, with follow-up including data collection of primary or secondary events for a duration (e.g. around three years of follow-up). In the example of the SCOT-HEART trial, the standard care strategy was compared with a CCTA guided strategy with follow-up observing the incidence of death related to heart disease or of non-fatal myocardial infarction over 1.7 years [9.14].

9.5. EXAMPLES OF CONTROLLED CLINICAL TRIALS

There are several examples in the literature on controlled clinical trials, with several prominent examples of diagnostic accuracy trials. In addition to the EVINCI trial [9.13], there is the Prospective Comparison of Cardiac PET–CT,

SPECT–CT Perfusion Imaging and CT Coronary Angiography with Invasive Coronary Angiography (PACIFIC) [9.16], the primary endpoint of which was diagnostic accuracy of CCTA, stress myocardial perfusion positron emission tomography (PET) or SPECT and hybrid imaging in relation to fractional flow reserve (FFR) measurement during invasive coronary angiography. For PET, an impaired hyperaemic blood flow of less than 2.30 $mL \cdot min^{-1} \cdot g^{-1}$ indicated ischaemic abnormalities, while SPECT employed standard segmental scoring for interpretation of ischaemic pathology [9.16]. The diagnostic accuracy results from the PACIFIC trial are shown in Fig. 9.2 and reveal a high accuracy of PET coronary flow reserve (CFR) in relation to invasive FFR.

9.6. EXAMPLES OF COMPARATIVE EFFECTIVENESS TRIALS

There are numerous examples of comparative effectiveness trials and a few are mentioned here to demonstrate the findings that can result from such trials. A recent review of this type of trial has been published [9.4] and selected stable ischaemic heart disease trials are reported in terms of their primary findings in Table 9.1.

These ischaemic heart disease trials largely failed to identify a significant difference between the effectiveness of a variety of diagnostic test strategies. In the What is the Optimal Method for Ischemia Evaluation in Women (WOMEN) trial [9.18], around 800 low to intermediate risk, symptomatic women were

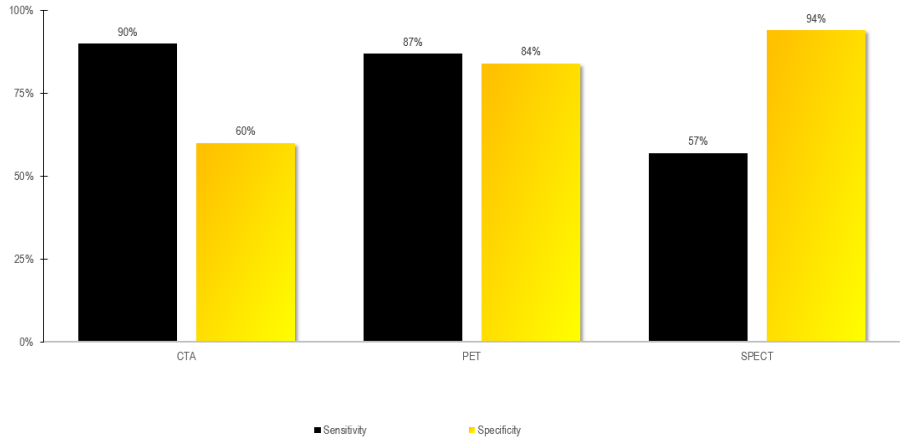

FIG. 9.2. Diagnostic accuracy results from the PACIFIC trial: Comparing imaging findings with invasive determination of fractional flow reserve.

TABLE 9.1. RECENT RANDOMIZED TRIALS IN STABLE ISCHAEMIC HEART DISEASE [9.4]

Trial	Randomization	*N*	Major endpoint	Trial *p* value
CRESCENT [9.17]	Coronary artery calcium plus selective CCTA in patients with coronary artery calcium > 0 vs ETT	350	1 year all-cause mortality, myocardial infarction, major stroke, unstable angina, unplanned CAD evaluation or late revascularization	0.011 favouring coronary artery calcium plus CCTA arm
PROMISE [9.15]	Anatomical (CCTA) vs functional test 67% nuclear 23% echocardiography 10% ETT	10 003	2.1 year death, myocardial infarction, unstable angina hospitalization or major complications	0.75
SCOT-HEART [9.14]	Standard evaluation vs CCTA	4 146	1.7 year coronary heart disease death or myocardial infarction	0.053
WOMEN [9.18]	Exercise SPECT vs ETT	824	2 year CAD death, myocardial infarction or hospitalization for acute coronary syndrome or heart failure	0.59

Note: CAD — coronary artery disease; CCTA — coronary computed tomography angiography; ETT — exercise treadmill/bicycle test; SPECT — single photon emission computed tomography.

randomized to exercise myocardial perfusion SPECT vs electrocardiography and were followed for major cardiovascular disease events for two years, revealing no differences in the primary endpoint ($p = 0.59$). The take home message from this trial was that in a lower risk, symptomatic woman, the use of the exercise treadmill/bicycle test (ETT) is a safe and equally effective test when compared with exercise myocardial perfusion SPECT.

A similar take home message may also be drawn from the SCOT-HEART and PROMISE trials [9.14, 9.19]. That is, that an anatomical strategy was similarly effective at 2–3 years of follow-up when compared with standard testing approaches, such as ETT or stress myocardial perfusion SPECT. However, there

are important differences between these two latter trials that are noteworthy, including the prevalence of obstructive CAD, which was 12% in the PROMISE and 42% in the SCOT-HEART trial. Thus, PROMISE enrolled a very low risk group, while SCOT-HEART enrolled an intermediate risk group, which might be the reason for the borderline *p* value in the SCOT-HEART trial. It may be that SCOT-HEART, which continued longer term follow-up, may further expand the differences between CCTA and standard testing approaches.

Not included in this review is the Clinical Evaluation of Magnetic Resonance Imaging in Coronary Heart Disease 2 (CE-MARC 2) trial [9.20], published in 2015. This multicentre, randomized controlled trial enrolled 1200 intermediate risk patients to one of three arms, including stress CMR imaging, myocardial perfusion SPECT or guideline directed care (based on the 2012 UK National Institute of Clinical and Healthcare Excellence Stable Chest Pain guidelines) [9.21]. Within the latter arm of guideline directed care, the testing algorithm included the use of CCTA for patients with a low pre-test risk, myocardial perfusion SPECT for an intermediate risk and invasive angiography for those with a high pre-test risk. The primary endpoint for the CE-MARC 2 trial was unnecessary, invasive coronary angiography defined by a preserved FFR value of greater than 0.80. Primary findings from CE-MARC 2 revealed similar 12 month rates of unnecessary invasive angiography for stress CMR and SPECT imaging (7.1% and 7.5%), but substantial higher rates of preserved FFR at angiography for those assigned to the guideline arm (28.8%). In fact, the use of stress CMR resulted in a nearly 80% relative odds reduction in the primary endpoint of unnecessary invasive angiography when compared with the guideline directed arm of the trial ($p < 0.001$).

These trials illustrate the complexity of trial design and, importantly, the challenges of deriving a clinical benefit for cardiovascular imaging patient cohorts. An exception to this is the Computed Tomography Versus Exercise Testing in Suspected Coronary Artery Disease (CRESCENT), published in 2016 [9.17], which enrolled 350 symptomatic patients and randomly allocated them to a strategy of selected CCTA (following an index coronary artery calcium scan) versus ETT. Clinical outcomes were defined as all-cause mortality, myocardial infarction, stroke, unstable angina, unplanned coronary artery disease (CAD) evaluation (e.g. emergency department visit) or late revascularization (beyond 90 days of follow-up). The results of this trial revealed a 68% relative risk reduction with index calcium scanning followed by selective CCTA as compared with ETT. At approximately one year of follow-up, event free survival was 97% for the selective CCTA arm as compared with 90% for the ETT arm ($p = 0.011$).

The Myocardial Perfusion CMR versus Angiography and FFR to Guide the Management of Patients with Stable Coronary Artery Disease (MR-INFORM) trial [9.22] enrolled a total of 918 stable chest pain patients randomized to stress

magnetic resonance perfusion imaging versus invasive coronary angiography with FFR guided care. The primary endpoint was all-cause mortality, myocardial infarction and repeat target vessel revascularization. Importantly, this trial was powered for non-inferiority of stress CMR as compared with invasive angiography, and the results revealed no difference in the primary endpoint at one year of follow-up ($p = 0.62$). These results reveal that the use of stress MRI is as safe and effective as an index evaluation strategy of invasive coronary angiography plus FFR. This trial added further support to non-invasive imaging as an index evaluation strategy being equally effective as invasive angiography.

These recent trials show promise that imaging guided strategies may be developed and that future adaptations to existing trial designs may more effectively link testing to therapeutic care so that improved clinical outcomes may ensue.

9.7. THERAPEUTIC RISK REDUCTION: GUIDING THERAPEUTIC DECISION MAKING

There are other randomized trials that employ imaging as an integral component of eligibility criteria, such as those trials comparing imaging ischaemia guided therapeutic strategies of medical therapy with coronary revascularization. There are two completed trials and an ongoing randomized trial that have compared ischaemia guided management approaches [9.11, 9.12]. These trials emulate the clinical evaluation algorithm for stable chest pain that includes index documentation of stress induced ischaemia followed by coronary angiography and either guideline directed medical therapy or coronary revascularization. Examples of these stable ischaemic heart disease trials are the Bypass Angioplasty Revascularization Investigation in Type 2 Diabetes (BARI 2D) trial [9.11] and the Clinical Outcomes Utilizing Revascularization and Aggressive Drug Evaluation (COURAGE) trial [9.12]. Both of these trials revealed no significant difference between medical therapy and revascularization at an approximately five year follow-up. Importantly, strict criteria in terms of a threshold level of ischaemia were not defined for either of these trials [9.23]. The International Study of Comparative Health Effectiveness with Medical and Invasive Approaches (ISCHEMIA), a recently completed randomized trial, employed a threshold of moderate–severe ischaemia (≥10% ischaemic myocardium on SPECT or PET, multisegmental wall motion abnormalities on stress echo and 2 mm or more ST segment depression on a stress electrocardiogram) as eligibility criteria along with a resting left ventricular ejection fraction (LVEF) of 35% or higher [9.24]. Subsequent randomization to an invasive strategy was compared with a conservative strategy as detailed in Fig. 9.3. The trial showed equipoise between an invasive and a conservative strategy for the management of patients

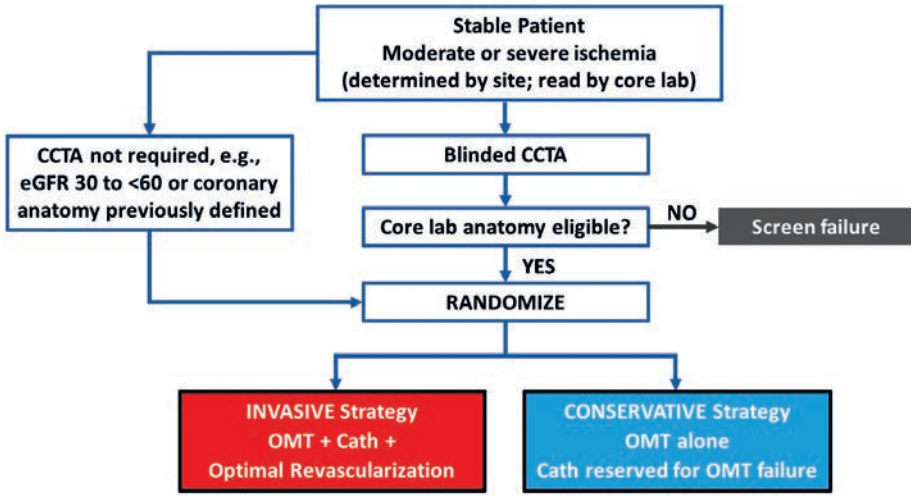

FIG. 9.3. ISCHEMIA trial comparison of an invasive versus a conservative strategy in eligible patients with moderate–severe ischaemia. The primary aim of the trial was to determine whether an initial invasive strategy of catherization (Cath) plus revascularization with optimal medical therapy (OMT) is superior to a conservative strategy of optimal medical therapy alone. CCTA — coronary computed tomography angiography; eGFR — estimated glomerular filtration rate. Source: see fig. 1 of Ref. [9.24].

with stable angina for the composite outcome of death from cardiovascular causes, myocardial infarction, or hospitalization for unstable angina, heart failure or resuscitated cardiac arrest.

9.8. ASSIMILATING EVIDENCE INTO EVALUATION ALGORITHMS

In several chapters in this publication, the authors identify strategic pathways or evaluation algorithms relating to a variety of clinical conditions in cardiovascular disease (see Refs [9.17, 9.25–9.30]). It remains vital for the cardiovascular imaging community to integrate clinical evidence into evaluation algorithms (see Fig. 9.3) so that both referring physicians and imagers may identify strategic opportunities to employ high quality evidence in routine daily clinical decision making with regard to optimal referral patterns to the imaging laboratory. Based on future trial findings, an optimal strategy will be highlighted and reflected in guideline accepted standards, and then accepted as an appropriate indication (in this case) for an invasive strategy (or not). Additional key findings may subsequently alter this evaluation algorithm.

9.9. KEY MESSAGES

(1) Comparative trials showed similar diagnostic accuracy of CCTA, SPECT and PET for the detection of obstructive CAD.
(2) There is a high degree of concordance between CCTA and invasive coronary angiography for the detection of obstructive lesions.
(3) Clinical trials are increasingly applying lesion specific ischaemia measurement with invasive FFR as the diagnostic endpoint. Invasive FFR, stress MRI and nuclear cardiology techniques have a high diagnostic accuracy.
(4) The comparative effectiveness of anatomical versus functional imaging strategies has been evaluated in recent randomized trials. In these trials, the non-invasive strategies included CCTA as the anatomical procedure, while functional testing approaches included ETT, stress myocardial perfusion SPECT and stress echocardiography. A synthesis of these trials reveals similar effectiveness and equivalent rates of cardiovascular disease outcomes at 2–3 years of follow-up. Thus, for a diagnostic evaluation of stable chest pain, both stress testing and CCTA are equally supported by randomized trial evidence.
(5) In lower risk symptomatic patients, a selective strategy of first determining the coronary artery calcium score (CACS) followed by selective imaging may improve clinical management and promote cost savings when compared with ETT.

REFERENCES TO CHAPTER 9

[9.1] FUSTER, V., Changing demographics: A new approach to global health care due to the aging population, J. Am. Coll. Cardiol. **69** (2017) 3002–3005.
[9.2] FUSTER, V., KELLY, B.B., VEDANTHAN, R., Global cardiovascular health: Urgent need for an intersectoral approach, J. Am. Coll. Cardiol. **58** (2011) 1208–1210.
[9.3] DOUGLAS, P.S., SHAW, L.J., NARULA, J., Randomized trials in cardiovascular imaging: Where to next? J. Am. Coll. Cardiol. Cardiovasc. Imag. **10** (2017) 381–383.
[9.4] SHAW, L.J., et al., Comparative effectiveness trials of imaging-guided strategies in stable ischemic heart disease, J. Am. Coll. Cardiol. Cardiovasc. Imag. **10** (2017) 321–334.
[9.5] SHAW, L.J., et al., Defining quality in cardiovascular imaging: A scientific statement from the American Heart Association, Circ. Cardiovasc. Imag. **10** (2017).
[9.6] FIHN, S.D., et al., 2012 ACCF/AHA/ACP/AATS/PCNA/SCAI/STS guideline for the diagnosis and management of patients with stable ischemic heart disease, J. Am. Coll. Cardiol. **60** (2012) 2564–2603.

[9.7] WOLK, M.J., et al., ACCF/AHA/ASE/ASNC/HFSA/HRS/SCAI/SCCT/SCMR/STS 2013 multimodality appropriate use criteria for the detection and risk assessment of stable ischemic heart disease, J. Am. Coll. Cardiol. **63** (2014) 380–406.

[9.8] HACHAMOVITCH, R., HAYES, S.W., FRIEDMAN, J.D., COHEN, I., BERMAN, D.S., Comparison of the short-term survival benefit associated with revascularization compared with medical therapy in patients with no prior coronary artery disease undergoing stress myocardial perfusion single photon emission computed tomography, Circulation **107** (2003) 2900–2907.

[9.9] HACHAMOVITCH, R., et al., Impact of ischaemia and scar on the therapeutic benefit derived from myocardial revascularization vs medical therapy among patients undergoing stress–rest myocardial perfusion scintigraphy, Eur. Heart J. **32** (2011) 1012–1024.

[9.10] HACHAMOVITCH, R., et al., Predicting therapeutic benefit from myocardial revascularization procedures: Are measurements of both resting left ventricular ejection fraction and stress-induced myocardial ischaemia necessary? J. Nucl. Cardiol. **13** (2006) 768–778.

[9.11] BARI 2-D STUDY GROUP, et al., A randomized trial of therapies for type 2 diabetes and coronary artery disease, N. Engl. J. Med. **360** (2009) 2503–2515.

[9.12] BODEN, W.E., et al., Optimal medical therapy with or without PCI for stable coronary disease, N. Engl. J. Med. **356** (2007) 1503–1516.

[9.13] NEGLIA, D., et al., Detection of significant coronary artery disease by noninvasive anatomical and functional imaging, Circ. Cardiovasc. Imag. **8** (2015).

[9.14] SCOT-HEART INVESTIGATORS, CT coronary angiography in patients with suspected angina due to coronary heart disease (SCOT-HEART): An open-label, parallel-group, multicentre trial, Lancet **385** (2015) 2383–2391.

[9.15] DOUGLAS, P.S., et al., Outcomes of anatomical versus functional testing for coronary artery disease, N. Engl. J. Med. **372** (2015) 1291–1300.

[9.16] DANAD, I., et al., Comparison of coronary CT angiography, SPECT, PET, and hybrid imaging for diagnosis of ischemic heart disease determined by fractional flow reserve, JAMA Cardiol. **2** (2017) 1100–1107.

[9.17] LUBBERS, M., et al., Calcium imaging and selective computed tomography angiography in comparison to functional testing for suspected coronary artery disease: The multicentre, randomized CRESCENT trial, Eur. Heart J. **37** (2016) 1232–1243.

[9.18] SHAW, L.J., et al., Comparative effectiveness of exercise electrocardiography with or without myocardial perfusion single photon emission computed tomography in women with suspected coronary artery disease: Results from the What is the Optimal Method for Ischemia Evaluation in Women (WOMEN) trial, Circulation **124** (2011) 1239–1249.

[9.19] HOFFMANN, U., et al., Prognostic value of noninvasive cardiovascular testing in patients with stable chest pain: Insights from the PROMISE trial (Prospective Multicenter Imaging Study for Evaluation of Chest Pain), Circulation **135** (2017) 2320–2332.

[9.20] RIPLEY, D.P., et al., Rationale and design of the Clinical Evaluation of Magnetic Resonance Imaging in Coronary Heart Disease 2 trial (CE-MARC 2): A prospective, multicenter, randomized trial of diagnostic strategies in suspected coronary heart disease, Am. Heart J. **169** (2015) 17–24.

[9.21] DANCY, L., O'GALLAGHER, K., MILTON, P., SADO, D., New NICE guidelines for the management of stable angina, Br. J. Gen. Pract. **68** (2018) 202–203.

[9.22] HUSSAIN, S.T., et al., Design and rationale of the MR-INFORM Study: Stress perfusion cardiovascular magnetic resonance imaging to guide the management of patients with stable coronary artery disease, J. Cardiovasc. Magn. Reson. **14** (2012) 65.

[9.23] MARON, D.J., et al., Initial invasive or conservative strategy for stable coronary disease, N. Engl. J. Med. **382** (2020) 1395–1407.

[9.24] MARON, D.J., et al., International Study of Comparative Health Effectiveness with Medical and Invasive Approaches (ISCHEMIA) trial: Rationale and design, Am. Heart J. **201** (2018) 124–135.

[9.25] KARTHIKEYAN, G., et al., Functional compared to anatomical imaging in the initial evaluation of patients with suspected coronary artery disease: An international, multi-center, randomized controlled trial (IAEA–SPECT/CTA study), J. Nucl. Cardiol. **24** (2017) 507–517.

[9.26] EINSTEIN, A.J., et al., Current worldwide nuclear cardiology practices and radiation exposure: Results from the 65 country IAEA Nuclear Cardiology Protocols Cross-sectional Study (INCAPS), Eur. Heart J. **36** (2015) 1689–1696.

[9.27] MIN, J.K., et al., Age- and sex-related differences in all-cause mortality risk based on coronary computed tomography angiography findings results from the international multicenter CONFIRM (coronary CT angiography evaluation for clinical outcomes: An international multicenter registry) of 23,854 patients without known coronary artery disease, J. Am. Coll. Cardiol. **58** (2011) 849–860.

[9.28] RIZVI, A., et al., Rationale and design of the CREDENCE trial: Computed Tomographic Evaluation of Atherosclerotic Determinants of Myocardial Ischaemia, BMC Cardiovasc. Disord. **16** (2016) 190.

[9.29] SCHULMAN-MARCUS, J., et al., Sex-specific associations between coronary artery plaque extent and risk of major adverse cardiovascular events: The CONFIRM long-term registry, J. Am. Coll. Cardiol. Cardiovasc. Imag. **9** (2016) 364–372.

[9.30] LEE, S.-E., LIN, F.Y., LU, Y., CHANG, H.-J., MIN, J.K., Rationale and design of the coronary computed tomographic angiography for selective cardiac catheterization: Relation to cardiovascular outcomes, cost effectiveness and quality of life (CONSERVE) trial, Am. Heart J. **186** (2017) 48–55.

Chapter 10

STABLE CORONARY ARTERY DISEASE

M.C. WILLIAMS, J. VITOLA, F. KENG, L.J. SHAW

Coronary artery disease (CAD) is most commonly caused by atherosclerotic plaque within the coronary arteries, which causes luminal narrowing and subsequent reduction in the blood flow to the myocardium. Ischaemic heart disease is another commonly used term for this condition, referring to the subsequent myocardial ischaemia rather than the causative disease in the coronary arteries. Other causative aetiologies for ischaemia include vasospasm, microvascular dysfunction, hypertensive disease, cardiomyopathies, thrombotic disease and coronary artery dissection.

'Stable CAD' refers to patients with symptoms related to CAD but without recent acute coronary syndrome (ACS). This has been defined as the presence of no ACS within the preceding three months. In clinical practice, there may be overlap between patients with stable CAD and ACS. This chapter covers the investigation of adult patients with known or suspected stable CAD, including those with new onset symptoms. It also covers asymptomatic patients, incidentally detected disease and pre-operative assessment.

Cardiovascular disease affects one in three adults and accounts for 31% of global deaths [10.1]. Among cardiovascular diseases, CAD is a major cause of morbidity and mortality globally [10.2]. The incidence of myocardial infarction and the related mortality rate have declined significantly over time in high income countries, mainly owing to initial treatment and primary and secondary preventive therapies. Conversely, mortality is either increasing or unchanged in some low to middle income countries [10.3]. Thus, the prevalence of CAD has remained relatively constant worldwide [10.4] and is projected to increase by 2030 [10.5]; and therefore the investigation of patients with stable CAD is an important clinical dilemma.

10.1. CLINICAL PRESENTATION

The clinical presentation of patients with CAD ranges from the asymptomatic presence of CAD to patients with ACS and myocardial infarction; it can also be responsible for sudden cardiac death. Chest pain is a common presentation and is responsible for over 1% of primary care consultations [10.6] and 6% of accident and emergency department attendances [10.7]. Key features in the evaluation of

TABLE 10.1. SYMPTOMS OF STABLE CORONARY ARTERY DISEASE [10.8]

Definition	Symptoms
Typical angina	Constricting discomfort in the chest, neck, shoulders, jaw or arms Triggered by physical exertion Relived by rest or glyceryl trinitrate within 5 minutes
Atypical angina	Two of the above features
Non-anginal chest pain	One or none of the above features
Other symptoms related to CAD (angina equivalent)	Breathlessness, pain in other locations, autonomic symptoms, non-specific features

chest pain include the type, location, severity and radiation of the pain along with the presence of associated symptoms. Features of anginal chest pain is classically described (see Table 10.1) and can be used to divide symptoms of chest pain into typical angina, atypical angina and non-anginal chest pain. Patients with CAD may present with symptoms other than chest pain such as breathlessness, pain in other locations, autonomic symptoms or non-specific features [10.8]. These features have been described as angina equivalent. Such alternative presentations of CAD are more frequent in patients with diabetes and in female and elderly patients [10.9]. They may also be misdiagnosed as secondary to respiratory or gastrointestinal diseases, thus leading to the undertreatment of important disease.

10.2. RISK PREDICTION MODELS AND PRE-TEST PROBABILITY

Since the 1990s, risk prediction and pre-test probability models have been an important component of the management of patients with chest pain [10.10]. Risk prediction models, such as the Framingham coronary heart disease risk score or Systematic Coronary Risk Evaluation (SCORE) risk charts are used to predict the risk of future events.[1] Pre-test probability models, such as the Diamond–Forrester model, are used to define the probability of having CAD and can divide patients into low risk, intermediate risk and high risk groups [10.11]. However, there are significant limitations in the use of these models.

[1] See www.heartscore.org

10.2.1. Advantages of prediction models

Pre-test probability and risk prediction models can be used to select patients for further investigation and to address treatments that can improve outcomes. In addition, patients at particularly low risk can be discharged without further investigations. A variety of pre-test probability and risk prediction models are available.

10.2.2. Disadvantages of prediction models

Prediction models are inherently limited by the data that are used to create them. Many of these models were developed prior to the availability of current imaging modalities or treatment options. In addition, they include a limited range of patients in terms of age, sex distribution and ethnicity [10.12]. Several prediction models have been found to be inadequate in population risk stratification. For example, the Diamond–Forrester model overestimates the probability of CAD, particularly in women and low risk populations [10.13]. In addition, among the population of patients referred with a clinical suspicion of CAD, many have a pre-test probability based on these prediction models of between 10% and 90%, and thus would benefit from further investigation.

10.3. ROLE OF BASIC INVESTIGATIONS

Basic investigations may be useful for patients with suspected CAD. These include:

— Blood pressure assessment;
— Blood tests;
— Chest X ray if pulmonary disease is suspected;
— Resting electrocardiogram (ECG) if stable CAD is suspected;
— Resting echocardiography if valvular heart disease or cardiomyopathy is suspected.

10.4. ROLE OF NON-INVASIVE IMAGING IN CLINICAL DECISION MAKING

Non-invasive imaging for patients with CAD can be used:

— To diagnose CAD;
— To identify the presence of normal coronary arteries;

— To assess the severity of CAD;
— To select patients appropriately for invasive coronary angiography who may benefit from revascularization;
— To guide and monitor treatment;
— To risk stratify patients prior to high risk non-cardiovascular surgery;
— To risk stratify patients after myocardial infarction;
— To risk stratify patients prior to invasive or non-invasive valvular surgery.

There are now many imaging modalities available to assess CAD [10.14–10.23]. Their advantages and disadvantages are listed in Table 10.2. Technical information with regard to the imaging modalities can be found in Part I, including the use of exercise or pharmacological stress agents. The selection of appropriate imaging tests is discussed in Chapter 8.

TABLE 10.2. ADVANTAGES AND DISADVANTAGES OF IMAGING MODALITIES TO ASSESS CORONARY ARTERY DISEASE

Investigation	Advantage	Disadvantage	Radiation dose (mSv)
Anatomical tests			
CCTA	Quick Provides information on stenosis severity and characteristics of atherosclerotic plaque	Risks of using iodinated contrast	2–5
CT CACS	Quick Additive to traditional risk factors in assessing cardiovascular risk	Severity of stenosis cannot be assessed	1–3
Coronary magnetic resonance angiography	No radiation dose	Technically challenging Risks of using gadolinium contrast Currently no established clinical indications Research tool only	0

TABLE 10.2. ADVANTAGES AND DISADVANTAGES OF IMAGING MODALITIES TO ASSESS CORONARY ARTERY DISEASE (cont.)

Investigation	Advantage	Disadvantage	Radiation dose (mSv)
Invasive coronary angiography	Opportunity to perform revascularization at the time of the procedure	Most expensive Invasive Risk of side effects (e.g. stroke, myocardial infarction, death) Risks of using iodinated contrast	4–6
Functional tests			
Stress ECG	No radiation	Risks of inducing stress Operator dependent Some patients may not be suitable (e.g. patients with chronic lung disease, obesity)	0
Stress CMR	No radiation	Risks of inducing stress May be expensive Risks of gadolinium contrast	0
SPECT	Can be performed with exercise or pharmacological stress	Risks of inducing stress	2–10
PET	Blood flow quantification possible	Risks of inducing stress May be expensive Availability varies	2–3
CT perfusion	Opportunity to add on to CCTA	Risks of inducing stress Risks of using iodinated contrast	5–10
CT fractional flow reserve	Does not involve stress imaging or additional radiation	Currently expensive	0

TABLE 10.2. ADVANTAGES AND DISADVANTAGES OF IMAGING MODALITIES TO ASSESS CORONARY ARTERY DISEASE (cont.)

Investigation	Advantage	Disadvantage	Radiation dose (mSv)
Fractional flow reserve during invasive coronary angiography	Current gold standard for the assessment of the functional significance of stenosis	Invasive May be operator dependent May be expensive	
Hybrid tests			
SPECT–CT	Provides combined information on perfusion and CAD	Risks of inducing stress Risks of using iodinated contrast	5–15
PET–CT	Provides combined information on perfusion and CAD	Risks of inducing stress Risks of iodinated contrast May be expensive	5–10
PET–MRI	Provides information on perfusion, myocardium and possibly CAD	Not widely available Research technique only	2–10

Note: CACS — coronary artery calcium score; CAD — coronary artery disease; CCTA — coronary computed tomography angiography; CMR — cardiac magnetic resonance; CT — computed tomography; ECG — electrocardiogram; ETT — exercise treadmill; MRI — magnetic resonance imaging; PET — positron emission tomography; SPECT — single photon emission computed tomography.

10.5. IMAGING ALGORITHMS BASED ON CLINICAL PRESENTATION

10.5.1. Investigation of suspected stable coronary artery disease

The approach to suspected stable CAD may be different depending on clinical presentation, and the choice of the type of investigation may also depend on local and patient factors. Figure 10.1 shows a possible algorithm.

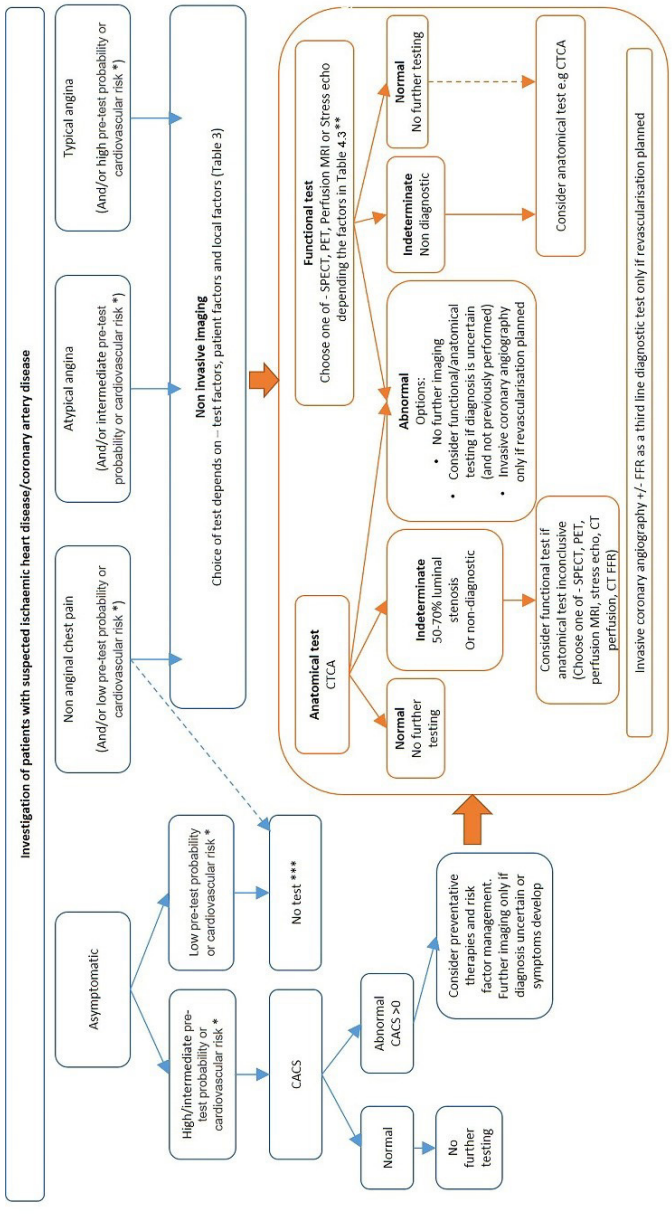

* Risk scores – up-to-date population specific risk scores may be used. However care should be taken as these may under/over estimate risk
** diagnostic accuracy of exercise tolerance test is poor, but this may be considered if no other options are available, especially for prognosis
*** a no test strategy may be appropriate for patients who are asymptomatic or particularly low risk

FIG. 10.1. Imaging algorithm for the investigation of patients with suspected CAD.

10.5.2. Important considerations when choosing a diagnostic test

Several factors should be taken into consideration when choosing a non-invasive diagnostic test for patients with suspected stable CAD:

(a) Patient factors:
- — Heart rate.
- — Body mass index.
- — Renal failure.
- — Metal implants.
- — Pregnancy.
- — Can they lie flat for the duration of the test?
- — Can they exercise?
- — Is the ECG interpretable?
- — Can medications be interrupted for the test?
- — Patient preference.
- — Contraindications to medications or contrast agents used.

(b) Test factors:
- — Diagnostic accuracy.
- — Radiation dose.
- — Contrast agent or tracer.
- — Method of stress (exercise or pharmacological).
- — Other medications used during test (e.g. beta blocker, glyceryl trinitrate).
- — Evidence from randomized controlled trials.
- — Cost of the test.
- — Cost and requirement or frequency of subsequent investigations.

(c) Local factors:
- — Local availability (e.g. scan facilities, infrastructure, local quality control/audit).
- — Local expertise (e.g. technologist, cardiologist, radiologist, nuclear medicine physician, medical physicist).
- — Local economic factors.

Importantly, a choice of doing no test may be appropriate for patients who are asymptomatic or particularly low risk.

10.5.3. Pre-operative risk assessment prior to non-cardiac surgery

Myocardial infarction during or shortly after surgery is an important cause of morbidity and mortality [10.24]. Up to 42% of complications of non-cardiac

surgery are attributable to cardiac complications [10.25]. Perioperative myocardial infarction occurs in 0.9% of patients undergoing major non-cardiac surgery and is most frequent in patients undergoing vascular surgery. The frequency of complications after non-cardiac surgery is likely to increase as more surgical procedures are performed on an increasingly ageing population. The frequency of cardiac complications during or after non-cardiac surgery varies depending on the type of surgery, the circumstances in which it is performed (elective or emergency) and patient factors such as known pre-existing disease [10.26]. It is therefore important to identify patients at risk of cardiac complications and risk stratify patients undergoing non-cardiac surgery (see Fig. 10.2).

Clinical assessment is essential in patients undergoing non-cardiac surgery, including assessment of medical history, symptoms and clinical examination. This may identify the presence of previously unknown CAD. Alternatively, it may identify patients at increased risk of CAD who may benefit from further non-invasive assessment. A variety of tools are available to assess cardiovascular risk prior to surgery, including the revised cardiac risk index. Non-invasive testing can provide information for patient counselling, perioperative management, surgical planning, anaesthetic technique, long term prognosis and the requirement for coronary artery revascularization. The consideration of whether non-invasive imaging may be required should be based on the cardiovascular risk status of the patient and the risk of complications from the proposed surgery. The 2014 European Society of Cardiology and European Society of Angiology guidelines on non-cardiac surgery stratify the types of surgery as low, intermediate and high risk (Table 10.3).

Most patients with stable CAD can undergo procedures of low or intermediate risk without further investigations. However, patients who are undergoing high risk surgery may benefit from further investigation and assessment by a multidisciplinary team. The choice of an anatomical or functional test will depend on the factors discussed in the previous section as well as whether

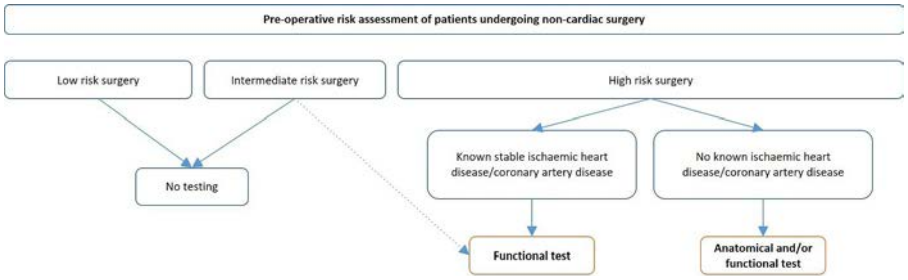

FIG. 10.2. Imaging algorithm for the pre-operative risk assessment of patients undergoing non-cardiac surgery.

TABLE 10.3. RISK ESTIMATES FOR SURGERY AND INTERVENTIONS
(see table 3 of Ref. [10.25])

Risk of cardiovascular complications based on surgical type only	Examples
Low <1%	Superficial surgery Breast Dental Endocrine (thyroid) Eye Reconstructive Carotid (asymptomatic) Minor gynaecology Minor orthopaedic (meniscectomy) Minor urological (transurethral resection of the prostate)
Intermediate 1–5%	Intraperitoneal (splenectomy, hiatus hernia repair, cholecystectomy) Carotid (symptomatic) Peripheral arterial angioplasty Endovascular aneurysm repair Head and neck surgery Major neurological or orthopaedic (hip and spine surgery) Major urological Major gynaecological Renal transplant Non-major intrathoracic
High >5%	Aortic surgery Major vascular surgery Open lower limb (revascularization, amputation, thromboembolectomy) Duodeno-pancreatic surgery Liver resection Bile duct surgery Oesophagectomy Repair of perforated bowel Adrenal resection Total cystectomy Pneumonectomy Pulmonary transplant Liver transplant

there is previous known stable CAD. Similarly, patients who are at intermediate or high cardiovascular risk may benefit from non-invasive investigation prior to intermediate or high risk surgery if it would alter management [10.24–10.26].

10.5.4. Incidental identification of CAD on imaging performed for other reasons

The heart and coronary arteries can be identified on imaging performed for other reasons and this may represent an opportunity to identify patients with previously undiagnosed CAD. This includes contrast or non-contrast non-ECG-gated computed tomography (CT) imaging performed for lung cancer screening, assessment of suspected cancer or trauma, among other reasons. These patients may benefit from the assessment of risk factors and preventive therapies [10.27]. If they are symptomatic, further assessment of suspected CAD may be required per Fig. 10.1.

The presence of coronary artery calcification on these non-dedicated CT images can be assessed using ordinal or semiquantitative scales. These images are suboptimal for determining the quantitative coronary artery calcium score (CACS) as this may over or underestimate risk depending on how the images are acquired. Nevertheless, based on the presence and amount of calcification, patients can be divided into four risk groups: very low risk; mildly increased risk; moderately increased risk; and moderately to severely increased risk [10.27]. Coronary artery calcification can also be identified on attenuation correction imaging performed during single photon emission computed tomography (SPECT)–CT and positron emission tomography (PET)–CT. This can be used to guide assessment of ischaemia and provide additional information to risk stratify patients.

The identification of vascular disease in other parts of the body may also highlight patients who are at risk of CAD. This includes vascular calcification identified on mammography and calcification within the aorta, carotid arteries or peripheral vessels. Such patients may benefit from the assessment of cardiovascular risk factors, the identification of symptoms that may represent undiagnosed CAD and the consideration of preventive therapies. Further non-invasive imaging will only be required in a small number of these patients who are symptomatic (see Fig. 10.1). Further information of CAD reporting and imaging can be found in Refs [10.28–10.30].

10.6. CONCLUSION

Chest pain is a frequent symptom throughout the world that requires assessment in both primary and secondary care. The assessment of patients with known or suspected CAD involves the assessment of symptoms, cardiovascular risk factors and the use of non-invasive imaging techniques. Different non-invasive imaging techniques will be of benefit for different patients. The choice of diagnostic test depends on: test factors such as diagnostic accuracy and radiation dose; patient factors such as heart rate, body mass index and the ability to lie supine; and local factors such as availability, expertise and cost. Ongoing research will refine current techniques and develop new and hybrid non-invasive imaging techniques. In addition, emerging research on clinical outcomes after treatment decisions based on non-invasive imaging techniques will help to guide the selection of non-invasive imaging tests.

10.7. KEY MESSAGES

(1) CAD is a major cause of morbidity and mortality globally, with cardiovascular disease affecting one in three adults.
(2) The most common symptom is chest pain, but alternative symptoms such as breathlessness should not be missed.
(3) Chest pain symptoms can be classified as typical angina, atypical angina and non-anginal chest pain.
(4) Coronary disease and cardiovascular risk probability models can classify patients into low, intermediate and high risk groups, but these models may under or overestimate risk for a significant proportion of patients.
(5) Choice of diagnostic test depends on: test factors such as diagnostic accuracy and radiation dose; patient factors such as heart rate, body mass index and the ability to lie supine; and local factors such as availability, expertise and cost.
(6) The cost of the index test and subsequent downstream testing should both be taken into consideration.
(7) A choice of doing no test may be appropriate for patients who are asymptomatic or particularly low risk.
(8) Anatomical testing with subsequent functional testing for intermediate or indeterminate disease is an appropriate testing strategy.
(9) Pre-operative assessment may be required for patients undergoing high risk surgery who are at intermediate to high risk of CAD.

(10) The assessment of coronary artery calcification on SPECT, PET or CT imaging performed for other reasons may identify additional patients who require treatment or help to clarify findings on perfusion imaging.

REFERENCES TO CHAPTER 10

[10.1] FIHN, S.D., et al., 2012 ACCF/AHA/ACP/AATS/PCNA/SCAI/STS guideline for the diagnosis and management of patients with stable ischemic heart disease, J. Am. Coll. Cardiol. **60** (2012) 2564–2603.

[10.2] TOWNSEND, N., BHATNAGAR, P., WILKINS, E., WICKRAMASINGHE, K., RAYNER, M., Cardiovascular Disease Statistics 2015, British Heart Foundation, London (2015).

[10.3] ROTH, G.A., et al., Global and regional patterns in cardiovascular mortality from 1990 to 2013, Circulation **132** (2015) 1667–1678.

[10.4] BHATNAGAR, P., WICKRAMASINGHE, K., WILKINS, E., TOWNSEND, N., Trends in the epidemiology of cardiovascular disease in the UK, Heart **102** (2016) 1945–1952.

[10.5] MOZAFFARIAN, D., et al., Heart disease and stroke statistics: 2016 update, Circulation **133** (2016) 38–360.

[10.6] NILSSON, S., et al., Chest pain and ischaemic heart disease in primary care, Br. J. Gen. Pract. **53** (2003) 378–382.

[10.7] GOODACRE, S., et al., The health care burden of acute chest pain, Heart **91** (2005) 229–230.

[10.8] NATIONAL INSTITUTE FOR HEALTH AND CARE EXCELLENCE, Recent-onset Chest Pain of Suspected Cardiac Origin: Assessment and Diagnosis, Clinical Guideline 95, NICE (2016).

[10.9] NABEL, E.G., et al., Women's Ischemic Syndrome Evaluation: Current Status and Future Research Directions, Section 3. Diagnosis and treatment of acute cardiac ischaemia: Gender issues, Circulation **109** (2004) 50–52.

[10.10] BRAUNWALD, E., et al., Diagnosing and managing unstable angina: Agency for Health Care Policy and Research, Circulation **90** (1994) 613–622.

[10.11] HAMBURGER, R., SPERTUS, J., WINCHESTER, D.E., Utility of the Diamond–Forrester classification in stratifying acute chest pain in an academic chest pain center, Crit. Pathw. Cardiol. **15** (2016) 56–59.

[10.12] DAMEN, J.A.A.G., et al., Prediction models for cardiovascular disease risk in the general population: Systematic review, BMJ **353** (2016) 2416.

[10.13] GENDERS, T.S.S., et al., A clinical prediction rule for the diagnosis of coronary artery disease: Validation, updating, and extension, Eur. Heart J. **32** (2011) 1316–1330.

[10.14] NEGLIA, D., et al., Detection of significant coronary artery disease by noninvasive anatomical and functional imaging, Circ. Cardiovasc. Imag. **8** (2015).

[10.15] DANAD, I., et al., Comparison of coronary CT angiography, SPECT, PET, and hybrid imaging for diagnosis of ischemic heart disease determined by fractional flow reserve, JAMA Cardiol. **2** (2017) 1100–1107.

[10.16] NIELSEN, L.H., et al., The diagnostic accuracy and outcomes after coronary computed tomography angiography vs conventional functional testing in patients with stable angina pectoris: A systematic review and meta-analysis, Eur. Heart J. Cardiovasc. Imag. **15** (2014) 961–971.

[10.17] TASK FORCE MEMBERS, et al., 2013 ESC guidelines on the management of stable coronary artery disease: The Task Force on the Management of Stable Coronary Artery Disease of the European Society of Cardiology, Eur. Heart J. **34** (2013) 2949–3003.

[10.18] MARK, D.B., et al., Economic outcomes with anatomical versus functional diagnostic testing for coronary artery disease, Ann. Intern. Med. **165** (2016) 94–102.

[10.19] WILLIAMS, M.C., et al., Use of coronary computed tomographic angiography to guide management of patients with coronary disease, J. Am. Coll. Cardiol. **67** (2016) 1759–1768.

[10.20] EINSTEIN, A.J., et al., Current worldwide nuclear cardiology practices and radiation exposure: Results from the 65 country IAEA Nuclear Cardiology Protocols Cross-sectional Study (INCAPS), Eur. Heart J. **36** (2015) 1689–1696.

[10.21] BAUMANN, S., et al., Comparison of coronary computed tomography angiography-derived vs invasive fractional flow reserve assessment: Meta-analysis with subgroup evaluation of intermediate stenosis, Acad. Radiol. **23** (2016) 1402–1411.

[10.22] DOUGLAS, P.S., et al., Clinical outcomes of fractional flow reserve by computed tomographic angiography-guided diagnostic strategies vs usual care in patients with suspected coronary artery disease: The prospective longitudinal trial of FFR_{CT} — Outcome and resource impacts study, Eur. Heart J. **36** (2015) 3359–3367.

[10.23] LU, M.T., et al., Noninvasive FFR derived from coronary CT angiography: Management and outcomes in the PROMISE trial, J. Am. Coll. Cardiol. Cardiovasc. Imag. **10** (2017) 1350–1358.

[10.24] SMILOWITZ, N.R., et al., Perioperative acute myocardial infarction associated with non-cardiac surgery, Eur. Heart J. **38** (2017) 2409–2917.

[10.25] KRISTENSEN, S.D., et al., 2014 ESC/ESA guidelines on non-cardiac surgery: Cardiovascular assessment and management, Eur. Heart J. **35** (2014) 2383–2431.

[10.26] FLEISHER, L.A., et al., 2014 ACC/AHA guideline on perioperative cardiovascular evaluation and management of patients undergoing noncardiac surgery, J. Am. Coll. Cardiol. **64** (2014) 77–137.

[10.27] PAKDAMAN, M.N., ROZANSKI, A., BERMAN, D.S., Incidental coronary calcifications on routine chest CT: Clinical implications, Trends Cardiovasc. Med. **27** (2017) 475–480.

[10.28] CURY, R.C., et al., Coronary Artery Disease: Reporting and Data System (CAD-RADS), J. Am. Coll. Cardiol. Cardiovasc. Imag. **9** (2016) 1099–1113.

[10.29] HECHT, H.S., et al., 2016 SCCT/STR guidelines for coronary artery calcium scoring of noncontrast noncardiac chest CT scans: A report of the Society of Cardiovascular Computed Tomography and Society of Thoracic Radiology, J. Cardiovasc. Comput. Tomogr. **11** (2017) 74–84.

[10.30] GIMELLI, A., et al., Strategies for radiation dose reduction in nuclear cardiology and cardiac computed tomography imaging, Eur. Heart J. **39** (2018) 286–296.

Chapter 11

ACUTE CORONARY SYNDROMES

S. DORBALA, G. KARTHIKEYAN, A. PEIX, D. PAEZ, J. VITOLA

Cardiovascular diseases remain a leading cause of mortality. In 2013, they accounted for 17.3 million deaths worldwide [11.1], including over 8 million deaths from coronary heart disease alone [11.2]. Acute chest pain is one of the most common cause of visits to the accident and emergency department; however, only 30% of such acute chest pain visits represent acute coronary syndromes (ACSs) [11.3, 11.4]. ACSs accounted for more than one million hospital discharges in the United States of America alone in 2010, and globally this burden is likely much larger [11.1]. The appropriate evaluation of ACS with early and safe discharge of patients without ACS combined with guideline directed management of ACSs can substantially reduce health care costs and improve clinical outcomes. Imaging plays a key role both in excluding ACSs and in managing and risk stratifying patients with documented ACSs.

11.1. DEFINITION OF ACUTE CORONARY SYNDROME

ACSs include three distinct pathophysiological entities: (i) unstable angina; (ii) myocardial infarction with ST segment elevation (STEMI); and (iii) myocardial infarction without ST segment elevation (NSTEMI). Unstable angina is defined as angina that is worsening in frequency or severity, occurring at rest or occurring for the first time but which does not result in myocyte necrosis [11.5, 11.6]. Myocardial infarction is diagnosed by a typical rise and fall of cardiac biomarkers (troponins > 99th percentile of the upper reference limit) along with at least one of the following: anginal symptoms, electrocardiogram (ECG) changes, evidence of myocardial scarring (regional wall motion abnormalities on imaging or evidence of loss of myocardial viability) or intracoronary thrombus (on angiography or at autopsy) [11.7]. The pathophysiology of each of these forms of ACS is distinct.

11.2. PATHOPHYSIOLOGY OF ACUTE CORONARY SYNDROME

Plaque instability with or without plaque rupture and thrombus formation is a key triggering event in ACSs [11.8]. Macrophage rich or inflamed plaques,

lipid laden plaques and plaques with thin cap fibroatheromas are more prone to rupture [11.9]. Macrophages release enzymes that degrade the extracellular matrix in the arteries and mediate plaque rupture; they also increase the thrombogenicity of the lipid laden plaque [11.9]. However, recent studies indicate that the composition of unstable atherosclerotic plaques has changed substantially over time [11.10]. This is likely at least in part owing to the aggressive primary and secondary prevention of coronary artery disease (CAD) since the 1990s, in particular the increased use of statin therapy for lipid lowering. Present day atherosclerotic plaques demonstrate lower fat content, a smaller inflammatory burden, lower calcium content and a smaller thrombus burden [11.10]. Plaque erosion is an increasingly common cause of ACS (30%) [11.11], and ACS without thrombosis is seen in 20% of patients [11.9]. Vasospasm, epicardial fat inflammation and microvascular disease have been implicated in ACS without thrombosis and in myocardial infarction with non-obstructive coronary arteries (MINOCA) [11.8, 11.9]. Unstable plaques, plaque erosion and plaque rupture result in angina and can progress to myocardial infarction and related complications of heart failure, mechanical complications, arrhythmic events or death. Imaging plays a key role in diagnosing ACS and its complications and in guiding management.

11.3. ROLE OF NON-INVASIVE IMAGING IN ACUTE CORONARY SYNDROME

The goals of evaluation in ACSs, and thus the choice of techniques used, vary from the acute (during acute chest pain/ACS) to subacute (immediate post-ACS) and chronic phase (late post-ACS) [11.5, 11.6]. During the acute phase, the pre-test risk of ACS based on clinical and ECG evaluation, laboratory and cardiac biomarkers and risk scores for ACS determine the choice of imaging [11.5, 11.6, 11.12, 11.13]. Invasive coronary angiography with ad hoc intravascular imaging, such as optical coherence tomography, intravascular ultrasound and haemodynamic assessment through fractional flow reserve prior to coronary revascularization are common in the evaluation of patients with documented ACS or in those with intermediate to high risk ACS. Non-invasive imaging is often reserved to identify complications, diagnose CAD in intermediate to low probability ACS patients or assess risk post-ACS [11.5, 11.6]. Depending on the clinical question being asked, echocardiography, cardiac magnetic resonance (CMR), coronary computed tomography angiography (CCTA) or radionuclide imaging such as single photon emission computed tomography (SPECT) or positron emission tomography (PET) may be used.

11.4. CLINICAL UTILITY OF NON-INVASIVE IMAGING IN ACUTE CORONARY SYNDROME

11.4.1. Echocardiography

Echocardiography provides critical information for the evaluation and management of all phases of ACS. Left ventricular function is routinely evaluated with echocardiography during hospitalization for ACS. Echocardiography contrast (except in patients with allergy to contrast) and strain imaging improve detection of regional wall motion abnormalities and left ventricular thrombus. Hand-held echocardiography can quickly exclude pericardial effusion or tamponade and is becoming indispensable in the evaluation of patients presenting to the emergency room with cardiac arrest. Transthoracic echocardiography (TTE) as well as transoesophageal echocardiography (TEE) can identify the aetiology of shock and haemodynamic collapse in patients with ACS, for example papillary muscle rupture, ventricular septal rupture and aortic dissection in patients in whom renal dysfunction precludes a contrast computed tomography (CT) scan or magnetic resonance imaging (MRI). Echocardiography not only identifies causes for haemodynamic collapse in ACS but can also guide placement and follow-up of left ventricular mechanical support devices. Pre-discharge stress echocardiography in stable patients after ACS can identify stress induced ischaemia and thereby help to stratify risk and to guide management. Finally, post discharge rest echocardiography is recommended at 6–12 weeks in patients with left ventricular ejection fraction (LVEF) ≤ 40% to determine the need for primary prevention internal cardioverter defibrillators [11.14]. Echocardiography has essentially no contraindications and is used universally in ACSs.

11.4.2. Coronary computed tomography angiography

CCTA can play a major role in non-invasively excluding anatomical obstructive CAD in patients with acute chest pain or suspected ACS with low to intermediate risk. Its role in NSTEMI and STEMI is limited except in specific cases (e.g. suspected spontaneous coronary artery dissection, to identify the aetiology of ACS). CCTA is of limited value in patients with known CAD or prior coronary revascularization (calcium and stents may limit the diagnostic accuracy of CCTA). In these cases, the clinical question is not coronary artery anatomy but rather the functional significance of obstructive CAD. A regular ECG rhythm, slow heart rate and normal renal function are required for CCTA. Very large body habitus may limit the quality of CCTA. Although triple rule out CCTA can be used to exclude CAD, pulmonary embolism and aortic dissection [11.15],

it is not routinely recommended owing to high radiation dose and suboptimal image quality.

11.4.3. Cardiac magnetic resonance imaging

CMR provides high resolution imaging of myocardial structure and function and plays an important role in the evaluation and management of patients with known or suspected ACS. CMR provides precise quantification of LVEF and regional wall motion abnormalities and left ventricular thrombus, even when echocardiography is limited. CMR with T1/T2 weighted imaging sequences and gadolinium contrast can accurately quantify myocardial scar and oedema [11.16], microvascular obstruction/no reflow phenomenon [11.17–11.19] and post-myocardial infarction complications including post-reperfusion myocardial haemorrhage [11.20]. Each of these parameters provides powerful prognostic information in patients with ACS and myocardial infarction. Myocarditis and alternate causes for symptoms can be diagnosed. Despite the excellent temporal and spatial resolution of CMR, limited access to it and its relatively long scan duration limit its routine use in ACS. Good renal function (estimated glomerular filtration rate (eGFR) > 30 $mL \cdot min^{-1} \cdot 1.73\ m^{-2}$) is required for the use of gadolinium contrast. CMR is contraindicated in most patients with implanted cardiac defibrillators and pacemakers, although CMR compatible devices are increasingly being used. Claustrophobia may limit CMR in certain individuals, despite the use of anxiolytics.

11.4.4. Radionuclide imaging: SPECT and PET

Radionuclide imaging is one of the oldest applications of non-invasive imaging in acute chest pain. In the early 1970s, prior to the discovery of cardiac troponins, ^{99m}Tc pyrophosphate SPECT was used to identify acute myocardial injury from ACS [11.21]. Currently, myocardial perfusion imaging (MPI) with SPECT (^{99m}Tc, ^{201}Tl) or PET (^{13}N ammonia or ^{82}Rb) is used at rest (for patients with acute chest pain, at high risk for CAD but low risk for ACS) or with stress (post-ACS) in the evaluation of ACSs. Extensive literature supports the diagnostic value of radionuclide MPI during chest pain and its prognostic value following ACS [11.22]. Radionuclide imaging has essentially no contraindications and is well tolerated by most patients. The quantitative evaluation of ischaemia and its ease of use and reproducibility are major strengths of radionuclide MPI. A very large body habitus may limit the quality of SPECT MPI; a two day study, attenuation correction or PET MPI may be considered in such cases.

11.5. CASE BASED APPROACH TO IMAGING IN ACUTE CORONARY SYNDROMES

This section illustrates the utility of imaging in ACSs using an algorithmic approach by presenting real life cases with distinct clinical presentations of suspected ACS.

11.5.1. Suspected ACS: Case 1

11.5.1.1. Clinical presentation

A 50 year old woman with no known CAD presented with substernal chest pain for 30 minutes. She had no coronary risk factors, other than a strong family history of premature CAD. She exercised regularly and had recently noted shortness of breath after 16 km of running. She was not on any medication. Her initial ECG in the emergency room showed sinus bradycardia (50 bpm), and inverted T waves in leads V2–V6. ECG remained unchanged after an hour. Her initial troponin T level was negative.

11.5.1.2. Discussion

Patients presenting with chest pain and suspected ACS are rapidly examined clinically. A 12 lead ECG and serum cardiac biomarker levels are obtained. Based on the results of this initial evaluation, an early invasive angiography may be appropriate in individuals with high risk features. In patients without high risk features, non-invasive imaging is considered (see Fig. 11.1).

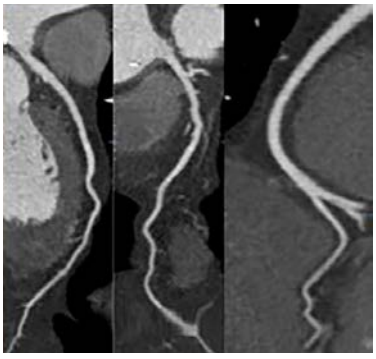

FIG. 11.1. CT coronary angiogram. The images show no obstructive CAD in the left anterior descending artery (left), left circumflex artery (middle) or the right coronary artery (right).

Non-invasive imaging with CCTA, rest MPI or stress imaging are powerful tools to identify the cause of symptoms, identify complications, quantify LVEF and provide assessment of risk (see Table 11.1).

In patients with low to intermediate risk of ACS and negative or equivocal troponin levels, CCTA (in patients without known CAD) or stress imaging (in patients with known CAD) can be considered. If high risk plaque or severe obstructive CAD is detected on CCTA, those patients are candidates for invasive coronary angiography. If not, and if the patient is low risk for ACS, medical management and outpatient stress testing are considered. CCTA has an excellent negative predictive value in excluding coronary atherosclerosis; absence of coronary plaque on CCTA portends a very low likelihood of adverse cardiac events [11.23].

TABLE 11.1. ROLE OF IMAGING IN PATIENTS WITH SUSPECTED ACS

Parameters assessed	Non-invasive imaging modality				
	Echocardiography	CCTA	CMR	SPECT MPI	PET MPI
Coronary artery anatomy					
Suspected ACS	−	+++*	−	−	−
NSTE-ACS	−	+++*	−	−	−
STE-ACS	−	−	−	−	−
Rest perfusion defect					
Suspected ACS	−	+	−	+++	+++
NSTE-ACS	−	−	−	−	−
STE-ACS	−	−	−	−	−
Regional wall motion abnormalities					
Suspected ACS	++	−	+	−	−
NSTE-ACS	++	−	+	−	−
STE-ACS	++	−	+	−	−
Haemodynamic collapse					
Suspected ACS	+++	+	+	−	−
NSTE-ACS	+++	+	+	−	−
STE-ACS	+++	+	+	−	−

TABLE 11.1. ROLE OF IMAGING IN PATIENTS WITH SUSPECTED ACS (cont.)

Parameters assessed	Non-invasive imaging modality				
	Echocardiography	CCTA	CMR	SPECT MPI	PET MPI
Guide mechanical circulatory support:					
Suspected ACS	+++	+	+	−	−
NSTE-ACS	+++	+	+	−	−
STE-ACS	+++	+	+	−	−

Note: ACS — acute coronary syndrome; CCTA — coronary computed tomography angiography; CMR — cardiac magnetic resonance; MPI — myocardial perfusion imaging; NSTE — non-ST-elevation; PET — positron emission tomography; SPECT — single photon emission computed tomography; STE — with ST segment elevation.

* No prior coronary artery disease or coronary revascularization and no contraindications to CCTA (regular rhythm, slow heart rate, no contrast allergy, normal renal function).

+++ Appropriate.

++ May be appropriate.

\+ Rarely appropriate.

− No routine indication.

A meta-analysis of four studies [11.24–11.28] shows that CCTA is safe in low and intermediate risk patients presenting to the accident and emergency department with chest pain. When compared with standard of care (without CCTA), CCTA reduced length of hospital stay but at the expense of increasing downstream invasive coronary angiography and coronary revascularization [11.29].

However, a more recent study in which CCTA was used in conjunction with high sensitivity troponin [11.30] shows that CCTA did not reduce length of stay nor did it increase invasive angiography or coronary revascularization compared with standard of care (which included repeated cardiac markers, hospital admission, non-invasive testing and referral to invasive coronary angiography).

The evaluation of stenosis severity and plaque characteristics on CCTA improves the specificity for ACS diagnosis compared with traditional CCTA (48.2% to 68.1%). The overall accuracy for ACS diagnosis also increased as the majority of patients with intermediate values of high sensitivity troponin with high risk plaque and ≥50% stenosis developed ACS (appropriate use criteria

95% CI, 0.84 (0.80–0.88) for high sensitivity troponin vs 0.74 (0.70–0.78) for conventional troponin) [11.30]. Considering the gradual transition from conventional troponin to high risk troponin in clinical practice, the role of CCTA in an emergency setting for acute chest pain continues to evolve [11.30].

11.5.2. Suspected ACS: Case 2

11.5.2.1. Clinical presentation

A 60 year old man, with prior angioplasty and stenting of the right coronary artery, presented to the accident and emergency department with new onset chest pain. An injection of ^{99m}Tc labelled radiopharmaceutical was given one hour after the chest pain ended. His coronary risk factors included high blood pressure and smoking. His presenting ECG did not demonstrate ST/T wave changes. His initial troponin T was 0.01 (borderline positive). Same day ^{99m}Tc-sestamibi MPI was performed at rest. Myocardial perfusion images showed a large and severe perfusion defect in the entire anterior and anteroseptal walls and in the apex (see Fig. 11.2(A)). On the same day, invasive coronary angiography was performed that demonstrated a 99% stenosis in the proximal left anterior descending coronary artery (see Fig. 11.2(B)), which was stented with excellent results (see Fig. 11.2(C)).

11.5.2.2. Discussion

Rest MPI during chest pain is appropriate when the ECG is normal or non-diagnostic for ischaemia and when conventional troponin is equivocal, or a single troponin measurement is elevated without additional evidence of ACS. It is rarely appropriate when high sensitivity troponin is negative [11.31]. Rest MPI soon after chest pain is also appropriate when CCTA cannot be obtained, is contraindicated or is limited (prior coronary stents). An approach to imaging in patients with suspected ACS is shown in Fig. 11.3.

Unlike the patient in Case 1, this patient had a prior right coronary artery stent, limiting the yield of CCTA. However, he had no prior history of myocardial infarction, making a rest pain sestamibi study appropriate. Perfusion defects in the anterior wall suggested severe CAD in the left anterior descending coronary artery, which was confirmed by invasive coronary angiography.

Since the rest MPI was normal, the patient was considered clinically stable, as he did not have ongoing chest pain, two troponin measurements had been normal six hours apart and the haemodynamics were stable, therefore stress imaging could be considered. Based on local expertise, exercise/vasodilator/dobutamine

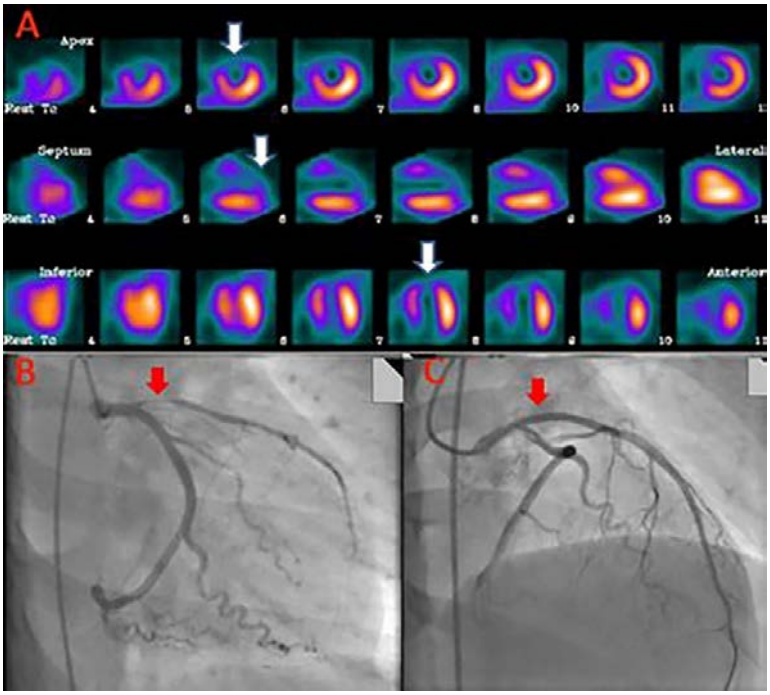

FIG. 11.2. Rest SPECT MPI and invasive coronary angiography. (A) The SPECT images depict short axis images (top row), vertical long axis images (middle row) and horizontal long axis images (bottom row). These images show a large sized and severe perfusion defect throughout the anterior and anteroseptal walls and the apex. (B) Invasive coronary angiography shows a tight stenosis in the proximal left anterior descending artery (indicated by arrow). (C) The stenosis was successfully stented (indicated by arrow).

MPI with SPECT or PET, exercise/dobutamine echocardiography or vasodilator CMR were options.

In addition to diagnosis, several studies have demonstrated that the magnitude of myocardial ischaemia and scar on MPI are powerful determinants of risk in patients with chest pain and suspected ACS. A prospective randomized observational study comparing stress only MPI versus CCTA [11.32] shows that 57% of the screened patients were not suited for CCTA owing to prior CAD or contraindications to CCTA. Time to diagnosis, length of hospital stay and cost were similar between CCTA and stress only SPECT. Negative CCTA and negative SPECT MPI had similarly low event rates, but an abnormal SPECT MPI had worse event free survival compared with an abnormal CCTA [11.32].

Cremer et al. [11.33] retrospectively evaluate emergency room patients with chest pain and two negative troponin values and non-diagnostic ECG. In

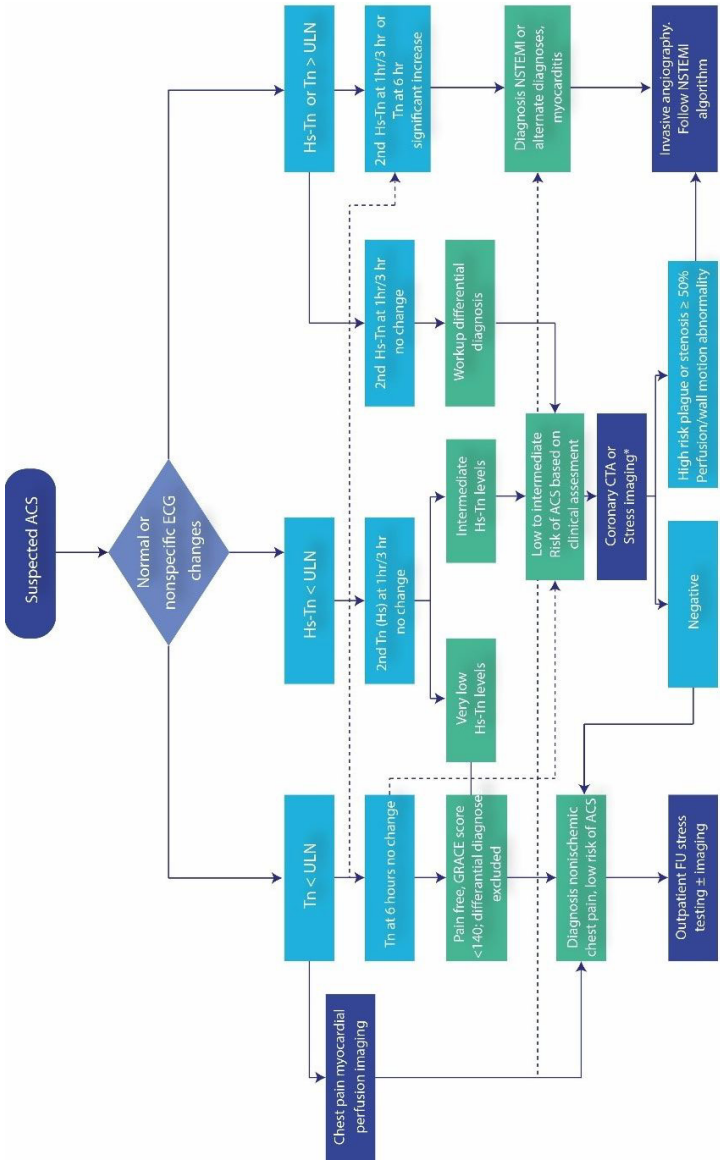

*FIG. 11.3. An approach to imaging patients with suspected ACS. CTA — computed tomography angiography; ECG — electrocardiogram; FU — follow-up; GRACE — Global Registry of Acute Coronary Events; Hs-Tn — high sensitivity troponin; NSTEMI — non-ST-elevation myocardial infarction; ULN — upper limit normal. *Stress imaging is superior to CCTA in patients with known CAD and performed in haemodynamically stable patients with two negative troponin values.*

this cohort, the presence and severity of obstructive CAD increased with the thrombolysis in myocardial infarction (TIMI) risk score. However, the yield of detecting ischaemia was low in patients with TIMI risk score ≤ 2 and no survival benefit was observed with early revascularization in these subjects [11.33].

11.5.3. NSTE-ACS: Case 3

11.5.3.1. Clinical presentation

A 68 year old man with prior coronary artery bypass graft had been discharged from hospital two weeks earlier with NSTEMI and revascularization of the left anterior descending coronary artery. He was readmitted with atypical chest pain and a troponin T = 0.03 ng/dL (normal value < 0.01 ng/dL). His rest ECG was unremarkable. Given the recent complicated intervention, he underwent for NSTEMI, and his impaired renal function (eGFR 40 $mL \cdot min^{-1} \cdot 1.73\ m^{-2}$), non-invasive imaging was preferred to guide management. A rest and stress ^{13}N ammonia PET was ordered. The medications he was taking included aspirin, clopidogrel, atenolol, atorvastatin and an angiotensin converting enzyme inhibitor. During the rest MPI scan, he complained of typical anginal symptoms and the stress test was cancelled. The rest MPI scan demonstrated a large and severe perfusion defect in the inferior and inferolateral wall, as well as in the apical four myocardial segments and apex (see Fig. 11.4(A)). Due to his recent myocardial infarction, it was not clear whether the defect represented viable and ischaemic myocardium, explaining his rest angina, or scar tissue. An ^{18}F-fluorodeoxyglucose (^{18}F-FDG) PET scan was therefore performed and showed mismatch in the entire inferolateral and the basal inferior wall consistent with viable myocardium, and a matched defect in the apical four myocardial segments and in the mid-inferior wall suggesting myocardial scar in the left anterior descending coronary artery territory. A coronary angiogram (see Fig. 11.4(B)) showed a tight stenosis with thrombus in the left circumflex coronary artery, which was revascularized.

11.5.3.2. Discussion

In patients with suspected NSTE-ACS in whom invasive coronary angiography is not performed, either owing to low risk ACS, physician/patient preference or contraindications to invasive angiography, management guided by non-invasive imaging is preferred.

CCTA can be limited in patients with documented CAD and prior stents presenting with acute chest pain. Stress testing is contraindicated in patients with acute symptoms suggesting ACS. As shown in this case, a rest MPI can be useful to guide management.

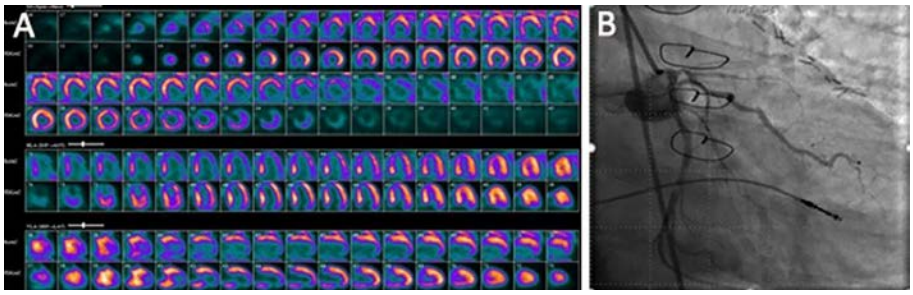

FIG. 11.4. Rest ^{13}N ammonia PET–CT, ^{18}F-FDG-PET–CT and invasive coronary angiography. The ^{13}N ammonia images (A) depict a large and severe perfusion defect in the entire inferior and inferolateral walls and apex. The ^{18}F-FDG images depict significant mismatch (hypoperfusion with preserved glucose utilization) in most of the inferior and inferolateral segments, consistent with hibernating myocardium. Invasive coronary angiogram (B) confirmed a tight stenosis in the left circumflex coronary artery, which was revascularized.

In a large prospective multicentre clinical study [11.34], 2475 patients with acute chest pain and non-diagnostic ECG changes were randomized to standard of care or rest MPI with ^{99m}Tc SPECT. In that study, rest ^{99m}Tc SPECT MPI reduced the hospital admission rate compared with standard of care (48% vs 56%, $p < 0.001$) and reduced 30 day major adverse cardiac events (rate of events with a negative MPI 3%, with an equivocal MPI 6%, with an abnormal MPI 20%, $p < 0.001$) [11.34].

In addition to MPI, metabolic imaging of ischaemic myocardium (^{18}F-FDG-PET) has been utilized to clarify the significance of perfusion abnormalities. The ischaemic myocardium preferentially uses glucose over fatty acids. ^{18}F-FDG-PET with glucose loading and insulin preparation as described by the American Society of Nuclear Cardiology is helpful in identifying a hypoperfused but metabolically active, hibernating myocardium [11.35]. ^{18}F-FDG-PET with fat loading (to suppress physiological glucose utilization by the myocardium) has been studied to identify inflamed coronary plaques [11.36].

More recently, ^{18}F sodium fluoride, a PET bone imaging agent, was repurposed to detect unstable plaques with microcalcification. In one recent prospective study of patients with stable ($N = 40$) and unstable coronary syndromes ($N = 40$), the target to background ratio of ^{18}F sodium fluoride PET, a marker of microcalcification, was significantly higher (1.66 (interquartile range 1.40–2.25) vs 1.24 (1.06–1.38), $p < 0.000\ 1$) in culprit plaques as compared with the highest uptake in the non-culprit plaques confirmed by intravascular ultrasound (coronary plaques) or histology (carotid plaques) [11.37].

Beyond radionuclide imaging, rest echocardiography can help to assess LVEF and to identify regional wall motion abnormalities. A biphasic response

(improvement in wall motion followed by worsening) or monophasic response (sustained improvement in wall motion) from rest to low dose dobutamine indicates myocardial viability.

Although CMR is time consuming, it has been used in patients with suspected ACS with cine imaging to identify contractile function and regional wall motion abnormalities. Furthermore, T2 weighted imaging can identify oedema; first pass perfusion imaging with gadolinium can be used to assess regional myocardial blood flow at rest or with stress; early gadolinium enhancement can help to identify microvascular integrity; and late gadolinium enhancement (LGE) is helpful to quantify the burden of scar tissue [11.38, 11.39]. The magnitude of myocardial fibrosis determined by T1 weighted LGE imaging is a powerful predictor of major adverse cardiovascular events [11.39]. The role of imaging before and after hospital discharge in patients with ACS is given in Table 11.2 and a proposed approach to imaging in patients with suspected NSTE-ACS is given in Fig. 11.5.

TABLE 11.2. ROLE OF IMAGING IN PATIENTS WITH ACS

Parameters assessed	Non-invasive imaging modality				
	Echocardiography	CCTA	CMR	SPECT MPI	PET MPI
	ACS: Before discharge				
LV systolic and diastolic function					
NSTE-ACS	+++	–	+++	–	–
STE-ACS	+++	–	+++	–	–
LV regional wall motion abnormalities					
NSTE-ACS	+++	–	+++	–	–
STE-ACS	+++	–	+++	–	–
RV structure and function					
NSTE-ACS	+++	–	+++	–	–
STE-ACS	+++	–	+++	–	–
Valve structure and function					
NSTE-ACS	+++	+	++	–	–
STE-ACS	+++	+	++	–	–

TABLE 11.2. ROLE OF IMAGING IN PATIENTS WITH ACS (cont.)

Parameters assessed	Non-invasive imaging modality				
	Echocardiography	CCTA	CMR	SPECT MPI	PET MPI
Thrombus					
NSTE-ACS	+++	+	+++	–	–
STE-ACS	+++	+	+++	–	–
Stress induced ischaemia					
NSTE-ACS	+++	–	+++	+++	+++
STE-ACS	+++	–	+++	+++	+++
Myocardial viability					
NSTE-ACS	+++	–	+++	+++	^{18}F-FDG-PET
STE-ACS	+++	–	+++	+++	
ACS: After discharge					
LV systolic function if LVEF < 40%					
NSTEMI	+++	–	+++	–	–
STEMI	+++	–	+++	–	–
Stress induced ischaemia					
NSTE-ACS	+++	–	+++	+++	+++
STE-ACS	+++	–	+++	+++	+++
Myocardial viability					
NSTE-ACS	+++	–	+++	+++	FDG-PET
STE-ACS	+++	–	+++	+++	

Note: ACS — acute coronary syndrome; CCTA — coronary computed tomography angiography; CMR — cardiac magnetic resonance; FDG — fluorodeoxyglucose; LV — left ventricular; LVEF — left ventricular ejection fraction; MPI — myocardial perfusion imaging; NSTE — non-ST-elevation; NSTEMI — non-ST-elevation myocardial infarction; PET — positron emission tomography; RV — right ventricular; SPECT — single photon emission computed tomography; STE — ST-elevation; STEMI — ST-elevation myocardial infarction.

+++ Appropriate.
++ May be appropriate.
+ Rarely appropriate.
– No routine indication.

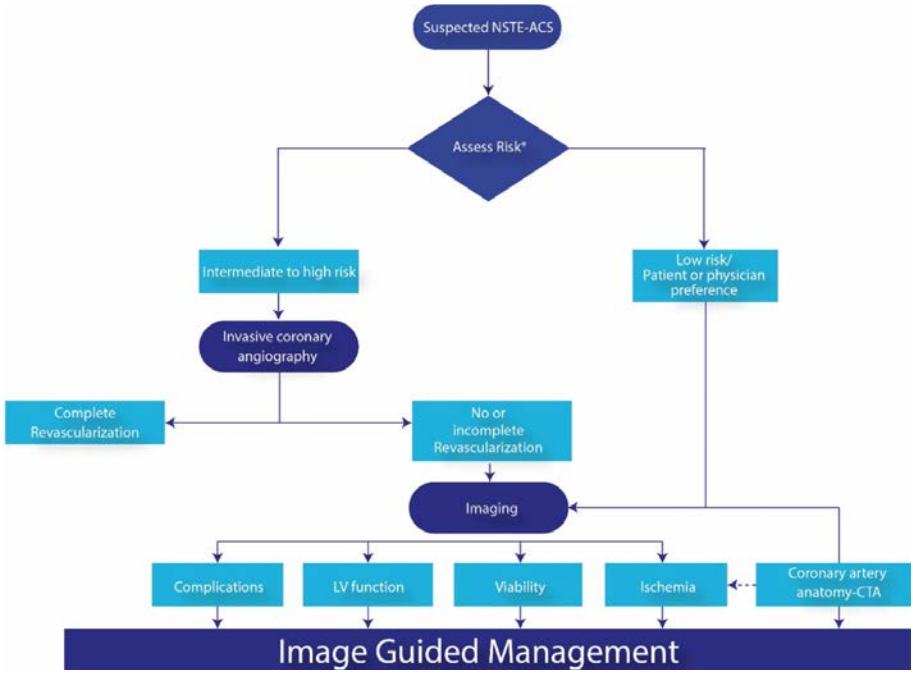

*FIG. 11.5. Role of imaging in suspected NSTE-ACS. * NSTE-ACS risk assessment: Low TIMI risk score (0) or GRACE score <109; low risk troponin negative female patients; absence of high risk features: refractory angina, electrical or haemodynamic instability. CTA — computed tomography angiography; LV — left ventricular.*

11.5.4. STE-ACS: Case 4

11.5.4.1. Clinical presentation

A 78 year old man with a history of hypertension, diabetes and chronic renal insufficiency (eGFR 45 $mL \cdot min^{-1} \cdot 1.73\ m^{-2}$) presented with an anterior wall STEMI and was submitted to urgent percutaneous coronary intervention of the left anterior descending coronary artery. During the procedure, the first septal perforator artery was occluded by the stent. The right coronary artery also showed a 99% ostial stenosis and the proximal left circumflex coronary artery showed a 60% stenosis. Immediately after the primary percutaneous coronary intervention, the patient's LVEF was 30% as determined by echocardiography. He was referred for vasodilator stress/rest ischaemia imaging and viability imaging for further evaluation. The rest and stress images, obtained with a ^{13}N ammonia PET, showed a large defect of severe intensity in the entire inferior wall,

in the mid and basal inferolateral walls with mild to moderate reversibility. The entire anteroseptal region showed mild reversibility consistent with the known jailed septal perforator artery. The ^{18}F-FDG-PET images demonstrate complete a mismatch between myocardial perfusion and glucose metabolism consistent with viability in the inferior wall (see Fig. 11.6). Based on these results, the right coronary artery was revascularized percutaneously.

11.5.4.2. Discussion

Pre-discharge vasodilator stress following ACS is safe in stable patients and can identify the magnitude of ischaemia and scar [11.38, 11.39]. If needed, myocardial viability can be assessed by additional ^{18}F-FDG-PET imaging.

Total and ischaemic perfusion defect size, LVEF, thallium lung uptake, infarct zone redistribution and multivessel CAD on thallium imaging are predictors of a high risk of cardiac events (cardiac death, non-fatal myocardial infarction, heart failure or unstable angina requiring hospitalization and revascularization) [11.40, 11.41].

A large prospective study enrolled 728 patients with myocardial infarction (both NSTEMI and STEMI) from 16 centres to undergo adenosine SPECT MPI who were then followed for one year. 2038 patients with high risk MPI (total perfusion deficit > 20%) and LVEF > 35% were randomized to medical therapy versus revascularization. The main findings of this study were that adenosine SPECT total perfusion defect size and ischaemic perfusion defect size were linearly related to cardiac events and death/reinfarction. Scan findings significantly enhanced risk stratification over TIMI risk score. Total and

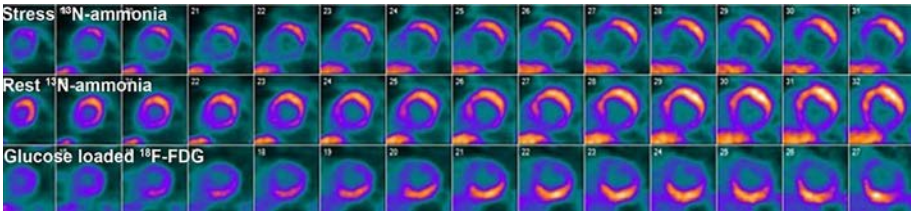

FIG. 11.6. Rest and stress ^{13}N ammonia PET–CT and ^{18}F-FDG-PET–CT images. Images are shown as short axis images from apex to base (left to right) with vasodilator stress ^{13}N ammonia (top row), rest ^{13}N ammonia (middle row) and glucose loaded ^{18}F-FDG images. These images show a large and severe perfusion defect in the entire inferior wall, inferolateral wall, septum and apex showing moderate reversibility on the rest images. The ^{18}F-FDG images show significant mismatch (hypoperfusion with preserved glucose utilization) in the inferior, inferolateral and inferoseptal walls (with the anterior, anteroseptal and anterolateral walls showing apparently reduced glucose uptake).

ischaemic perfusion deficit size and LVEF < 35% were powerful predictors of death or reinfarction. This study established that the extent, severity and reversibility of the myocardial perfusion defect, and LVEF are strong predictors of high risk in patients with ACS [11.22, 11.40, 11.41].

The extent of microvascular obstruction, myocardial scar, ischaemia and viability on CMR provide information used for the risk stratification of patients with ACS [11.16]. LVEF on echocardiography, CMR or radionuclide MPI can be used to determine eligibility for primary prevention internal cardioverter defibrillators post-ACS.

11.5.5. STE-ACS: Case 5

11.5.5.1. Clinical presentation

A 60 year old male with no prior CAD was admitted with chest pain and an anterior wall STEMI. He was treated with recombinant tissue plasminogen activator within 20 minutes of arrival in the accident and emergency department, about 6 h after the onset of chest pain. His symptoms resolved and the follow-up ECG showed an anterior wall myocardial infarction with 1 mm ST elevation in leads V3–V6, unchanged from the post-recombinant tissue plasminogen activator ECG. He developed sudden onset of shortness of breath with a systolic blood pressure of 80 mmHg, no chest pain and no cardiac murmur. An emergency bedside echocardiogram (see Fig. 11.7) shows a flail mitral valve (A) with severe eccentric mitral regurgitation (B).

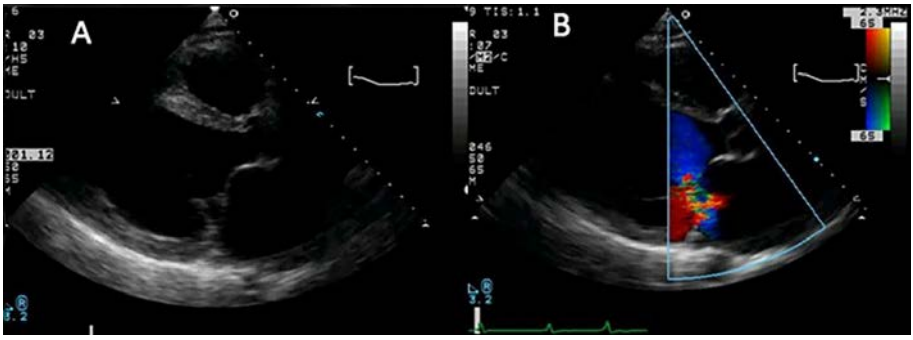

FIG. 11.7. 2-D and colour Doppler echocardiography to evaluate complications in acute STEMI. 2-D echocardiography shows (A) a flail mitral valve prolapsing into the left atrium with (B) severe eccentric mitral regurgitation.

11.5.5.2. Discussion

Echocardiography has several indications in patients with STE-ACS. It can identify causes of haemodynamic instability or shock and provide alternate explanations for a clinical presentation. Echocardiography is vital to identify ventricular septal rupture, papillary muscle rupture with acute mitral valve dysfunction, and tamponade following rupture of the left ventricular free wall in an ACS patient with haemodynamic compromise. In individuals with suspected rupture of the papillary muscle and severe mitral regurgitation, TEE may be indicated if the transthoracic study is not conclusive. Echocardiography is used to guide the placement of mechanical support devices in patients in shock. Large STEMIs can predispose a patient to left ventricular thrombus formation that, when identified, is an indication for anticoagulation.

CMR (see Fig. 11.8) plays an important role in the evaluation, risk assessment and management of patients with STEMI, in addition to echocardiography and radionuclide imaging (see Fig. 11.9). LGE, microvascular obstruction/no reflow phenomenon and peri-infarct zone are powerful predictors of post-infarct mortality independent of LVEF [11.18, 11.19].

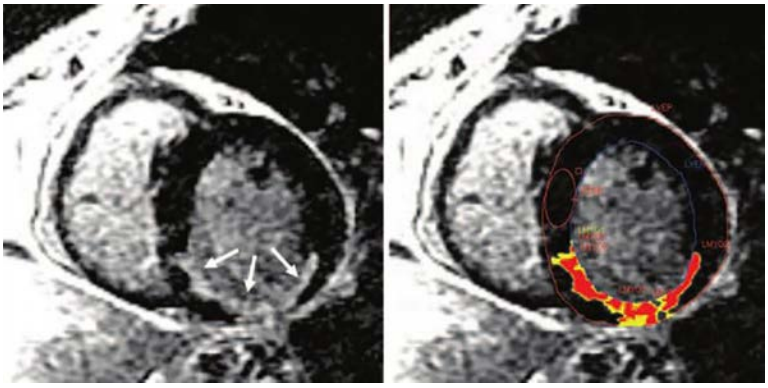

FIG. 11.8. LGE images post-inferior-wall myocardial infarction. The inferior, inferoseptal and inferolateral walls show LGE (left) with peri-infarct zone (right, yellow) indicating high risk.

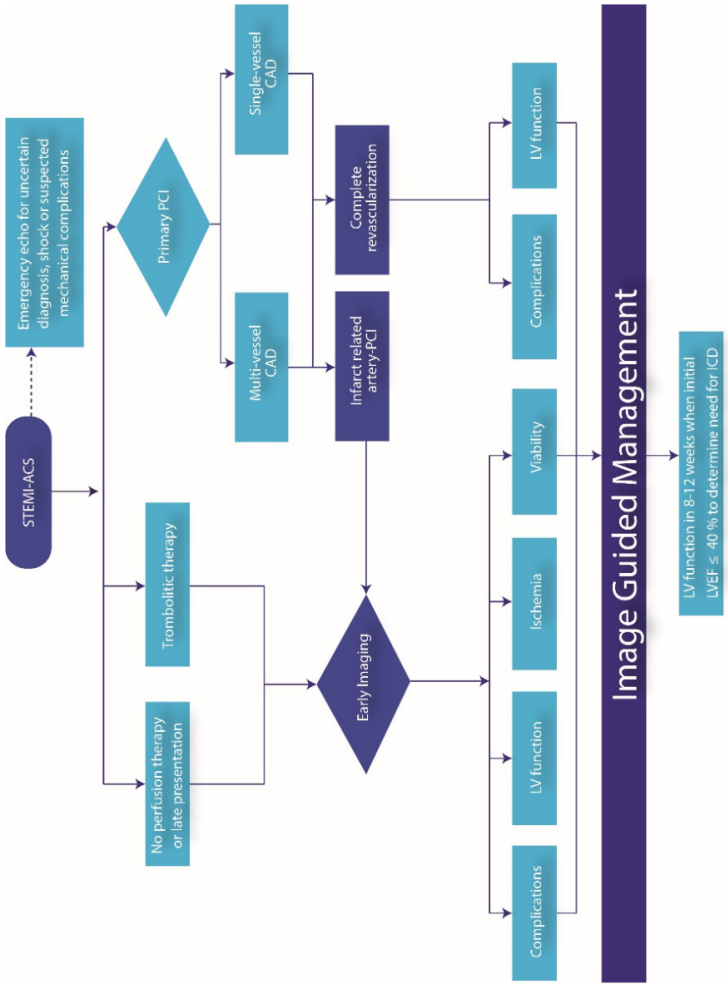

FIG. 11.9. Role of imaging in STEMI-ACS. In low TIMI risk score (0) or 1, GRACE score < 109; negative troponin; absence of high risk features. In complications and left ventricular (LV) function: Echocardiography, cardiac magnetic resonance (CMR). For ischaemia and viability: Radionuclide imaging, echocardiography or CMR. CAD — coronary artery disease; ICD — implantable cardioverter defibrillator; LVEF — left ventricular ejection fraction; PCI — percutaneous coronary intervention.

11.6. MYOCARDIAL INFARCTION WITH NON-OBSTRUCTIVE CORONARY ARTERIES

MINOCA comprises about 30–35% of cases of ACS [11.12, 11.42]. The causes for MINOCA include myocarditis, Takotsubo cardiomyopathy, spontaneous recanalization post-myocardial infarction, vasospasm, hypertrophic and dilated cardiomyopathies, coronary microvascular dysfunction and thrombophilic disorders. Multimodality imaging may be very helpful in identifying the underlying aetiology for MINOCA.

11.7. KEY MESSAGES

(1) Acute chest pain and suspected ACS is one of the most common reasons for emergency room visits.
(2) ACSs can present as unstable angina, myocardial infarction with ST elevation or without ST elevation.
(3) MINOCA comprises about 30–35% of cases of ACS.
(4) The management of ACS, particularly intermediate to high risk ACS, based on clinical evaluation, ECG and risk scores, includes invasive angiography with revascularization.
(5) Non-invasive cardiovascular imaging provides key additional information that is essential to stratify risk, identify complications and guide management of ACS.
(6) Assessment of left ventricular function, using echocardiography, is important during hospitalization for ACS and during follow-up to determine eligibility for primary prevention implantable cardioverter defibrillators.
(7) In ACS, the magnitude of microvascular obstruction, extent of scar and non-coronary aetiologies of symptoms can be identified by CMR.
(8) In patients with suspected or low risk ACS and no known prior CAD, coronary anatomy can be assessed non-invasively with CCTA to exclude CAD and to characterize coronary plaque.
(9) Ischaemia testing is indicated in ACS patients with incomplete or no revascularization either prior to or after discharge. Rest and stress MPI (SPECT or PET) are most commonly used; echocardiography and CMR are also options.
(10) The extent of viable myocardium, in addition to ischaemia testing, can guide revascularization decisions. MPI (SPECT or PET), ^{18}F-FDG-PET (hibernation), CMR (scar on gadolinium enhanced imaging) and low dose dobutamine stress echocardiography are all options.

REFERENCES TO CHAPTER 11

[11.1] BENJAMIN, E.J., et al., Heart disease and stroke statistics: 2017 update, Circulation **135** (2017) 146–603.

[11.2] ROTH, G.A., et al., Global and regional patterns in cardiovascular mortality from 1990 to 2013, Circulation **132** (2015) 1667–1678.

[11.3] KOHN, M.A., KWAN, E., GUPTA, M., TABAS, J.A., Prevalence of acute myocardial infarction and other serious diagnoses in patients presenting to an urban emergency department with chest pain, J. Emerg. Med. **29** (2005) 383–390.

[11.4] RAFF, G.L., HOFFMANN, U., UDELSON, J.E., Trials of imaging use in the emergency department for acute chest pain, J. Am. Coll. Cardiol. Cardiovasc. Imag. **10** (2017) 338–349.

[11.5] ROFFI, M., et al., 2015 ESC guidelines for the management of acute coronary syndromes in patients presenting without persistent ST-segment elevation, Eur. Heart J. **37** (2016) 267–315.

[11.6] AMSTERDAM, E.A., et al., 2014 AHA/ACC guideline for the management of patients with non-ST-elevation acute coronary syndromes, Circulation **130** (2014) 344–426.

[11.7] THYGESEN, K., et al., Third universal definition of myocardial infarction, Circulation **126** (2012) 2020–2035.

[11.8] LIBBY, P., Mechanisms of acute coronary syndromes and their implications for therapy, N. Engl. J. Med. **368** (2013) 2004–2013.

[11.9] CREA, F., LIBBY, P., Acute coronary syndromes: The way forward from mechanisms to precision treatment, Circulation **136** (2017) 1155–1166.

[11.10] PASTERKAMP, G., DEN RUIJTER, H.M., LIBBY, P., Temporal shifts in clinical presentation and underlying mechanisms of atherosclerotic disease, Nat. Rev. Cardiol. **14** (2017) 21–29.

[11.11] ARBUSTINI, E., et al., Plaque erosion is a major substrate for coronary thrombosis in acute myocardial infarction, Heart **82** (1999) 269–272.

[11.12] IBANEZ, B., et al., 2017 ESC guidelines for the management of acute myocardial infarction in patients presenting with ST-segment elevation, Eur. Heart J. **39** (2018) 119–177.

[11.13] O'GARA, P.T., et al., 2013 ACCF/AHA guideline for the management of ST-elevation myocardial infarction, Circulation **127** (2013) 362–425.

[11.14] SIONTIS, G.C., et al., Outcomes of non-invasive diagnostic modalities for the detection of coronary artery disease: Network meta-analysis of diagnostic randomised controlled trials, BMJ **21** (2018) 360–504.

[11.15] DE LA MORA CERVANTES, R., DENNIE, C., Triple rule-out cardiac computed tomography: Is it finally a reality? Minerva Cardioangiol. **65** (2017) 225–234.

[11.16] LOCKIE, T., NAGEL, E., REDWOOD, S., PLEIN, S., Use of cardiovascular magnetic resonance imaging in acute coronary syndromes, Circulation **119** (2009) 1671–1681.

[11.17] PLEIN, S., et al., Assessment of non-ST-segment elevation acute coronary syndromes with cardiac magnetic resonance imaging, J. Am. Coll. Cardiol. **44** (2004) 2173–2181.

[11.18] YAN, A.T., et al., Characterization of microvascular dysfunction after acute myocardial infarction by cardiovascular magnetic resonance first-pass perfusion and late gadolinium enhancement imaging, J. Cardiovasc. Magn. Reson. **8** (2006) 831–837.

[11.19] YAN, A.T., et al., Characterization of the peri-infarct zone by contrast-enhanced cardiac magnetic resonance imaging is a powerful predictor of post-myocardial infarction mortality, Circulation **114** (2006) 32–39.

[11.20] CARRICK, D., et al., Myocardial hemorrhage after acute reperfused ST-segment-elevation myocardial infarction: Relation to microvascular obstruction and prognostic significance, Circ. Cardiovasc. Imag. **9** (2016).

[11.21] PARKEY, R.W., et al., A new method for radionuclide imaging of acute myocardial infarction in humans, Circulation **50** (1974) 540–546.

[11.22] DAKIK, H.A., et al., Prognostic value of exercise 201Tl tomography in patients treated with thrombolytic therapy during acute myocardial infarction, Circulation **94** (1996) 2735–2742.

[11.23] SCHLETT, C.L., et al., Prognostic value of CT angiography for major adverse cardiac events in patients with acute chest pain from the emergency department: 2-year outcomes of the ROMICAT trial, J. Am. Coll. Cardiol. Cardiovasc. Imag. **4** (2011) 481–491.

[11.24] GOLDSTEIN, J.A., et al., The CT-STAT (Coronary Computed Tomographic Angiography for Systematic Triage of Acute Chest Pain Patients to Treatment) trial, J. Am. Coll. Cardiol. **58** (2011) 1414–1422.

[11.25] LINDE, J.J., et al., Long-term clinical impact of coronary CT angiography in patients with recent acute-onset chest pain: The randomized controlled CATCH trial, J. Am. Coll. Cardiol. Cardiovasc. Imag. **8** (2015) 1404–1413.

[11.26] HULTEN, E., et al., Outcomes after coronary computed tomography angiography in the emergency department: A systematic review and meta-analysis of randomized, controlled trials, J. Am. Coll. Cardiol. **61** (2013) 880–892.

[11.27] HOFFMANN, U., et al., Coronary CT angiography versus standard evaluation in acute chest pain, N. Engl. J. Med. **367** (2012) 299–308.

[11.28] LITT, H.I., et al., CT angiography for safe discharge of patients with possible acute coronary syndromes, N. Engl. J. Med. **366** (2012) 1393–1403.

[11.29] HULTEN, E., et al., Meta-analysis of coronary CT angiography in the emergency department, Eur. Heart J. Cardiovasc. Imag. **14** (2013) 607.

[11.30] FERENCIK, M., et al., Highly sensitive troponin I followed by advanced coronary artery disease assessment using computed tomography angiography improves acute coronary syndrome risk stratification accuracy and work-up in acute chest pain patients: Results from ROMICAT II trial, J. Am. Coll. Cardiol. Cardiovasc. Imag. **8** (2015) 1272–1281.

[11.31] RYBICKI, F.J., et al., 2015 ACR/ACC/AHA/AATS/ACEP/ASNC/NASCI/SAEM/SCCT/SCMR/SCPC/SNMMI/STR/STS appropriate utilization of cardiovascular imaging in emergency department patients with chest pain: A joint document of the American College of Radiology Appropriateness Criteria Committee and the American College of Cardiology Appropriate Use Criteria Task Force, J. Am. Coll. Cardiol. **67** (2016) 853–879.

[11.32] NABI, F., et al., Optimizing evaluation of patients with low-to-intermediate-risk acute chest pain: A randomized study comparing stress myocardial perfusion tomography incorporating stress-only imaging versus cardiac CT, J. Nucl. Med. **57** (2016) 378–384.

[11.33] CREMER, P.C., et al., Myocardial perfusion imaging in emergency department patients with negative cardiac biomarkers: Yield for detecting ischemia, short-term events, and impact of downstream revascularization on mortality, Circ. Cardiovasc. Imag. **7** (2014) 912–919.

[11.34] UDELSON, J.E., et al., Myocardial perfusion imaging for evaluation and triage of patients with suspected acute cardiac ischemia: A randomized controlled trial, JAMA **288** (2002) 2693–2700.

[11.35] DILSIZIAN, V., et al., ASNC imaging guidelines/SNMMI procedure standard for positron emission tomography (PET) nuclear cardiology procedures, J. Nucl. Cardiol. **23** (2016) 1187–1226.

[11.36] ROGERS, I.S., et al., Feasibility of FDG imaging of the coronary arteries: Comparison between acute coronary syndrome and stable angina, J. Am. Coll. Cardiol. Cardiovasc. Imag. **3** (2010) 388–397.

[11.37] JOSHI, N.V., et al., ^{18}F-fluoride positron emission tomography for identification of ruptured and high-risk coronary atherosclerotic plaques: A prospective clinical trial, Lancet **383** (2014) 705–713.

[11.38] KWONG, R.Y., et al., Detecting acute coronary syndrome in the emergency department with cardiac magnetic resonance imaging, Circulation **107** (2003) 531–537.

[11.39] STEEL, K., et al., Complementary prognostic values of stress myocardial perfusion and late gadolinium enhancement imaging by cardiac magnetic resonance in patients with known or suspected coronary artery disease, Circulation **120** (2009) 1390–1400.

[11.40] MAHMARIAN, J.J., et al., Adenosine sestamibi SPECT post-infarction evaluation (INSPIRE) trial: A randomized, prospective multicenter trial evaluating the role of adenosine Tc-99m sestamibi SPECT for assessing risk and therapeutic outcomes in survivors of acute myocardial infarction, J. Nucl. Cardiol. **11** (2004) 458–469.

[11.41] BROWN, K.A., et al., Early dipyridamole ^{99m}Tc-sestamibi single photon emission computed tomographic imaging 2 to 4 days after acute myocardial infarction predicts in-hospital and postdischarge cardiac events: Comparison with submaximal exercise imaging, Circulation **100** (1999) 2060–2066.

[11.42] PASUPATHY, S., TAVELLA, R., BELTRAME, J.F., Myocardial Infarction with Nonobstructive Coronary Arteries (MINOCA): The past, present, and future management, Circulation **135** (2017) 1490–1493.

Chapter 12

HEART FAILURE

X. ZHOU, I. CARVAJAL, M.A. VANNAN

Non-invasive imaging plays a key role in the evaluation and management of a patient with a clinical diagnosis of heart failure [12.1]. The taking of a clinical history, the determination of signs and symptoms, and physical examination are indispensable first steps in the evaluation of a patient with suspected or known heart failure. Thereafter, non-invasive imaging is used to further characterize the heart failure, with the aim of confirming or establishing the aetiology, classifying the type and stage of heart failure, targeting therapies and assigning a prognosis. This chapter provides a roadmap of how to appropriately use the various imaging modalities in the assessment of heart failure, with an emphasis on initial testing. Some of the essential questions to be answered during initial testing are:

— What is the global and regional left ventricular function?
— What is the size of the left ventricle?
— What is the left ventricular myocardial morphology?
— Is there myocardial ischaemia and/or viability?
— What is the size and function of other chambers: left atrium, right ventricle?
— Are there significant associated or causative valve disease?
— Are there pericardial abnormalities?

12.1. GLOBAL AND REGIONAL LEFT VENTRICULAR FUNCTION

Ejection fraction is the most commonly used index to assess global left ventricular systolic function [12.2, 12.3]. When the left ventricular ejection fraction (LVEF) is <40%, there is universal consensus that this indicates heart failure with reduced ejection fraction (HFrEF). When the LVEF is >50%, this is classified as heart failure with preserved ejection fraction (HFpEF), and an LVEF of 41–49% represents heart failure with medium range ejection fraction (HFmrEF, according to the European Society of Cardiology guidelines) or borderline ejection fraction (HFpEF-borderline, according to the American College of Cardiology/American Heart Association guidelines). Some of the patients with a LVEF of >40% may be those whose ejection fraction was previously <40% (i.e. patients who have improved from HFrEF to HFpEF-borderline or even HFpEF). This classification has prognostic significance, determines the selection

of appropriate drug therapy and aids in decision making on the timing and appropriateness of device therapy (see Fig. 12.1).

LVEF is most commonly measured or estimated by 2-D echocardiography. While this is practical, there are many challenges when using 2-D echocardiography. There is the limitation imposed by inadequate acoustic windows, which can in many instances be overcome by the use of microbubble contrast echocardiography. However, even contrast echocardiography cannot overcome the fundamental geometric assumptions made in 2-D imaging, and operator variability in acquiring the images. 3-D echocardiography does not assume pre-fixed geometric shapes of the left ventricle and shows promise for routine use. However, it is also limited by the need for adequate acoustic windows for reliable data. Cardiac magnetic resonance (CMR) is currently the alternative technique for the measurement of ejection fraction, and the first line technique preferred over echocardiography in some instances. Radionuclide ventriculography is also a method of measuring LVEF, although it is used less frequently now with the evolution of CMR for this particular purpose. Radionuclide ventriculography is still a useful technique when echocardiography is suboptimal and CMR cannot be done. Computed tomography (CT) is rarely performed for the sole purpose of measuring LVEF.

Regional function is most commonly assessed by the visual examination of myocardial thickening and wall motion. The degree of abnormality is classified as hypokinetic, akinetic or dyskinetic muscle with scores assigned to each abnormality. The sum of the scores assigned to each region is then used as a semiquantitative measure of the severity, with higher scores representing more severe regional dysfunction. The presence of significant regional dysfunction

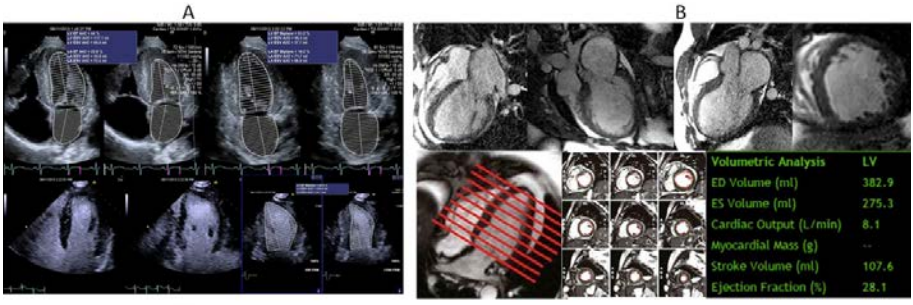

FIG. 12.1. (A) The upper panel shows standard 2-D echocardiographic methods with and without contrast; (B) Left ventricular volumes and LVEF measured using CMR. In about 30% of patients undergoing echocardiography for heart failure, contrast is useful to salvage suboptimal images to allow measurement of LVEF. CMR is not limited by acoustic windows and is a better method when accurate and reproducible measurements of LVEF are necessary.

in the setting of HFrEF, HFmrEF or HFpEF generally points to an ischaemic aetiology for heart failure. However, global left ventricular dysfunction in heart failure may also be associated with regional dysfunction. Echocardiography and CMR are the two most useful imaging modalities to assess regional myocardial function in terms of thickening and motion.

12.2. LEFT VENTRICULAR SIZE AND SHAPE

Left ventricular size can be measured as a dimension or volume. The former is practical and simple, and the latter is a better descriptor of size than a dimension, but requires more data and takes time to compute. The measurement of left ventricular volume is especially relevant when there is significant regional dysfunction. Left ventricular dimension as an index of left ventricular size is not recommended in the latter situation. Both end diastolic and end systolic left ventricular size and volume has prognostic significance and are indices that can be used to assess the effectiveness of heart failure therapies [12.4]. Left ventricular global shape measured as the sphericity index or reginal shape measured as endocardial curvature are also critical determinants of global and regional left ventricular function but whether these should be measured selectively or routinely is not currently established. Thus, only the measurement of left ventricular size is presently recommended in routine practice. 2-D echocardiography is used to measure left ventricular dimensions and volumes, although the measured volumes are smaller than those measured with CMR. Contrast echocardiography improves the accuracy of 2-D echocardiography for measurement of volumes, but they still prove to be smaller than CMR volumes and have the disadvantage of geometric assumption for the calculation of volume. CMR is the reference standard for left ventricular volume and when accurate, reproducible left ventricular volume measurements are necessary for clinical purposes. 3-D echocardiography is superior to 2-D echocardiography and may prove to be a practical alternative to CMR, at least in those with adequate acoustic windows.

12.3. MYOCARDIAL MORPHOLOGY AND FUNCTION

There are three key attributes of myocardial morphology that can be assessed by imaging. The first is myocardial thickness. Myocardial thickness is the mass of the myocardium bounded internally by the endocardium and externally by the epicardium. There are regional variations in myocardial thickness with the apex of the heart being the thinnest part of the left ventricular myocardium. Myocardial thickness is a key component of left ventricular mass, which in turn is a key

determinant of prognosis in heart failure. The ratio of myocardial thickness to the left ventricular cavity size (volume) is an index of regional wall tension that plays a significant role in left ventricular remodelling [12.5].

The second attribute of myocardial morphology is whether it is excessively trabeculated. The endocardium of the left ventricle of an adult may show some noticeable trabeculations at the apex, lateral, inferior and posterior walls. These are shallow finger like projections. The interventricular septum and the anterior walls of the left ventricle are almost never trabeculated in the adult; the adult left ventricular myocardium is largely compacted. Excessive trabeculation in regions where there is usually some trabeculation or presence of trabeculation in areas where there is usually none may be indicative of a cardiomyopathy such as isolated left ventricular non-compaction as the aetiology of heart failure. Conversely, excessive trabeculation may merely be a marker of extreme left ventricular dilatation that causes exaggeration of the normally present trabeculation. The latter is more likely in older age groups. Myocardial trabeculations play a role in myocardial deformation (strain) and excessive, abnormal trabeculations may potentially contribute to abnormal myocardial strain and adverse left ventricular remodelling (see Fig. 12.2).

The third attribute that is crucial to left ventricular function is the presence, extent and amount of myocardial scarring and fibrosis. Scarring usually follows injury to the myocardium such as infarction: the loss of myocytes triggers fibroblast activation that results in replacement fibrosis, but the total myocardial mass is decreased and in general there is thinning of the myocardium. Alternatively, increased myocardial stress such as hypertension can activate the fibroblasts, which causes diffuse interstitial (reactive) fibrosis and expansion of the extracellular volume. In this case, total myocardial mass is increased and myocardial hypertrophy is present. However, cell death by apoptosis or other mechanisms can result in myocyte loss, which is then replaced by replacement fibrosis, maintaining increased myocardial mass and myocardial hypertrophy. These structural changes are essential determinants of natural history and clinical outcomes of heart failure syndromes. They influence the selection and success of therapeutic strategies, and provide targets for newer therapies [12.6].

Myocardial function is measured as strain. Although myocardial strain has been previously measured by CMR in normal and abnormal left ventricles, it has only recently evolved into a practical index of myocardial function. This has been mainly due to the development of speckle tracking echocardiography (STE), which allows the measurement of myocardial strain. This technology has become ubiquitous in echocardiography and therefore the assessment of myocardial strain has become widespread in many heart failure syndromes. There is now general agreement, based on the published evidence, that global longitudinal strain measured by echocardiography is a sensitive marker of

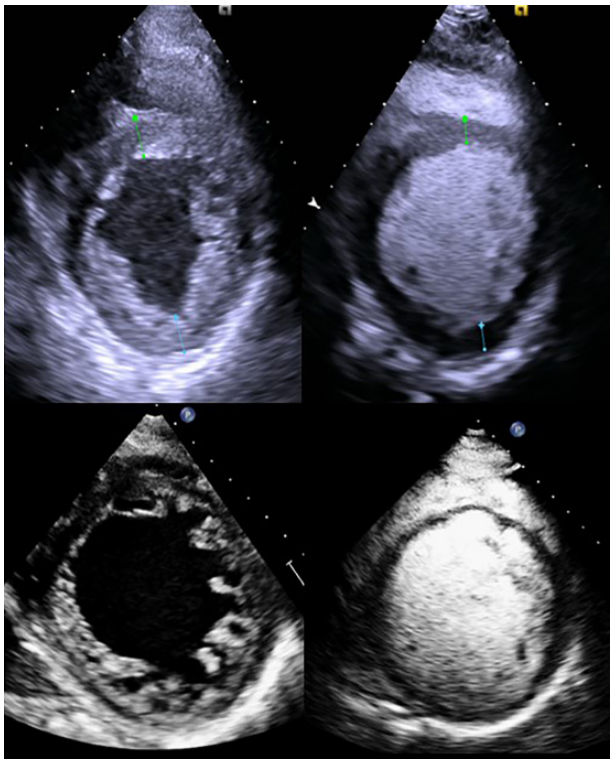

FIG. 12.2. Trabeculated endocardium and compacted myocardium. Excessive trabeculation has implications for myocardial function. Even though the myocardium appears relatively compacted with only minor trabeculations (top row), contrast echocardiography on the right clearly shows that the compacted myocardial edge and the myocardium are thinner than in the non-contrast echo. This is even better illustrated in a patient with heart failure and dilated left ventricle (bottom row). In the non-contrast echocardiography, excessive trabeculation is noted; contrast echocardiography shows the compacted myocardial edge beyond the trabeculations and is shown to be uniformly thin all around. The ratio of the trabeculated to compacted myocardial thickness and the ratio of the compacted myocardial thickness to the total myocardial mass have a diagnostic value for non-compaction and are also determinants of myocardial function (strain) for any given ejection fraction.

myocardial dysfunction and predates a reduction in LVEF. Global circumferential strain may also offer incremental prognostic value to global longitudinal strain, especially in the assessment of myocardial viability [12.7]. Myocardial strain is also a good index of regional function but the noise in echocardiographic techniques limits their use for this purpose. However, this is a target for future developments in this field since regional function is a key part of the assessment of myocardial ischaemia, especially during stress testing. STE is the primary

technique used in the routine assessment of myocardial strain. It is practical, and repeat testing is easily carried out. CMR is the other modality that can be used for myocardial strain measurements, but the usual method of myocardial tagging is cumbersome for routine use. More recently, feature tracking algorithms applied to cine-CMR steady state free precession (SSFP) images have been investigated for the measurement of myocardial strain. If these methods prove to be accurate and practical, CMR may be used more often for myocardial strain measurements in the future.

12.4. MYOCARDIAL ISCHAEMIA OR VIABILITY

The most common aetiology for heart failure is myocardial ischaemia or infarct due to obstructive coronary artery disease (CAD). The latter is a treatable cause of ischaemic myocardial dysfunction and hence it is important to include or exclude the presence of obstructive CAD. Non-obstructive CAD or microvascular dysfunction can also cause ischaemic heart failure and, although these are not the result of epicardial CAD, they can often be treated based on the underlying aetiology. Thus, testing for myocardial ischaemia is a key step in the first time evaluation of heart failure. In addition, the assessment of myocardial viability may be important when making decisions about revascularization in the setting of ischaemic heart failure and significant left ventricular dysfunction (LVEF < 30%) [12.8].

Stress and rest single photon emission computed tomography (SPECT) or positron emission tomography (PET) are the most commonly used methods to assess myocardial ischaemia and viability in heart failure. The assessment of the presence and severity of myocardial ischaemia by both these techniques has proven their diagnostic and prognostic value in patients with heart failure [12.9, 12.10]. CT coronary artery calcium score (CACS) and coronary computed tomography angiography (CCTA) are emerging as useful tests that provide adjunctive, and often useful, information on the probability of the presence of obstructive CAD and/or coronary plaque morphology (see Chapter 6).

Stress and rest echocardiography and CMR are the other two non-invasive tests for the assessment of myocardial ischaemia (see Chapters 4 and 5). Dobutamine or vasodilator stress echocardiography have both been shown to be useful methods to evaluate myocardial ischaemia and viability. In addition, exercise echocardiography can be used to test for myocardial ischaemia. These echocardiographic based tests have been shown to have good diagnostic and prognostic value in patients with left ventricular dysfunction. The addition of contrast has further extended their utility through the enhancement of endocardial borders and by providing information on microvascular integrity

(myocardial contrast echocardiography). The feasibility and reliability of myocardial contrast echocardiography, however, has not been demonstrated in large studies and is not recommended. Despite the plethora of data with stress echocardiography, a challenge is the assessment of ischaemia or viability in left ventricular dysfunction with thinned out walls. Thus, CMR has emerged as an alternative to echocardiography and is often the second line test after SPECT–PET. Stress and rest CMR myocardial perfusion imaging (MPI) also has excellent spatial resolution for the evaluation of wall thickening, which improves the reliability of the test.

12.5. LEFT ATRIUM AND RIGHT VENTRICLE

The size of the left atrium [12.11] is an independent predictor of outcomes in heart failure (see Fig. 12.3). It is also an important marker of abnormalities in diastolic filling of the left ventricle in all categories of heart failure. Similarly, left atrial function and strain are emerging as sensitive indicators of myocardial dysfunction and predictors of outcome in heart failure. However, these measurements will need further investigations before they are recommended as routine measurements in patients with heart failure. Currently, measurement of left atrial volume on bi-plane echocardiography is implemented as an adjunct assessment of left ventricular diastolic dysfunction along with tissue Doppler to

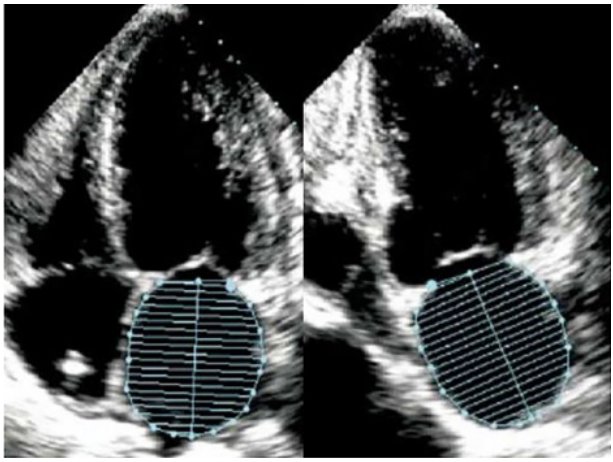

FIG. 12.3. Prognostic value of left atrial volume in heart failure. These images show the standard echocardiographic method to measure bi-plane left atrial volume which is then indexed to the body surface area.

estimate prognosis in heart failure. 3-D echocardiography and CMR are alternative techniques that are performed selectively to evaluate the left atrial volume.

The right ventricular ejection fraction (RVEF) is a powerful indicator of outcomes in left sided heart failure [12.12]. CMR is the preferred technique to measure the RVEF, but it is not practical in all patients with heart failure. Therefore, a number of 2-D echocardiographic indices of right ventricular systolic function have been used as a surrogate for RVEF, and many of these have shown good correlation with RVEF. These indices have also been prognostically valuable. 3-D echocardiography holds promise to measure RVEF, but this needs further validation and the feasibility for routine use remains to be determined. Right ventricular myocardial strain is another parameter that may be incremental to RVEF or even superior to RVEF in the prognostication of heart failure, but this needs to be confirmed in future studies (see Fig. 12.4).

12.6. VALVE DISEASE

The most common valve disease in heart failure is a result of left ventricular dysfunction. Secondary mitral regurgitation, also referred to as functional mitral regurgitation, is the most common valve disease in the heart failure population. Some degree of mitral regurgitation is seen in the majority of patients with heart failure, with severe mitral regurgitation being present in about a third of the patients with systolic heart failure. While there is a good understanding of the mechanisms of secondary mitral regurgitation, the treatment strategies for this are more controversial and are still being debated. However, there is universal agreement that significant functional mitral regurgitation worsens prognosis in heart failure [12.13] and, if unresolved with maximum tolerated guideline directed medical therapy, other interventions must be considered for the optimal treatment of mitral regurgitation. The options, generally, are surgical mitral valve repair or replacement, with the latter lately being shown to be better than repair to prevent recurrent mitral regurgitation. Cardiac resynchronization therapy has also been shown to be useful to reduce mitral regurgitation if not to abolish it. More recently, catheter based therapies for mitral regurgitation such as repair with a mitral clip or other annuloplasty device, and replacement with specifically designed valves for the mitral position, have shown promise. These minimally invasive transcatheter therapies may yet transform the solutions for a problem for which there are limited options, if any.

Another valve disease that is being increasingly recognized as an important contributor to morbidity in heart failure is functional tricuspid regurgitation. While the data are compelling, the options for treatment are even more limited than those for functional mitral regurgitation, with surgical repair being the only

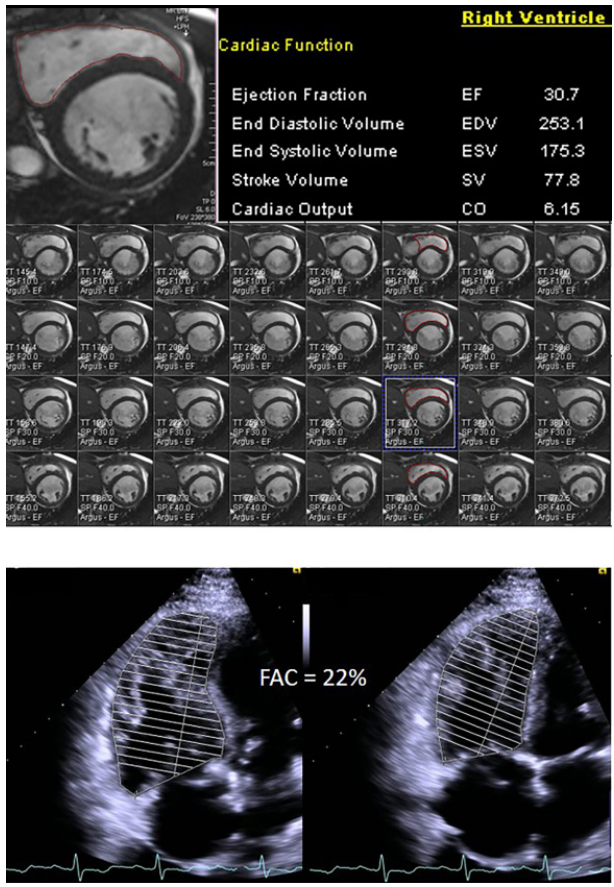

FIG. 12.4. Predictive value of right ventricular function in heart failure. The upper part of the figure shows the CMR approach to measuring right ventricular volumes and ejection fraction. CMR is the recommended method for this purpose. The powerful predictive value of RVEF in patients with left heart failure is shown in the lower half with ejection fraction of <30% portending a bad prognosis. Echocardiography is the standard and the most common method used to assess right ventricular function in daily practice. RVEF cannot be measured by 2-D echocardiography and several Doppler echocardiography indices are used as a surrogate for RVEF instead.

option until recently. However, surgery for functional tricuspid regurgitation alone was not enthusiastically embraced given that many of these patients had varying degrees of right ventricular systolic dysfunction and did not benefit from the abolishment of tricuspid regurgitation. However, the emergence of transcatheter devices for tricuspid valve repair is promising and hence routine assessment of tricuspid regurgitation may become essential in heart failure.

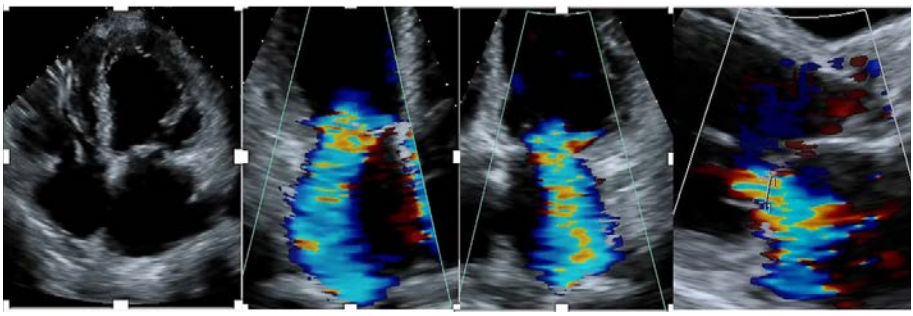

FIG. 12.5. Functional mitral regurgitation in heart failure. The image on the far left shows a four chamber view of the heart. The next three images show the severity of mitral regurgitation as assessed by colour Doppler in the three chamber view, four chamber view and long axis parasternal view, respectively.

Figure 12.5 illustrates the significance of functional mitral regurgitation and tricuspid regurgitation in heart failure.

12.7. KEY MESSAGES

(1) The prevalence of heart failure is increasing, in part owing to an ageing population.
(2) Heart failure is the among the top indications for performing a non-invasive imaging test worldwide.
(3) Non-invasive imaging modalities have unique and overlapping capabilities that mean that multiple testing is often done in the evaluation of heart failure.
(4) The increase in therapeutic options beyond medical treatment to include device therapies has further increased the volume of non-invasive imaging tests in patients with heart failure.
(5) The above factors have required the medical community to develop algorithms for non-invasive testing based on the key questions in the management of patients with heart failure, rather than on a modality based approach.
(6) Echocardiography, nuclear cardiology, CMR and CT CACS or CCTA all have a role in the initial and subsequent evaluation of heart failure depending on the clinical presentation. However, it is very unlikely that all four tests are necessary in each patient with heart failure.
(7) Echocardiography is the first test in almost all initial evaluations of heart failure. It provides both anatomical and haemodynamic data that have diagnostic and prognostic value.

(8) If CAD is strongly suspected as the cause of heart failure based on clinical presentation and echocardiography, then nuclear scintigraphy is usually the next step with maximum yield. In specific circumstances, CCTA may be an alternative test or may be done in addition to nuclear scintigraphy.
(9) If primary cardiac muscle disease is strongly suggested by initial clinical presentation and echocardiography, then CMR is often the best next step. Occasionally, nuclear scintigraphy may be useful instead of CMR.
(10) If there is suggestion of significant valve disease either as a cause of heart failure or a result of heart failure, then echocardiography with selective use of CMR is often sufficient for a comprehensive evaluation.

REFERENCES TO CHAPTER 12

[12.1] PATEL, M.R., et al., 2013 ACCF/ACR/ASE/ASNC/SCCT/SCMR appropriate utilization of cardiovascular imaging in heart failure, J. Am. Coll. Cardiol. **61** (2013) 2207–2231.
[12.2] YANCY, C.W., et al., 2013 ACCF/AHA guideline for the management of heart failure, J. Am. Coll. Cardiol. **62** (2013) 147–239.
[12.3] PONIKOWSKI, P., et al., 2016 ESC guidelines for the diagnosis and treatment of acute and chronic heart failure: The Task Force for the Diagnosis and Treatment of Acute and Chronic Heart Failure of the European Society of Cardiology (ESC), Eur. J. Heart Fail. **18** (2016) 891–975.
[12.4] MARWICK, T.H., Ejection fraction pros and cons: JACC state-of-the-art review, J. Am. Coll. Cardiol. **72** (2018) 2360–2379.
[12.5] KONSTAM, M.A., ABBOUD, F.M., Ejection fraction: Misunderstood and overrated (changing the paradigm in categorizing heart failure), Circulation **135** (2017) 717–719.
[12.6] KONSTAM, M.A., KRAMER, D.G., PATEL, A.R., MARON, M.S., UDELSON, J.E., Left ventricular remodeling in heart failure: Current concepts in clinical significance and assessment, J. Am. Coll. Cardiol. Cardiovasc. Imag. **4** (2011) 98–108.
[12.7] GONZÁLEZ, A., SCHELBERT, E.B., DÍEZ, J., BUTLER, J., Myocardial interstitial fibrosis in heart failure: Biological and translational perspectives, J. Am. Coll. Cardiol. **71** (2018) 1696–1706.
[12.8] BAX, J.J., DELGADO, V., Myocardial viability as integral part of the diagnostic and therapeutic approach to ischemic heart failure, J. Nucl. Cardiol. **22** (2015) 229–245.
[12.9] DJAILEB, L., et al., Suboptimal performance of cardiovascular magnetic resonance imaging for the assessment of myocardial viability at the early phase of an acute coronary syndrome: Usefulness of SPECT myocardial perfusion imaging, J. Nucl. Cardiol. **26** (2019) 1365–1367.
[12.10] LÖFFLER, A.I., KRAMER, C.M., Myocardial viability testing to guide coronary revascularization, Interv. Cardiol. Clin. **7** (2018) 355–365.

[12.11] ROSSI, A., et al., Independent relationship of left atrial size and mortality in patients with heart failure: An individual patient meta-analysis of longitudinal data (MeRGE heart failure), Eur. J. Heart Fail. **11** (2009) 929–936.

[12.12] GHIO, S., Prognostic value of right ventricular function in chronic HF, Cardiol. Rev. **19** (2002) 9–15.

[12.13] NASSER, R., et al., Evolution of functional mitral regurgitation and prognosis in medically managed heart failure patients with reduced ejection fraction, J. Am. Coll. Cardiol. Heart Fail. **5** (2017) 652–659.

Chapter 13

CARDIOMYOPATHIES

R. GIUBBINI, S. DORBALA, E. MILAN

Cardiomyopathy is an intrinsic structural disorder of the myocardium that may result in ventricular dysfunction and can progress to clinical heart failure. It is a major public health issue, affecting more than 5.8 million people in the United States of America and more than 23 million people worldwide [13.1]. Heart failure is not a specific entity, but a clinical syndrome with different characteristics depending on age, sex, race, ethnicity, left or right ventricular dysfunction, and aetiology.

A basic pathophysiological difference characterizing patients with different aetiologies of heart failure is the presence of reduced or preserved left ventricular ejection fraction (LVEF). This distinction is not trivial, since the treatment of heart failure with reduced ejection fraction (HFrEF) is well established, while that is not the case for heart failure with preserved ejection fraction (HFpEF). Several risk factors, such as ischaemic heart disease, hypertension, smoking, obesity, diabetes mellitus and infectious diseases, are associated with the development of heart failure as well as its severity and prognosis.

Cardiomyopathies can be classified as primary or secondary disorders. A primary cardiomyopathy is an isolated disease of the myocardium and can be genetic or acquired. Secondary cardiomyopathies are due to systemic disorders with involvement of the myocardium. Another approach to classifying cardiomyopathies is to differentiate conditions that cause primarily left ventricular systolic or diastolic dysfunction. Based on their morphological and haemodynamic characteristics, cardiomyopathies have traditionally been divided into three main categories: dilated cardiomyopathy, hypertrophic cardiomyopathy and restrictive cardiomyopathy (see Table 13.1).

Non-invasive imaging modalities can help to determine whether abnormalities are present in the myocardium, valves, pericardium or vessels. The information collected with imaging can also provide important prognostic information. Echocardiography is the most common imaging technique used for the initial diagnosis and management of cardiomyopathy. However, other imaging modalities, including nuclear cardiology (myocardial perfusion imaging, MPI, with either single photon emission computed tomography, SPECT, or positron emission tomography, PET), cardiac magnetic resonance (CMR) imaging and cardiac computed tomography (CCT), play an important role, depending on the underlying aetiology of the cardiomyopathy.

TABLE 13.1. MAIN AETIOLOGIES FOR DIFFERENT CARDIOMYOPATHIES

Dilated cardiomyopathy	Hypertrophic cardiomyopathy	Restrictive cardiomyopathy
Idiopathic	Idiopathic	Idiopathic
Familiar	Familial	Familial
Drugs and medications (alcohol, chemotherapy)	Storage disease (lysosomal, glycogen)	Infiltrative (amyloidosis, sarcoidosis)
Myocarditis (infective/toxic/immune)	Syndromic	Storage disease (Anderson–Fabry, haemochromatosis)
Endocrine (diabetes mellitus, thyroid disease)	Deficiency disease (carnitine, phosphorylase B kinase)	Non-infiltrative

As the first line imaging procedure, echocardiography helps to clarify several important pathophysiological mechanisms, such as systolic versus diastolic left ventricular dysfunction, valvular and pericardial diseases, and probable non-ischaemic versus ischaemic cardiomyopathy. The latter can be further investigated with MPI and CMR to establish the presence of inducible myocardial ischaemia and scarring [13.2], and coronary computed tomography angiography (CCTA) to establish the presence of obstructive coronary artery disease (CAD) [13.3–13.5].

Multimodality imaging is particularly useful in the differential diagnosis of HFpEF that can be secondary to severe tricuspid regurgitation, restrictive cardiomyopathy, constrictive pericarditis and hypertrophic cardiomyopathy [13.4]. The role of multimodality imaging in restrictive cardiomyopathies has been recently reviewed in Ref. [13.6].

13.1. HYPERTROPHIC CARDIOMYOPATHY

Hypertrophic cardiomyopathy is a genetic myocardial disorder, phenotypically affecting 0.2% (1 in 500) of the general adult population, independent of sex and ethnicity. The typical pathological findings of the disease are myocyte hypertrophy and hyperplasia, myocyte disarray, small vessel disease

and fibrosis. Fibrosis can present as interstitial fibrosis (increased collagen without evidence of cardiomyocyte loss) and replacement fibrosis (increased collagen with evidence of cardiomyocyte loss).

The clinical features of hypertrophic cardiomyopathy can vary; in the majority of patients it is a benign condition, asymptomatic and with a normal life expectancy. However, hypertrophic cardiomyopathy is the most frequent cause of sudden cardiac death in the young and in athletes under 35 years of age. Heart failure and atrial fibrillation are the most relevant complications [13.7–13.9]. Echocardiography is recommended in all patients with hypertrophic cardiomyopathy on diagnosis and during follow-up. CMR can be considered depending on the clinical presentation and can provide useful information on morphology and architecture. CCTA and MPI can be used to exclude CAD and myocardial ischaemia. PET is the best method for evaluating microvascular ischaemia [13.10].

13.2. DILATED CARDIOMYOPATHY

Dilated cardiomyopathy is the most common form of non-ischaemic cardiomyopathy and has multiple potential underlying aetiologies (see Table 13.1). Its phenotype is typically characterized by dilatation of all four cardiac chambers with associated left and right ventricular systolic dysfunction. Concomitant functional mitral regurgitation is also common. Transthoracic echocardiography findings that may suggest a specific aetiology of dilated cardiomyopathy include focal posterolateral akinesis or dyskinesis suggestive of dystrophin related dilated cardiomyopathy or mild dilatation with akinetic or dyskinetic segments in a non-coronary distribution suggestive of inflammatory or infectious aetiologies. CMR may suggest a specific aetiology, especially haemochromatosis, sarcoidosis and myocarditis. CMR also permits the localization of involved segments amenable to endomyocardial biopsy.

The main role of CCT is currently the exclusion of obstructive CAD, although it can also provide an accurate assessment of ventricular ejection fraction.

SPECT and PET myocardial perfusion scintigraphy can quantify myocardial perfusion to exclude an ischaemic aetiology of the condition. Nuclear imaging in dilated cardiomyopathy can demonstrate either a homogeneous distribution of blood flow or patchy (non-vascular) perfusion abnormalities on MPI, and uniform glucose metabolism on ^{18}F-fluorodeoxyglucose (FDG) PET images. This is in contrast with ischaemic cardiomyopathy, where left ventricular segments demonstrate discrete reductions in perfusion and/or reduced glucose utilization in territories corresponding to an extravascular distribution.

13.3. RESTRICTIVE CARDIOMYOPATHY

Tummala et al. [13.11] report that restrictive cardiomyopathy (RCM) is characterized by impaired diastolic filling with restrictive physiology, reduced diastolic volume of either or both ventricles, normal or near normal ventricular systolic function and wall thickness, and biatrial enlargement:

> "Echocardiography can demonstrate characteristic morphologic and physiologic patterns of RCM. Differentiating RCM from chronic constrictive pericarditis is a common diagnostic dilemma, not always evident on echocardiography... CMR and CCT offer complementary information to echocardiography, particularly in the anatomical assessment of the pericardium for thickening, inflammation, and calcification, as well as the evaluation of respiratory phasic changes in ventricular filling..."

Tissue characterization with CMR allows the further characterization of other underlying disorders potentially contributing to the restrictive physiology. PET is the most sensitive modality for identifying the areas of increased ^{18}F-FDG uptake indicative of inflammation [13.11].

13.4. SPECIFIC CARDIOMYOPATHIES

13.4.1. Cardiac amyloidosis

Nuclear imaging is particularly useful in characterizing cardiac amyloidosis. Amyloidosis is characterized by the loss of the natural structure of proteic precursors and subsequent aggregation of insoluble fibrillar compound. Fibrils are sustained by a secondary antiparallel β-foils structure. Amyloid deposits are found in the extracellular tissue of many organs and deposits can be either focal or systemic. Cardiac involvement is a leading cause of morbidity and mortality owing to systemic amyloidosis. Myocardium, conduction system and vascular structures can be affected. Typically, it shows characteristics of restrictive cardiomyopathy but both diastolic and systolic function are compromised [13.12]. The most frequent types of systemic amyloidosis with cardiac involvement are [13.13]:

(a) Acquired monoclonal immunoglobulin light chain amyloidosis due to plasma cell proliferation producing light chain gamma globulins;

(b) The hereditary, transthyrenin related form, which can be caused by over 100 mutations of transthyrenin, a transport protein mainly synthesized by the liver;
(c) Wild type (non-mutant) transthyretin related amyloidosis or systemic 'senile' amyloidosis, which mainly affects the hearts of elderly men.

In all three forms, myocardial involvement is frequent and carries major clinical consequences. Furthermore, among the rarely encountered causes of cardiac amyloidosis is apolipoprotein derived disease. Apolipoprotein A-IV is a glycoprotein that is instrumental in the metabolism and transport of dietary lipids [13.14]. Treatment of monoclonal immunoglobulin light chain amyloidosis requires treatment of the underlying plasma cell dyscrasia with chemotherapy and treatment for heart failure. Transthyrenin related amyloidosis is primarily formed in the liver and orthotopic liver transplantation is a rational and effective treatment for this form of amyloidosis.

Treatment of systemic senile amyloidosis is normally restricted to symptomatic relief with conventional heart failure therapy [13.15]. However, some younger patients may be eligible for heart transplantation.

The diagnosis of cardiac amyloidosis is based on: (i) biopsy positive Red Congo/Thioflavin + polarized light microscopy; (ii) genetic analysis and mass spectrometry to identify the protein precursor; and (iii) contrast magnetic resonance (MR) with gadolinium, showing delayed enhancement of the myocardium in a non-subendocardial distribution.

The literature shows the utility of ^{99m}Tc diphosphonate scintigraphy for identifying the infiltration of cardiac amyloidosis, specifically in the transthyretin mutation form [13.16]. The high affinity of ^{99m}Tc diphosphonate for the amyloid substance is probably due to a high calcium tissue concentration in patients with amyloidosis. In fact, the calcium concentration in livers infiltrated with amyloid is about 254 mg/g, compared with 6.8 mg/g found in the liver of healthy subjects [13.17]. Myocardial uptake is quantified using a simple visual score that compares myocardial uptake with blood pool and bone uptake (0 = no uptake, 1 = blood pool, 2 > blood pool < bone, 3 > bone uptake (see Fig. 13.1)). A combination of gadolinium late enhancement on CMR and ^{99m}Tc diphosphonate scintigraphy could be sufficient for the diagnosis and follow-up of therapy decision making in patients with cardiac amyloidosis (see Fig. 13.2).

13.4.2. Cardiac sarcoidosis

Manoushagian et al. [13.18] report that "Sarcoidosis is a multisystem disorder that is characterized histologically by non-caseating, non-necrotic granulomas. Although it most commonly manifests in the lungs or with

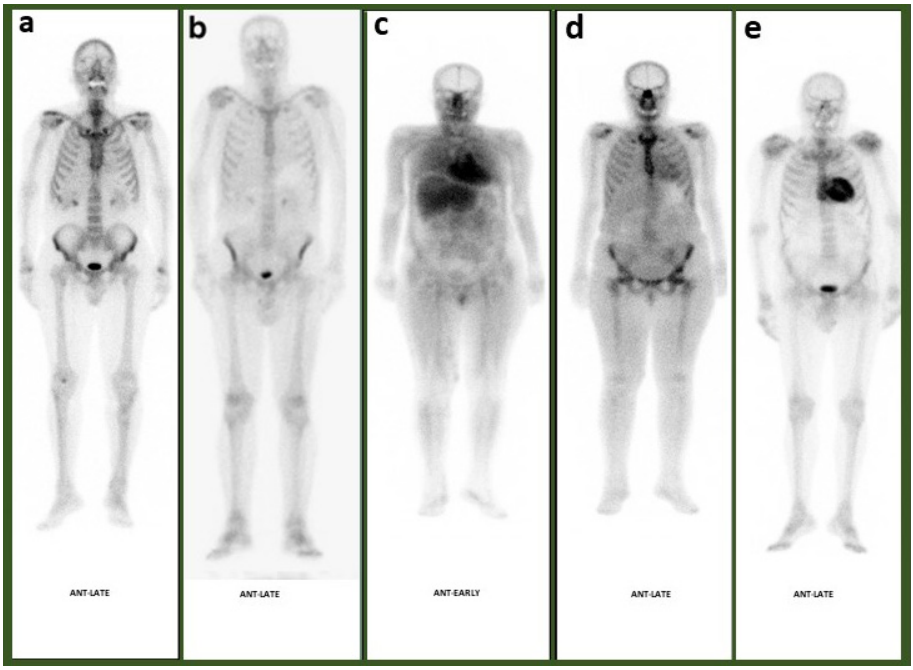

FIG. 13.1. (a, b) Two representative cases of bone scans in patients with a score of 0–1 and a final diagnosis of monoclonal immunoglobulin light chain amyloidosis; (c, d) early and late scans in a second patient; (e) a late scan of a third patient; (c, d, e) patients with a score of 3, which relates to transthyrenin amyloidosis.

lymphadenopathy, it can affect any organ." Only 40–50% of patients with cardiac sarcoidosis evident at autopsy had the diagnosis made during their lifetime. Cardiac sarcoidosis diagnosis depends on the detection method, and it has a wide range of clinical manifestations, ranging from an asymptomatic presentation to sudden cardiac death [13.8]. Cardiac sarcoidosis is the second leading cause of death due to sarcoidosis in the United States of America [13.19], making diagnosing and monitoring the progression of this disease a task of utmost importance [13.18]. Diagnosis is traditionally based on the Guidelines of the Japanese Ministry of Health and Welfare (see Ref. [13.20]), revised in 2006, which consider histological, clinical, biological and diagnostic procedures, and on those published in 2014 by the Heart Rhythm Society (see Ref. [13.21]). A comparison between the two guidelines was recently published in Refs [13.20, 13.22].

Areas of active cardiac inflammation demonstrate increased glucose metabolism and therefore increased ^{18}F-FDG uptake on PET. On the contrary, MPI (by SPECT or PET with perfusion tracers) can show areas of hypoperfusion due to inflammation and vascular compression due to oedema or myocardial fibrosis

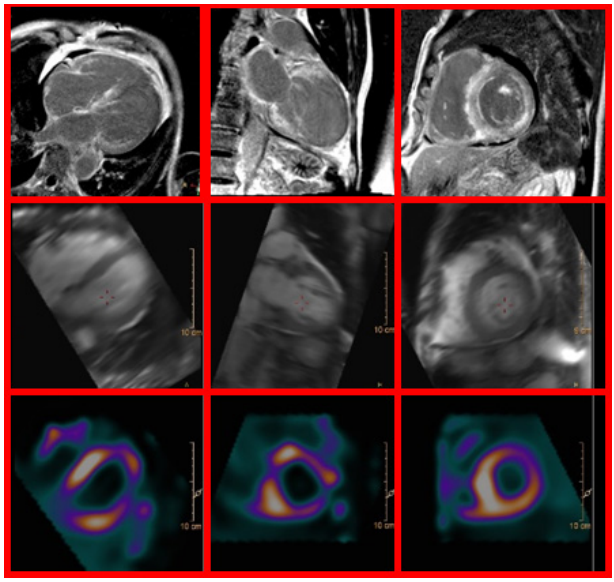

FIG. 13.2. An example of a combination of gadolinium late enhancement on CMR (T1 weighted images in the upper line; T2 weighted in the second line) and ^{99m}Tc diphosphonate scintigraphy (bottom line), which shows a myocardial infiltration.

and scar. Depending on the degree of active inflammation on ^{18}F-FDG PET and resting perfusion defects on MPI, the disease can be staged as: no evidence of activity (no inflammation or scar), early stage (active inflammation with mild or no scar), progressive disease (active inflammation with moderate scar) or fibrous disease (minimal or no inflammation with severe scar) [13.18–13.23].

The evaluation of myocardial uptake of ^{18}F-FDG PET in cardiac sarcoidosis is not a trivial issue because the metabolic utilization of glucose can be physiological and ischaemia may affect myocardial uptake. Therefore, adequate patient preparation aimed to suppress myocardial utilization is mandatory (see Chapter 3).

The presence of obstructive coronary disease and myocardial ischaemia should be excluded by stress imaging, CCTA or, when needed, invasive coronary angiography.

Evaluation of myocardial uptake requires an accurate quality control to exclude attenuation artefacts due to misalignment between PET and CT or the presence of attenuators (devices, prosthetic valves, coronary calcification). Both attenuation corrected and uncorrected images should be considered. Semiquantitative measurements can be helpful in serial follow-up after appropriate treatment, as it is in other non-cardiac localizations. It has been

reported that an increase in standardized uptake value maximum and mean on repeat PET are negatively correlated with the patient's clinical outcome [13.24]. Integrated PET–MR or PET–CT and MR fusion imaging [13.25] could be useful in increasing the specificity of MR findings and for follow-up.

13.4.3. Anderson–Fabry disease

Anderson–Fabry disease is a lysosomal disease due to a deficit of alpha-galactosidase with a progressive accumulation of glycosphingolipids inside cells of different tissues [13.26]. It is a recessive X linked transmitted disease. The organs commonly affected are the kidneys, heart, skin, vascular districts, central nervous system, eyes and audiovestibular apparatus. The cardiac variant of the disease is characterized by an accumulation of glycosphingolipids in myocardiocytes, the endothelium, smooth muscle cells with the involvement of the myocardium, the endocardium, valves, conduction tissue and intramyocardial vessels [13.27]. Therefore, myocardial hypertrophy and diastolic dysfunction, cell death and systolic dysfunction, myocardial fibrosis and arrhythmias can be observed. The vacuolization of endothelial and smooth muscle cells affects the microcirculation. Anderson–Fabry cardiomyopathy can mimic both an obstructive or non-obstructive cardiomyopathy, and angina is relatively frequent. Cardiac damage begins in the early stages of the disease and an early diagnosis is crucial to improve patient management. Ultrasound shows a characteristic pattern with binary appearance of left ventricular myocardial borders that can be useful to differentiate Anderson–Fabry cardiomyopathy from hypertrophic cardiomyopathy [13.28].

CMR with late gadolinium enhancement (LGE) identified pathology, as well as the novel T1 mapping techniques and PET with perfusion tracer, can detect microvascular damage in a very early phase of the disease [13.29].

13.5. CLASSIFICATION OF CARDIOMYOPATHIES ACCORDING TO LEFT VENTRICULAR SYSTOLIC OR DIASTOLIC DYSFUNCTION

Another approach to classifying cardiomyopathies is to differentiate conditions that cause primarily left ventricular systolic or diastolic dysfunction:

(a) Predominant left ventricular systolic dysfunction:
    (i) Ischaemic.
    (ii) Dilated cardiomyopathy:

— Primary inherited;
— Post-partum;
— Post-chemotherapy;
— Tachycardia induced.

(iii) Toxicity related:
— Induced by drugs;
— Induced by alcohol;
— Induced by heavy metals;
— Post-chemotherapy.

(iv) Valvular.

(v) Endocrine:
— Thyrotoxicosis;
— Hypothyroidism;
— Pheochromocytoma;
— Adrenal insufficiency.

(vi) Inflammatory.

(vii) Human immunodeficiency virus.

(viii) Viral myocarditis.

(b) Predominant left ventricular diastolic dysfunction:

(i) Hypertrophic cardiomyopathy:
— Idiopathic;
— Hypertensive.

(ii) Inflammatory:
— Chagas disease;
— Sarcoidosis.

(iii) Infiltrative:
— Anderson–Fabry disease;
— Cardiac amyloidosis;
— Haemochromatosis.

13.6. KEY MESSAGES

(1) Cardiomyopathies are increasingly being detected in both routine and non-routine imaging examinations.

(2) Non-invasive imaging plays an important role in the diagnostic work-up and management of patients with cardiomyopathy.

(3) Although echocardiography is the most common imaging technique used for initial diagnosis and management, other imaging techniques, including nuclear cardiac imaging, CMR and CCT, have important roles in the evaluation, treatment and estimation of prognosis in these patients.

REFERENCES TO CHAPTER 13

[13.1] BUI, A.L., HORWICH, T.B., FONAROW, G.C., Epidemiology and risk profile of heart failure, Nat. Rev. Cardiol. **8** (2011) 30–41.

[13.2] MAHRHOLDT, H., WAGNER, A., JUDD, R.M., SECHTEM, U., KIM, R.J., Delayed enhancement cardiovascular magnetic resonance assessment of non-ischaemic cardiomyopathies, Eur. Heart J. **26** (2005) 1461–1474.

[13.3] YANCY, C.W., et al., 2013 ACCF/AHA guideline for the management of heart failure, Circulation **128** (2013) 240–327.

[13.4] NAGUEH, S.F., CHANG, S.M., NABI, F., SHAH, D.J., ESTEP, J.D., Cardiac imaging in patients with heart failure and preserved ejection fraction, Circ. Cardiovasc. Imag. **10** (2017).

[13.5] EDELMAN, R.R., HESSELINK, J.R., ZLATKIN, M.B., CRUES, J.V. (Eds), Clinical Magnetic Resonance Imaging, 3rd edn, Elsevier, New York (2006).

[13.6] HABIB, G., et al., Multimodality imaging in restrictive cardiomyopathies: An EACVI expert consensus document in collaboration with the "Working Group on myocardial and pericardial diseases" of the European Society of Cardiology, endorsed by the Indian Academy of Echocardiography, Eur. Heart J. Cardiovasc. Imag. **18** (2017) 1090–1121.

[13.7] ELLIOTT, P.M., et al., 2014 ESC Guidelines on diagnosis and management of hypertrophic cardiomyopathy, Eur. Heart J. **35** (2014) 2733–2779.

[13.8] MARON, B.J., Hypertrophic cardiomyopathy: A systematic review, JAMA **287** (2002) 1308–1320.

[13.9] CARDIM, N., et al., Role of multimodality cardiac imaging in the management of patients with hypertrophic cardiomyopathy: An expert consensus of the European Association of Cardiovascular Imaging Endorsed by the Saudi Heart Association, Eur. Heart J. Cardiovasc. Imag. **16** (2015) 280.

[13.10] SCIAGRÀ, R., Positron-emission tomography myocardial blood flow quantification in hypertrophic cardiomyopathy, Q. J. Nucl. Med. Mol. Imag. **60** (2016) 354–361.

[13.11] TUMMALA, L.S., YOUNG, R.K., SINGH, T., JANI, S., SRICHAI, M.B., Role of non-invasive imaging in the work-up of cardiomyopathies, Curr. Atheroscler. Rep. **17** (2015) 486.

[13.12] FALK, R.H., Diagnosis and management of the cardiac amyloidoses, Circulation **112** (2005) 2047–2060.

[13.13] GERTZ, M.A., LACY, M.Q., DISPENZIERI, A., Amyloidosis: Recognition, confirmation, prognosis, and therapy, Mayo Clin. Proc. **74** (1999) 490–494.

[13.14] BOIS, M.C., et al., Apolipoprotein A-IV-associated cardiac amyloidosis, J. Am. Coll. Cardiol. **69** (2017) 2248–2249.

[13.15] TUZOVIC, M., et al., Cardiac amyloidosis: Diagnosis and treatment strategies, Curr. Oncol. Rep. **19** (2017) 46.

[13.16] RAPEZZI, C., et al., Usefulness and limitations of ^{99m}Tc-3,3-diphosphono-1,2-propanodicarboxylic acid scintigraphy in the aetiological diagnosis of amyloidotic cardiomyopathy, Eur. J. Nucl. Med. Mol. Imag. **38** (2011) 470–478.

[13.17] YOOD, R.A., SKINNER, M., COHEN, A.S., LEE, V.W., Soft tissue uptake of bone seeking radionuclide in amyloidosis, J. Rheumatol. **8** (1981) 760–766.
[13.18] MANOUSHAGIAN, S.J., LAKHTER, V., PATIL, P.V., Multimodality imaging in the diagnosis and management of cardiac sarcoidosis, J. Nucl. Cardiol. **24** (2017) 29–33.
[13.19] SCHATKA, I., BENGEL, F.M., Advanced imaging of cardiac sarcoidosis, J. Nucl. Med. **55** (2014) 99–106.
[13.20] HULTEN, E., et al., Cardiac sarcoidosis: State of the art review, Cardiovasc. Diag. Ther. **6** (2016) 50–63.
[13.21] BIRNIE, D.H., et al., HRS expert consensus statement on the diagnosis and management of arrhythmias associated with cardiac sarcoidosis, Heart Rhythm. **11** (2014) 1305–1323.
[13.22] BLANKSTEIN, R., WALLER, A.H., Evaluation of known or suspected cardiac sarcoidosis, Circ. Cardiovasc. Imag. **9** (2016).
[13.23] CHAREONTHAITAWEE, P., et al., Joint SNMMI–ASNC expert consensus document on the role of ^{18}F-FDG PET/CT in cardiac sarcoid detection and therapy monitoring, J. Nucl. Cardiol. **24** (2017) 1341–1353.
[13.24] LEE, P.-I., CHENG, G., ALAVI, A., The role of serial FDG PET for assessing therapeutic response in patients with cardiac sarcoidosis, J. Nucl. Cardiol. **24** (2017) 19–28.
[13.25] NENSA, F., TEZGAH, E., POEPPEL, T., NASSENSTEIN, K., SCHLOSSER, T., Diagnosis and treatment response evaluation of cardiac sarcoidosis using positron emission tomography/magnetic resonance imaging, Eur. Heart J. **36** (2015) 550.
[13.26] SWEET, M.E., MESTRONI, L., TAYLOR, M.R.G., Genetic infiltrative cardiomyopathies, Heart Fail. Clin. **14** (2018) 215–224.
[13.27] KUBO, T., Fabry disease and its cardiac involvement, J. Gen. Fam. Med. **18** (2017) 225–229.
[13.28] PIERONI, M., et al., Fabry's disease cardiomyopathy: Echocardiographic detection of endomyocardial glycosphingolipid compartmentalization, J. Am. Coll. Cardiol. **47** (2006) 1663–1671.
[13.29] TOMBERLI, B., et al., Coronary microvascular dysfunction is an early feature of cardiac involvement in patients with Anderson–Fabry disease, Eur. J. Heart Fail. **15** (2013) 1363–1373.

Chapter 14

PERICARDIAL DISEASES

G. HONG, P. RAGGI, M.C. WILLIAMS

The pericardium is composed of layers of collagen fibrils and elastin fibres, and it consists of a parietal and a visceral layer. In healthy conditions, the space between the pericardial layers is filled with a very small amount of viscous fluid. Under the visceral layer of the pericardium lies the epicardial adipose tissue, a stratum of adipose tissue mostly composed of beige adipose cells with mechanical, thermal and nutritional functions.

Pericardial diseases are relatively common in clinical practice and may present either as isolated diseases or as a manifestation of a systemic disorder. Although the potential aetiologies are varied and complex, the pericardium has a relatively non-specific response to different noxious stimuli, typically consisting of inflammation of the pericardial layers and increased production of pericardial fluid.

Diseases of the pericardium may arise from infections (viral, bacterial, fungal) or from other causes, including but not limited to: radiation, mechanical injury, myocardial infarction, metabolic diseases and malignancies; or they may be idiopathic. The typical presentation of pericardial diseases is described in the following sections.

14.1. ACUTE PERICARDITIS

14.1.1. Definition and clinical presentation

Acute pericarditis is characterized by an inflammatory process in response to external noxious stimuli with accumulation of fluid in the pericardial space. It has been reported in approximately 0.1–0.2% of hospitalizations and about 5% of patients presenting to an emergency room with chest pain not due to acute coronary syndromes. Idiopathic cases, most of which are probably viral in aetiology, are the most common causes of acute pericarditis. Other aetiologies of acute pericarditis include bacterial infections, malignancies and autoimmune disorders. The symptoms and signs of acute pericarditis are often

non-specific [14.1–14.4]. To make a diagnosis of acute pericarditis at least two of the following should be present:

(a) Sharp chest pain that worsens with movements, typically taking a deep breath or leaning forward;
(b) A pericardial friction rub on auscultation; the rub could have a systolic, a diastolic or a systolic and diastolic phase;
(c) Diffuse, concave ST segment elevation on the surface electrocardiogram (ECG) (see Fig. 14.1), with or without PR segment depression;
(d) New or increasing pericardial fluid accumulation (i.e. effusion) at ultrasound investigation.

An example of a surface 12 lead ECG showing diffuse ST segment elevation (black arrows) is reported in Fig. 14.1 as well as long axis (left) and short axis (right) parasternal views showing accumulation of a small amount of fluid in the pericardial space.

Pericarditis should also be suspected in a patient with persistent fever and pericardial effusion or new unexplained cardiomegaly on chest radiography. For all patients with suspected acute pericarditis, the initial evaluation should include a comprehensive history and physical examination, selective blood work (assessing for markers of inflammation or myocardial damage), chest radiography, electrocardiography and echocardiography. Most acute pericarditis

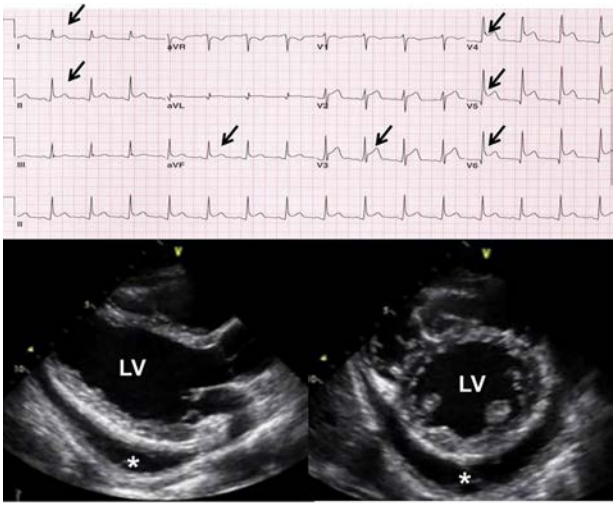

FIG. 14.1. Example of widespread ST elevation in a case of pericardial disease (top) and pericardial effusion at echo (asterisks, bottom).

cases follow a benign course and are likely due to an acute viral infection that most often heals spontaneously. The focus of initial diagnostic approaches should be on excluding treatable aetiologies (e.g. tuberculosis) or those that may carry a poor prognosis (e.g. primary malignancies and metastatic diseases). For most patients with acute idiopathic or viral pericarditis, medical therapy with non-steroidal anti-inflammatory drugs is recommended by practitioners.

14.1.2. Imaging algorithms and modalities for acute pericarditis based on clinical presentation

Multimodality imaging can be very helpful in making the diagnosis of acute pericarditis, as discussed below [14.5].

14.1.2.1. Echocardiography

Echocardiography is often the first imaging test to be used and frequently the only one being performed to exclude the presence of pericarditis. An echocardiographic examination can be completely normal, including the absence of any pericardial effusion. However, the presence of fluid accumulation in the pericardial space in a patient with known or suspected pericarditis supports the diagnosis. Large and/or haemodynamically significant pericardial effusions are rare as an initial presentation of acute pericarditis [14.6].

14.1.2.2. Cardiac computed tomography

The utility of cardiac computed tomography (CCT) extends not only to the confirmation of the presence of fluid accumulation in the pericardial sac, but to the exclusion of associated disease processes in the pulmonary parenchyma, the mediastinum and the lymph nodes (tuberculosis, cancer, sarcoidosis). Thickening of the pericardium in the absence of calcification and fluid accumulation confirms the diagnosis of acute pericarditis. Intravenous iodine administration may enhance the focal or diffuse thickening of the visceral and parietal surfaces of the pericardium. Finally, assessment of the computed tomography (CT) attenuation (i.e. density) of the pericardial fluid may help to differentiate a purulent exudate (20–60 HU) from a transudate (typically less than 10 HU) [14.7].

14.1.2.3. Cardiac magnetic resonance

On T2 weighted imaging the inflamed pericardium appears thickened and a layer of intermediate signal intensity next to the bright signal emanating from the epicardial fat; it may also show late enhancement after gadolinium injection.

Late gadolinium enhancement (LGE) may also provide evidence of myocardial inflammation due to the concurrent presence of myocarditis. The combined use of CT and cardiac magnetic resonance (CMR) can provide more definitive evidence of pericarditis in cases where the diagnosis is unclear due to atypical presentation of the syndrome, absence of elevation in biomarkers of inflammation and ECG signs of pericarditis [14.8].

14.2. CARDIAC TAMPONADE

As discussed above, the pericardial space is almost a virtual space and normally contains a small amount of viscous fluid (10–50 mL). Even a small accumulation of fluid, if it occurs rapidly, can cause a quick increase in the intrapericardial space and impinge on the filling of the ventricles, ultimately limiting cardiac output. Tamponade refers to the stage where the underfilling of the left ventricle during diastole causes a severe reduction of forward cardiac output with hypotension, reduced perfusion of vital organs and eventually shock. The main factors that affect the development of haemodynamic compromise are the rapidity of fluid accumulation as well as its volume, the presence of adhesions in the pericardial space, and the presence of pulmonary hypertension. In the latter case, the high right ventricular pressures oppose the external compression of the ventricular cavities.

A rapid diagnosis of cardiac tamponade is essential for the favourable outcome of patients suffering from this condition. Echocardiography is typically the first and most useful tool to be employed both for diagnostic and therapeutic purposes in cardiac tamponade. Pericardial fluid is typically seen as an echolucent rim either in a specific region of the pericardium if the effusion is small or loculated, or all around the myocardium if the effusion is larger (see Fig. 14.2). Smaller collections may be visible only during the ventricular systole, while larger collections are visible during the entire ventricular cycle. The most sensitive and specific view for the diagnosis of pericardial effusion is an accumulation of fluid around the free wall of the right atrium in the apical four chamber view obtained while the patient lies in the left lateral decubitus. Larger effusions gradually extend to the anterior wall of the right ventricle.

B mode and Doppler echocardiography offer important clues for the diagnosis of cardiac tamponade such as the maximum diameter of the fluid collection (see Fig. 14.2), diastolic collapse of the free wall of the right atrium and/or right ventricle, a >20% inspiratory variation in the transmitral blood inflow velocity, a distended inferior vena cava without respiratory variation in diameter, and retrograde flow in the inferior vena cava during inspiration (see Fig. 14.3).

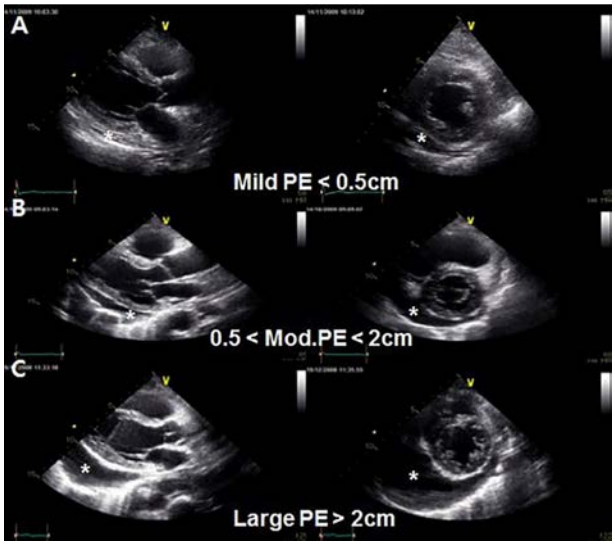

FIG. 14.2. Examples of assessment of severity of pericardial effusion based on the maximum diameter of the effusion on B mode echocardiography. The effusion is identified by the asterisk: (A) small pericardial effusion behind the left ventricle; (B) moderate pericardial effusion; (C) large pericardial effusion in the same location.

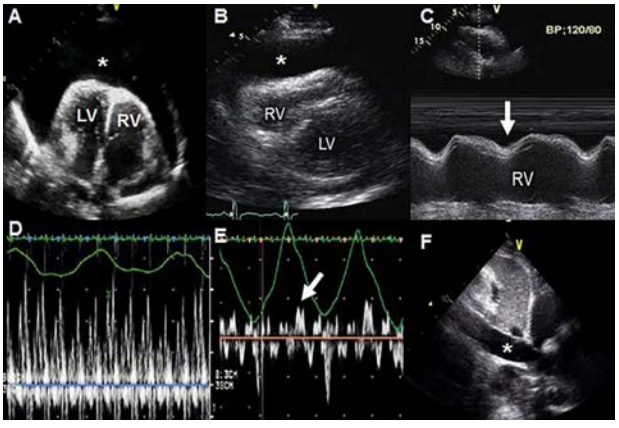

FIG. 14.3. Cardiac tamponade results from impaired ventricular filling: (A) large pericardial fluid accumulation (asterisk) seen in an apical four chamber view; (B) pericardial fluid accumulation (asterisk) shown in a parasternal short axis view between the free wall of the right ventricle and the parietal pericardium; (C) M mode echocardiography shows diastolic collapse of the free wall of the right ventricle; (D) transmitral Doppler flow recording shows a marked decrease in flow velocity with inspiration; (E) Doppler recording shows reversal of flow in the inferior vena cava; (F) inferior vena cava (asterisk) is distended and shows no collapse with inspiration.

Transthoracic echocardiography can also prove useful in planning pericardiocentesis to evacuate the pericardial effusion both for therapeutic and diagnostic reasons. Indications for a therapeutic intervention are based on the clinical scenario (see Fig. 14.4). The aetiology of pericardial tamponade can be investigated by analysing the fluid collected during the diagnostic tap. A transudate is more likely to suggest a benign aetiology while an exudative or bloody fluid collection are suggestive of bacterial mycobacterial infections or malignant aetiologies.

14.2.1. Cardiac computed tomography

In cases with a high suspicion for pericardial effusion but non-diagnostic echocardiography, additional thoracic imaging with CT is helpful in establishing the presence of an effusion. A CT scan is not routinely recommended unless both transthoracic and transoesophageal echocardiography are non-diagnostic, or unless there is concern for other pericardial pathology (e.g. pericardial thickening and constrictive pericarditis). CT may be useful when quantification and localization of pericardial fluid is important, when the effusion is complex, when epicardial fat may be suspected to be the source of the increased pericardial thickness or when pleural effusions need to be excluded.

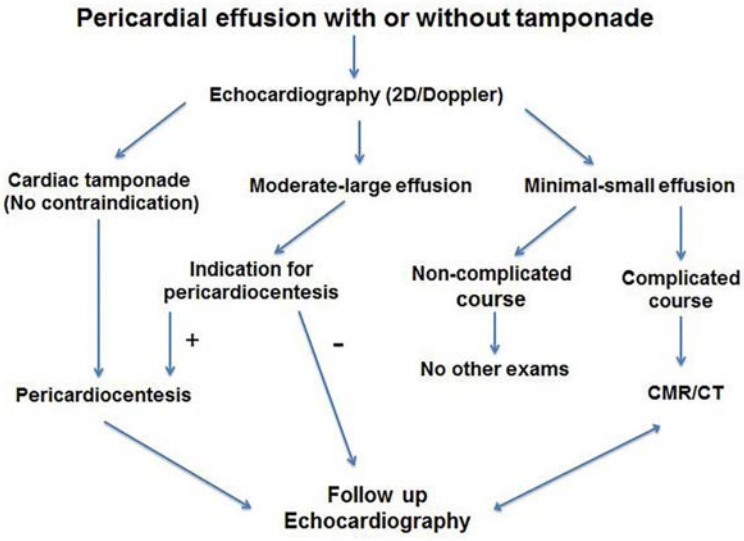

FIG. 14.4. Imaging algorithms based on clinical presentation.

14.2.2. Cardiac magnetic resonance

As is the case for CCT, CMR may be useful when the quantification and localization of pericardial fluid is important, when the effusion is complex, when epicardial fat thickness needs to be assessed and pleural effusions need to be excluded. It is useful for characterizing the nature of the effusion.

14.3. CONSTRICTIVE PERICARDITIS

14.3.1. Definition and clinical presentation

Constrictive pericarditis is a medical condition characterized by a thickened, fibrotic and at times calcified pericardium, limiting the diastolic filling of the heart and as a consequence its ability to propel forward a sufficient cardiac output [14.9]. The diagnosis of constrictive pericarditis is often overlooked and frequently confused with other causes of heart failure. In fact, the symptoms of patients with constrictive pericarditis are similar to those of patients suffering from heart failure with both reduced and preserved ejection fraction, such as peripheral oedema, anasarca, shortness of breath and fatigue with exertion and sometimes even at rest. The pathophysiology of these symptoms is increased systemic venous pressure due to reduced filling of the right ventricle and reduced left ventricular output because of its diminished filling. Other physical examination signs exhibited by patients with constrictive pericarditis are elevated jugular venous pressure, pulsus paradoxus, Kussmaul's sign (paradoxical increase of jugular venous pressure with inspiration) and pericardial knock.

Initial investigations for patients with suspected constrictive pericarditis include a 12 lead ECG, chest X ray and echocardiography. The surface ECG may reveal a diffuse low voltage. The chest X ray may show calcification along the profile of the cardiac silhouette, dilated right and left atria, and pleural effusions. The typical echocardiographic findings are discussed below.

The differential diagnosis of constrictive pericarditis includes restrictive cardiomyopathy and liver cirrhosis or other protein losing enteropathies. Patients who do not exhibit signs of decompensation, such as anasarca, cachexia, weight loss, hypoalbuminemia due to protein losing enteropathy and/or impaired hepatic function due to chronic congestion or cardiogenic cirrhosis, may be treated conservatively. For patients with advanced and worsening symptoms, however, the only treatment option is pericardiectomy, which may often reveal to be a complex surgical intervention with high morbidity and mortality rates [14.10, 14.11].

14.3.2. Imaging modalities for constrictive pericarditis

14.3.2.1. Echocardiography

There are unique features of constrictive pericarditis that render echocardiography a reliable method to diagnose this condition. The most salient ones are respiratory variation in ventricular filling, evidence of interventricular dependence, and increased longitudinal motion of the heart.

The respiratory variation in ventricular filling is the result of the dissociation of intrathoracic and intracardiac pressure change during the respiratory phases. During normal inspiration, the intrathoracic pressure drops, and this is transmitted to the cardiac chambers. However, in constrictive pericarditis the intracardiac pressures do not fall to the same extent as the intrathoracic pressure, and the difference in pressure change with inspiration results in reduced filling of the left heart chambers. The reduction in inspiratory filling can be visualized as a reduction in mitral inflow velocity and a shift of the interventricular septum toward the left ventricle (septal bounce). Left heart filling increases during expiration and this causes a shift of the interventricular septum toward the right ventricle, this time causing a reduced filling of the right heart chambers with diastolic reversal of flow in the hepatic veins. Finally, the septal mitral annulus e′ velocity, measured with tissue Doppler imaging, is increased not reduced, as seen in several forms of cardiomyopathies. The septal annulus e′ is also greater than the lateral e′ velocity owing to the reduced mobility of the lateral wall of the left ventricle. Salient structural and haemodynamic echocardiographic clues in patients with constrictive pericarditis are listed below (see Fig. 14.5) [14.12, 14.13]:

(a) Two dimensional and M mode echocardiography:
   - — Increased pericardial thickness with or without calcification (seen in about 40% of patients).
   - — Dilated right and left atria.
   - — Distended inferior vena cava, showing no collapse during inspiration.
   - — Septal bounce on M mode: an abrupt posterior motion of the ventricular septum in early diastole during inspiration. This is believed to be due to underfilling of the left ventricle.

(b) Doppler echocardiography:
   - — High E mitral inflow velocity (due to rapid early filling and sudden ending of diastolic filling).
   - — Prominent septal mitral annulus e′ velocity on tissue Doppler.
   - — Mitral inflow velocity drops 25–40% and tricuspid velocity increases (40–60%) following inspiration.

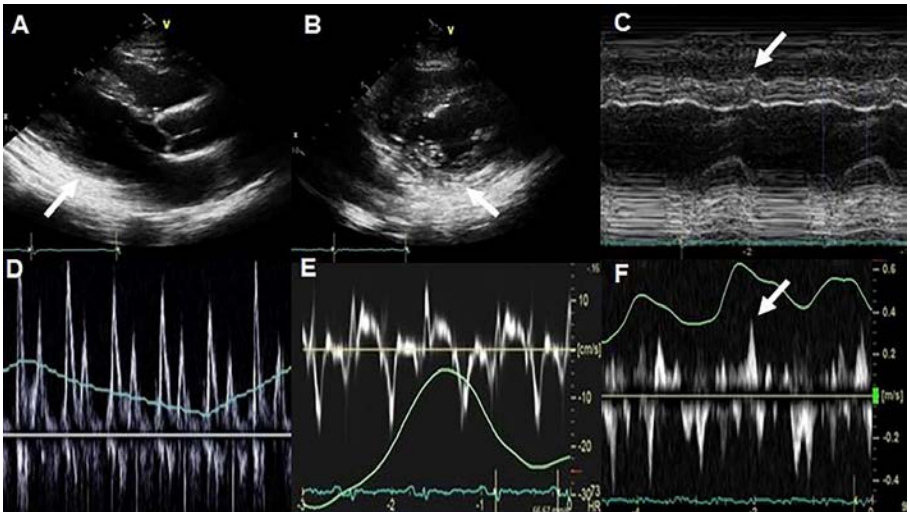

FIG. 14.5. Echocardiographic study of a patient with constrictive pericarditis. 2-D echocardiography showing pericardial thickening and calcification: (A) parasternal long axis view (arrow); (B) parasternal short axis view (arrow); (C) M mode echocardiography shows interventricular dependence (arrow); (D) pulsed wave Doppler recording of mitral inflow velocity showing respiratory variation; (E) septal e' velocity of tissue Doppler imaging is about 14 cm/s; (F) hepatic vein pulsed wave Doppler shows diastolic flow reversal with expiration (arrow) [14.14–14.17].

— Hepatic venous flow reversal with expiration.
— Normal or increased velocity of early diastolic transmitral flow on colour M mode echocardiography.

14.3.2.2. Cardiac computed tomography

CCT can provide useful clues to establish the diagnosis of constrictive pericarditis and to plan future surgical interventions (see Fig. 14.6). Helpful findings on CCT include increased pericardial thickness and calcification. Additional findings suggestive of constrictive pericarditis include a dilated inferior vena cava, deformed ventricular contours and angulation of the ventricular septum. On cine CT the absence of pulmonary parenchymal pulsations in synchrony with the cardiac cycle, especially in the presence of focal or diffuse pericardial thickening, is suggestive of constrictive pericarditis. CT is useful in planning pericardiectomy especially in patients with prior cardiothoracic surgeries in order to visualize viable vascular structures and accurately measure the distance between critical cardiovascular structures [14.18].

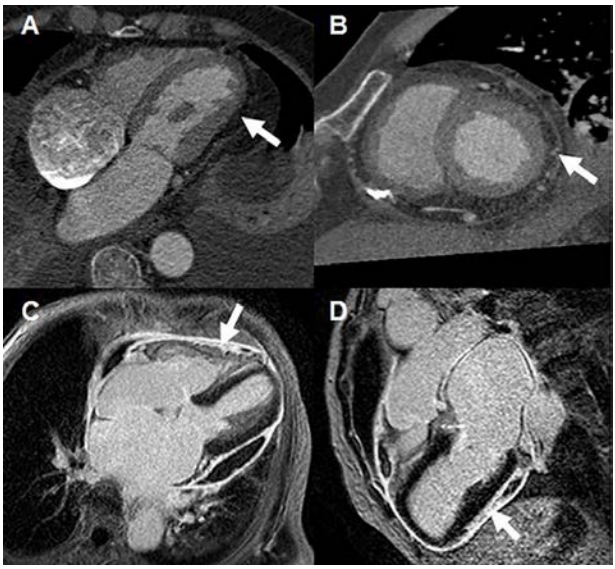

FIG. 14.6. Four chamber (A) and short axis (B) CCT views demonstrating increased pericardial thickness (arrows). The asterisk in panel B points at a small area of calcification along the lower portion of the free wall of the right ventricle. On 4-chamber (C) and left ventricular outflow (D) CMR views the pericardium shows delayed hyperenhancement (arrows).

14.3.2.3. Cardiac magnetic resonance

The normal pericardium has a low intensity signal on CMR (see Fig. 14.6). Findings suggestive of constrictive pericarditis on CMR are a thickened pericardium that may enhance during delayed gadolinium imaging, dilated atria and distended inferior vena cava, ventricular interdependence with septal bounce on cine MRI.

Patients with constrictive pericarditis and pericardial LGE have greater fibroblast proliferation, chronic inflammation and pericardial thickening compared with those without LGE. Pericardial LGE might also be a predictor of reversibility of constrictive pericarditis following treatment with anti-inflammatory agents. CMR imaging in patients being considered for pericardiectomy can provide additional detailed anatomical information that might alter the decision to proceed with surgery based on the likelihood of resolution with medical therapy alone [14.19].

14.3.2.4. Positron emission tomography

In contrast to CT and MR imaging relying on anatomical structure and function, positron emission tomography (PET) imaging reflects the in vivo metabolism of ^{18}F-fluorodeoxyglucose (FDG). Both methods can be combined with PET imaging to associate metabolic findings with anatomy, so-called cardiac hybrid imaging. Usually, inflammatory processes involving the pericardium show a mild to moderate ^{18}F-FDG uptake but also no increased ^{18}F-FDG uptake can be observed. In contrast, proliferative neoplastic disorders commonly exhibit a markedly increased ^{18}F-FDG uptake that is often congruent with a localized mass of tissue [14.20, 14.21].

14.4. KEY MESSAGES

(1) Pericardial disease represents a wide spectrum of processes involving or damaging the pericardium.
(2) Acute pericarditis, pericardial effusion with or without cardiac tamponade, and constrictive pericarditis are the most common pericardial diseases in clinical practice.
(3) Imaging is essential for an appropriate diagnosis of pericardial disease and its complications and plays an important role in its management. The different imaging modalities are often complementary and the choice of one or multiple imaging modalities is driven by the clinical context or conditions of the patient.
(4) Echocardiography remains an initial imaging test in most scenarios because of its ease of use, wide availability, bedside availability, cost effectiveness and comprehensive assessment of both anatomy and physiology.
(5) 2-D echocardiography has several weaknesses, mainly related to its dependence on a good acoustic window and its inability to image the entire pericardium. New developments may be helpful to reduce or avoid some of these limitations.
(6) Strain imaging has entered the clinical arena mainly to assess the impact of various pathological conditions on ventricular function. 3-D echocardiography has the potential to provide a complete evaluation of the entire pericardium in any anatomical plane, and, therefore, to detect loculated effusions.
(7) CT is a widely available technique with a short acquisition time. CT is particularly sensitive for identifying pericardial calcification.
(8) CT density measurements may enable a better initial characterization of pericardial fluid than echocardiography.

(9) CMR is a useful additional test for the diagnosis of many pericardial diseases, especially if echocardiography is equivocal, localized disease is suspected, echocardiographic image quality is suboptimal or if additional pathology is suspected.
(10) CMR can provide information on the extent of pericardial disease and abnormalities in surrounding structures, and it allows an accurate measurement of pericardial and related structures. It can also provide information about associated myocarditis.

REFERENCES TO CHAPTER 14

[14.1] LANGE, R.A., HILLIS, L.D., Clinical practice: Acute pericarditis, N. Engl. J. Med. **351** (2004) 2195–2202.
[14.2] IMAZIO, M., GAITA, F., LEWINTER, M., Evaluation and treatment of pericarditis: A systematic review, JAMA **314** (2015) 1498–1506.
[14.3] TROUGHTON, R.W., ASHER, C.R., KLEIN, A.L., Pericarditis, Lancet **363** (2004) 717–727.
[14.4] IMAZIO, M., ADLER, Y., Management of pericardial effusion, Eur. Heart J. **34** (2013) 1186–1197.
[14.5] YARED, K., BAGGISH, A.L., PICARD, M.H., HOFFMANN, U., HUNG, J., Multimodality imaging of pericardial diseases, J. Am. Coll. Cardiol. Cardiovasc. Imag. **3** (2010) 650–660.
[14.6] COSYNS, B., et al., European Association of Cardiovascular Imaging (EACVI) position paper: Multimodality imaging in pericardial disease, Eur. Heart J. Cardiovasc. Imag. **16** (2015) 12–31.
[14.7] KLEIN, A.L., et al., American Society of Echocardiography clinical recommendations for multimodality cardiovascular imaging of patients with pericardial disease: Endorsed by the Society for Cardiovascular Magnetic Resonance and Society of Cardiovascular Computed Tomography, J. Am. Soc. Echocardiogr. **26** (2013) 965–1012.
[14.8] VERHAERT, D., et al., The role of multimodality imaging in the management of pericardial disease, Circ. Cardiovasc. Imag. **3** (2010) 333–343.
[14.9] CAMERON, J., OESTERLE, S.N., BALDWIN, J.C., HANCOCK, E.W., The etiologic spectrum of constrictive pericarditis, Am. Heart J. **113** (1987) 354–360.
[14.10] LING, L.H., et al., Constrictive pericarditis in the modern era: Evolving clinical spectrum and impact on outcome after pericardiectomy, Circulation **100** (1999) 1380–1386.
[14.11] BERTOG, S.C., et al., Constrictive pericarditis: Etiology and cause-specific survival after pericardiectomy, J. Am. Coll. Cardiol. **43** (2004) 1445–1452.
[14.12] SCHNITTGER, I., BOWDEN, R.E., ABRAMS, J., POPP, R.L., Echocardiography: Pericardial thickening and constrictive pericarditis, Am. J. Cardiol. **42** (1978) 388–395.

[14.13] ENGEL, P.J., et al., M-mode echocardiography in constrictive pericarditis, J. Am. Coll. Cardiol. **6** (1985) 471–474.

[14.14] AGATSTON, A.S., RAO, A., PRICE, R.J., KINNEY, E.L., Diagnosis of constrictive pericarditis by pulsed Doppler echocardiography, Am. J. Cardiol. **54** (1984) 929–930.

[14.15] BOONYARATAVEJ, S., OH, J.K., TAJIK, A.J., APPLETON, C.P., SEWARD, J.B., Comparison of mitral inflow and superior vena cava Doppler velocities in chronic obstructive pulmonary disease and constrictive pericarditis, J. Am. Coll. Cardiol. **32** (1998) 2043–2048.

[14.16] HA, J.W., et al., Annulus paradoxus: Transmitral flow velocity to mitral annular velocity ratio is inversely proportional to pulmonary capillary wedge pressure in patients with constrictive pericarditis, Circulation **104** (2001) 976–978.

[14.17] OH, J.K., et al., Diagnostic role of Doppler echocardiography in constrictive pericarditis, J. Am. Coll. Cardiol. **23** (1994) 154–162.

[14.18] CUMMINGS, K.W., GREEN, D., JOHNSON, W.R., JAVIDAN-NEJAD, C., BHALLA, S., Imaging of pericardial diseases, Semin. Ultrasound CT MR **37** (2016) 238–254.

[14.19] ALDWEIB, N., FARAH, V., BIEDERMAN, R.W.W., Clinical utility of cardiac magnetic resonance imaging in pericardial diseases, Curr. Cardiol. Rev. **14** (2018) 200–212.

[14.20] MAURER, A.H., BURSHTEYN, M., ADLER, L.P., STEINER, R.M., How to differentiate benign versus malignant cardiac and paracardiac ^{18}F FDG uptake at oncologic PET/CT, Radiographics **31** (2011) 1287–1305.

[14.21] ERBA, P.A., SOLLINI, M., LAZZERI, E., MARIANI, G., FDG-PET in cardiac infections, Semin. Nucl. Med. **43** (2013) 377–395.

Chapter 15

PRIMARY VALVE DISEASES

M.H. Al-MALLAH, M. VANNAN, X. ZHOU

15.1. CAUSES OF VALVE DISEASE

Rheumatic heart disease remains the primary aetiology of valvular heart diseases in developing countries. It is the most common aetiology of primary valvular diseases in patients younger than 55 years of age [15.1]. The prevalence ranges from 0.5 per 1000 patients in developed countries to 21 per 1000 patients in developing countries. In contrast, degenerative valvular disease is the most common cause of primary valvular disease in developed countries owing to the ageing population. Other common aetiologies of valvular heart disease include congenital abnormalities (primarily bicuspid aortic valve or mitral valve prolapse). In contrast, secondary valvular disease can arise from endocarditis, ischaemic heart disease, heart failure, trauma, infiltrative diseases (carcinoid), medications and drug use [15.2].

15.2. SIGNS, SYMPTOMS AND DIAGNOSIS OF VALVULAR HEART DISEASE

The signs and symptoms of valvular heart disease depend on the type of valvular disease. Most patients develop shortness of breath or chest pain as the degree of severity worsens. Patients may also have decreased exercise capacity, palpitations, atrial fibrillation, presyncope/syncope and signs of congestive heart failure (lower extremity oedema, lung crackles, ascites). However, a significant proportion of patients remain asymptomatic despite having severe valvular pathologies.

After a detailed and thorough history and physical examination, echocardiography is the first imaging tool to be utilized in the assessment of patients with valvular heart disease. Echocardiography offers the advantage of ease of accessibility, portability and cost efficiency. In addition, it does not involve the use of ionizing radiation. Transthoracic echocardiography (TTE) provides good visualization of the valve anatomy and the primary pathology, and can quantify stenosis/regurgitation and their mechanisms. However, in patients

with poor echocardiography windows, more detailed assessment is needed using transoesophageal echocardiography (TEE) [15.3]. This is mostly needed when surgical or percutaneous interventions are planned. In these cases, TEE can help to determine the feasibility of valve sparing surgery or valve repair versus the need for valve replacement.

15.3. CLASSIFICATION OF THE SEVERITY OF PRIMARY VALVULAR PATHOLOGIES

The current guidance of the European Society of Cardiology [15.4], the American College of Cardiology and the American Heart Association [15.5, 15.6] and the American Society of Echocardiography [15.7] varies in the measures recommended to classify primary valvular disease. These are primarily based on echocardiographic measures, as shown in Table 15.1 for valvular stenosis.

15.4. PRE-OPERATIVE IMAGING EVALUATIONS IN PATIENTS WITH RHEUMATIC MITRAL STENOSIS

Imaging plays an important role in the pre-operative planning of patients with severe rheumatic mitral stenosis. TTE is a good initial tool to assess valve morphology, calcification, subvalvular apparatus and chordae. However, if these cannot be adequately assessed by TTE, then TEE should be performed. In recent years, computed tomography (CT) has been used to assess the left atrial appendage. Its accuracy has been confirmed in multiple studies and a meta-analysis [15.8]. In selected patients with coronary risk factors, the coronary anatomy needs to be assessed as discussed below. Repeat imaging is indicated in patients with new or worsening symptoms. For patients with mitral or aortic valve disease who are not yet candidates for intervention, guidelines recommend

TABLE 15.1. GRADING OF THE SEVERITY OF STENOTIC LESIONS

	Severe aortic stenosis	Mitral stenosis
Haemodynamic measures	Peak velocity > 4 m/s Mean gradient > 40 mm Hg	Diastolic pressure half-time > 150 ms or > 220 ms in very severe mitral stenosis
Valve area	<1.0 cm^2 or indexed valve area of <0.6 cm^2/m^2	<1.5 cm^2 is defined as severe mitral stenosis and <1.0 cm^2 as very severe mitral stenosis

a repeat echocardiographic assessment every 3–5 years, 1–2 years and 6–12 months in asymptomatic patients with mild, moderate and severe disease, respectively [15.6]. For mitral stenosis patients, guidelines recommend repeat testing every 3–5 years, 1–2 years and 6–12 months in asymptomatic patients with mitral valve area of >1.5 cm^2, 1–1.5 cm^2 and <1 cm^2, respectively [15.6]. Patients with significant aortic valve calcification and mild or moderate aortic stenosis should be re-evaluated yearly.

15.5. ROLE OF CMR IMAGING IN PATIENTS WITH PRIMARY VALVE DISEASE

Cardiac magnetic resonance (CMR) imaging can be used as an alternative to echocardiography in the assessment of valve disease when echocardiography assessment is suboptimal. Currently, CMR is the gold standard for the assessment of left and right ventricular volumes and ejection fraction [15.9]. These are essential for the decision making process, especially in patients with regurgitant lesions where the type of intervention is influenced by the volume of the ventricles and the ejection fraction. In addition, CMR provides an excellent assessment of the anatomy and dimensions of the ascending aorta, pulmonary artery and great vessels, which are important parameters in the clinical decision making process in both aortic and pulmonary valve pathologies. Finally, although CMR can provide a good assessment of valve morphology and function, the temporal resolution of standard sequences is inferior to echocardiography (~25 frames/s). However, high temporal resolution sequences could be adopted (60–70 frames/s) if needed. Phase contrast imaging provides an opportunity to assess valve haemodynamics, regurgitant volume and regurgitant fraction. In patients with decreased left ventricular ejection fraction (LVEF), CMR with late gadolinium enhancement (LGE) could hint to the possible aetiology of left ventricular dysfunction and predict the probability of left ventricular function improvement in these patients (e.g. myocardial hibernation or infarction of the inferolateral wall and of the posteromedial papillary muscle as a cause of functional MR).

Most prosthetic valves (mechanical, biological) are magnetic resonance imaging (MRI) compatible in the 1.5 T field, although often a metal artefact from either the valve prosthesis or the repair metal ring is seen around the valve, limiting the ability to assess the valve itself. Nonetheless, precautions can be taken to optimize the image quality and the precision of measurements. The safety of imaging prosthetic valves in 3 T magnetic field scanners must be ascertained before proceeding with the examination, as safety is less well established with stronger magnetic fields.

A new 4-D flow sequence allows the visualization of flow vortices through valves, in the cardiac chambers and in the great vessels, which might have implications for the remodelling of these structures. Currently, this is a tool for research only, but with promising future clinical applications.

15.6. ASSESSMENT OF CORONARY ANATOMY IN PATIENTS WITH PRIMARY VALVULAR HEART DISEASE PRIOR TO SURGICAL INTERVENTIONS

In patients scheduled for valvular interventions, coronary anatomy assessment is recommended in middle aged and elderly patients with cardiovascular risk factors. Coronary angiography has been the most commonly used test to assess coronary anatomy. However, in patients with low to intermediate pre-test likelihood of coronary artery disease (CAD), coronary computed tomography angiography (CCTA) has emerged as an accurate alternative to invasive angiography. A meta-analysis of 1107 patients who underwent cardiac computed tomography (CCT) prior to cardiac surgery showed a pooled sensitivity of 93% and a specificity of 89% [15.10].

In patients who have had prior coronary artery bypass surgery and have been referred for subsequent valvular heart disease surgery, CCT plays an important role in surgical planning. It provides information on the location of the right ventricle and grafts in relation to the sternum and sternal wires. A meta-analysis of 900 patients who underwent CT prior to reoperation showed that CCT was associated with decreased stroke risk in these patients, but not with a difference in death or myocardial infarction [15.11].

15.7. FOLLOW-UP OF PATIENTS WITH PROSTHETIC VALVES

TTE should be performed right after valvular replacement or repair to establish a baseline gradient across these valves. TTE should also be performed when a change in symptoms occurs. However, metallic valves may be difficult to assess via TTE owing to artefacts, and TEE should be considered when visualization is limited by TTE. CCT has recently emerged as an alternative to echocardiography where reduced opening of a mechanical valve is suspected and not properly visualized with ultrasound. Metallic leaflet motion can be assessed using retrospective gating on CT, without the need for contrast or heart rate control (see Fig. 15.1) [15.12]. If contrast is injected, possible causes of mechanical valve dysfunction such as pannus or thrombus can be identified [15.13].

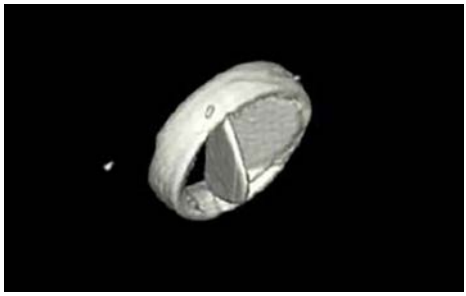

FIG. 15.1. Non-contrast enhanced CT of a patient with a metallic aortic valve shown during systole. The leaflet in the right upper portion of the image is frozen in a closed position. This causes an increased transvalvular gradient, which can be measured by Doppler echocardiography.

In patients with fever and suspected endocarditis, TTE is the suggested initial test. However, another test is often needed, including TEE or CCT. Positron emission tomography–computed tomography (PET–CT) has recently been identified as a useful tool in such patients and will be further discussed in Chapter 18. CMR has a limited role in the assessment of endocarditis [15.14].

15.8. ROLE OF IMAGING IN PLANNING PERCUTANEOUS INTERVENTIONS FOR AORTIC STENOSIS

After confirming the diagnosis of severe aortic stenosis by TTE or TEE, pre-procedural planning to identify patient suitability for transcutaneous aortic valve replacement should be performed. This is most commonly performed by CCT with contrast. It is the preferred tool given its high spatial resolution. CCT provides an accurate assessment of the aortic annulus (see Fig. 15.2), major and minor diameters, sinus of Valsalva and sinotubular junction diameters, and an assessment of the left ventricular outflow tract. These are essential in the choice of the prosthetic valve diameter.

A very important measurement is the distance between the coronary ostia and aortic annulus, which is essential to avoid acute coronary ostia occlusion during the procedure. CCT also helps in determining the most appropriate access, as it gives an accurate assessment of the tortuosity and calcification of the ascending and descending aorta, as well as in the iliac and femoral arteries (see Fig. 15.3) [15.15]. After implantation, echocardiography is the main test to assess implant function and paravalvular regurgitation. CT has been used to identify hypoattenuating valvular lesions that suggest the presence of thrombus on the prosthetic leaflets.

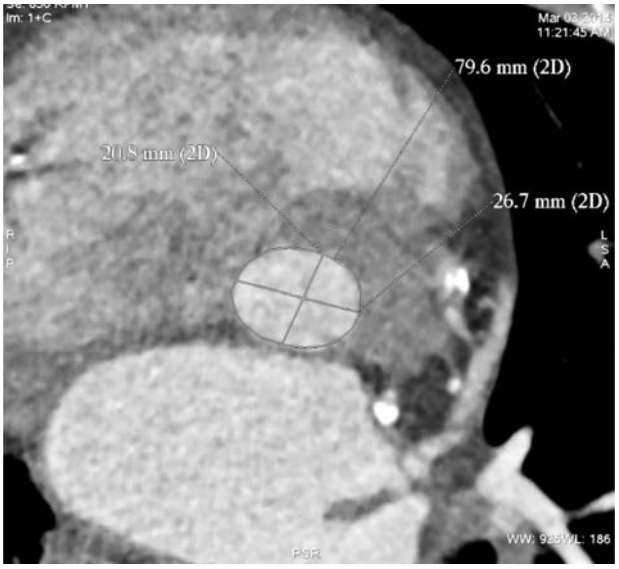

FIG. 15.2. Aortic annulus tracing of a patient prior to transcatheter aortic valve replacement. The long and short axes are measured as well as the perimeter.

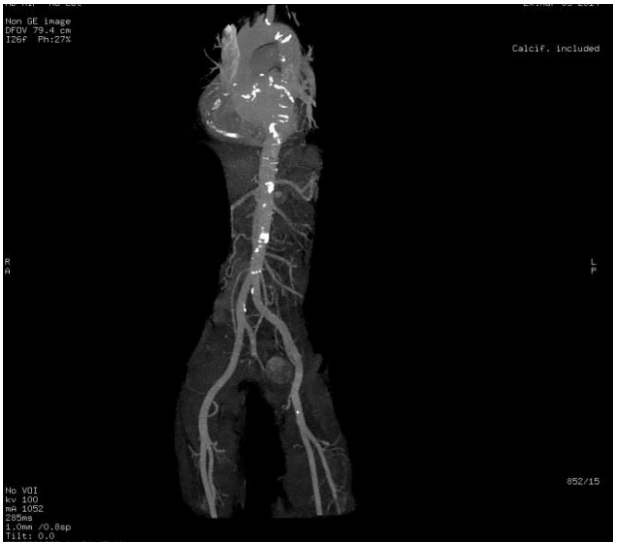

FIG. 15.3. Reconstruction of the ascending and descending aorta in a patient being prepared for transcatheter aortic valve replacement. There is mild tortuosity and moderate calcification in the descending aorta. No calcifications are noted in the femoral and iliac arteries.

15.9. ROLE OF NUCLEAR CARDIOLOGY IN PATIENTS WITH PRIMARY VALVE DISEASE

Nuclear cardiology has a limited role in the assessment of primary valve disease. The left ventricular volume and function can be assessed using multigated angiocardiography scanning when echocardiography is suboptimal and CMR cannot be performed. However, the valves cannot be visualized with nuclear imaging techniques.

Recent data suggest that PET imaging with ^{18}F sodium fluoride may have a role in predicting aortic stenosis progression in patients with aortic valve calcifications. However, more data are needed prior to adoption of this imaging approach in routine clinical practice [15.16].

15.10. FOLLOW-UP AND TREATMENT OF PATIENTS WITH ADVANCED VALVULAR HEART DISEASE

Patients with severe valvular heart disease should be followed up by a multidisciplinary team including clinical cardiologists, cardiac surgeons, interventional cardiologists, imaging specialists, pharmacists, physical therapists, nutritionists and nurses. Other specialties could be involved depending on the presence of other comorbidities. This ‘heart team’ should have regular meetings especially when making decisions about therapeutic intervention. The European Society of Cardiology guidelines recommend that these patients be followed in a heart valve centre that can provide advanced interventions [15.2, 15.17]. Non-invasive imaging support to these interventions is essential and includes advanced echocardiography (3-D echocardiography, intraoperative echocardiography), CT and MRI. Table 15.2 summarizes the role of the different imaging modalities in valvular heart disease.

TABLE 15.2. COMPARISON OF DIFFERENT IMAGING MODALITIES IN THE ASSESSMENT OF VALVULAR HEART DISEASES

	Echo	CT	MRI	Nuclear
Valve morphology	++	++	++	–
Valve calcification	++	+++	+	+

TABLE 15.2. COMPARISON OF DIFFERENT IMAGING MODALITIES IN THE ASSESSMENT OF VALVULAR HEART DISEASES (cont.)

	Echo	CT	MRI	Nuclear
Haemodynamic assessment				
Valve stenotic area	+++	++	+++	−
Valve regurgitant fraction	+++	+	+++	−
Left ventricular function	+++	++	+++	++
Right ventricular function	++	+	+++	+
Native valve infection	+++	+	++	+
Prosthetic valve infection	++	++	+	+++

+++ Extremely useful.
++ Very useful.
+ Rarely appropriate.
− No routine indication.

15.11. CASE PRESENTATION

A 43 year old man was referred for cardiac evaluation because his primary care physician heard a murmur during a routine check-up. He was a smoker and had a strong family history of CAD. The patient was asymptomatic from a cardiac standpoint. Blood pressure was 145/60 and his pulse was 90 bpm. The findings on the echocardiogram are shown in Fig. 15.4. The patient had a suspected bicuspid aortic valve with severe aortic regurgitation (see Fig. 15.4). His LVEF was estimated to be 50–55%. His left ventricle appeared to be dilated. He underwent CMR, which confirmed the bicuspid morphology of the aortic valve, severe aortic regurgitation and severe left ventricular dilation (see Fig. 15.5). In addition, his ascending aorta was normal and the aortic MR angiography showed no aortic coarctation (see Fig. 15.6). Given his risk factors and family history, he underwent CCTA, which showed no obstructive CAD (see Fig. 15.7). He was referred to surgery and underwent aortic valve replacement with a mechanical aortic valve prosthesis.

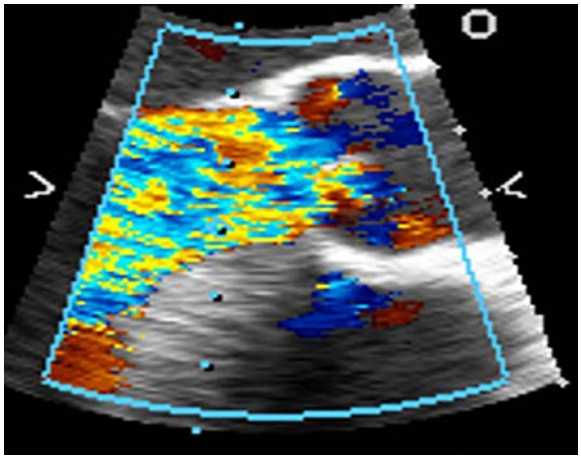

FIG. 15.4. Parasternal long axis view of the aortic valve with colour Doppler indicating severe aortic insufficiency.

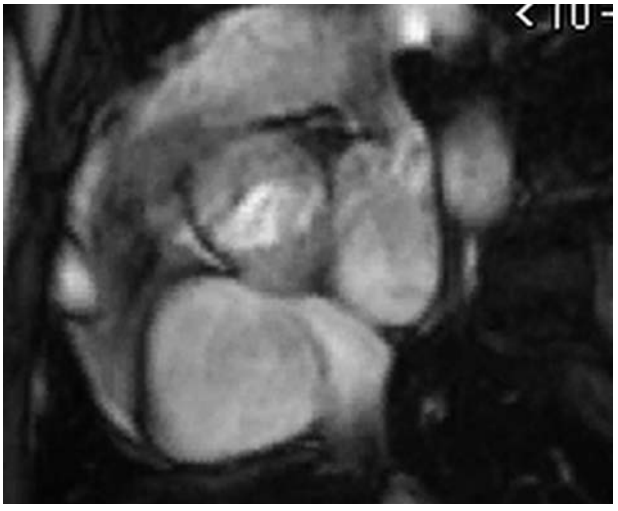

FIG. 15.5. CMR thin cut short axis view of the aortic valve showing a bicuspid aortic valve.

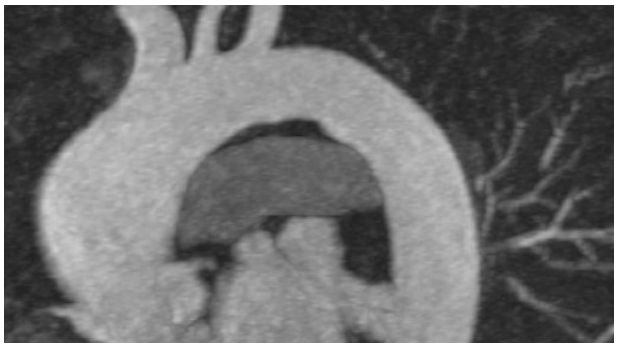

FIG. 15.6. Reconstructed long axis view of the aortic arch and descending aorta. In this patient with a bicuspid aortic valve, there is no evidence of coarctation of the aorta.

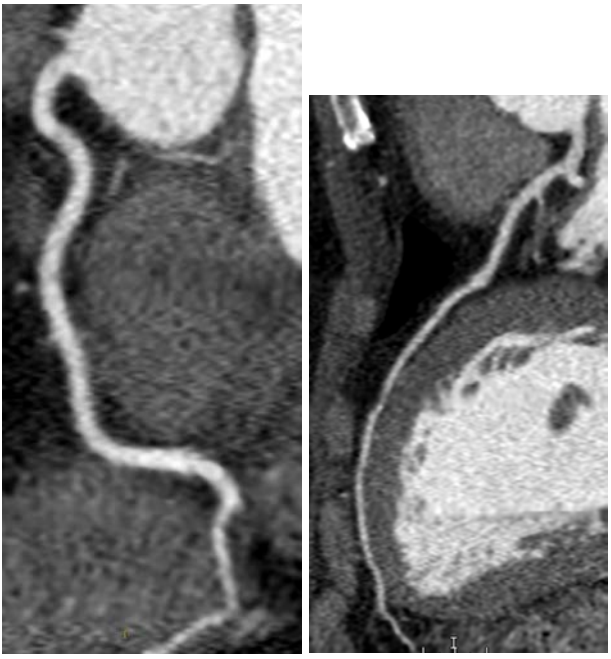

FIG. 15.7. Pre-operative CCTA of a patient with a bicuspid aortic valve and severe aortic insufficiency. There is no evidence of obstructive disease in the coronary arteries and the patient was referred for surgery without the need of invasive coronary angiography.

15.12. KEY MESSAGES

(1) Rheumatic valvular heart disease remains the main cause of primary valvular heart disease in developing countries.
(2) Degenerative valvular heart disease is the main cause of primary valvular disease in developed countries.
(3) Different valvular pathologies have similar clinical presentations and require a high index of suspicion, a thorough history and a physical exam to establish the correct diagnosis.
(4) Echocardiography is the primary imaging tool for the diagnosis and assessment of primary valvular heart disease to establish the diagnosis and its severity.
(5) In patients with primary valvular disease, a follow-up echocardiogram is recommended when symptoms change or after a certain period of time depending on the initial severity of the disease.
(6) CMR adds incremental value by confirming the diagnosis in controversial or borderline cases and assessing left ventricular and right ventricular volumes.
(7) CCTA is an acceptable alternative to invasive coronary angiography in low to intermediate risk patients with severe primary cardiac pathologies being prepared for valve surgery.
(8) CT plays an important role in planning percutaneous valve interventions, while echocardiography is the main tool of periprocedural monitoring.
(9) In patients with low flow, low gradient aortic stenosis, severe aortic valve calcifications favour the diagnosis of severe aortic stenosis.
(10) In patients with prosthetic valves and increased gradients, CCT is an alternative to fluoroscopy to assess valve leaflet dysfunction.
(11) Primary valvular heart disease should be managed by a multidisciplinary team, ideally in a dedicated valve centre staffed with clinical cardiologists, imaging specialists, interventional cardiologists and surgeons.

REFERENCES TO CHAPTER 15

[15.1] REMENYI, B., CARAPETIS, J., WYBER, R., TAUBERT, K., MAYOSI, B.M., Position statement of the World Heart Federation on the prevention and control of rheumatic heart disease, Nat. Rev. Cardiol. **10** (2013) 284–292.
[15.2] IUNG, B., VAHANIAN, A., Epidemiology of acquired valvular heart disease, Can. J. Cardiol. **30** (2014) 962–970.
[15.3] PODLESNIKAR, T., DELGADO, V., BAX, J.J., Imaging of valvular heart disease in heart failure, Card. Fail. Rev. **4** (2018) 78–86.

[15.4] BAUMGARTNER, H., et al., 2017 ESC/EACTS guidelines for the management of valvular heart disease, Eur. Heart J. **38** (2017) 2739–2791.

[15.5] NISHIMURA, R.A., et al., 2017 AHA/ACC focused update of the 2014 AHA/ACC guideline for the management of patients with valvular heart disease, J. Am. Coll. Cardiol. **70** (2017) 252–289.

[15.6] NISHIMURA, R.A., et al., 2014 AHA/ACC guideline for the management of patients with valvular heart disease: Executive summary, J. Am. Coll. Cardiol. **63** (2014) 57–185.

[15.7] ZOGHBI, W.A., et al., Recommendations for noninvasive evaluation of native valvular regurgitation, J. Am. Soc. Echocardiogr. **30** (2017) 303–371.

[15.8] ROMERO, J., et al., Detection of left atrial appendage thrombus by cardiac computed tomography in patients with atrial fibrillation: A meta-analysis, Circ. Cardiovasc. Imag. **6** (2013) 185–194.

[15.9] ALJIZEERI, A., SULAIMAN, A., ALHULAIMI, N., ALSAILEEK, A., AL-MALLAH, M.H., Cardiac magnetic resonance imaging in heart failure: Where the alphabet begins! Heart Fail. Rev. **22** (2017) 385–399.

[15.10] OPOLSKI, M.P., et al., CT angiography for the detection of coronary artery stenoses in patients referred for cardiac valve surgery: Systematic review and meta-analysis, J. Am. Coll. Cardiol. Cardiovasc. Imag. **9** (2016) 1059–1070.

[15.11] KIRMANI, B.H., BRAZIER, A., SRISKANDARAJAH, S., AZZAM, R., KEENAN, D.J., A meta-analysis of computerized tomography scan for reducing complications following repeat sternotomy for cardiac surgery, Interact. Cardiovasc. Thorac. Surg. **22** (2016) 472–479.

[15.12] MOSS, A.J., et al., Complementary role of cardiac CT in the assessment of aortic valve replacement dysfunction, Open Heart **3** (2016).

[15.13] AL-MALLAH, M.H., ALJIZEERI, A., VILLINES, T.C., SRICHAI, M.B., ALSAILEEK, A., Cardiac computed tomography in current cardiology guidelines, J. Cardiovasc. Comput. Tomogr. **9** (2015) 514–523.

[15.14] VON KNOBELSDORFF-BRENKENHOFF, F., SCHULZ-MENGER, J., Role of cardiovascular magnetic resonance in the guidelines of the European Society of Cardiology, J. Cardiovasc. Magn. Reson. **18** (2016) 6–24.

[15.15] MARWAN, M., ACHENBACH, S., Role of cardiac CT before transcatheter aortic valve implantation (TAVI), Curr. Cardiol. Rep. **18** (2016) 21.

[15.16] DWECK, M.R., et al., Assessment of calcification and inflammation with positron emission tomography in aortic stenosis and atherosclerosis, Lancet **381** (2013) 11.

[15.17] CHAMBERS, J.B., et al., Standards defining a ‘Heart Valve Centre’: ESC Working Group on Valvular Heart Disease and European Association for Cardiothoracic Surgery viewpoint, Eur. Heart J. **38** (2017) 2177–2183.

Chapter 16

CARDIO-ONCOLOGY

C.Y. SHIM, E. MILAN, R. GIUBBINI, S. DORBALA, P. RAGGI

Cancer survivorship is increasing through improved preventive strategies and novel anticancer drugs. Recent data show that cancer survivorship is increasing in the most common ten cancers [16.1]. Cancer is now becoming a chronic illness, and both short and long term cardiotoxic effects of cancer therapies are increasingly apparent. In addition, cancer survivors have cardiovascular disease more frequently than the general population. Cancer treatment toxicity further contributes to cardiovascular disease. Heart failure is the most common clinical presentation of cardiotoxicity. In clinical practice, the measurement of left ventricular ejection fraction (LVEF) to monitor for the occurrence of cardiotoxicity is widely assessed with radionucleotide ventriculography or 2-D echocardiography [16.2]. Novel parameters and new imaging techniques have been developed to overcome the limitations of isolated evaluation of LVEF [16.3]. A diagnostic approach based on the integrated use of different imaging techniques allows the early detection of cardiotoxicity, improving the therapeutic management, clinical outcomes and the quality of life of cancer patients.

16.1. DEFINITION

Cardio-oncology is a new multidisciplinary specialty with the purpose of identifying patients who are at a higher risk for developing cardiotoxicity so that appropriate surveillance, treatment and follow-up strategies may be instituted early. According to the 2014 American Society of Echocardiography and European Association of Cardiovascular Imaging expert consensus statement [16.4], the definition of cancer therapy related cardiac dysfunction is a decrease in the LVEF of over 10 percentage points, to a value of less than 53% during treatment. This definition of cardiotoxicity is more focused on myocardial dysfunction and consequent heart failure. Type 1 cardiotoxicity, associated with anthracycline use, is characterized by myocardial injury and is more likely to be irreversible, even with intervention or termination of the offending agent. Type 2 cardiotoxicity, associated with trastuzumab use, has a higher likelihood of recovery after discontinuation of the offending agent.

16.2. CLINICAL PRESENTATIONS

There are diverse clinical presentations associated with cancer therapy. Although chemotherapy associated cardiovascular abnormalities have been more in focus in current clinical practice, radiotherapy associated cardiovascular complications may occur after chest radiotherapy for breast cancer and lymphoma. Some cardiovascular complications occur during or after active therapy, but many of them usually appear after a long latent period, hence the need for long term monitoring. Although cardiotoxicity often refers to left ventricular dysfunction, there is a wide range of other common chemotherapy related cardiovascular complications, such as myocardial ischaemia, hypertension, thromboembolism, pericardial effusion and arrhythmias. The role of imaging is important for the detection of vascular complications and pericardial complications [16.5]. Common cardiovascular abnormalities associated with chemotherapy include:

(a) Myocardial complications:
  — Left ventricular dysfunction;
  — Heart failure.
(b) Vascular complications:
  — Hypertension;
  — Coronary vasospasm;
  — Venous thromboembolism;
  — Arterial thrombosis;
  — Pulmonary hypertension.
(c) Pericardial complications:
  — Pericardial effusion.

Common cardiovascular abnormalities associated with radiotherapy include:

(a) Myocardial complications:
  — Left ventricular dysfunction;
  — Heart failure.
(b) Vascular complications:
  — Aortic calcification;
  — Valvular complications;
  — Valve stenosis.
(c) Pericardial complications:
  — Pericardial effusion;
  — Constrictive pericarditis.

16.2.1. Asymptomatic left ventricular dysfunction

Numerous chemotherapeutic agents are associated with left ventricular dysfunction. The most frequently implicated therapeutic agents are anthracycline, a monoclonal antibody targeting the HER2 pathway, and tyrosine kinase inhibitors such as vascular endothelial growth factor pathway inhibitors [16.6]. Asymptomatic left ventricular dysfunction or heart failure may occur during active treatment or in the later survivorship phase.

As described in Table 16.2, the toxicity mechanisms of chemotherapeutic agents are classified into two types, and several risk factors predisposing to developing these complications have been identified in a large number of basic, clinical and epidemiological studies. The damage caused by anthracyclines (type I damage) occurs in a cumulative dose dependent manner [16.4]. Electron microscopy shows various degrees of myocyte damage, therefore myocardial damage is deemed irreversible, although myocardial function may be preserved and compensation optimized through anti-remodelling therapy [16.4]. In contrast, type II cancer therapy related cardiac dysfunction is exemplified by trastuzumab. It is not dose dependent, it does not lead to apoptosis and is often reversible.

Risk factors for type I cancer therapeutics related cardiac dysfunction are being either very young or old, being female, having hypertension, pre-existing cardiac disease, undergoing mediastinal radiation therapy and higher cumulative anthracycline dosing. In terms of the risk factors of type II cancer therapeutics

TABLE 16.2. TYPE I AND II CANCER THERAPEUTICS RELATED CARDIAC DYSFUNCTION

	Type I	Type II
Chemotherapeutic agent	Doxorubicin (anthracycline)	Trastuzumab (HER2 targeting antibody)
Mechanism	Free radical formation, oxidative stress/damage	Blocked ErbB2 signalling
Response to anti-remodelling therapy	Irreversible, but may stabilize	Reversible by 2–4 months after interruption of the agent
Dose relationship	Cumulative dose dependent	Not dose dependent
Ultrastructure	Vascular swelling processing to myofibrillar disarray and necrosis	No abnormalities

related cardiac dysfunction, the concurrent use of anthracyclines is the most significant risk factor.

The most commonly used parameter for monitoring left ventricular function with echocardiography is LVEF. In order to evaluate the effect of chemotherapy on left ventricular function, imaging at baseline before chemotherapy, and sequential imaging during follow-up is very helpful. To discover subclinical left ventricular dysfunction before the development of a poor ejection fraction, 2-D speckle tracking echocardiography (STE) has recently been introduced [16.7]. Abnormalities of left ventricular global longitudinal strain occur early and predict the development of left ventricular dysfunction. Other imaging modalities, such as multigated blood-pool imaging and cardiac magnetic resonance (CMR) have been used in the evaluation of LVEF [16.4, 16.8, 16.9].

16.2.2. Heart failure

Heart failure is the most common clinical manifestation of cardiotoxicity induced by chemotherapy. The onset of clinical symptoms and signs such as shortness of breath, chest discomfort, generalized or peripheral oedema is usually proceeded by subclinical or asymptomatic myocardial dysfunction. Therefore, early detection and monitoring of left ventricular dysfunction are beneficial for the restoration of left ventricular function and to prevent irreversible myocardial injury. As mentioned in the prior paragraph, symptoms and signs of heart failure may be stabilized after optimal medical therapy including angiotensin converting enzyme inhibitors and beta blockade. Figure 16.1 shows a typical example of type I chemotherapeutic agent induced cardiac dysfunction; the patient presented with stage C heart failure and was stabilized with medical therapy despite the presence of myocardial fibrosis on CMR imaging.

16.2.3. Vascular disease

Various types of vascular toxicity can be secondary to exposure to chemotherapeutic agents. Vasospasm, thrombosis, acute coronary syndrome (ACS), stroke, systemic hypertension and pulmonary hypertension can be associated with some specific chemoagents. Figure 16.2 illustrates a case of acute ST-elevation myocardial infarction (STEMI) induced by arterial thrombosis on the ascending aorta. A round shaped echogenic mass on the multimodality imaging and total occlusion of the distal right coronary artery were noted.

Fluorouracil (also known as 5-FU), which is frequently used for the treatment of gastrointestinal malignancy, can cause ischaemic syndromes ranging from angina to myocardial infarction by inducing vasospasm. A high dose of fluorouracil (>800 $mg \cdot m^{-2} \cdot day^{-1}$) especially if in combination with cisplatin,

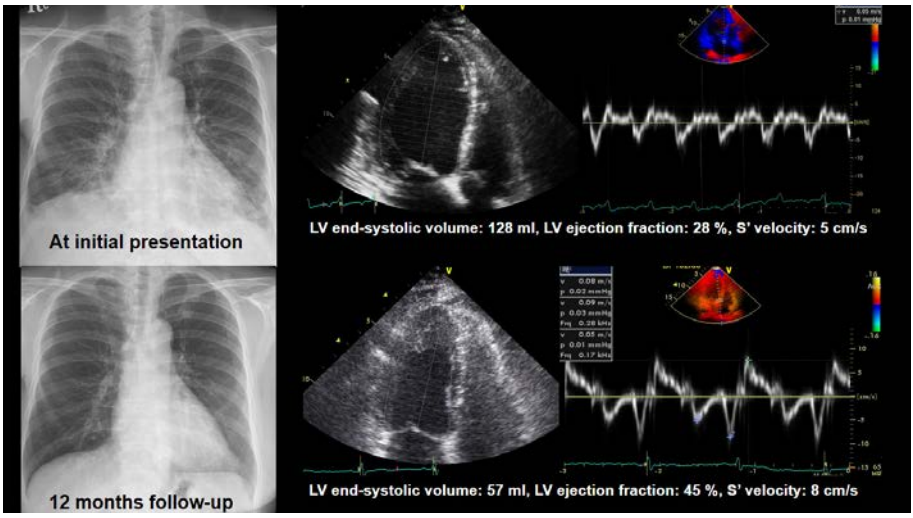

FIG. 16.1. A case of a 51 year old woman, diagnosed with breast cancer and treated with doxorubicin therapy ten years ago (cumulative dose of 550 mg/m^2). The patient presented with a cough and with shortness of breath even at rest. Decreased LVEF at initial presentation of symptoms (28%); improved LVEF after optimal medical treatment for heart failure (45%).

is well known to contribute to fluorouracil induced cardiotoxicity. Thalidomide and cisplatin are well known to increase the risk of thromboembolism [16.10]. Several tyrosine kinase inhibitors have been reported to have specific cardiotoxic side effects. For instance, sunitinib, used for the treatment of renal cell carcinoma among other cancers, frequently causes heart failure and hypertension. Bevacizumab [16.11, 16.12], used for the treatment of colorectal cancer among other things, increases the risk of arterial thrombosis [16.13].

16.2.4. Pericardial disease

Pericardial effusion is frequently found in cancer patients. It may be secondary to infiltration of the malignancy itself or a secondary inflammatory process, including cardiotoxicity. Pericarditis has been described in patients undergoing therapy with cyclophosphamide, cytarabine and bleomycin.

Pericarditis is common in patients undergoing radiotherapy. An acute exudative process is rare in patients receiving radiotherapy and more typically, pericarditis occurs within weeks of completing treatment and usually resolves spontaneously. Delayed chronic pericarditis several weeks to years after radiation exposure is not uncommon and may evolve into constrictive pericarditis in 5–20% of patients. The median time range between irradiation and open pericardiectomy

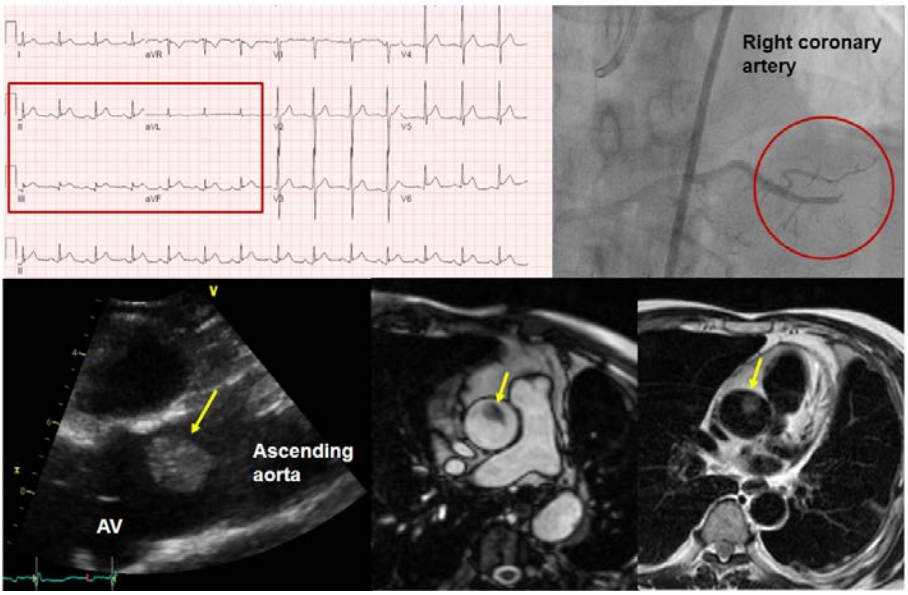

FIG. 16.2. A case of a 67 year old man with a diagnosis of metastatic mesothelioma. Cisplatin based chemotherapy had been started one month earlier. The patient was experiencing acute chest pain at rest for one hour with ST segment elevation on the inferior leads. Thrombotic occlusion at the distal right coronary artery was shown on the coronary angiogram. A round hypermobile mass on the ascending aorta was seen on the echocardiogram, compatible with a thrombus on CMR imaging (iso-signal intensity on T1 weighted imaging, slightly high signal intensity on T2 weighted imaging).

for constrictive pericarditis has been reported to be 13 years [16.14]. Figure 16.3 shows an example of constrictive pericarditis caused by radiation therapy. The patient presented with dyspnoea and peripheral oedema. Typical haemodynamic features of constrictive pericarditis were documented on echocardiogram.

16.2.5. Valvular complications

Radiotherapy can also promote valvular stenosis, especially of the aortic valve and mitral valve. Fibrosis and calcification of the valves are hallmarks of radiation related valve damage. Radiation increases fibroelastic growth factors that in turn increase fibroblast proliferation, collagen synthesis and extracellular matrix deposition. It also induces osteogenic phenotypes by increasing osteogenic factors that lead to valve calcification. The progression of valvular disease induced by radiation exposure is slow and can be as long as 20 years. In a study of 300 asymptomatic patients who received a minimum of 35 Gy to the

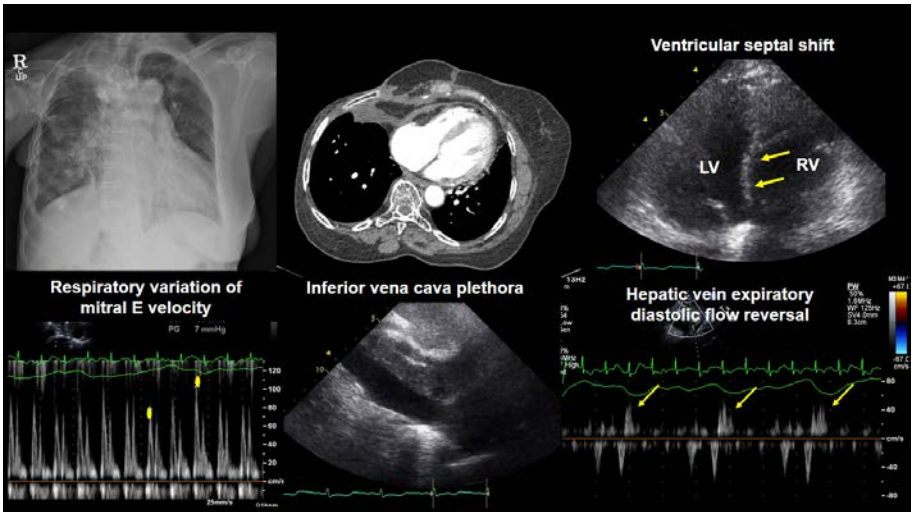

FIG. 16.3. A case of a 74 year old woman treated with radiotherapy for breast cancer 20 years previously. The patient presented with dyspnoea and orthopnoea with generalized oedema that had begun three months previously. A ventricular septal shift with typical constrictive physiology was evident on the echocardiogram.

mediastinum for Hodgkin's lymphoma [16.15], the incidence of mild to severe aortic regurgitation was increased by 60%, and the relative risk of valve surgery at 15 years after radiotherapy was ninefold higher compared with controls.

16.3. IMAGING ALGORITHMS BASED ON CLINICAL PRESENTATION

Imaging algorithms in guidelines are mainly focused on asymptomatic patients [16.10]. Requirements for LVEF assessment are reserved for anthracyclines and HER2 therapeutics. All other conventional chemotherapies and immune therapies do not require routine LVEF assessment. Among the imaging assessment modalities, a physician can choose radionuclide ventriculography, computed tomography (CT), echocardiography or CMR imaging, mostly based on local expertise.

16.4. SELECTION OF AN IMAGING MODALITY

A physician selecting an imaging modality should consider a few important factors. The ideal modality allows the detection of early myocardial changes, provides information associated with future development of cardiotoxicity and has long term prognostic value. Hence, the imaging modality should be accurate and reproducible. Although LVEF assessment is relatively simple, it has pitfalls. Its value is dependent on loading conditions, and reduction in LVEF is often a late phenomenon.

16.5. ECHOCARDIOGRAPHY

Assessment of LVEF assessment by 2-D measurement is fairly accurate but not as accurate as that obtained with CMR or 3-D echocardiography. Furthermore, its measurement is affected by left ventricular loading conditions, and the reduction in LVEF is often a late phenomenon. Therefore, global longitudinal strain by 2-D STE has been recommended for the detection of early subclinical myocardial dysfunction before LVEF drops (see Fig. 16.4). However, strain imaging has also pitfalls as it is vendor or software specific, it lacks the evidence of long term randomized clinical trials and there are sparse data on its reproducibility in non-academic clinical centres.

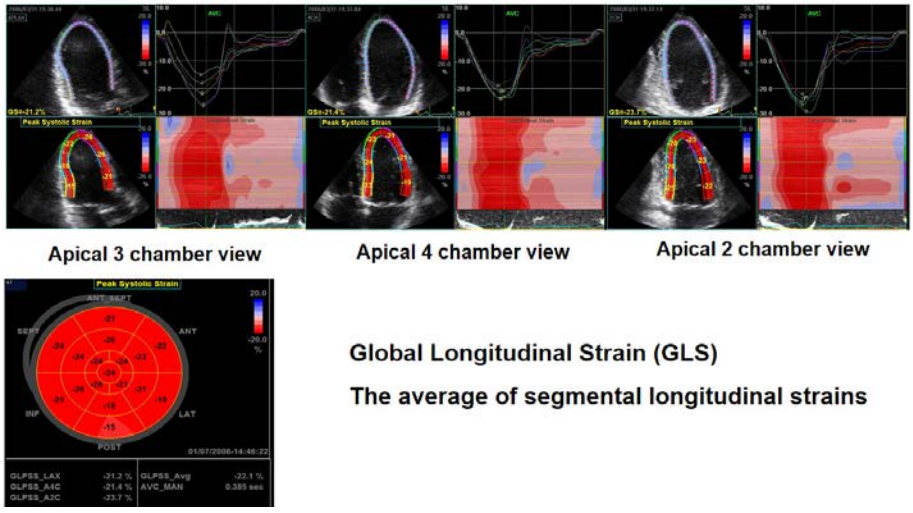

FIG. 16.4. Global longitudinal strain assessed by 2-D STE.

In 2014, the American Society of Echocardiography and the European Association of Cardiovascular Imaging issued an expert consensus on the multimodality imaging evaluation of adult patients exposed to chemotherapeutic agents [16.10]. Imaging algorithms for type I cardiotoxicity and type II cardiotoxicity were based on initial echocardiographic evaluation. Before initiation of a regimen potentially associated with type I or type II cardiotoxicity, a baseline evaluation of LVEF and global longitudinal strain and the measurement of serum troponin levels are recommended. If any of these are abnormal, a cardiology consultation is recommended [16.4]. For type I cardiotoxic regimens, follow-up echocardiography is recommended at the completion of therapy and six months later for doses of <240 mg/m^2 or equivalent [16.4]. Once this dose is exceeded, measurements of LVEF, global longitudinal strain and troponin are recommended before each additional 50 mg/m^2 [16.4]. For a type II cardiotoxic regimen, the measurement of LVEF, global longitudinal strain and troponin is recommended every three months during therapy and six months after completion [16.4].

16.6. NUCLEAR IMAGING

Multigated radionuclide angiography using in vivo ^{99m}Tc labelled erythrocytes allows the visualization of the cardiac blood-pool through a gamma camera with gated acquisition. The acquisition of gated images during the cardiac cycle provides accurate and highly reproducible information on LVEF, RVEF, left ventricular volumes and segmental wall motion evaluation [16.15] (see Fig. 16.5). However, its use may be hampered by soft tissue attenuation and it exposes the patient to ionizing radiation, particularly relevant in cases with repeated studies for monitoring purposes.

Technetium-99m gated blood-pool single photon emission computed tomography (SPECT) is characterized by the acquisition of 3-D images providing data on left and right ventricular function and wall motion. A good correlation between gated blood-pool SPECT and multigated radionuclide angiography in LVEF estimation has been reported [16.16].

Iodine-123-metaiodobenzylguanidine (^{123}I-MIBG) SPECT is a promising technique for the detection of early anthracycline injury and for the identification of patients at high risk of developing cardiotoxicity [16.17]. MIBG is a norepinephrine analogue showing the same uptake, storage and release mechanisms of norepinephrine. However, unlike norepinephrine, MIBG is not metabolized, therefore, labelled with ^{123}I, it can be used for the evaluation of cardiac sympathetic innervation and possible adrenergic derangement. After ^{123}I-MIBG injection, early (15 min) and late (4 h) images are acquired. The

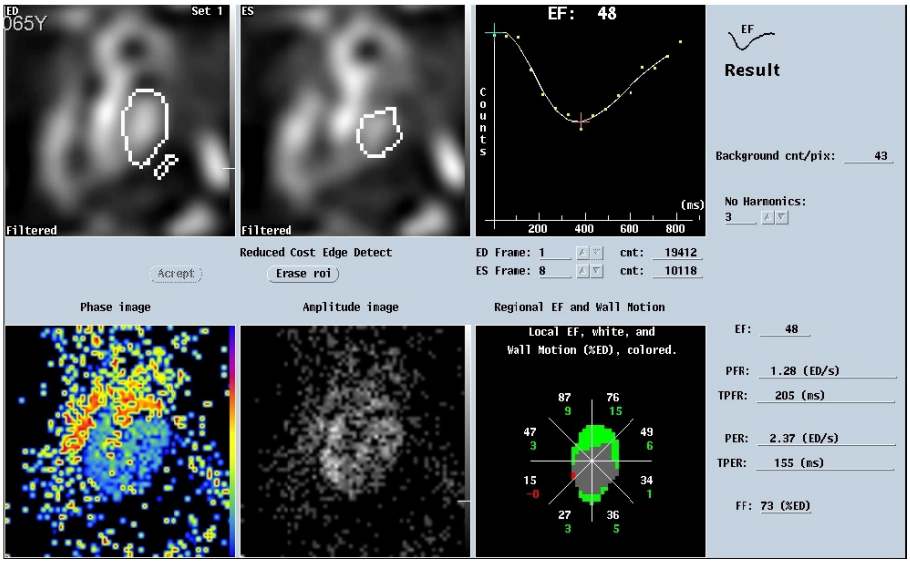

FIG. 16.5. A case of a 65 year old woman diagnosed with breast cancer, treated with trastuzumab therapy. The patient had a history of hypertension treated with diuretics for ten years, dyslipidaemia and was a smoker. The radionuclide angiography showed a decrease in LVEF due to cardiotoxicity (before treatment, LVEF = 67%; after treatment, LVEF = 48%).

most frequently used parameters are the heart to mediastinal ratio and washout rate. An increased concentration of norepinephrine in the cardiac synaptic space and a reduction in the presynaptic space induces a decrease in MIBG cardiac uptake (reduction of heart to mediastinal ratio) and accelerates the washout rate. In asymptomatic patients treated with anthracyclines, investigators have demonstrated that ^{123}I-MIBG is useful for the assessment of myocardial sympathetic innervation and helpful in the identification of patients at risk of developing cardiotoxicity [16.17].

Positron emission tomography (PET) is the gold standard for evaluating myocardial metabolism and perfusion owing to its high spatial and temporal resolution and routinely available attenuation correction providing high diagnostic sensibility and accuracy. The role of this technique in the early detection of cardiotoxicity is still debated. However, ^{18}F-fluorodeoxyglucose (FDG) uptake is a marker of glucose utilization in the myocardium and it has been demonstrated that in patients treated with doxorubicin, a progressive increase of cardiac ^{18}F-FDG uptake can be considered a biomarker of cardiotoxicity owing to the enhanced expression of glucose transporters GLUT-1 and GLUT-4 [16.18, 16.19].

16.7. CARDIAC MAGNETIC RESONANCE IMAGING

Recent advances in CMR allow the detection of early myocardial changes by assessing extracellular volume and fibrosis (T1 mapping) and interstitial oedema (T2 mapping). Therefore, CMR provides new insights into mechanisms of cardiovascular disease in cancer patients. Currently, T1 mapping can be measured prior to and after contrast (gadolinium) injection and can be used to calculate extracellular volume. Extracellular volume measurement with CMR reflects the myocardial collagen content in the interstitial tissue, therefore it may potentially be useful to monitor a patient's response to anti-remodelling therapies [16.20]. The role of multimodality imaging in cardio-oncology has been recently reviewed [16.21].

16.8. KEY MESSAGES

(1) Cancer survivorship is increasing through improved preventive strategies and novel anticancer therapies. Thus, survivors frequently develop cardiovascular diseases.
(2) Chemotherapeutic agents have direct and indirect cardiovascular toxicities.
(3) Left ventricular function needs to be monitored in cancer patients treated with anthracycline and monoclonal antibodies targeting HER2 inhibitors.
(4) Vascular toxicity can occur in some patients treated with newer cancer therapeutics.
(5) Pericardial effusion in cancer patients can be caused by direct invasion of the underlying malignancy or a secondary inflammatory process.
(6) Pericarditis and constrictive pericarditis are common in patients undergoing chest radiotherapy.
(7) Valvular stenosis due to fibrosis and calcification can occur after radiotherapy and most commonly affects the left side valves.
(8) The determination of left ventricular global longitudinal strain by 2-D STE can detect subclinical myocardial dysfunction before LVEF drops.
(9) Nuclear imaging such as radionuclide ventriculography and MIBG are helpful for monitoring cardiotoxicity.
(10) CMR imaging is an emerging tool for investigating mechanisms of cardiovascular disease in cancer patients.

REFERENCES TO CHAPTER 16

[16.1] MILLER, K.D., et al., Cancer treatment and survivorship statistics, 2016, CA Cancer J. Clin. **66** (2016) 271–289.

[16.2] NARAYAN, H.K., et al., Detailed echocardiographic phenotyping in breast cancer patients: Associations with ejection fraction decline, recovery, and heart failure symptoms over 3 years of follow-up, Circulation **135** (2017) 1397–1412.

[16.3] SAIKI, H., et al., Risk of heart failure with preserved ejection fraction in older women after contemporary radiotherapy for breast cancer, Circulation **135** (2017) 1388–1396.

[16.4] PLANA, J.C., et al., Expert consensus for multimodality imaging evaluation of adult patients during and after cancer therapy: A report from the American Society of Echocardiography and the European Association of Cardiovascular Imaging, Eur. Heart J. Cardiovasc. Imag. **15** (2014) 1063–1093.

[16.5] HERRMANN, J., et al., Vascular toxicities of cancer therapies, Circulation **133** (2016) 1272–1289.

[16.6] CHEN, M.H., KERKELÄ, R., FORCE, T., Mechanisms of cardiac dysfunction associated with tyrosine kinase inhibitor cancer therapeutics, Circulation **118** (2008) 84–95.

[16.7] THAVENDIRANATHAN, P., et al., Use of myocardial strain imaging by echocardiography for the early detection of cardiotoxicity in patients during and after cancer chemotherapy: A systematic review, J. Am. Coll. Cardiol. **63** (2014) 2751–2568.

[16.8] FALLAH-RAD, N., et al., The utility of cardiac biomarkers, tissue velocity and strain imaging, and cardiac magnetic resonance imaging in predicting early left ventricular dysfunction in patients with human epidermal growth factor receptor II-positive breast cancer treated with adjuvant trastuzumab therapy, J. Am. Coll. Cardiol. **57** (2011) 2263–2270.

[16.9] JIJI, R.S., KRAMER, C.M., SALERNO, M., Non-invasive imaging and monitoring cardiotoxicity of cancer therapeutic drugs, J. Nucl. Cardiol. **19** (2012) 377–388.

[16.10] ABDEL-RAZEQ, H., et al., Thromboembolic events in cancer patients on active treatment with cisplatin-based chemotherapy: Another look! Thromb J. **16** (2018) 2.

[16.11] CHU, T.F., et al., Cardiotoxicity associated with tyrosine kinase inhibitor sunitinib, Lancet **370** (2007) 2011–2019.

[16.12] SCHMIDINGER, M., et al., Cardiac toxicity of sunitinib and sorafenib in patients with metastatic renal cell carcinoma, J. Clin. Oncol. **26** (2008) 5204–5212.

[16.13] SCHUTZ, F.A.B., JE, Y., AZZI, G.R., NGUYEN, P.L., CHOUEIRI, T.K., Bevacizumab increases the risk of arterial ischemia: A large study in cancer patients with a focus on different subgroup outcomes, Ann. Oncol. **22** (2011) 1404–1412.

[16.14] SZPAKOWSKI, N., DESAI, M.Y., Radiation-associated pericardial disease, Curr. Cardiol. Rep. **27** (2019) 97.

[16.15] GUJRAL, D.M., LLOYD, G., BHATTACHARYYA, S., Radiation-induced valvular heart disease, Heart **102** (2016) 269–276.

[16.16] PELLETIER-GALARNEAU, M., et al., Assessment of left ventricular ejection fraction with cardiofocal collimators: Comparison between IQ-SPECT, planar equilibrium radionuclide angiography, and cardiac magnetic resonance, J. Nucl. Cardiol. **26** (2019) 1857–1864.

[16.17] STOKKEL, M.P., DE WIT-VAN DER VEEN, L.J., BOEKHOUT, A., I-123-MIBG myocardial imaging in trastuzumab-based cardiotoxicity: The first experience, Nucl. Med. Commun. **34** (2013) 19–24.

[16.18] GORLA, A.K.R., SOOD, A., PRAKASH, G., PARMAR, M., MITTAL, B.R., Substantial increase in myocardial FDG uptake on interim PET/CT may be an early sign of adriamycin-induced cardiotoxicity, Clin. Nucl. Med. **41** (2016) 462–463.

[16.19] BAUCKNEHT, M., et al., Doxorubicin effect on myocardial metabolism as a prerequisite for subsequent development of cardiac toxicity: A translational ^{18}F-FDG PET/CT observation, J. Nucl. Med. **58** (2017) 1638–1645.

[16.20] HUANG, H., et al., Accuracy of left ventricular ejection fraction by contemporary multiple gated acquisition scanning in patients with cancer: Comparison with cardiovascular magnetic resonance, J. Cardiovasc. Magn. Reson. **19** (2017) 34.

[16.21] PLANA, J.C., THAVENDIRANATHAN, P., BUCCIARELLI-DUCCI, C., LANCELLOTTI, P., Multi-modality imaging in the assessment of cardiovascular toxicity in the cancer patient, J. Am. Coll. Cardiol. Cardiovasc. Imag. **11** (2018) 1173–1186.

Chapter 17

ADULT CONGENITAL HEART DISEASE

F. KENG, S. DORBALA, S.L. PARTINGTON

Improvements in both medical and surgical care in patients with congenital heart disease have resulted in increased longevity and, therefore, an increased prevalence of adults with congenital heart disease [17.1]. As more such patients survive into adulthood, the development of the subspecialty of adult congenital heart disease (ACHD) has increased in significance. The majority of ACHD patients have undergone surgical repairs in childhood, and lifelong follow-up is recommended. Many patients with ACHD do not recognize subtle changes in exercise capacity, and serial imaging is important to monitor them for haemodynamic and anatomical sequelae. Despite advances in the management of ACHD patients, their mortality is still seven times higher than comparable peers without such conditions, and disease progression in intervened and non-intervened individuals into adulthood is a major factor to be considered. The need for non-invasive imaging of these patients both for diagnostic, management and prognostic purposes has led to significant developments in cardiac imaging to cater for this unique group of patients.

17.1. GUIDELINES

Guidelines are available for the management of ACHD patients. The American College of Cardiology and the American Heart Association published guidelines in 2018 [17.2] and 2015 [17.3], the Canadian Cardiac Society and the European Society of Cardiology published guidelines in 2009 [17.4] and 2020 [17.5].

17.2. CLINICAL PRESENTATION

The clinical presentation of ACHD is varied. ACHD patients may be totally asymptomatic and present with an abnormal electrocardiogram (ECG), chest X ray or auscultatory findings. ACHD patients may still present with cyanosis, right or left ventricular heart failure symptoms, palpitations, cerebrovascular accidents, infective endocarditis and, rarely, chest discomfort. To be able to identify the presence and type of congenital heart disease, a list of

the specific disease entities is included in Section 17.4, with the various roles of cardiac imaging.

17.3. IMAGING MODALITIES

In general, echocardiography (transthoracic echocardiography, TTE, transoesophageal echocardiography, TEE) is the mainstay of imaging investigations for ACHD, as it is widely available and easily accessible. Echocardiography provides anatomical data with good spatial and temporal resolution and functional and haemodynamic parameters and is devoid of radiation risks. Echocardiography contrast is sometimes used to further delineate structure and perfusion, and although there is some controversy over the safety of echocardiography contrast in patients with right to left shunts, there are no known serious adverse events in patients with right to left shunts [17.6]. Expertise and training in ACHD are vitally important so that appropriate images are obtained to optimally define all the pertinent aspects of the congenital heart lesion and to appropriately interpret the findings.

Cardiac computed tomography (CCT) is also an excellent modality for ACHD when interpreted by expert readers [17.7, 17.8]. It provides excellent spatial resolution for structural heart lesions and extracardiac structures, particularly the branch pulmonary arteries and the aorta, structures not well seen by echocardiography. Haemodynamic surveillance is not well performed by CCT; although prospective or retrospective CCT can be used to quantify ventricular size and function [17.9]. The risks of radiation exposure and iodinated contrast injection are other considerations, bearing in mind that low dose CT protocols reduce the dose of radiation required. Furthermore, the use of a low dose CCT for structural imaging may be sufficient for the purpose of diagnosing a variety of types of ACHD. This modality can be considered when echocardiography does not answer all the clinical questions or when cardiac and extracardiac structural questions remain. Similarly, various contraindications for cardiac magnetic resonance (CMR) may necessitate this modality.

CMR is another excellent modality for structural cardiac and extracardiac imaging and allows for the surveillance of the long term cardiac complications of ACHD [17.10, 17.11]. CMR has excellent tissue border delineation, tissue characterization and phase contrast flow assessment and allows for 3-D imaging of the heart and extracardiac structures. CMR is the ideal modality for the quantification of ventricular volumes and function [17.12, 17.13], valvular regurgitation [17.14], and shunt and collateral burden calculation [17.15] that allows for serial comparisons without the need for ionizing radiation. Equipment expertise can limit the general utility of CMR. Some metallic implants, including

older generation pacemakers, result in safety issues in CMR and artefacts from other implanted metallic devices such as stents and coils can limit image quality in some patients. Gadolinium contrast injection is often necessary, although sequences allowing for non-contrast enhanced MR angiography are available, and the referrer should be aware of the risks of gadolinium injection. Again, CMR can be considered when echocardiography does not offer complete resolution of the clinical questions and when quantification of ventricular size and function or quantification of flow is required.

Nuclear cardiac imaging has only a small role to play in ACHD, limited to shunt detection and quantitation, demonstration of myocardial ischaemia and viability, myocardial functional analysis, and possibly detection of infective processes in native and postoperative patients [17.16].

17.4. SPECIFIC DISEASE ENTITIES

17.4.1. Atrial septal defect

Of the various forms of atrial septal defect (ASD), including the patent foramen ovale, the secundum variety is the most common, followed by the primum and sinus venosus types. Anomalous pulmonary venous return is common in secundum and sinus venous atrial level defects and should be assessed prior to planning the type of repair to be carried out. The major haemodynamic consequence of haemodynamically significant ASDs are the increased right heart blood flow resulting in right sided chamber enlargement and, rarely, the subsequent development of pulmonary hypertension and reversal of shunt flow causing Eisenmenger's syndrome.

TTE would be the investigation of choice for the location of the defect or defects and the haemodynamic consequences on the right heart (see Fig. 17.1), thus guiding medical or surgical therapies. The non-invasive nature of this test makes it the ideal modality for follow-up assessment after intervention and for gauging the progression of disease in non-intervened individuals. It can also demonstrate associated cardiac and extracardiac abnormalities. TEE is sometimes needed for clearer delineation of the size and rims of the ASD to assess suitability for percutaneous device closure. Injection of agitated saline in the form of a bubble study can identify small shunts not confirmed by colour Doppler. Following percutaneous and open surgical closure, the echocardiography can identify the type and success of the procedure.

Contrast CCT can demonstrate the defect and pulmonary venous anatomy with great accuracy. However, it involves radiation exposure, and contrast injection and flow cannot be quantified by CCT, although right ventricular size

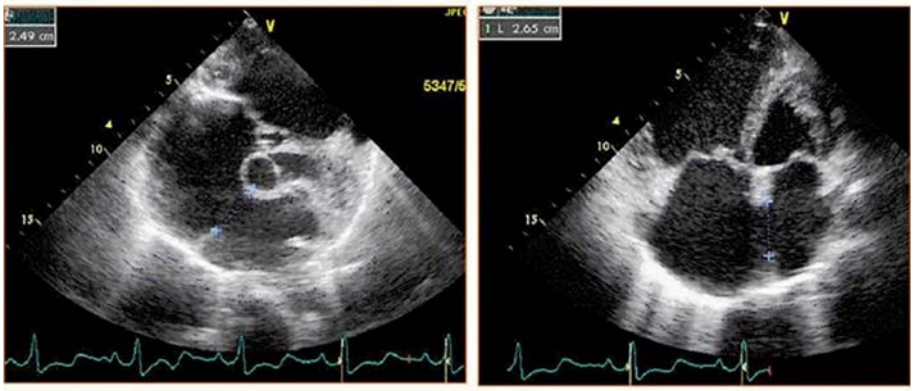

FIG. 17.1. Secundum ASD. This young patient presented with right heart failure symptoms at 18 years of age. Clinical examination revealed a systolic murmur. A chest X ray showed cardiomegaly. Transthoracic echocardiogram clearly shows a haemodynamically significant shunt that was very large. The ASD was deemed too large for percutaneous closure and thus surgical closure was recommended. A contrast CCTA (not shown) was carried out prior to surgery that did not show any evidence of coronary abnormalities.

can. New CCT techniques have drastically reduced the radiation dose required for such examinations.

CMR with or without contrast is another modality for assessment of cardiac shunts. CMR accurately delineates the location of the lesion, the pulmonary venous anatomy and also the haemodynamic consequences of the lesion by quantification of the volume of shunting [17.15] and right ventricular size [17.12, 17.13]. However, it suffers from the paucity of expertise and equipment, and the cost involved is usually higher compared with echocardiography. The role of nuclear imaging is extremely limited for shunt assessment.

Cardiac catheterization is sometimes needed to assess the severity of a shunt when both a right and left heart study can be performed. It also offers an accurate assessment of pulmonary pressures that is extremely important when there is concern about pulmonary arterial hypertension, as if pulmonary vascular resistance is sufficiently elevated, shunt closure is contraindicated and medical treatment for pulmonary hypertension should be considered. Coronary artery disease (CAD) may need to be assessed in older individuals if surgical ASD closure is required. Catheterization can also provide the therapeutic option of catheter based closure of the ASD.

17.4.2. Ventricular septal defect

Of the four major types of ventricular septal defect (VSD), the peri-membranous variety is the most common, the others being outlet, inlet and muscular types. Some may close spontaneously over time, but the vast majority result in some residual shunts in adults. The VSD may be associated with other structural heart defects, in particular right ventricular outflow tract obstruction and aortic regurgitation. Large VSDs that remain unrepaired into adulthood frequently develop pulmonary vascular disease progressing to Eisenmenger's syndrome.

TTE with Doppler is the main investigative modality in VSDs. It can demonstrate the number and location of defects. The haemodynamics of the VSD can also be assessed by TTE, including the velocity of shunt flow across the VSD, with a high velocity systolic flow signal suggesting a small, restrictive defect and a low velocity flow suggesting a large, non-restrictive defect. TTE also identifies the consequences of a haemodynamically significant VSD, including left ventricular dilation or the presence of pulmonary hypertension. Following VSD repair, TTE allows for assessment of the presence of residual VSD, demonstrates other associated cardiac conditions and is crucial in the longitudinal follow-up of patients (see Fig. 17.2).

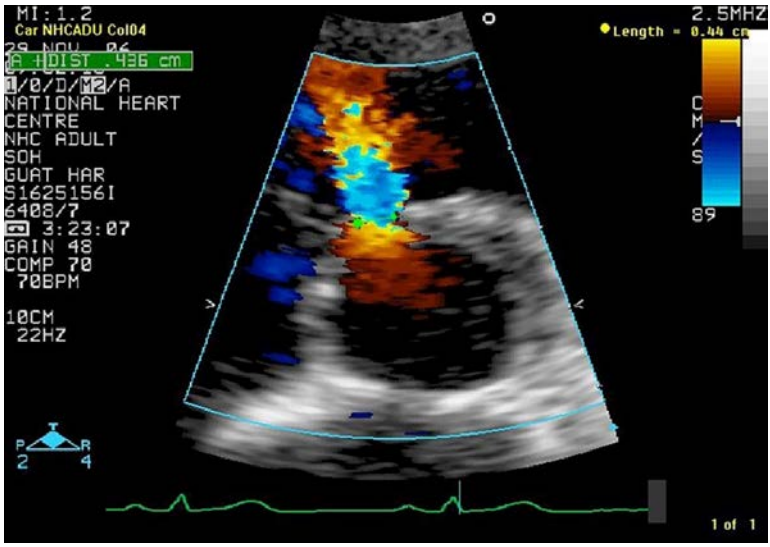

FIG. 17.2. Short axis peri-membranous VSD in a middle aged man presenting with an asymptomatic heart murmur, showing a left to right shunt across the membranous portion of the ventricular septum. Coronary angiography was performed to assess the shunt and also the coronary arteries before surgery was recommended.

CMR and CCT are also useful in this context, especially when the TTE or TEE cannot define the lesion completely. Other advantages include the accurate delineation of concomitant cardiac lesions. The disadvantages have been previously discussed.

Cardiac catheterization can be considered for shunt quantification and pulmonary pressure assessments if there is concern for pulmonary hypertension that may preclude VSD repair. Again, cardiac catheterization is primarily used when percutaneous device closure is considered, together with simultaneous assessment of the coronary arteries. The nuclear role is again limited to shunt assessment and perhaps the detection of infections around the lesion.

17.4.3. Atrioventricular septal defect

Atrioventricular septal defect (AVSD) can be either complete or partial, and involves a primum ASD and inlet VSD, with the defect occurring across the atrioventricular valve, thus resulting in a wide range of dysfunction of the mitral and tricuspid valves. AVSD is commonly associated with Down's syndrome. To survive into adulthood, many patients would have undergone surgical correction, and without surgical correction, many patients develop pulmonary hypertension and Eisenmenger's syndrome, particularly if there is a large VSD component. Imaging modalities must recognize the sequalae following AVSD repair including residual ASD, VSD and atrioventricular valve regurgitation and/or stenosis.

TTE and TEE are again the mainstay of imaging for both unoperated and operated patients. Indices such as the shunt and haemodynamic consequences of the lesion can be assessed, together with associated valvular lesions.

CCT and CMR can be used when echocardiography does not answer the anatomical or haemodynamic question. Cardiac catheterization can be considered when other non-invasive methods prove equivocal, and is sometimes required when open surgical correction is considered, particularly to assess the pulmonary vascular resistance or when coronary artery stenosis needs to be ruled out prior to surgical repair in an older patient.

17.4.4. Patent ductus arteriosus

Patent ductus arteriosus (PDA), an abnormal communication between the aorta and the pulmonary artery, is often associated with other congenital heart defects, especially ASD and VSD. Once recognized, transcatheter or open surgical ligation offers a permanent cure.

Doppler echocardiography would be the initial technique of choice for the detection of this lesion when suspected. A good parasternal long axis right ventricular outflow tract view can often demonstrate the abnormal flow into

the main pulmonary artery from the aorta and can give an indication of the haemodynamic consequences of the PDA including pulmonary pressure and left ventricular dilation. When echocardiography images are inadequate, CMR or CCT can be employed for a clearer delineation of the PDA, with CMR providing shunt fraction data. TTE is also important for routine follow-up of these patients (see Fig. 17.3).

Cardiac catheterization is used to delineate the location, size, severity and morphology of the shunt, to evaluate the pulmonary vascular resistance and to determine whether percutaneous occlusion of the PDA is possible.

17.4.5. Left sided heart obstructive lesions (aortic valve disease, coarctation of aorta)

Left sided heart obstructive lesion syndromes include many possible obstructive lesions such as supramitral ring, mitral stenosis, subvalvular atrial stenosis, valvular atrial stenosis, supravalvular atrial stenosis and aortic coarctation. These lesions can occur in isolation or in combination with one another. The combination of supramitral ring, mitral stenosis from a parachute mitral valve, subaortic stenosis and aortic coarctation is called Shone's syndrome. Overall, left sided obstructive lesions are rather common in the population, mostly due to the common occurrence of bicuspid aortic valve (0.5–2% of live births).

TTE can be used to demonstrate the haemodynamic consequences of obstructive lesions on the left and right heart. Quantification of the stenotic or regurgitant flow across the mitral and aortic valves and left sided heart obstructive lesion and gradient across the aortic arch is the forte of Doppler echocardiography.

CCT and CMR can also be used to accurately assess left sided obstructive lesions and in particular the aortic arch that is frequently not well seen by TTE.

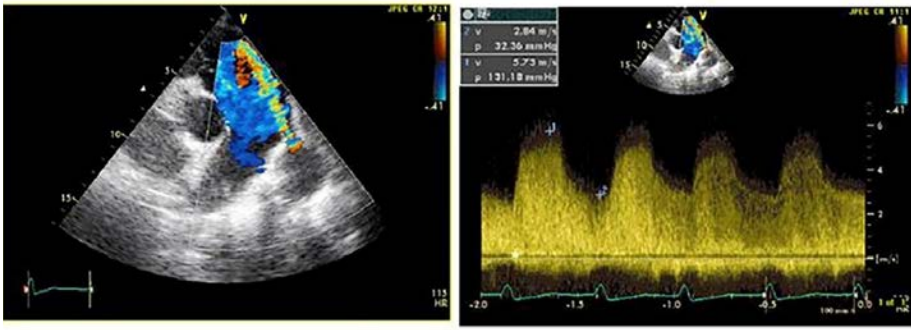

FIG. 17.3. PDA with haemodynamics.

CCT and CMR can assess the dimensions of the entire aorta, the relation of aortic narrowing to the head and neck vessels and collateral circulation around any arch narrowing, so that the need for intervention can be assessed and the mode of intervention, transcatheter or open surgical repair, can be planned.

Cardiac catheterization gives accurate haemodynamic data for lesions when non-invasive techniques are insufficient, equivocal or discordant. Percutaneous interventions for the aortic valve and aortic coarctation can be considered in select cases. The coronary arteries may need to be assessed if open surgery is required for correction of congenital defects in older patients.

17.4.6. Right ventricular outflow tract obstruction (pulmonary stenosis)

Congenital conditions involving right ventricular outflow tract obstruction include tricuspid valve disease, pulmonary valve disease, infundibular obstruction, sub-infundibular obstruction and supravalvular obstructions including branch pulmonary artery stenosis. Right ventricle to pulmonary artery conduits implanted for repairs of various types of congenital heart defect frequently stenose or become regurgitant, causing haemodynamic problems.

Both TTE and TEE offer diagnosis of such lesions, with accurate assessment of the site, dimensions and haemodynamic consequences of any obstructive lesions. Echocardiography is also important in the follow-up of patients both before and after surgery.

CMR and CCT are other alternatives for imaging when echocardiography images are suboptimal. Such imaging can clearly delineate right ventricle to pulmonary artery conduits and the entire pulmonary tree, structures that are not well seen by TTE. CMR can provide haemodynamic data of pulmonary flow including stenotic and regurgitant flow and the relative proportion of right and left pulmonary artery flow to assess the haemodynamic significance of branch pulmonary artery stenosis.

Cardiac catheterization offers accurate real time haemodynamic indices when other imaging techniques prove equivocal. Percutaneous intervention of an obstruction can be considered if suitable, including placement of percutaneous pulmonary valves and dilation and stenting of pulmonary artery stenosis. Again, if open surgical intervention is required, coronary angiography may be necessary.

17.4.7. Coronary artery abnormalities

Patients with coronary artery abnormalities include those born with anomalous coronary artery origins and others with congenital heart disease in which surgical reimplantation of coronary arteries is required, such as patients with transposition of the great arteries with arterial switch surgery or patients with

aortic stenosis following a Ross–Yacoub procedure. Coronary artery problems can also occur in some patients with supravalvular aortic stenosis such as in those with Williams syndrome.

Although TTE can demonstrate coronary origins, it suffers from the problem of image quality, and cannot demonstrate the entire course of the artery. It can sometimes pick up evidence of an arteriovenous fistula.

CCT with contrast is the technique of choice for delineating the entire course of the coronary artery in relation to other cardiac structures and great vessels. The origin and the course of the artery is important to ascertain the need for intervention in these cases. Arteriovenous fistulas can be demonstrated accurately and easily, both in course, origin and drainage.

CMR with or without contrast is also a good technique for delineating the proximal course of coronary arteries, but is frequently limited at demonstrating the distal coronary arteries. CMR can demonstrate myocardial scar if there is concern for prior coronary infarct.

The role of nuclear stress imaging is important to look for the physiological consequences of coronary artery obstruction, ischaemia, in the myocardial territory subtended by the abnormal coronary, which may include coronary compression and fistulous connections, among other things, which may then require percutaneous or open surgical intervention [17.16].

Cardiac catheterization sometimes clinches the diagnosis, but it may not be able to delineate the course of the coronary artery in relation to other cardiac structures and great vessels. Frequently, CCT is required when angiography fails to locate the usual origin of coronary arteries. An atrioventricular fistula can be easily demonstrated.

17.4.8. Pulmonary hypertension and Eisenmenger's syndrome

Pulmonary hypertension, irrespective of its cause, is a progressive disease that causes significant morbidity and mortality. Early recognition and treatment are necessary to prevent disease progression.

TTE is the best modality for easy estimates of pulmonary pressures and to assess for the cause of raised pulmonary pressures. TTE identifies right ventricular outflow tract obstruction as described above, so that elevated right ventricular systolic pressures due to right heart obstruction can be differentiated from elevated right ventricular systolic pressures from pulmonary hypertension. Once diagnosed, echocardiography can also be used to monitor disease progression or regression after medical or surgical therapies.

CMR and CCT can provide alternative techniques for imaging the pulmonary arteries, giving excellent delineation of the entire pulmonary tree.

Cardiac catheterization gives an accurate assessment of right ventricular and pulmonary pressures, right ventricular outflow tract gradients and pulmonary vascular resistance and can demonstrate in real time changes in pressures with pulmonary vasodilators to demonstrate reversibility in pulmonary artery pressure. It can also demonstrate the sometime distal nature of pulmonary artery stenosis in its entire course.

17.4.9. Tetralogy of Fallot

Tetralogy of Fallot has four components resulting from the anterior deviation of the conal septum: (i) varying degrees of right ventricular outflow tract obstruction; (ii) VSD; (iii) overriding aorta; and (iv) right ventricular hypertrophy. The degree of right ventricular outflow tract obstruction can range from only mild subpulmonary stenosis to the most severe form involving complete absence of the main pulmonary artery (tetralogy of Fallot with pulmonary atresia). The majority of patients undergo surgical repair in infancy or childhood, which generally involves patching the narrowing in the right ventricular outflow tract, resulting in varying degrees of pulmonary regurgitation. Many patients with repaired tetralogy of Fallot undergo a pulmonary valve replacement in adulthood, with cardiac imaging being used to aid in the decision making for the timing of the valve replacement. Survival following tetralogy of Fallot repair is excellent, but there is a threefold increase in mortality beginning in the third postoperative decade of life [17.17], highlighting the importance of regular surveillance of these patients.

TTE would be the initial method of choice for assessing tetralogy of Fallot, both before and after surgery. It gives the structural and haemodynamic indices necessary for the monitoring tetralogy of Fallot following repair including the assessment of pulmonary regurgitation, residual right ventricular outflow tract obstruction and residual shunts and lesions that may require further therapy (see Fig. 17.4).

Evaluation of patients with repaired tetralogy of Fallot is one of the most common ACHD referrals for CMR. CMR is acknowledged as the gold standard for assessing the haemodynamic sequalae of pulmonary regurgitation with guidelines for determining timing of pulmonary valve replacement based on the presence of symptoms or right ventricular size and function [17.2, 17.18]. It also provides information on the presence of right ventricular outflow tract aneurysms, branch pulmonary arteries, residual VSD and left ventricular size and function that can also be affected following tetralogy of Fallot repair (see Figs 17.5–17.7).

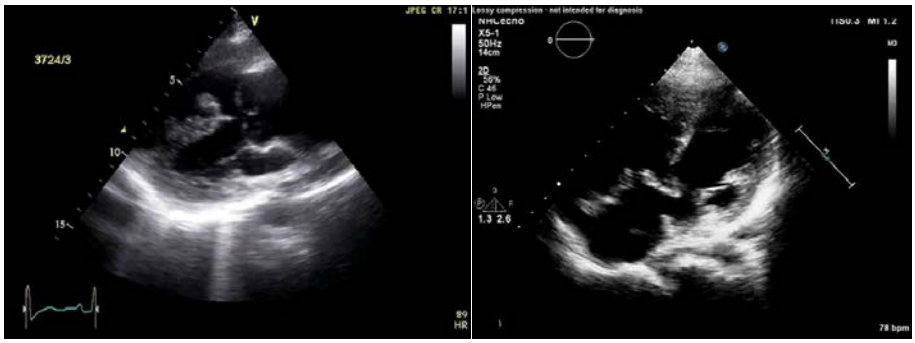

FIG. 17.4. Tetralogy of Fallot, previously undiagnosed in a young male, necessitating surgical correction. The transthoracic echocardiogram demonstrates the malalignment VSD, overriding aorta and right ventricular hypertrophy.

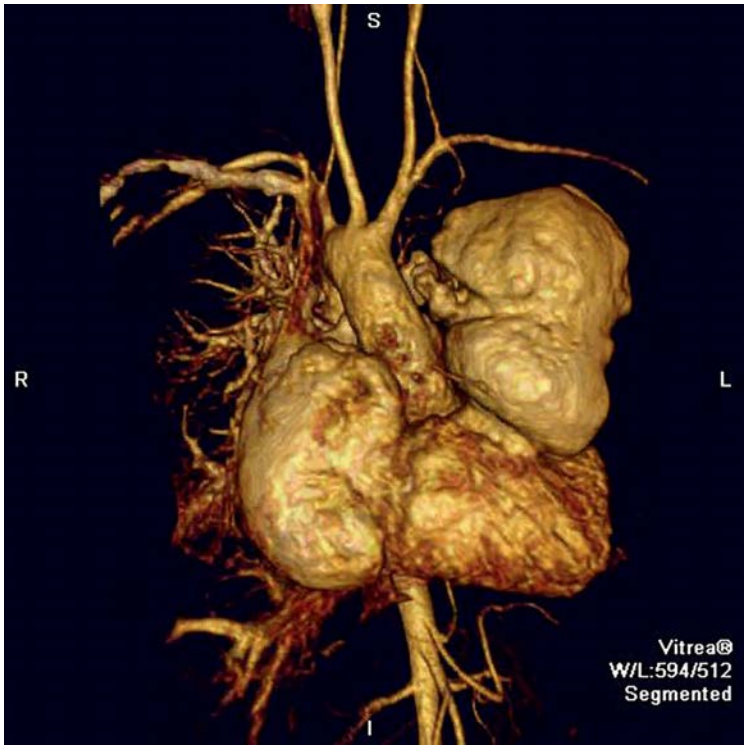

FIG. 17.5. MR angiogram with 3-D volume rendered reconstruction in a patient with repaired tetralogy of Fallot demonstrating a large right ventricular outflow tract aneurysm at the site of the right ventricular outflow tract patch.

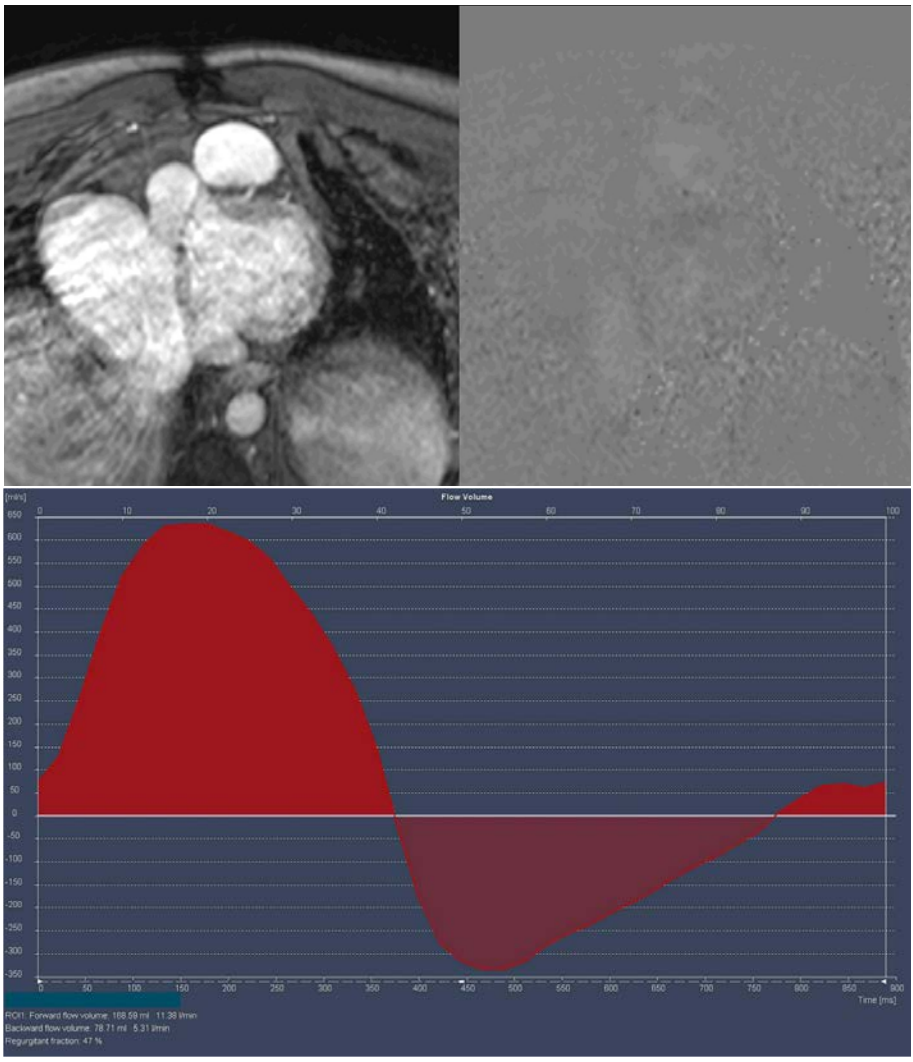

FIG. 17.6. MR Phase contrast flow assessment across the main pulmonary artery in a patient with repaired tetralogy of Fallot with a transannular patch demonstrating severe pulmonary regurgitation with a regurgitant fraction of 47%.

CCT can be considered in patients who cannot undergo CMR, as it can also give the structural information required including quantification of right ventricular size and function if unable to obtain a CMR [17.9]. Cardiac catheterization is required before corrective surgery, and can also be used post-surgery to detect coronary problems, residual shunts and abnormal haemodynamics.

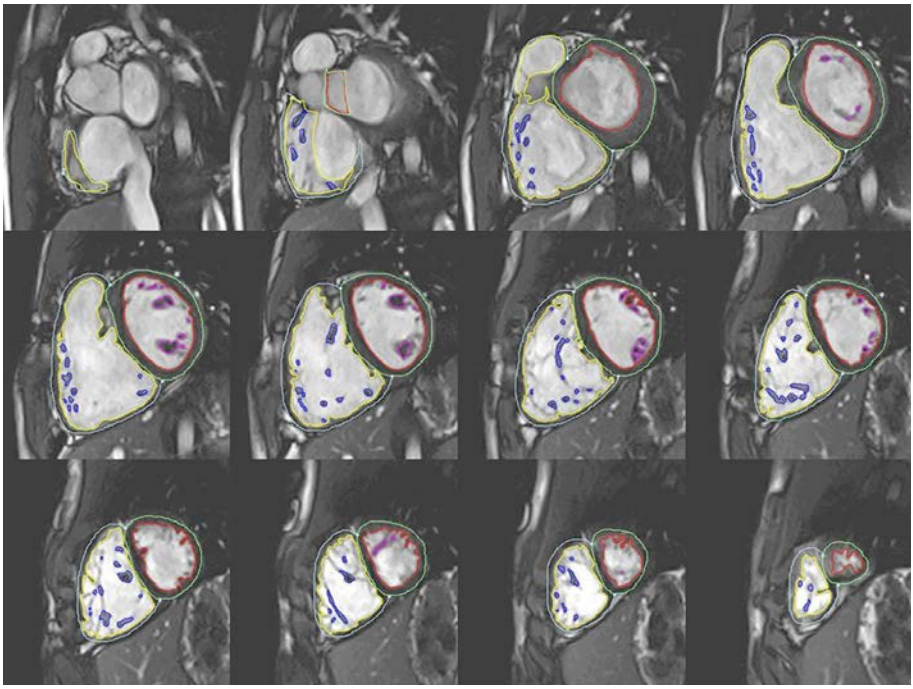

FIG. 17.7. Steady state free procession CMR short axis stack in a patient with repaired tetralogy of Fallot demonstrating the end diastolic ventricular contours used to calculate the right ventricular end diastolic volume.

17.4.10. Dextrotransposition of the great arteries

Dextrotransposition of the great arteries (D-TGA) is characterized by atrioventricular concordance and ventriculoarterial discordance. Deoxygenated blood flows from the right atrium to the right ventricle to the aorta, while oxygenated blood flows from the left atrium to the left ventricle to the pulmonary artery. This results in cyanotic congenital heart disease and, without intervention, the mortality rate in the first year of life is very high. From the late 1950s until the mid-1990s, surgical repair involved atrial switch surgery in which systemic venous (deoxygenated) blood is rerouted leftward through the atrium to the mitral valve and the left ventricle by intra-atrial baffles. Pulmonary venous blood is redirected rightwards to the tricuspid valve and right ventricle. Following the atrial switch, the right ventricle is the systemic ventricle, which frequently develops ventricular dysfunction early in life, and the left ventricle is the subpulmonic ventricle. Common complications after the atrial switch

include venous pathway stenosis, baffle leak, systemic right ventricular systolic dysfunction and tricuspid regurgitation.

In the 1990s, the arterial switch operation succeeded the atrial switch as the preferred treatment for D-TGA. The great arteries are transected above the sinuses, the aorta is brought posteriorly to align with the left ventricle while the pulmonary arteries are brought anteriorly where they straddle the aorta to come into alignment with the right ventricle. A coronary artery translocation is performed when the aorta is translocated. Late complications after the arterial switch operation include neo-aortic dilation and regurgitation, supravalvular pulmonic stenosis, branch pulmonary artery stenosis and coronary artery obstruction [17.19, 17.20] (see Fig. 17.8).

Given the very different surgical repairs for D-TGA with different post-surgical anatomy and late complications, an expert imager should have detailed knowledge of both the native and corrected anatomy for follow-up purposes.

Echocardiography is the mainstay of imaging for D-TGA. Adults who have survived with the defect would have had surgical correction performed, or had some shunt to allow for survival, and echocardiography would be able

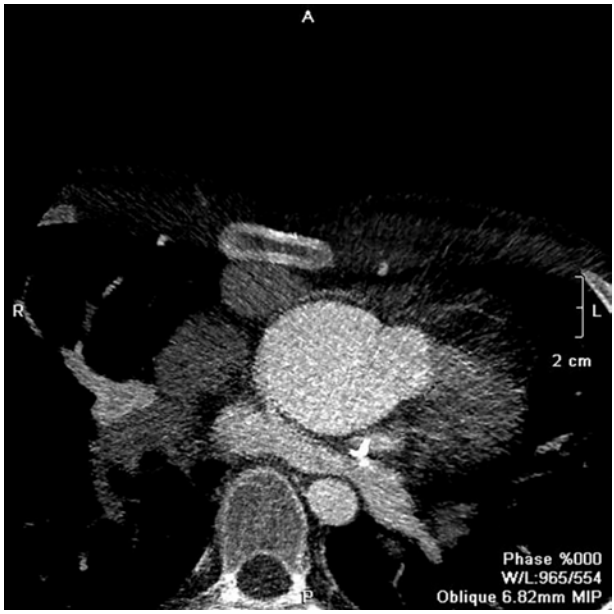

FIG. 17.8. CCT in a patient with D-TGA with arterial switch surgery requiring coronary artery translocation demonstrating narrowing of the left coronary artery as it courses between the aorta and the main pulmonary artery.

to show the native abnormalities or the components of the surgical correction. Following atrial switch, the atrial baffles can be assessed for leak or stenosis and the systemic right ventricular function should be assessed. Following arterial switch, main and branch pulmonary artery stenosis and neo-aortic root dilation and regurgitation can be assessed. Assessment of the anatomy and physiological consequence of the correction can sometimes be challenging and expertise is required to ensure that appropriate echocardiography views are obtained to visualize the atrial baffles following atrial switch and the branch pulmonary arteries following arterial switch.

CCT (see Fig. 17.8) and CMR can also demonstrate the surgical anatomy well, including atrial baffles and the branch pulmonary arteries. The coronary artery origins can also be assessed by CCT and CMR, which is important after arterial switch surgery. CMR can quantify systemic right ventricular size and function following atrial switch surgery.

Cardiac catheterization is usually employed post-surgery to assess the atrial baffles for leaks or obstruction following atrial switch and branch pulmonary artery stenosis and coronary obstruction following arterial switch. Catheter based interventions can also be performed for baffle stenosis or leaks and pulmonary artery stenosis.

As myocardial ischaemia from obstructed coronary arteries can occur following arterial switch surgery, ACHD guidelines recommend at least one assessment for coronary artery patency which can be done non-invasively [17.3]. Nuclear stress imaging for ischaemia can be employed.

17.4.11. Congenitally corrected transposition of the great arteries

Congenitally corrected transposition of the great arteries (CCTGA) (also known as L-loop TGA or physiologically corrected TGA) is characterized by atrioventricular discordance and ventriculoarterial discordance. The right ventricle acts as the systemic ventricle and frequently develops dysfunction early in life. Patients with isolated CCTGA are acyanotic, may not be diagnosed until adulthood and generally do not require surgical repairs. The majority of patients with CCTGA have associated defects including VSD, abnormal tricuspid valve and pulmonary outflow obstruction, may have symptoms or murmurs detected at younger ages and may have required intervention for the associated lesions in childhood.

TTE in expert hands should be able to demonstrate this double discordance; however, it is sometimes difficult to distinguish the ventricles or the great vessels accurately, given the abnormal ventricular position. The right ventricle can be identified by the presence of the moderator band and its association with the tricuspid valve, which is more apically displaced than the mitral valve. The

function of the systemic right ventricle, the tricuspid valve function and pulmonary stenosis and right ventricular outflow tract obstruction should be assessed.

CMR gives good structural delineation and also provides data for the systemic right ventricular and the subpulmonary left ventricular function. Most adults with CCTGA will have systemic right ventricular dysfunction. Cardiac catheterization is indicated when other forms of imaging prove equivocal. It provides functional and haemodynamic indices.

17.4.12. Ebstein's anomaly

This rare congenital defect involves an abnormal tricuspid valve and right ventricle with apical displacement of the septal tricuspid leaflet; the anterior tricuspid valve leaflet is generally large and redundant. The apical displacement of the septal and posterior tricuspid valve leaflets results in atrialization of the right ventricle. ASD and patent foramen ovale are common in Ebstein's anomaly. The wide spectrum of severity of this condition can result in foetal hydrops in the most severe form and, in milder cases, the tricuspid regurgitation can be minor, patients may not develop symptoms and may go undiagnosed until adulthood.

TTE is the imaging modality of choice for Ebstein's anomaly. It can demonstrate the size and function of the right ventricle, the distortion of the tricuspid valve, the degree of valvular stenosis or regurgitation and the presence of ASD. Post-surgical repair patients can also be assessed for residual disease, obstructions and function.

CMR and CCT offer excellent structural delineation of the right heart, and CMR can also determine haemodynamic indices. Cardiac catheterization is rarely needed, unless there are high risk patients in need of surgical repair, in which function and structural integrity is important, as in the case of older adults where knowing the coronary anatomy is essential prior to an intervention.

17.4.13. Single ventricle diseases

Single ventricle diseases are congenital, are characterized by a functioning single ventricle and encompass a plethora of defects. Such conditions are very often associated with a whole host of shunts and valvular, structural and obstructive defects. Presentation is usually in the neonatal period, with either heart failure or cyanosis, requiring quick surgical intervention. The series of surgeries generally culminates in a Fontan procedure that involves connecting the superior and inferior vena cava to the pulmonary arteries without a ventricular pumping chamber ejecting to the pulmonary arteries. A baffle is created either within the right atrium (lateral tunnel Fontan) or outside the heart involving a tube graft (extracardiac Fontan) to connect the inferior vena cava to the pulmonary

artery. The one functional ventricular pumping chamber ejects oxygenated blood through the aorta to the systemic circulation. A minute proportion may remain undiagnosed into adulthood, when symptoms progress to clinical significance.

TTE and TEE are the mainstay of imaging for single ventricle diseases. They can visualize both native and postoperative features of abnormal structure, function and shunts, and obstructions, together with haemodynamic consequences. Following Fontan, TTE can assess obstruction or leak in the Fontan baffle and ventricular and valve function.

CMR and CCT are extremely useful in complex congenital heart imaging, providing high resolution structural images in pre and postoperative patients. This is complemented by functional analysis and haemodynamic flow data obtained by CMR. The information gathered may obviate the need for initial cardiac catheterization, and also give the interventionist foresight as to how to approach interventional studies. CMR can better assess the Fontan baffle and branch pulmonary artery connection compared with TTE and can better assess for Fontan baffle leak, stenosis and Fontan thrombosis. CMR can also quantify the collateral vessel flow that frequently develops in Fontan patients.

During invasive angiography, many indices can be gathered, such as haemodynamic indices, shunts and collaterals in both preoperative and postoperative patients.

17.5. KEY MESSAGES

(1) Congenital heart disease should be considered when an imaging modality shows unusual and distorted cardiac structures. It should be noted how the great veins connect to the atria, how the atria connect to the ventricles and how the ventricles connect to the great arteries.
(2) Haemodynamic indices are vital for management. The best assessment is invasive, but echocardiography and magnetic resonance imaging are good non-invasive modalities.
(3) ACHD cases will likely benefit from more intensive imaging via true 3-D techniques for better structural appreciation, and this can be most easily achieved with low dose CCT or CMR.
(4) Appreciation of anatomy for structural congenital heart disease is required to properly interpret the various imaging modalities. Postoperative cases are even more difficult to interpret, and operative records are essential for interpretation.
(5) Specialized training in ACHD imaging is important and essential to the correct interpretation of such images.

(6) Finally, cost, expertise and availability may ultimately determine the modalities of choice for individual patients, and no available algorithm can fit all circumstances.

REFERENCES TO CHAPTER 17

[17.1] MARELLI, A.J., MACKIE, A.S., IONESCU-ITTU, R., RAHME, E., PILOTE, L., Congenital heart disease in the general population: Changing prevalence and age distribution, Circulation **115** (2007) 163–172.

[17.2] STOUT, K.K., et al., 2018 AHA/ACC guideline for the management of adults with congenital heart disease: A Report of the American College of Cardiology/American Heart Association Task Force on Clinical Practice Guidelines, Circulation **139** (2018) e698–e800.

[17.3] BHATT, A.B., et al., Congenital heart disease in the older adult: A scientific statement from the American Heart Association, Circulation **131** (2015) 1884–1931.

[17.4] SILVERSIDES, S.K., et al., Canadian Cardiovascular Society 2009 Consensus Conference on the management of adults with congenital heart disease: Complex congenital cardiac lesions, Can. J. Cardiol. **26** (2010) e98–117.

[17.5] BAUMGARTNER, H., et al., 2020 ESC guidelines for the management of adult congenital heart disease, Eur. Heart J. **42** (2020) 563–645.

[17.6] KALRA, A., SHROFF, G.R., ERLIEN, D., GILBERTSON, D.T., HERZOG, C.A., Perflutren-based echocardiographic contrast in patients with right-to-left intracardiac shunts, J. Am. Coll. Cardiol. Cardiovasc. Imag. **7** (2014) 206–207.

[17.7] HAN, B.K., et al., Computed tomography imaging in patients with congenital heart disease, Part I. Rationale and utility: An expert consensus document of the Society of Cardiovascular Computed Tomography, J. Cardiovasc. Comput. Tomogr. **9** (2015) 475–492.

[17.8] HAN, B.K., et al., Computed tomography imaging in patients with congenital heart disease, Part 2. Technical recommendations: An expert consensus document of the Society of Cardiovascular Computed Tomography, J. Cardiovasc. Comput. Tomogr. **9** (2015) 493–513.

[17.9] TAKX, R.A.P., et al., Quantification of left and right ventricular function and myocardial mass: Comparison of low-radiation dose 2nd generation dual-source CT and cardiac MRI, Eur. J. Radiol. **81** (2012) 598–604.

[17.10] KILNER, P.J., et al., Recommendations for cardiovascular magnetic resonance in adults with congenital heart disease from the respective working groups of the European Society of Cardiology, Eur. Heart J. **31** (2010) 794–805.

[17.11] PARTINGTON, S.L., VALENTE, A.M., Cardiac magnetic resonance in adults with congenital heart disease, Methodist Debakey Cardiovasc. J. **9** (2013) 156–162.

[17.12] CLARKE, C.J., GURKA, M.J., NORTON, P.T., KRAMER, C.M., HOYER, A.W., Assessment of the accuracy and reproducibility of RV volume measurements by CMR in congenital heart disease, J. Am. Coll. Cardiol. Cardiovasc. Imag. **5** (2012) 28–37.

[17.13] MOOIJ, C.F., DE WIT, C.J., GRAHAM, D.A., POWELL, A.J., GEVA, T., Reproducibility of MRI measurements of right ventricular size and function in patients with normal and dilated ventricles, J. Magn. Reson. Imag. **28** (2008) 67–73.

[17.14] CAWLEY, P.J., MAKI, J.H., OTTO, C.M., Cardiovascular magnetic resonance imaging for valvular heart disease, Circulation **119** (2009) 468–478.

[17.15] POWELL, A.J., TSAI-GOODMAN, B., PRAKASH, A., GREIL, G.F., GEVA, T., Comparison between phase-velocity cine magnetic resonance imaging and invasive oximetry for quantification of atrial shunts, Am. J. Cardiol. **91** (2003) 1523–1525.

[17.16] PARTINGTON, S.L., et al., Clinical applications of radionuclide imaging in the evaluation and management of patients with congenital heart disease, J. Nucl. Cardiol. **23** (2016) 45–63.

[17.17] NOLLERT, G., et al., Long-term results of total repair of tetralogy of Fallot in adulthood: 35 years follow-up in 104 patients corrected at the age of 18 or older, Thorac. Cardiovasc. Surg. **45** (1997) 178–181.

[17.18] GEVA, T., Repaired tetralogy of Fallot: The roles of cardiovascular magnetic resonance in evaluating pathophysiology and for pulmonary valve replacement decision support, J. Cardiovasc. Magn. Reson. **13** (2011) 9–33.

[17.19] BONNET, D., et al., Long-term fate of the coronary arteries after the arterial switch operation in newborns with transposition of the great arteries, Heart **76** (1996) 274–279.

[17.20] TANEL, R.E., WERNOVSKY, G., LANDZBERG, M.J., PERRY, S.B., BURKE, R.P., Coronary artery abnormalities detected at cardiac catheterization following the arterial switch operation for transposition of the great arteries, Am. J. Cardiol. **76** (1995) 153–157.

Chapter 18

ENDOCARDITIS

D. SOBIC SARANOVIC, G. KARTHIKEYAN, E. MILAN

Infective endocarditis is a focus of infection of the endocardial surface and native heart valve, or an infection of intracardiac prosthetic material. The latter refers to all types of prosthetic valves, intracardiac patches and shunts, annuloplasty rings and cardiac implanted electronic devices (CIEDs); these include pacemakers, implantable cardioverter defibrillators and ventricular assist devices.

18.1. EPIDEMIOLOGY AND CLINICAL PRESENTATION

The incidence of infective endocarditis is 3–10 per 100 000 people per year, and it is associated with a high in-hospital mortality (20%) [18.1–18.3]. In low income countries, rheumatic heart disease remains the major risk factor for infective endocarditis at a younger age (35–40 years), while in developed countries the most frequent risk factors are degenerative valve disease, diabetes, cancer, intravenous drug use and congenital heart disease, and infective endocarditis occurs in older patients (>60 years) [18.4, 18.5]. Infective endocarditis is more common in left sided native valves than in right sided valves. CIED and prosthetic valve endocarditis occurs in over 6% of all implantable devices, carries significant morbidity and mortality and has a substantial financial impact on the healthcare system [18.5]. Gram-positive bacteria, Staphylococcus, Streptococcus and Enterococcus are the most common causes of infective endocarditis and are found in 90% of all cases. *Staphylococcus aureus* is the most frequent [18.6]. A gram-negative bacterial or fungal infection is rare but usually fatal [18.7].

Clinical presentation of infective endocarditis is diverse and non-specific. It ranges from acute sepsis to fever of unknown origin with constitutional symptoms such as chills, poor appetite and weight loss. Infective endocarditis may also present with a complication such as heart failure, stroke, systemic embolism or metastatic infection (spondylodiscitis, vertebral osteomyelitis, metastatic abscesses) in 30% of patients [18.8–18.10]. Clinical examination typically reveals a cardiac murmur, which is present in up to 85% of patients and several associated findings such as nail splinter haemorrhages, emboli, Osler’s nodes, Janeway and Bowman lesions of the eye, Roth spots, petechiae and clubbing [18.11]. Early diagnosis, antibiotic therapy and/or surgery are

crucial for patient outcomes. Blood cultures are essential to ascertain the diagnosis of infective endocarditis, but false negative results are obtained in several clinical scenarios, especially in patients exposed to prior antibiotic therapies and in patients infected with rare and fastidious bacteria known as HACEK (Haemophilus species, Aggregatibacter species, *Cardiobacterium hominis*, *Eikenella corrodens* and Kingella species) [18.12, 18.13]. In this light, multimodality diagnostic imaging plays an essential role in the diagnosis and management of infective endocarditis.

18.2. DIAGNOSTIC IMAGING

The advantages and disadvantages of several non-invasive imaging modalities in infective endocarditis are briefly summarized in Table 18.1.

TABLE 18.1. DIAGNOSTIC PERFORMANCE OF MULTIMODALITY IMAGING IN INFECTIVE ENDOCARDITIS

Procedure	Advantages	Limitations
TTE	Widely available Easy and quick to perform Repeatable	Poor sensitivity (particularly in the presence of prosthetic material)
TEE	Widely available Easy to perform	Limited usefulness in the presence of mechanical heart valves
CT	High spatial resolution Better characterization of paravalvular complications	Radiation exposure False positive in physiological postsurgical fluid collection
MRI	High spatial resolution Excellent soft tissue characterization and valvular morphology	Time consuming Limited availability Not suitable for prosthetic valve and CIED infective endocarditis
WBC SPECT–CT	High specificity Detection of peripheral embolism Detection of infection foci after recent surgery (less than 1 month) Useful in detection of infection in CIEDs	Time consuming Blood products handling Lower spatial resolution and contrast Artefacts in SPECT–CT False negative in candida and Enterococcus infection Moderate radiation exposure

TABLE 18.1. DIAGNOSTIC PERFORMANCE OF MULTIMODALITY IMAGING IN INFECTIVE ENDOCARDITIS (cont.)

Procedure	Advantages	Limitations
^{18}F-FDG PET–CT	High spatial resolution High sensitivity Detection of peripheral embolism Detection of other sources of fever or bacteraemia in patients with CIEDs	Need for adequate preparation of patients May demonstrate residual inflammatory changes in recent surgery without infection Possible uptake in active thrombi, cardiac tumours, metastasis and foreign body reactions Possible false negative test in patients with small vegetations or prolonged antibiotic therapy Not useful for infectious brain embolisms because of high glucose metabolism in the brain Moderate radiation exposure

Note: CIED — cardiac implanted electronic device; CT — computed tomography; FDG — fluorodeoxyglucose; MRI — magnetic resonance imaging; PET — positron emission tomography; SPECT — single photon emission computed tomography; TEE — transoesophageal echocardiography; TTE — transthoracic echocardiography; WBC — white blood cells.

18.3. ECHOCARDIOGRAPHY

Echocardiography is crucial for the diagnosis, detection of cardiac complications and follow-up of infective endocarditis cases. Transthoracic echocardiography (TTE) is the method of choice in cases of suspected native or prosthetic valve infective endocarditis. For native valve infective endocarditis, TTE has 50–90% sensitivity and 90% specificity, but the sensitivity is lower (40–70%) in prosthetic valve infective endocarditis. TTE can assess ventricular function, the haemodynamic severity of valve lesions and the presence of abscesses [18.14, 18.15]. Transoesophageal echocardiography (TEE) is indicated if TTE is inconclusive, or negative but with high clinical suspicion of infective endocarditis, in cases with positive TTE findings when complications are suspected or when intracardiac devices and leads are present. For native valve infective endocarditis, the sensitivity of TEE is 90–100%, and the specificity is 90%. For prosthetic valve infective endocarditis, the pooled sensitivity is 86%

(range 77–92%) [18.14–18.16]. If TEE is negative and the clinical suspicion is still high, the use of other diagnostic imaging modalities is warranted.

18.4. MULTISLICE GATED CARDIAC COMPUTED TOMOGRAPHY

Multislice gated cardiac computed tomography (CCT) provides cross-sectional 3-D images of the valves and heart. It is more accurate than echocardiography for the detection of paravalvular complications, such as abscesses, pseudoaneurysms or fistulas. In aortic infective endocarditis, computed tomography (CT) may be used in addition to define the size, anatomy and calcification of the aortic valve, root and ascending aorta, which may inform surgical planning. In pulmonary and right sided endocarditis, CT may reveal concomitant pulmonary disease, including abscesses and infarcts. CT for the diagnosis of infective endocarditis overall has 97% sensitivity and 88% specificity. False positive multislice gated CCT findings include physiological postsurgical fluid collections, possibly interfering with infective endocarditis diagnosis. Multislice gated CCT imaging should be done within seven days of suspicion of infective endocarditis if an initial TEE is negative or inconclusive and the clinical suspicion of infective endocarditis is still high [18.17–18.19]. Multislice gated CCT can also be employed for the evaluation of coronary artery disease (CAD) in patients scheduled for surgical intervention for infective endocarditis in whom an invasive coronary angiogram may be contraindicated (i.e. large vegetations on the leaflets of the aortic valve).

18.5. CARDIAC MAGNETIC RESONANCE

Cardiac magnetic resonance (CMR) may be helpful in distinguishing infective vegetation from a tumour if there is a clinical doubt. This technique offers high spatial resolution, excellent characterization of soft tissue and valvular morphology. However, it is a time consuming procedure, with limited availability, and it is not suitable for suspected infection of CIEDs [18.20, 18.21].

Brain magnetic resonance imaging (MRI) is important for the evaluation of possible complications of infective endocarditis, such as acute ischaemic lesions, microabscesses, mycotic aneurysms and microhaemorrhages. Brain MRI allows for a better lesion characterization in patients with infective endocarditis and neurological symptoms [18.22, 18.23]. It has no impact on the diagnosis of infective endocarditis in patients with neurological symptoms, as they already have one minor Duke criterion (see Table 18.2); but MRI may influence the therapeutic strategy, particularly the timing of surgery [18.24].

TABLE 18.2. DEFINITION OF INFECTIVE ENDOCARDITIS ACCORDING TO THE MODIFIED DUKE CRITERIA

Definite infective endocarditis	Possible infective endocarditis	Not infective endocarditis
Pathological criteria: Pathological culture or histological examination of vegetation, vegetation that has embolized, or intracardiac abscess specimen Clinical criteria 2 major criteria 1 major criterion and 3 minor criteria 5 minor criteria	1 major criterion and 1 minor criterion 3 minor criteria	Definite alternate diagnosis Resolution of symptoms with antibiotic therapy for ≤4 days No evidence of infective endocarditis at surgery or autopsy, with antibiotic therapy for ≤4 days Does not meet criteria for possible infective endocarditis

18.6. NUCLEAR MOLECULAR AND FUNCTIONAL IMAGING

Both ^{18}F-fluorodeoxyglucose (FDG) positron emission tomography–computed tomography (PET–CT) and single photon emission computed tomography–computed tomography (SPECT–CT) using ^{99m}Tc-hexamethylpropyleneamine oxime (^{99m}Tc-HMPAO) labelled leukocytes are important supplementary methods in cases of suspected infective endocarditis that remain inconclusive after TEE.

18.6.1. ^{18}F-FDG PET–CT

The use of ^{18}F-FDG PET–CT in cases of suspected infective endocarditis is based on the higher accumulation of ^{18}F-FDG in infected cells or tissue where glucose metabolism is increased (activated leukocytes, monocytes, macrophages and CD4+ T lymphocytes). The sensitivity of ^{18}F-FDG PET–CT for the diagnosis of native valve infective endocarditis is 14%, for extracardiac complications except in the brain 14–100%, and the specificity is 80%. ^{18}F-FDG PET–CT has a sensitivity of 73–100% and a specificity of 71–100% for the diagnosis of prosthetic valve infective endocarditis [18.25–18.27]. For the diagnosis of cardiac device related infections (device, lead and pocket infection),

^{18}F-FDG PET–CT has 80–89% sensitivity and 86–100% specificity, which a reported 100% sensitivity and 80% specificity for infection of ventricular assist devices [18.28–18.30].

The main added value of ^{18}F-FDG PET–CT is the reduction in the rate of misdiagnosed infective endocarditis, classified in the 'possible infective endocarditis' category, which increases the sensitivity of the modified Duke score from 70% to 97% [18.24, 18.31]. In addition, whole body imaging with this technique allows the detection of infectious emboli and mycotic aneurysms. However, caution needs to be taken when interpreting ^{18}F-FDG PET–CT given the possibility of false positive and false negative findings in patients with suspected infective endocarditis. False positive results can result from recent thoracic or cardiac surgery or interventional procedures (less than two months old, because of postsurgical inflammation), recent thrombi, soft atherosclerotic plaques, vasculitis, primary cardiac tumours, cardiac metastasis from a non-cardiac tumour, and foreign body reactions or inadequate patient preparation without suppression of physiological accumulation of the radiopharmaceutical in the myocardium [18.32, 18.33]. False negative findings may result from prior antibiotic administration, small size vegetations or elevated blood glucose concentration [18.34].

An additional promising role of ^{18}F-FDG PET–CT may be to monitor the response to antimicrobial treatment in patients with established infective endocarditis. However, current data are insufficient to make a general recommendation at the time of writing.

18.6.2. SPECT–CT with labelled leukocytes

Leukocyte scintigraphy with SPECT–CT is highly specific for infection because granulocytes are recruited to the site of infection [18.35]. However, since infectious vegetations contain few granulocytes, a positive leukocyte scintigraphy could visualize granulocytes in the inflamed tissue surrounding the valve involved in infective endocarditis or those present during the resolving phase. The added value of this imaging technique has been demonstrated in cases with persisting diagnostic uncertainty in prosthetic valve infective endocarditis, and intracardiac device related, pacemaker related, and ventricular assist device related infective endocarditis [18.36]. Furthermore, leukocyte scintigraphy with SPECT–CT can detect extracardiac complications.

A positive leukocyte scintigraphy with SPECT–CT correlates with high infectious activity and predicts poor prognosis in infective endocarditis. In addition, a positive scan may reveal an abscess or perivalvular infection and indicate the need for surgical intervention. In contrast, negative scans indicate the absence of infectious activity and are consistently associated with a favourable

clinical outcome once antimicrobial therapy is initiated. Furthermore, negative scans may help to exclude extensive perivalvular infection and the need for surgery in patients with definite infective endocarditis.

The high specificity of leukocyte scintigraphy with SPECT–CT may be particularly helpful when diagnostic uncertainty remains after ^{18}F-FDG PET–CT. For patients with suspected prosthetic valve endocarditis, a sequential work-up strategy of ^{18}F-FDG PET–CT and leukocyte scintigraphy with SPECT–CT has been proposed if echocardiography is inconclusive. In this work-up, patients with negative ^{18}F-FDG PET–CT as well as those showing an intense focal ^{18}F-FDG PET–CT signal in a cardiac valve area do not need additional scanning. However, patients with low, diffuse ^{18}F-FDG PET–CT uptake around a valve prosthesis will need leukocyte scintigraphy with SPECT–CT, particularly if scanned in the first two months after cardiac surgery [18.24, 18.37]. Leukocyte scintigraphy has some limitations (laborious and demanding preparation, four patient visits required, the risk of missing small infectious foci owing to the lower spatial resolution of SPECT), whereas ^{18}F-FDG PET–CT provides better spatial resolution, improved opportunities for quantification, whole body imaging for identification of extra cardiac complications, more feasible logistics and increased comfort for patients.

18.6.3. Imaging algorithms based on clinical presentation

An integrated imaging strategy in suspected infective endocarditis is important. This is especially the case when infective endocarditis is still highly probable despite a negative TTE and TEE. Advanced imaging techniques, such as multislice gated CCT, CMR, ^{18}F-FDG PET–CT, and leukocyte scintigraphy with SPECT–CT, may help to establish an early diagnosis of infective endocarditis and detect its complications. The existing evidence justifies the addition of these diagnostic methods to the modified Duke criteria for diagnosing infective endocarditis. The proposed algorithm is in line with the existing published guidelines of the European Society of Cardiology [18.24], the American College of Cardiology, and the American Heart Association from 2014 [18.38] and 2015 [18.18] (see Figs 18.1–18.3).

The clinical diagnosis of infective endocarditis is based on the modified Duke criteria incorporated in the infective endocarditis guidelines [18.39]. Morphological and biological criteria for infective endocarditis are defined in the modified Duke criteria and are used in order to classify diagnostic probability of infective endocarditis as definite, possible or rejected (see Table 18.2).

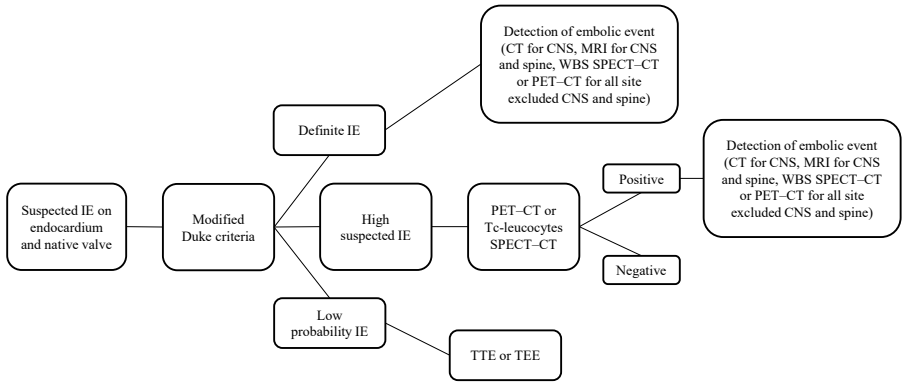

FIG. 18.1. Algorithms for native valve and endocardial infective endocarditis (IE). CT — computed tomography; CNS — central nervous system; MRI — magnetic resonance imaging; PET — positron emission tomography; SPECT — single photon emission computed tomography; TEE — transoesophageal echocardiography; TTE — transthoracic echocardiography; WBS — whole body scanning.

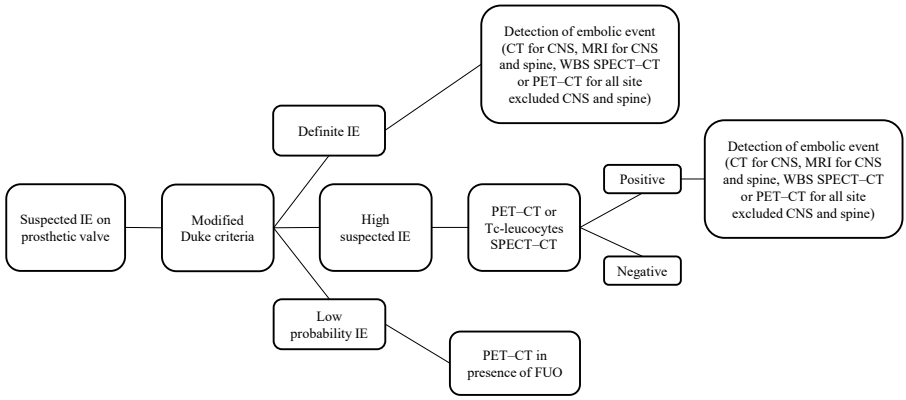

FIG. 18.2. Algorithm for infective endocarditis (IE) of prosthetic valves and CIEDs. CT — computed tomography; CNS — central nervous system; FUO — fever of unknown origin; MRI — magnetic resonance imaging; PET — positron emission tomography; SPECT — single photon emission computed tomography; WBS — whole body scanning.

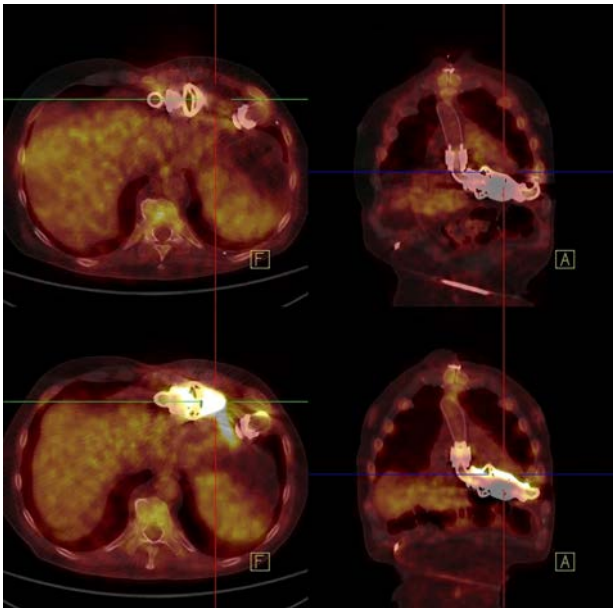

FIG. 18.3. Patients with infected ventricular assist devices. ^{18}F-FDG PET–CT baseline: high accumulation of ^{18}F-FDG in the pocket containing the ventricular assist device (bottom row). After antibiotic therapy, a follow-up ^{18}F-FDG PET–CT one year later shows no further accumulation of ^{18}F-FDG in the pocket containing the ventricular assist device (top row). (Courtesy of D. Sobic Saranovic, Clinical Center of Serbia.)

18.7. KEY MESSAGES

(1) Infective endocarditis is associated with a high morbidity and mortality worldwide.
(2) Blood cultures are essential for the correct diagnosis and treatment of endocarditis.
(3) TTE is the first-line imaging modality to diagnose infective endocarditis due to its versatility, low cost and no risk of radiation exposure.
(4) TEE is often necessary to confirm the diagnosis of infective endocarditis when this condition is suspected but TTE is negative.
(5) CT affords excellent imaging of paravalvular complications.
(6) Magnetic resonance offers high resolution images of the valve leaflets and provides accurate tissue characterization.

(7) Nuclear imaging with either SPECT or PET allows the detection of inflammatory cardiac foci, infected pulse generator pockets, and vegetations of infective endocarditis adherent on implanted cardiac devices not otherwise detectable with other imaging techniques.

REFERENCES TO CHAPTER 18

[18.1] PANT, S., et al., Trends in infective endocarditis incidence, microbiology, and valve replacement in the United States from 2000 to 2011, J. Am. Coll. Cardiol. **65** (2015) 2070–2076.

[18.2] DAYER, M.J., et al., Incidence of infective endocarditis in England, 2000–13: A secular trend, interrupted time-series analysis, Lancet **385** (2015) 1219–1228.

[18.3] THUNY, F., et al., Excess mortality and morbidity in patients surviving infective endocarditis, Am. Heart J. **164** (2012) 94–101.

[18.4] SECKELER, M.D., HOKE, T.R., The worldwide epidemiology of acute rheumatic fever and rheumatic heart disease, Clin. Epidemiol. **3** (2011) 67–84.

[18.5] HOEN, B., DUVAL, X., Clinical practice: Infective endocarditis, N. Engl. J. Med. **368** (2013) 1425–1433.

[18.6] FOWLER, V.G., Jr., et al., *Staphylococcus aureus* endocarditis: A consequence of medical progress, JAMA **293** (2005) 3012–3021.

[18.7] MOREILLON, P., QUE, Y.-A., Infective endocarditis, Lancet **363** (2004) 139–149.

[18.8] DURANTE-MANGONI, E., et al., Current features on infective endocarditis in elderly patients: Results of the International Collaboration on Endocarditis Prospective Cohort Study, Arch. Intern. Med. **168** (2008) 2095–2103.

[18.9] CAHILL, T.J., PRENDERGAST, B.D., Infective endocarditis, Lancet **387** (2016) 882–893.

[18.10] THUNY, F., et al., Risk of embolism and death in infective endocarditis: Prognostic value of echocardiography: A prospective multicenter study, Circulation **112** (2005) 69–75.

[18.11] SILVERMAN, M.E., UPSHAW, C.B., Jr., Extracardiac manifestations of infective endocarditis and their historical descriptions, Am. J. Cardiol. **100** (2007) 1802–1807.

[18.12] LEE, A., MIRRETT, S., RELLER, L.B., WEINSTEIN, M.P., Detection of bloodstream infections in adults: How many blood cultures are needed? J. Clin. Microbiol. **45** (2007) 3546–3548.

[18.13] RIEDEL, S., et al., Timing of specimen collection for blood cultures from febrile patients with bacteremia, J. Clin. Microbiol. **46** (2008) 1381–1385.

[18.14] HABIB, G., et al., Recommendations for the practice of echocardiography in infective endocarditis, Eur. J. Echocardiogr. **11** (2010) 202–219.

[18.15] VIEIRA, M.L.C., GRINBERG, M., POMERANTZEFF, P.M.A., ANDRADE, J.L., MANSUR, A.J., Repeated echocardiographic examinations of patients with suspected infective endocarditis, Heart **90** (2004) 1020–1024.

[18.16] DE CASTRO, S., et al., Diagnostic accuracy of transthoracic and multiplane transesophageal echocardiography for valvular perforation in acute infective endocarditis: correlation with anatomic findings, Clin. Infect. Dis. **30** (2000) 825–826.

[18.17] FEUCHTNER, G.M., et al., Multislice computed tomography in infective endocarditis: Comparison with transesophageal echocardiography and intraoperative findings, J. Am. Coll. Cardiol. **53** (2009) 436–444.

[18.18] BADDOUR, L.M., et al., Infective endocarditis in adults: Diagnosis, antimicrobial therapy, and management of complications: A scientific statement for healthcare professionals from the American Heart Association, Circulation **132** (2015) 1435–1486.

[18.19] ENTRIKIN, D.W., PUSHPENDER, G., KON, N.D., CARR, J.J., Imaging of infective endocarditis with cardiac CT angiography, J. Cardiovasc. Comput. Tomogr. **6** (2012) 399–405.

[18.20] PAZOS-LÓPEZ, P., et al., Value of CMR for the differential diagnosis of cardiac masses, J. Am. Coll. Cardiol. Cardiovasc. Imag. **7** (2014) 896–905.

[18.21] KRISHNAMURTHY, R., CHEONG, B., MUTHUPILLAI, R., Tools for cardiovascular magnetic resonance imaging, Cardiovasc. Diagn. Ther. **4** (2014) 104–125.

[18.22] DUVAL, X., et al., Effect of early cerebral magnetic resonance imaging on clinical decisions in infective endocarditis: A prospective study, Ann. Intern. Med. **152** (2010) 497–504.

[18.23] HESS, A., et al., Brain MRI findings in neurologically asymptomatic patients with infective endocarditis, Am. J. Neuroradiol. **34** (2013) 1579–1584.

[18.24] HABIB, G., et al., 2015 ESC guidelines for the management of infective endocarditis, Eur. Heart J. **36** (2015) 3075–3123.

[18.25] SALOMÄKI, S.P., et al., ^{18}F-FDG positron emission tomography/computed tomography in infective endocarditis, J. Nucl. Cardiol. 24 (2017) 195–206.

[18.26] KOUIJZER, I.J.E., The value of ^{18}F-FDG PET/CT in diagnosing infectious endocarditis, Eur. J. Nucl. Med. Mol. Imag. **40** (2013) 1102–1107.

[18.27] VAN RIET, J., et al., ^{18}F-FDG PET/CT for early detection of embolism and metastatic infection in patients with infective endocarditis, Eur. J. Nucl. Med. Mol. Imag. **37** (2010) 1189–1197.

[18.28] PETROVIC, J., SOBIC-SARANOVIC, D., TRIFUNOVIC, D., DRASKOVIC, D., IVANOVIC, B., Unexpected and unique ^{18}F-FDG PET/CT finding in a patient with prosthetic valves and septicaemia, Eur. Heart J. Cardiovasc. Imag. **20** (2019) 1181.

[18.29] LANCELLOTTI, P., HABIB, G., OURY, C., NCHIMI, A., Positron emission tomography/computed tomography imaging in device infective endocarditis: Ready for prime time, Circulation **132** (2015) 1076–1080.

[18.30] GRAZIOSI, M., et al., Role of ^{18}F-FDG PET/CT in the diagnosis of infective endocarditis in patients with an implanted cardiac device: A prospective study, Eur. J. Nucl. Med. Mol. Imag. **41** (2014) 1617–1623.

[18.31] TLILI, G., et al., High performances of ^{18}F-fluorodeoxyglucose PET–CT in cardiac implantable device infections: A study of 40 patients, J. Nucl. Cardiol. **22** (2015) 787–798.

[18.32] ŠAPONJSKI, J., et al., The detection of endocarditis, post implantation grafts, arteritis and other related disorders by ^{18}F-FDG PET/CT, Hell. J. Nucl. Med. Suppl. **20** (2017) S37–S44.

[18.33] GOMES, A., et al., Diagnostic value of imaging in infective endocarditis: A systemic review, Lancet Infect. Dis. **17** (2017) 1–14.

[18.34] SARRAZIN, J.-F., et al., Usefulness of fluorine-18 positron emission tomography/computed tomography for identification of cardiovascular implantable electronic device infections, J. Am. Coll. Cardiol. **59** (2012) 1616–1625.

[18.35] ERBA, P.A., et al., Image acquisition and interpretation criteria for ^{99m}Tc-HMPAO-labelled white blood cell scintigraphy: Results of a multicentre study, Eur. J. Nucl. Med. Mol. Imag. **41** (2014) 615–623.

[18.36] ERBA, P.A., et al., Radiolabeled WBC scintigraphy in the diagnostic workup of patients with suspected device-related infections, J. Am. Coll. Cardiol. Cardiovasc. Imag. **6** (2013) 1075–1086.

[18.37] ERBA, P.A., et al., Added value of ^{99m}Tc-HMPAO-labeled leukocyte SPECT/CT in the characterization and management of patients with infectious endocarditis, J. Nucl. Med. **53** (2012) 1235–1243.

[18.38] NISHIMURA, R.A., et al., 2014 AHA/ACC guideline for the management of patients with valvular heart disease: Executive summary, J. Am. Coll. Cardiol. **63** (2014) 2438–2388.

[18.39] LI, J.S., et al., Proposed modifications to the Duke criteria for the diagnosis of infective endocarditis, Clin. Infect. Dis. **30** (2000) 633–638.

BIBLIOGRAPHY TO CHAPTER 18

AHMED, F.Z., et al., Early diagnosis of cardiac implantable electronic device generator pocket infection using ^{18}F-FDG PET/CT, Eur. Heart J. Cardiovasc. Imag. **16** (2015) 521–530.

BRUUN, N.E., HABIB, G., THUNY, F., SOGAARD, P., Cardiac imaging in infectious endocarditis, Eur. Heart J. **35** (2014) 624–632.

CAHILL, T.J., et al., Challenges in infective endocarditis, J. Am. Coll. Cardiol. **69** (2017) 325–344.

ERBA, P.A., et al., Recommendations on nuclear and multimodality imaging in IE and CIED infections, Eur. J. Nucl. Med. Mol. Imag. **45** (2018) 1795–1815.

IUNG, B., ERBA, P.A., PETROSILLO, N., LAZZERI, E., Common diagnostic flowcharts in infective endocarditis, Q. J. Nucl. Med. Mol. Imag. **58** (2014) 55–65.

JAMAR, F., et al., EANM/SNMMI guideline for ^{18}F-FDG use in inflammation and infection, J. Nucl. Med. **54** (2013) 647–658.

JUNEAU, D., et al., Positron emission tomography and single-photon emission computed tomography imaging in the diagnosis of cardiac implantable electronic device infection, Circ. Cardiovasc. Imag. **10** (2017).

MILLAR, B.C., PRENDERGAST, B.D., ALAVI, A., MOORE, J.E., ^{18}FDG-positron emission tomography (PET) has a role to play in the diagnosis and therapy of infective endocarditis and cardiac device infection, Int. J. Cardiol. **167** (2013) 1724–1736.

SARRZIN, J.-F., PHILIPPON, F., TROTTIER, M., TESSIER, M., Role of radionuclide imaging for diagnosis of device and prosthetic valve infections, World J. Cardiol. **8** (2016) 534–546.

TRAYKOV, V., et al., Clinical practice and implementation of guidelines for the prevention, diagnosis and management of cardiac implantable electronic device infections: Results of a worldwide survey under the auspices of the European Heart Rhythm Association, Europace **8** (2019) 1270–1279.

Chapter 19

IMAGING CORONARY ATHEROSCLEROSIS WITH COMPUTED TOMOGRAPHY AND POSITRON EMISSION TOMOGRAPHY

P. RAGGI, E. ALEXANDERSON, L.J. SHAW

The application of cardiovascular imaging has expanded to include the search for unstable plaques at high risk of rupturing and causing acute coronary events. A vulnerable plaque has been described histologically as a plaque with a large lipid core covered by a thin fibrous cap, microcalcifications as opposed to large calcified plates, and inflammatory cell infiltration at the margins of the plaque. Several of these components of the atherosclerotic plaque can be visualized and quantified by means of molecular imaging. In addition, it has recently become apparent that plaques exhibiting characteristics of vulnerability may be associated with inducible myocardial ischaemia even in the absence of luminal obstruction. This chapter reviews the application of positron emission tomography (PET) and computed tomography (CT) for anatomical and functional imaging of coronary atherosclerosis.

19.1. MOLECULAR IMAGING

Cardiovascular imaging modalities in pursuit of vulnerable atherosclerotic plaques were developed in an attempt to obtain information that may help to predict an event. To date, this important aim has been achieved only partially, but it has not deterred investigators from continuing to search for the vulnerable patient. A vulnerable patient not only harbours high risk plaques but also hosts a vulnerable blood (i.e. propensity to thromboembolism), a vulnerable myocardium (i.e. propensity to arrhythmias and accelerated apoptosis) and — potentially — a vulnerable nervous system (enhanced sympathetic drive, enhanced myocardial susceptibility to mental stimuli) [19.1]. Hence, the search for vulnerable or high risk plaques is only an aspect of a more complex search for the substrate responsible for catastrophic events.

Molecular imaging with PET allows investigators to image some of the components of a high risk plaque. PET tracers are either ^{18}F based, such as ^{18}F-fluorodeoxyglucose (FDG) and sodium fluoride (^{18}F-NaF), or ^{68}Ga based, such as ^{68}Ga-DOTA-TATE and ^{68}Ga-DOT.

^{18}F-FDG is a glucose analogue actively taken up by cells with a high metabolic rate and it has been used extensively to identify vascular inflammation.

In initial experiments, ^{18}F-FDG uptake was thought to be restricted to metabolically active macrophages within the plaque [19.2]. More recently, however, it has been shown that smooth muscle cells and endothelial cells also demonstrate an increased uptake of ^{18}F-FDG in inflamed atherosclerotic plaques [19.3].

An inherent limitation of ^{18}F-FDG use for coronary artery imaging is the preferential uptake by the myocardium that clouds the uptake by the much smaller coronary vessels. To maximize uptake of ^{18}F-FDG by all metabolically active cells within atherosclerotic plaques, patients are asked to fast or follow a low carbohydrate or a high lipid diet for 12–24 hours before imaging. A euglycemic hyperinsulinaemic clamp at times is utilized to optimize uptake of ^{18}F-FDG. Retrospective and observational studies showed an association between arterial ^{18}F-FDG uptake and adverse events [19.4, 19.5]. High ^{18}F-FDG uptake was demonstrated in the aorta and carotid arteries in patients with metabolic syndrome and diabetes [19.6–19.8], and regression of ^{18}F-FDG uptake was shown after treatment with statins [19.9, 19.10] and pioglitazone [19.11, 19.12]. Most data were acquired in large size arteries owing to the competing myocardial uptake of ^{18}F-FDG. In two small studies, the investigators were able to demonstrate a change in ^{18}F-FDG uptake limited to the left main coronary artery trunk that is easier to isolate from the myocardium than the rest of the coronary tree [19.12, 19.13].

Numerous reports have clearly shown that coronary artery calcium (CAC) is an excellent marker of risk [19.14, 19.15]. However, CAC provides static information on the condition of coronary artery plaques, and nascent plaques may behave differently from stable plaques where CAC is a representation of healed disease. ^{18}F-NaF has been in use for a long time to image bone metastases [19.16], but it was only recently reported as a useful tracer to image atherosclerosis. ^{18}F-NaF accumulates in plaques accruing calcium apatite and all nascent plaques accrue microcalcifications that may evolve into larger deposits. Owing to its main application, preliminary reports of ^{18}F-NaF as an atherosclerosis imaging agent issued from oncological observations. In 75 patients submitted to whole body imaging, 10–12% of large artery (aorta, carotid and femoral arteries) calcifications showed active ^{18}F-NaF uptake [19.17]. In a subsequent study, Morbelli et al. [19.18] show that there is a poor correlation between large artery calcification and ^{18}F-NaF uptake that is better correlated with risk factors for atherosclerosis. In addition, in 45 oncological patients where large artery uptake of ^{18}F-FDG and ^{18}F-NaF was compared, Derlin et al. [19.19] find a poor correlation between tracers with a coincident uptake of ^{18}F-NaF and ^{18}F-FDG in only 6.5% of the vascular sites. Hence, these ^{18}F based tracers identify different pathological processes that do not necessarily co-exist. They also demonstrate different imaging characteristics; in an initial report, coronary artery uptake of

^{18}F-FDG could not be assessed in 50% of 119 volunteers, of whom 40 had had a prior cardiovascular or cerebrovascular history, owing to myocardial spillover of ^{18}F-FDG despite a day of carbohydrate free, high fat diet [19.20]. In contrast, ^{18}F-NaF uptake was quantifiable in 96% of the coronary arteries, and it showed a modest correlation (r = 0.65) with CAC. Interestingly, 41% of patients with severe calcification showed no ^{18}F-NaF activity, suggesting that large calcium deposits may hide inactive atherosclerotic processes. Conversely, ^{18}F-NaF uptake may occur in non-calcified areas pointing at the presence of microcalcification within developing atherosclerotic plaques. Density of calcified plaques has been found to be inversely correlated with the uptake of ^{18}F-NaF [19.21], and plaques with features of instability on coronary computed tomography angiography (CCTA) (partially calcified plaques, with positive remodelling, large lipid cores and microcalcifications) had the highest ^{18}F-NaF uptake [19.22]. This suggests that ^{18}F-NaF imaging may be a valuable tool to identify patients harbouring plaques with potential for rupture and acute coronary events.

The initial proof that ^{18}F-NaF could identify patients with vulnerable plaques was provided in a study that involved patients with either acute coronary syndromes (ACSs), stable angina or undergoing carotid endarterectomy [19.23]. In that study, ^{18}F-NaF localized preferentially in culprit arteries of patients with ACSs and in ruptured carotid artery plaques of patients with cerebrovascular events. A similar finding was reported in two subsequent publications of patients with stroke or transient ischaemic attacks [19.24, 19.25].

These preliminary data support the notion that ^{18}F-NaF can identify unstable plaques in patients with active cardiovascular syndromes. However, they do not yet prove that this tracer may be useful to predict events in asymptomatic patients, nor do they show any evidence of the prognostic utility of this tracer. In an initial pursuit of this quest, researchers investigated the prevalence of plaques with high uptake of ^{18}F-NaF in patients at risk of events based on their clinical profile. Raggi et al. [19.26] submitted 88 ambulatory, asymptomatic patients with diabetes mellitus and several concomitant risk factors to ^{18}F-NaF imaging. They report a surprisingly low prevalence of coronary artery uptake of 15%, despite a high prevalence of CAC and a median haemoglobin A1c of 7.5%. In a study of 98 patients living with HIV, the prevalence of coronary ^{18}F-FDG uptake was compared to that of ^{18}F-NaF [19.27]. Interestingly, the prevalence of coronary artery uptake of ^{18}F-NaF and ^{18}F-FDG was substantially higher compared to that of ambulatory patients with diabetes described above (78% and 19%, respectively), suggesting that patients with HIV have a large burden of active disease. However, the proportion of patients with low and high risk that exhibited uptake of either ^{18}F based tracer was similar, stressing the frequently noted discordance between clinical and imaging data: several high risk patients did not show uptake, while several low risk patients did. ^{68}Ga-DOT is a PET tracer with high affinity for the

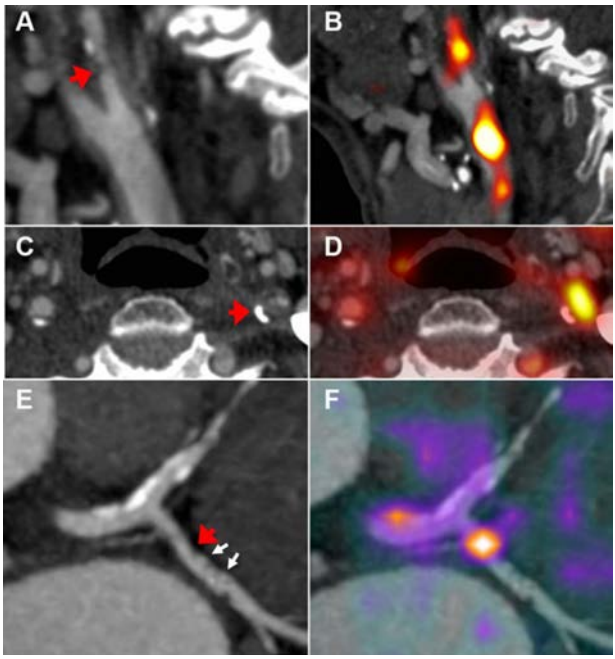

FIG. 19.1. Examples of PET molecular imaging of atherosclerosis. Sagittal (A) and axial (C) CT angiographic views showing a plaque in the left internal carotid stenosis (red arrows). Fused sagittal (B) and axial (D) PET–CT images, showing high uptake of ^{18}F-FDG in the carotid artery of this symptomatic patient. (E) CCTA showing calcification in the left anterior coronary artery (bright signal at the bifurcation with the circumflex coronary artery) and only mild luminal disease in the left circumflex coronary artery (red arrow) with spotty calcification (white arrows). (F) Fused ^{68}Ga-DOTA-TATE PET–CT showing high uptake in plaque visualized in the left circumflex coronary artery. Source: fig. 4 of Ref. [19.29].

somatostatin receptor type 2 expressed on the surface of activated macrophages. In a recent publication, Tarkin et al. [19.28] report that ^{68}Ga-DOT preferentially accumulates in the culprit vessel of patients with ACSs, and in plaques with high risk features in patients with stable coronary artery disease (CAD). The uptake of ^{68}Ga-DOT was directly proportional to the risk profile of the patients investigated. Of interest, the uptake of ^{68}Ga-DOT was lower in patients taking high intensity statins, suggesting that these drugs have an anti-inflammatory activity at the plaque level. Representative examples of molecular imaging of active atherosclerotic disease are shown in Figs 19.1 and 19.2.

There are currently several limitations to the implementation of molecular imaging for risk stratification:

(a) The discordance between clinical and imaging data renders the task of identifying patients that should be submitted to imaging exceedingly difficult.
(b) There are no internationally accepted reporting standards to differentiate high from low risk patients based on imaging findings.
(c) Although lower than for other types of nuclear based imaging test currently in use, the radiation dose is not negligeable.
(d) The cost of the equipment is high and its availability limited.
(e) The identification of a single unstable or vulnerable plaque may be insufficient to predict the occurrence of an event since plaques may rupture or fissure but then repair in a dynamic and constantly changing pattern. Therefore, an assessment of the global burden of disease rather than the identification of a single unstable plaque may be more helpful to assess with greater certainty the level of risk.
(f) Most importantly, there has been no published data to show that plaque imaging has prognostic benefit over and above simple markers of overall plaque burden such as CAC. Therefore, despite the exciting recent developments we are still in the developmental phase of this new era of cardiovascular 'imaging for prevention'.

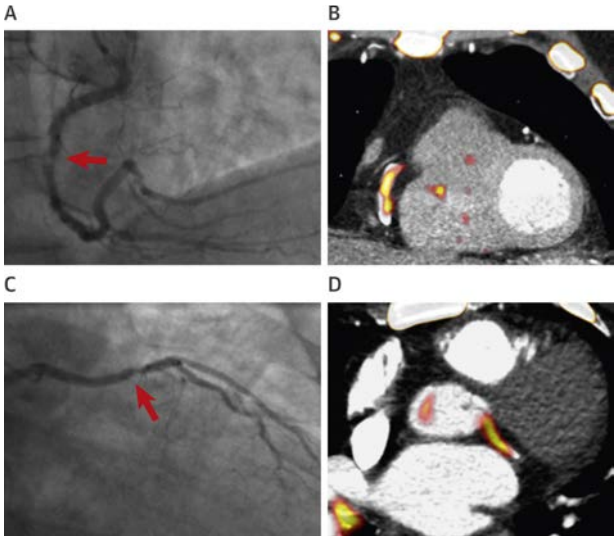

FIG. 19.2. Two examples of patients suffering an ACS. Culprit lesions in the right (A) and circumflex (C) coronary artery on invasive angiography. (B) and (D) show the fused CT and invasive angiography studies with intense uptake of ^{18}F-NaF in the respective culprit lesions. Source: fig. 5 of Ref. [19.30].

19.2. PLAQUE FEATURES ON CCTA THAT PREDICT OUTCOME AND MYOCARDIAL ISCHAEMIA

There is a large body of evidence that demonstrates the high sensitivity and excellent negative predictive value of CCTA to rule out obstructive CAD [19.31]. However, beyond its utility to diagnose obstructive CAD, CCTA is emerging as a technique to identify the presence and of non-obstructive coronary artery lesions carrying prognostic information [19.32, 19.33]. Using intravascular ultrasound, investigators demonstrated that CCTA can assess plaque features with good to excellent accuracy [19.34]. The characteristics that define a high risk plaque on CCTA include positive (i.e. outward) vessel remodelling, low attenuation (i.e. density of <30–50 HU), spotty calcifications and napkin ring sign (necrotic core in the context of the plaque). These features provide prognostic information beyond the degree of stenosis [19.35, 19.36]. Using CCTA for suspected CAD, it has been shown that positive vessel remodelling and low CT attenuation plaques were independently associated with the risk of future ACSs, and provided incremental prognostic information beyond clinical characteristics and luminal stenosis [19.37]. In the Rule Out Myocardial Infarction/Ischaemia Using Computer Assisted Tomography II (ROMICAT II) trial [19.38], both luminal stenosis of >50% (relative risk of 34.4) and high risk plaque features were associated with a significant risk of ACS (relative risk of 32.0). After multivariable adjustment, high risk plaque features remained independently associated with risk of events. High risk features were also associated with an increased risk of events in patients with isolated non-obstructive (<50%) CAD [19.37]. Further evidence of the prognostic utility of plaque features identified by CCTA were provided by the recent subanalysis of randomized trials [19.39, 19.40].

Interestingly, plaque characteristics have also been shown to be predictive of the inducibility of myocardial ischaemia [19.41]. In an early observation, myocardial ischaemia on single photon emission computed tomography (SPECT) imaging was associated with the number of plaques with mixed features (calcified and non-calcified areas) on CCTA (odds ratio, OR 1.64, $p = 0.01$) [19.42]. Several subsequent publications confirmed that plaque features (mainly positive vessel remodelling and low CT attenuation plaques) are associated with either inducible myocardial ischaemia on PET [19.42, 19.43] or abnormal fractional flow reserve measured either invasively [19.35, 19.42, 19.44] or non-invasively on CCTA [19.44–19.46]. Local oxidative stress and endothelial dysfunction may predispose to the development of myocardial ischaemia in the absence of obstructive disease remains as shown in animal laboratory experiments [19.47].

These novel findings raise an important concern as to the appropriate way to approach treatment in patients with non-obstructive lesions that nevertheless induce ischaemia: should they be submitted to revascularization? Or should

medical preventive therapies alone be intensified? And even before posing these questions, is CCTA reliable, reproducible and sufficiently available to start basing assumptions and treatment options on the results of this test?

The introduction of dual energy CT may represent an important advancement in the ability to further characterize coronary artery plaques. In fact, it is expected that dual energy CT will help to differentiate lipid rich and fibrous non-calcified plaques, which often show an overlapping density profile [19.48]. The utilization of two energy sources in dual energy CT should achieve better material decomposition (i.e. differentiation of different tissues), with improved plaque characterization.

19.3. KEY MESSAGES

(1) Molecular imaging will likely contribute to our understanding of the role of inflammation and other markers of plaque instability to the prognosis of patients at risk.
(2) CCTA is highly sensitive to establish the diagnosis of obstructive CAD.
(3) In addition, there is a growing role for CCTA in the identification of high risk plaque features that are associated with future risk of an ACS.
(4) Ongoing research developments show that anatomical findings may be a good marker of physiologically important limitation of myocardial perfusion. These measures may eventually help to fully comprehend a patient's clinical risk.

REFERENCES TO CHAPTER 19

[19.1] NAGHAVI, M., et al., From vulnerable plaque to vulnerable patient: A call for new definitions and risk assessment strategies: Part I, Circulation **108** (2003) 1664–1672.

[19.2] RUDD, J.H., et al., Imaging atherosclerotic plaque inflammation with [^{18}F]-fluorodeoxyglucose positron emission tomography, Circulation **105** (2002) 2708–2711.

[19.3] FOLCO, E.J., et al., Hypoxia but not inflammation augments glucose uptake in human macrophages: Implications for imaging atherosclerosis with ^{18}fluorine-labeled 2-deoxy-D-glucose positron emission tomography, J. Am. Coll. Cardiol. **58** (2011) 603–614.

[19.4] FIGUEROA, A.L., et al., Measurement of arterial activity on routine FDG PET/CT images improves prediction of risk of future CV events, J. Am. Coll. Cardiol. Cardiovasc. Imag. **6** (2013) 1250–1259.

[19.5] MARNANE, M., et al., Carotid plaque inflammation on ^{18}F-fluorodeoxyglucose positron emission tomography predicts early stroke recurrence, Ann. Neurol. **71** (2012) 709–718.

[19.6] TAHARA, N., et al., Vascular inflammation evaluated by [^{18}F]-fluorodeoxyglucose positron emission tomography is associated with the metabolic syndrome, J. Am. Coll. Cardiol. **49** (2007) 1533–1539.

[19.7] KIM, T.N., et al., Vascular inflammation in patients with impaired glucose tolerance and type 2 diabetes: Analysis with ^{18}F-fluorodeoxyglucose positron emission tomography, Circ. Cardiovasc. Imag. **3** (2010) 142–148.

[19.8] TAHARA, N., et al., Positive association between serum level of glyceraldehyde-derived advanced glycation end products and vascular inflammation evaluated by [^{18}F]fluorodeoxyglucose positron emission tomography, Diabetes Care **35** (2012) 2618–2625.

[19.9] TAHARA, N., et al., Simvastatin attenuates plaque inflammation: Evaluation by fluorodeoxyglucose positron emission tomography, J. Am. Coll. Cardiol. **48** (2006) 1825–1831.

[19.10] ISHII, H., et al., Comparison of atorvastatin 5 and 20 mg/d for reducing F-18 fluorodeoxyglucose uptake in atherosclerotic plaques on positron emission tomography/computed tomography: A randomized, investigator-blinded, open-label, 6-month study in Japanese adults scheduled for percutaneous coronary intervention, Clin. Ther. **32** (2010) 2337–2347.

[19.11] MIZOGUCHI, M., et al., Pioglitazone attenuates atherosclerotic plaque inflammation in patients with impaired glucose tolerance or diabetes a prospective, randomized, comparator-controlled study using serial FDG PET/CT imaging study of carotid artery and ascending aorta, J. Am. Coll. Cardiol. Cardiovasc. Imag. **4** (2011) 1110–1118.

[19.12] NITTA, Y., et al., Pioglitazone decreases coronary artery inflammation in impaired glucose tolerance and diabetes mellitus: Evaluation by FDG-PET/CT imaging, J. Am. Coll. Cardiol. Cardiovasc. Imag. **6** (2013) 1172–1182.

[19.13] SINGH, P., et al., Coronary plaque morphology and the anti-inflammatory impact of atorvastatin, Circ. Cardiovasc. Imag. **9** (2016).

[19.14] POLONSKY, T.S., et al., Coronary artery calcium score and risk classification for coronary heart disease prediction, JAMA **303** (2010) 1610–1616.

[19.15] YEBOAH, J., et al., Comparison of novel risk markers for improvement in cardiovascular risk assessment in intermediate-risk individuals, JAMA **308** (2012) 788–795.

[19.16] BLAU, M., GANATRA, R., BENDER, M.A., ^{18}F-fluoride for bone imaging, Semin. Nucl. Med. **2** (1972) 31–37.

[19.17] DERLIN, T., et al., Feasibility of ^{18}F-sodium fluoride PET/CT for imaging of atherosclerotic plaque, J. Nucl. Med. **51** (2010) 862–865.

[19.18] MORBELLI, S., et al., Divergent determinants of ^{18}F-NaF uptake and visible calcium deposition in large arteries: Relationship with Framingham Risk Score, Int. J. Cardiovasc. Imag. **30** (2014) 439–447.

[19.19] DERLIN, T., et al., Correlation of inflammation assessed by ^{18}F-FDG PET, active mineral deposition assessed by ^{18}F-fluoride PET, and vascular calcification in atherosclerotic plaque: A dual-tracer PET/CT study, J. Nucl. Med. **52** (2011) 1020–1027.

[19.20] DWECK, M.R., et al., Coronary arterial ^{18}F-sodium fluoride uptake, J. Am. Coll. Cardiol. **59** (2012) 1539–1548.

[19.21] FIZ, F., et al., ^{18}F-NaF uptake by atherosclerotic plaque on PET/CT imaging: Inverse correlation between calcification density and mineral metabolic activity, J. Nucl. Med. **56** (2015) 1019–1023.

[19.22] KITAGAWA, T., et al., ^{18}F-sodium fluoride positron emission tomography for molecular imaging of coronary atherosclerosis based on computed tomography analysis, Atherosclerosis **263** (2017) 385–392.

[19.23] JOSHI, N.V., et al., ^{18}F-fluoride positron emission tomography for identification of ruptured and high-risk coronary atherosclerotic plaques: A prospective clinical trial, Lancet **383** (2014) 705–713.

[19.24] COCKER, M.S., et al., [^{18}F]-NaF PET/CT identifies active calcification in carotid plaque, J. Am. Coll. Cardiol. Cardiovasc. Imag. **10** (2017) 486–468.

[19.25] VESEY, A.T., et al., ^{18}F-fluoride and ^{18}F-fluorodeoxyglucose positron emission tomography after transient ischemic attack or minor ischemic stroke, Circ. Cardiovasc. Imag. **10** (2017).

[19.26] RAGGI, P., et al., ^{18}F-Sodium fluoride imaging of coronary atherosclerosis in ambulatory patients with diabetes mellitus, Arterioscler. Thromb. Vasc. Biol. **39** (2019) 276–284.

[19.27] GUARALDI, G., et al., ^{18}Fluoride-based molecular imaging of coronary atherosclerosis in HIV infected patient, Atherosclerosis **297** (2020) 127–135.

[19.28] TARKIN, J.M., et al., Detection of atherosclerotic inflammation by ^{68}Ga-DOTATATE PET compared to [^{18}F]FDG PET imaging, J. Am. Coll. Cardiol. **69** (2017) 1774–1791.

[19.29] TARKIN, J.M., et al., Imaging atherosclerosis, Circ. Res. **118** (2016) 750–769.

[19.30] DAGHEM, M., BING, R., FAYAD, Z.A., DWECK, M.R., Noninvasive imaging to assess atherosclerotic plaque composition and disease activity: Coronary and carotid applications, J. Am. Coll. Cardiol. Cardiovasc. Imag. **13** (2020) 1055–1068.

[19.31] STEIN, P.D., YAEKOUB, A.Y., MATTA, F., SOSTMAN, H.D., 64-slice CT for diagnosis of coronary artery disease: A systematic review, Am. J. Med. **121** (2008) 715–725.

[19.32] MIN, J.K., et al., Prognostic value of multidetector coronary computed tomographic angiography for prediction of all-cause mortality, J. Am. Coll. Cardiol. **50** (2007) 1161–1170.

[19.33] MIN, J.K., et al., Age- and sex-related differences in all-cause mortality risk based on coronary computed tomography angiography findings results from the international multicenter CONFIRM (Coronary CT Angiography Evaluation for Clinical Outcomes: An international multicenter registry) of 23,854 patients without known coronary artery disease, J. Am. Coll. Cardiol. **58** (2011) 849–860.

[19.34] PUNDZIUTE, G., et al., Head-to-head comparison of coronary plaque evaluation between multislice computed tomography and intravascular ultrasound radiofrequency data analysis, J. Am. Coll. Cardiol. Cardiovasc. Interv. **1** (2008) 176–182.

[19.35] MOTOYAMA, S., et al., Computed tomographic angiography characteristics of atherosclerotic plaques subsequently resulting in acute coronary syndrome, J. Am. Coll. Cardiol. **54** (2009) 49–57.

[19.36] OTSUKA, K., et al., Napkin-ring sign on coronary CT angiography for the prediction of acute coronary syndrome, J. Am. Coll. Cardiol. Cardiovasc. Imag. **6** (2013) 448–457.

[19.37] MOTOYAMA, S., et al., Plaque characterization by coronary computed tomography angiography and the likelihood of acute coronary events in mid-term follow-up, J. Am. Coll. Cardiol. **66** (2015) 337–346.

[19.38] PUCHNER, S.B., et al., High-risk plaque detected on coronary CT angiography predicts acute coronary syndromes independent of significant stenosis in acute chest pain: Results from the ROMICAT-II trial, J. Am. Coll. Cardiol. **64** (2014) 684–692.

[19.39] WILLIAMS, M.C., et al., Coronary artery plaque characteristics associated with adverse outcomes in the SCOT-HEART study, J. Am. Coll. Cardiol. **73** (2019) 291–301.

[19.40] FERENCIK, M., et al., Use of high-risk coronary atherosclerotic plaque detection for risk stratification of patients with stable chest pain: A secondary analysis of the PROMISE randomized clinical trial, JAMA Cardiol. **3** (2018) 144–152.

[19.41] CONTE, E., et al., Evaluation of coronary plaque characteristics with coronary computed tomography angiography in patients with non-obstructive coronary artery disease: A long-term follow-up study, Eur Heart J. Cardiovasc. Imag. **18** (2017) 1170–1178.

[19.42] LIN, F., et al., Multidetector computed tomography coronary artery plaque predictors of stress-induced myocardial ischemia by SPECT, Atherosclerosis **197** (2008) 700–709.

[19.43] DRIESSEN, R.S., et al., Effect of plaque burden and morphology on myocardial blood flow and fractional flow reserve, J. Am. Coll. Cardiol. **71** (2018) 499–509.

[19.44] NAKAZATO, R., et al., Additive diagnostic value of atherosclerotic plaque characteristics to non-invasive FFR for identification of lesions causing ischaemia: Results from a prospective international multicentre trial, Eurointervention **12** (2016) 473–481.

[19.45] GAUR, S., et al., Coronary plaque quantification and fractional flow reserve by coronary computed tomography angiography identify ischaemia-causing lesions, Eur. Heart J. **37** (2016) 1220–1227.

[19.46] PARK, H.B., et al., Atherosclerotic plaque characteristics by CT angiography identify coronary lesions that cause ischemia: A direct comparison to fractional flow reserve, J. Am. Coll. Cardiol. Cardiovasc. Imag. **8** (2015) 1–10.

[19.47] LAVI, S., et al., The interaction between coronary endothelial dysfunction, local oxidative stress, and endogenous nitric oxide in humans, Hypertension **51** (2008) 127–133.

[19.48] ANDREINI, D., Dual energy coronary computed tomography angiography for detection and quantification of atherosclerotic burden: Diagnostic and prognostic significance, Rev. Esp. Cardiol. **69** (2016) 885–887.

ABBREVIATIONS

ACHD	adult congenital heart disease
ACS	acute coronary syndrome
ASD	atrial septal defect
AVSD	atrioventricular septal defect
CAC	coronary artery calcium
CACS	coronary artery calcium score
CAD	coronary artery disease
CAD–RADS	Coronary Artery Disease – Reporting and Data System
CCT	cardiac computed tomography
CCTA	coronary computed tomography angiography
CCTGA	congenitally corrected transposition of the great arteries
CFR	coronary flow reserve
CIED	cardiac implanted electronic device
CMR	cardiac magnetic resonance
CRESCENT	Computed Tomography Versus Exercise Testing in Suspected Coronary Artery Disease
CT	computed tomography
CZT	cadmium zinc telluride
D-TGA	dextrotransposition of the great arteries
ECG	electrocardiogram
eGFR	estimated glomerular filtration rate
ETT	exercise treadmill/bicycle test
EVINCI	Evaluation of Integrated Cardiac Imaging for the Detection and Characterization of Ischemic Heart Disease
FDG	fluorodeoxyglucose
FFR	fractional flow reserve
GSPECT	gated single photon emission computed tomography
HFmrEF	heart failure with medium range ejection fraction
HFpEF	heart failure with preserved ejection fraction
HFrEF	heart failure with reduced ejection fraction
INCAPS	IAEA Nuclear Cardiology Protocols Study
LGE	late gadolinium enhancement
LVEF	left ventricular ejection fraction
MBF	myocardial blood flow
MIBG	metaiodobenzylguanidine
MINOCA	myocardial infarction with non-obstructive coronary arteries
MPI	myocardial perfusion imaging
MR	magnetic resonance

MRI	magnetic resonance imaging
NSTEMI	non-ST-elevation myocardial infarction
PDA	patent ductus arteriosus
PET	positron emission tomography
PROMISE	Prospective Multicenter Imaging Study for Evaluation of Chest Pain
QALY	quality adjusted life years
RVEF	right ventricular ejection fraction
SCOT-HEART	Scottish Computed Tomography of the Heart
SPECT	single photon emission computed tomography
SSFP	steady state free precession
STE	speckle tracking echocardiography
STEMI	ST-elevation myocardial infarction
TEE	transoesophageal echocardiography
TGA	transposition of the great arteries
TIMI	thrombolysis in myocardial infarction
TTE	transthoracic echocardiography
VSD	ventricular septal defect
WOMEN	What is the Optimal Method for Ischemia Evaluation in Women

CONTRIBUTORS TO DRAFTING AND REVIEW

Alexanderson, E.	National Institute of Cardiology “Ignacio Chávez”, Mexico
Al-Mallah, M.H.	King Abdul-Aziz Cardiac Center, Saudi Arabia
Berman, D.	Cedars-Sinai Medical Center, United States of America
Bucciarelli-Ducci, C.	Bristol Heart Institute, United Kingdom
Carrasco, J.	National Institute of Cardiology “Ignacio Chávez”, Mexico
Carvajal, I.	National Institute of Cardiology “Ignacio Chávez”, Mexico
Cuevas, D.	National Institute of Cardiology “Ignacio Chávez”, Mexico
Dominguez, B.	National Institute of Cardiology “Ignacio Chávez”, Mexico
Dondi, M.	International Atomic Energy Agency
Dorbala, S.	Brigham and Women’s Hospital, United States of America
Garcia, E.V.	Emory University, United States of America.
Giubbini, R.	University of Brescia and Spedali Civili, Italy
Hong, G.	Severance Cardiovascular Hospital, Republic of Korea
Karthikeyan, G.	All India Institute of Medical Sciences, India
Keng, F.	National Heart Centre Singapore, Singapore
Lanzelloti, P.	University of Liège Hospital, Belgium
Lara, V.	National Institute of Cardiology “Ignacio Chávez”, Mexico

Maeve, A.	National Institute of Cardiology “Ignacio Chávez”, Mexico
Milan, E.	Nuclear Medicine Department, Treviso Hospital, Italy
Neglia, D.	Fondazione Toscana “Gabriele Monasterio”, Italy
Paez, D.	International Atomic Energy Agency
Partington, S.L.	Children’s Hospital of Philadelphia, United States of America
Peix, A.	Institute of Cardiology and Cardiovascular Surgery, Cuba
Pérez, M.	National Institute of Cardiology “Ignacio Chávez”, Mexico
Qian, Z.	Piedmont Heart Institute, United States of America
Raggi, P.	Mazankowski Alberta Heart Institute, Canada.
Shaw, L.J.	Emory University, United States of America
Shim, C.Y.	Severance Cardiovascular Hospital, Republic of Korea
Sobic Saranovic, D.	Clinical Center of Serbia, Serbia
Sureshkumar, S.	International Atomic Energy Agency
Vannan, M.A.	Piedmont Atlanta Hospital, United States of America
Vitola, J.	Quanta Diagnóstico Nuclear, Brazil
Williams, M.C.	University of Edinburgh, United Kingdom
Zhou, X.	Chinese People’s Liberation Army General Hospital, China

IAEA
International Atomic Energy Agency

No. 26

ORDERING LOCALLY

IAEA priced publications may be purchased from the sources listed below or from major local booksellers.

Orders for unpriced publications should be made directly to the IAEA. The contact details are given at the end of this list.

NORTH AMERICA

Bernan / Rowman & Littlefield
15250 NBN Way, Blue Ridge Summit, PA 17214, USA
Telephone: +1 800 462 6420 • Fax: +1 800 338 4550
Email: orders@rowman.com • Web site: www.rowman.com/bernan

REST OF WORLD

Please contact your preferred local supplier, or our lead distributor:

Eurospan Group
Gray's Inn House
127 Clerkenwell Road
London EC1R 5DB
United Kingdom

Trade orders and enquiries:
Telephone: +44 (0)176 760 4972 • Fax: +44 (0)176 760 1640
Email: eurospan@turpin-distribution.com

Individual orders:
www.eurospanbookstore.com/iaea

For further information:
Telephone: +44 (0)207 240 0856 • Fax: +44 (0)207 379 0609
Email: info@eurospangroup.com • Web site: www.eurospangroup.com

Orders for both priced and unpriced publications may be addressed directly to:

Marketing and Sales Unit
International Atomic Energy Agency
Vienna International Centre, PO Box 100, 1400 Vienna, Austria
Telephone: +43 1 2600 22529 or 22530 • Fax: +43 1 26007 22529
Email: sales.publications@iaea.org • Web site: www.iaea.org/publications

This publication provides comprehensive guidance on the rationale and implementation of integrated cardiovascular imaging for practitioners. Imaging experts from IAEA Member States can embrace optimal strategies of cardiovascular imaging to address an array of clinical conditions. By applying high quality evidence published in peer reviewed literature, vast opportunities are available to improve the lives of patients at risk of and diagnosed with cardiovascular disease, many of whom will benefit from the use of cardiovascular imaging to guide optimal therapeutic decision making.

International Atomic Energy Agency
Vienna